

# **The Identification of Anti-hormone Induced Genes as Potential Therapeutic Targets in Breast Cancer**

**Victoria Shaw**

Thesis presented for the degree of  
Doctor of Philosophy

October 2007

**Tenovus Centre for Cancer Research  
Cardiff University**

UMI Number: U584191

All rights reserved

INFORMATION TO ALL USERS

The quality of this reproduction is dependent upon the quality of the copy submitted.

In the unlikely event that the author did not send a complete manuscript and there are missing pages, these will be noted. Also, if material had to be removed, a note will indicate the deletion.



UMI U584191

Published by ProQuest LLC 2013. Copyright in the Dissertation held by the Author.  
Microform Edition © ProQuest LLC.

All rights reserved. This work is protected against  
unauthorized copying under Title 17, United States Code.



ProQuest LLC  
789 East Eisenhower Parkway  
P.O. Box 1346  
Ann Arbor, MI 48106-1346

## DECLARATION

This work had not previously been accepted in substance for any degree and is not concurrently submitted in candidature for any degree.

Signed VShaw (candidate) Date 25/10/07

## STATEMENT 1

This thesis is being submitted in partial fulfilment of the requirements for the degree of PhD

Signed VShaw (candidate) Date 25/10/07

## STATEMENT 2

This thesis is the result of my own independent work/investigation, except where otherwise stated. Other sources are acknowledged by explicit references.

Signed VShaw (candidate) Date 25/10/07

## STATEMENT 3

I hereby give consent for my thesis, if accepted, to be available for photocopying and for inter-library loan, and for the title and summary to be made available to outside organisations

Signed VShaw (candidate) Date 25/10/07

## ~ Acknowledgements ~

I would like to express my gratitude to my supervisors Prof. Robert Nicholson and Dr. Julia Gee. Their guidance, support and enthusiasm has been instrumental throughout my PhD and especially whilst writing this thesis.

Thank you to all the Staff at the Tenovus Centre for Cancer Research, I learnt so much from each of you and had a lot of fun. Extra special thanks to Richard McClelland, I really don't know what I would have done with out you. I am also extremely grateful to Denise Barrow and the rest of the tissue culture team and the ICC girls, especially Michelle James for there help in preparing cell pellet arrays. Thanks also to Carol Dutkowski for the proof reading.

The people credited with keeping me sane throughout the completion of this thesis are my closest friends. Thank you Anna, Kathryn, Hannah, Alastair, Kathryn, Sara, Rachel, Cindy and Dylan, it would have been much harder without you.

Finally and most importantly thank you to my amazing Mum and Dad for their unconditional love, support, understanding and encouragement when it was most needed. This is for both of you.

*Superhero thesis writer,  
Fixing to save the world from my room  
~Malcolm Middleton*

## ~ Summary ~

Tamoxifen, a competitive inhibitor of oestradiol binding to the oestrogen receptor (ER), remains a key anti-hormonal treatment for ER+ve breast cancer although its effectiveness is limited by development of resistance. It is hypothesised that in addition to blockade of pro-proliferative/anti-apoptotic genes, anti-oestrogens exert an early protective effect, inducing cell survival and pro-invasive genes that enable a subset of cells to escape the anti-tumour effects of the anti-oestrogens and facilitate disease progression. It was hoped that identification of such early compensatory events in this thesis and their subsequent therapeutic targeting in combination with anti-oestrogens would be able to improve anti-tumour response. Proof of this principle exists since co-targeting of anti-oestrogen-induced epidermal growth factor receptor (EGFR) alongside tamoxifen has been reported to improve growth inhibition in ER+ve MCF-7 human breast cancer cells and delay acquisition of resistance.

After filtering, hierarchical clustering and ontological investigation, 8 possible compensatory genes were identified as anti-oestrogen (tamoxifen and faslodex)-induced /oestrogen-suppressed at an early time point in MCF-7 cells *in vitro* using cDNA microarrays (bearing 1200 cancer-related genes), comparing anti-oestrogen with oestrogen (E2) treatment and control (oestrogen deprived) conditions. RT-PCR and protein investigation gave further insight into expression levels of these genes based on ER occupancy. Genes induced by both an anti-oestrogen-occupied ER and an unoccupied ER versus E2 treatment were the Rnd family member RhoE and nucleoside diphosphate kinase NME3 implicated in migration and cell survival respectively, and the anti-apoptotic transcription factor NFkB1. The adhesive junction protein  $\delta$ -catenin, cell survival elements 14-3-3 $\zeta$  and chaperone Bag-1 and nuclear serine/threonine kinase NDR implicated in progression were all induced by an anti-oestrogen occupied ER but not by an unoccupied ER versus E2 treatment. Co-treating with the NFkB inhibitor parthenolide and faslodex suppressed NFkB1 DNA binding, transcriptional activity and improved growth inhibition of MCF-7 cells. These data demonstrate that several genes of adverse potential are induced during the anti-oestrogen-responsive phase, and that their co-targeting has promise to improve anti-tumour response.

## ~ Contents ~

### Chapter 1

1. Introduction	2
1.1 Breast cancer	2
1.1.1 Statistics and risk factors	2
1.1.2 Oestrogens & breast cancer	3
1.1.2.1 Oestrogen receptor	4
1.1.3 Endocrine therapy	11
1.1.3.1 Anti-oestrogens	12
1.1.3.2 Oestrogen deprivation	17
1.1.4 Anti-hormone resistance and growth factor signalling	21
1.1.4.1 ErbB receptor signalling	22
1.1.4.2 Inhibition of growth factor signalling in resistance & its limitations	25
1.1.5 Molecular mechanism for oestrogen repression of gene expression	27
1.1.5.1 Competition for co-activators by the oestrogen bound ER $\alpha$ complex	28
1.1.5.2 Recruitment of co-repressors by the oestrogen bound ER $\alpha$ complex	28
1.1.5.3 ER $\alpha$ protein/protein interactions sequestering other transcription factors	29
1.1.5.4 Role for Er $\beta$ in oestrogen mediated repression of gene expression	30
1.1.6 Proof of principle that oestrogen suppresses growth regulatory genes that increase on anti-oestrogen treatment: targeting potential of epidermal growth factor receptor	31

1.2 Microarrays	33
1.2.1 Technology overview	33
1.2.1.1 cDNA microarrays	34
1.2.1.2 Oligonucleotide microarrays	35
1.2.1.3 Comparison of cDNA and oligonucleotide microarrays	36
1.3 Microarray technology in breast cancer research	37
1.3.1 Expression profiling in clinical samples	37
1.3.2 Microarrays in breast cancer cell lines and model systems	40
1.4 Project aims	43
<b>Chapter 2</b>	
<b>2 Materials and methods</b>	<b>47</b>
2.1 Materials and equipment	47
2.2 Cell Culture	51
2.2.1 Routine maintenance and passaging of MCF-7 cells	51
2.2.2 Experimental medium	52
2.2.3 Development of a tamoxifen and faslodex resistant cell lines	53
2.3 RNA extraction	54
2.3.1 Cell culture for RNA extraction	54
2.3.2 Tri-reagent extraction	54
2.3.2.1 Measurement of total RNA concentration	56
2.3.2.2 Agarose gel electrophoresis of total RNA	56
2.3.3 DNase treatment and RNA purification	57
2.4 Northern blotting	57
2.4.1 Use of ionising radiation	57

2.4.2 Formaldehyde gel electrophoresis	58
2.4.3 Probe production	59
2.4.4 Hybridization	59
2.4.5 Removal of radioactivity from membranes	60
2.5 cDNA atlas array procedure	61
2.5.1 Probe synthesis form total RNA	61
2.5.2 Column chromatography	61
2.5.3 Pre-hybridization of nylon arrays	62
2.5.4 hybridization	62
2.5.5 Washing	63
2.5.6 Stripping arrays for re-hybridization	64
2.6 Array analysis	64
2.6.1 AtlasImage 2.7	64
2.6.2 GeneSifter	65
2.6.2.1 Normalisation and log transformation	65
2.6.2.2 Boxplots and scatter plots	66
2.6.2.3 Pairwise comparison	67
2.6.3.4 Hierarchical clustering	67
2.6.2.5 Statistical array analysis	67
2.7 Semi-quantitative RT-PCR	67
2.7.1 Reverse transcription (RT)	67
2.7.2 Semi-quantitative polymerase chain reaction	68
2.8 Protein isolation	70



2.8.1 Cell culture for western blotting	70
2.8.2 Cell lysis	71
2.8.2.1 Lowry protein concentration assay	72
2.9 Sodium Dodecyl Sulphate-Polyacrylamide Gel electrophoresis	72
2.10 Western blotting	74
2.10.1 Detection and analysis	75
2.11 Immunocytochemistry	76
2.11.1 Optimisation	76
2.11.2 RhoE coverslip assay	77
2.11.2.1 Coverslip cell culture	77
2.11.2.2 Paraformaldehyde/vanadate fix for RhoE	77
2.11.2.3 RhoE ICC assay	78
2.11.3 Use of cell pellet arrays	79
2.11.3.1 De-wax sections	79
2.11.3.2 Immunocytochemistry assay	79
2.11.3.3 Pronase retrieval	80
2.11.3.4 Pressure cooking retrieval	80
2.11.3.5 Microwave retrieval	80
2.11.4 Immunocytochemical analysis	82
2.11.5 Statistical analysis	83
2.12 TransAM assay	83
2.12.1 Cell culture fro TransAM assay	83
2.12.2 Preparation of whole cell extract	84
2.12.3 NFkB transcription factor assay	85

2.12.3.1 Binding of NFκB isoforms to the NFκB consensus sequence	85
2.12.3.2 Binding of primary antibody	86
2.12.3.3 Binding of secondary antibody	87
2.12.3.4 Colorimetric reaction	87
2.13 NFκB transfection assay	87
2.13.1 Cell culture and transfection	87
2.13.2 Cell lysis	89
2.13.3 Luciferase assay	89
2.13.4 In situ β-galactosidase fixation, staining and quantification	89
2.14 Parthenolide growth inhibition assay	90
<b>Chapter 3</b>	
<b>3 Results</b>	<b>93</b>
<b>3.1 Array analysis</b>	<b>93</b>
3.1.1 Clontech Atlas™ Human 1.2 Nylon arrays	93
3.1.2 Array analysis software: data log transformation & normalisation	95
3.1.3 Scatter plots to validate array profiles & performance	96
3.1.4 Detailed evaluation of array performance for day 7 & 10 samples	99
3.1.5 Anti-oestrogen induced gene selection by expression profiling	102
3.1.5.1 Venn diagrams	102
3.1.5.1.1 Genes induced at both day 7 & 10 versus untreated control	102
3.1.5.1.2 Gene induced at both day 7 & 10 versus oestradiol	103
3.1.5.1.3 Anti-oestrogen induced genes	104
3.1.5.2 Hierarchical clustering to further explore gene profiles	105

3.2 Detailed ontological analysis of the 60 anti-oestrogen induced genes & selection for validation	109
3.2.1 Broad profiling of molecular function & cancer related ontology for the anti-oestrogen induced genes	109
3.2.2 Anti-oestrogen induced genes selected for verification	111
3.2.3 Ontological results of the 8 genes selected for verification	113
3.2.3.1 RhoE	113
3.2.3.2 Delta Catenin	114
3.2.3.3 Bag-1	115
3.2.3.4 14-3-3 zeta	116
3.2.3.5 Hif-1 $\alpha$	119
3.2.3.6 NME3	120
3.2.3.7 NF $\kappa$ B1	121
3.2.3.8 NDR1 protein kinase	126
3.3 Full array profiles & PCR validation for the 8 selected genes	128
3.3.1 RhoE	129
3.3.1.1 Summary	129
3.3.1.2 Array profile	129
3.3.1.3 RT-PCR profile with array RNA	129
3.3.1.4 RT-PCR validation profile	130
3.3.3 Bag-1	134
3.3.3.1 Summary	134
3.3.3.2 Array profile	134
3.3.3.3 RT-PCR profile with array RNA	135
3.3.3.4 Validation RT-PCR	135

3.3.4 14-3-3 $\xi$	136
3.3.4.1 Summary	136
3.3.4.2 Array profile	136
3.3.4.3 RT-PCR profile with array RNA	137
3.3.4.4 Validation PCR profile	137
3.3.5 Hif-1 $\alpha$	139
3.3.5.1 Summary	139
3.3.5.2 Array profile	139
3.3.5.3 RT-PCR profile with array RNA	140
3.3.5.4 Validation RT-PCR profile	140
3.3.6 NME3	142
3.3.6.1 Summary	142
3.3.6.2 Array profile	142
3.3.6.3 RT-PCR profile with array RNA	143
3.3.6.4 Validation RT-PCR	143
3.3.7 NF $\kappa$ B1	144
3.3.7.1 Summary	144
3.3.7.2 Array profile	144
3.3.7.3 RT-PCR profile with array RNA	145
3.3.7.4 Validation RT-PCR profile	145
3.3.8 NDR	146
3.3.8.1 Summary	146
3.3.8.2 Array profile	146
3.3.8.3 RT-PCR profile with array PCR	147

3.4 Investigation at protein level	148
3.4.1 RhoE	149
3.4.1.1 Oestradiol and anti-hormonal treatments	149
3.4.1.1.1 Immunocytochemistry	149
3.4.1.1.2 Western blotting	150
3.4.1.2 Resistance	150
3.4.1.2.1 Western blotting	150
3.4.2 Delta Catenin	151
3.4.2.1 Oestradiol and anti-hormonal treatments	151
3.4.2.1.1 Immunocytochemistry	151
3.4.2.2 Resistance	153
3.4.2.2.1 Immunocytochemistry	153
3.4.3 Bag-1	154
3.4.3.1 Oestradiol and anti-hormonal treatments	154
3.4.3.1.1 Immunocytochemistry	154
3.4.3.2 Resistance	155
3.4.3.2.1 Immunocytochemistry	155
3.4.4 14-3-3 $\zeta$	157
3.4.4.1 Oestradiol and anti-hormonal treatments	157
3.4.4.1.1 Immunocytochemistry	157
3.4.4.1.2 Western blotting	159
3.4.5 Hif-1 $\alpha$	160
3.4.5.1 Oestradiol and anti-hormonal treatments	160
3.4.5.1.1 Immunocytochemistry	160

3.4.5.1.2 Western blotting	160
3.4.6 NME3	162
3.4.6.1 Oestradiol and anti-hormonal treatments	162
3.4.6.1.1 Immunocytochemistry	162
3.4.7 NFkB1	164
3.4.7.1 Oestradiol and anti-hormonal treatments	164
3.4.7.1.1 Immunocytochemistry	164
3.4.7.1.2 NFkB DNA binding activity in MCF-7 cells with oestradiol and anti-hormone treatments	166
3.4.7.1.3 NFkB reporter assay in MCF-7 cells with anti-hormone treatments and in the presence and absence of NFkB blockade	167
3.4.7.1.4 Inhibitor growth studies	167
3.4.7.2 Resistance	168
3.4.7.2.1 Immunocytochemistry	168
3.4.7.2.2 NFkB DNA binding activity	169
3.4.7.2.3 Inhibitor growth studies	169
<b>Chapter 4</b>	
4 Discussion	171
4.1 Anti-oestrogens induce EGFR/Her2 during response: link to compensatory signalling and improved therapeutic response	171
4.2 Model system and project comparisons	172
4.3 Arrays were suitable to identify anti-oestrogen induced genes	173
4.4 Overall patterns of gene expression	174
4.5 Identification of genes co-induced by anti-oestrogens	176
4.5.1 Further exploration of induced genes using Venn diagrams	178

4.6 Ontological investigation of the 60 anti-oestrogen induced genes	179
4.7 Further investigation of the anti-oestrogen induced genes	181
4.7.1 Genes identified that were induced by anti-oestrogens alone or by both anti-oestrogens and oestrogen deprivation	183
4.7.2 Some anti-oestrogen induced genes identified persist through to acquired resistance	191
4.7.3 Several genes induced may confer additional adverse features to the breast cancer cell in the appropriate context	193
4.8 Implications for therapy and future directions	199
4.8.1 Oestrogen receptor blockade in combination with targeting of anti-hormone induced genes could prove worthwhile in improving the anti-tumour properties of anti-hormones	201
4.8.2 Inhibiting these new gene targets, where their increased expression is retained, could also prove valuable in treating resistance	204
4.8.3 Targeting of anti-hormones induced genes that may become important according to cell context (notably those driving invasive behaviour) may subvert progression and improve outlook	205
<b>Chapter 5</b>	
5 Appendix	207
5.1 Publications arising as a result of this thesis	207
5.2 Preparation of cell pellet arrays	208
5.2.1 Cell culture	208
5.2.2 Cell fixation	208
5.2.3 Paraffin Embedding	209
5.2.4 Cell array preparation	210
<b>Chapter 6</b>	
6 References	212

## ~ Abbreviations ~

AD - Activation domain  
AF-1/2 - activation function 1/2  
AI - aromatase inhibitors  
AP-1 - activator protein-1  
ARNT - aryl hydrocarbon receptor nuclear translocator  
ATAC - arimidex tamoxifen alone or in combination  
BMP - bone morphogenic protein  
cAMP - cyclic AMP  
CDC25C - cell division cycle 23 C  
cDNA - complimentary DNA  
CDK2 - cyclin dependent kinase 2  
CRE - cAMP response element  
CREB - cAMP response element binding protein  
CVS - central venous system  
BAD - BCL2 antagonist of cell death  
Bag-1 - BCL2 associated athanogene  
BAX - BCL2 associated X protein  
BID - BH3 interacting domain death agonist  
DBD - DNA binding domain  
DCIS - ductal breast carcinoma *in situ*  
DNA - deoxyribonucleic acid  
E2 - Oestrogen/Oestradiol  
ED - oestrogen deprivation  
EGF - epidermal growth factor  
EGFR - epidermal growth factor receptor  
EMT - epithelial mesenchymal transition  
ER+ve - oestrogen receptor positive  
ER-ve - oestrogen receptor negative  
ERE - Oestrogen response element  
ER - oestrogen receptor  
EST - expressed sequence tag  
FACS - fluorescent-activated cell sorting  
FSH - follicle stimulating hormone  
FTI - farnesyltransferase small molecule inhibitor  
GAPDH - glyceraldehydes-3 phosphate dehydrogenase  
GPCR - G-protein coupled receptor  
HAT - histone acetyl-transferase  
HDAC1 - SMRT/histone deacetylase 1  
Hif-1 $\alpha$  - hypoxia inducible factor 1 $\alpha$   
HRT - hormone-replacement therapy  
Hsp - heat shock protein  
I $\kappa$ B - inhibitor of  $\kappa$ B  
IKK - I $\kappa$ B kinase  
IL-6 - interleukin 6  
IGF-R - insulin like growth factor receptor



Ink4D - cyclin dependent kinase inhibitor D  
LBD - Ligand binding domain  
LCoR - ligand-dependent co-repressor  
LH - luteinizing hormone  
LH-RH - luteinizing hormone releasing hormone  
LTED - long term oestrogen deprivation  
MAPK - mitogen activated protein kinase  
MINDACT - microarray in node negative disease may avoid chemotherapy  
MMP7 - matrix metallo proteinase 7  
Mob1 - Mps one binder  
mRNA - messenger RNA  
MTA2 - metastasis associated 1 family member 2  
NCoR - nuclear receptor co-regulator  
NDPK - nucleoside diphosphate kinase  
NDR - nuclear DBf2-related protein  
NFkB - nuclear factor kappa B  
NIK - NFkB inducing protein  
NLS - nuclear localisation signal  
NPI - Nottingham prognostic index  
NPRAP - neural plakophilin related ARM repeat protein  
PDGR - platelet derived growth factor  
PI3K - phosphoinositide kinase 3  
PIC - pre-initiation complex  
PMA - phorbol 12-myristate 13-acetate  
PR - progesterone receptor  
pVHL - von Hippel-Lindau tumour suppressor  
RANTES - regulated upon activation, normal T-cell expressed and secreted  
REA - repressor of ER $\alpha$  activity  
RERG - ras-related and oestrogen regulated growth inhibitor  
RHD - rel homolog domain  
RNA - ribonucleic acid  
RSK - p90 ribosomal s6 kinase  
RTK - receptor tyrosine kinase  
RT-PCR - reverse transcription polymerase chain reaction  
SAFB1 - scaffold attachment factor B1  
SEM - standard error of the mean  
SERMS - selective oestrogen receptor modulators  
SERDS - selective oestrogen receptor down regulators  
SMRT - silencing mediator of retinoic acid receptor  
TCF/LEF - T-cell factor/lymphoid enhancing factor  
TFIIH - transcription factor II H  
TGF $\alpha/\beta$  - transforming growth factor  $\alpha/\beta$   
TIF-1 - transcriptional intermediary-2  
TKI - tyrosine kinase inhibitor  
TNF $\alpha$  - tumour necrosis factor  $\alpha$   
VCAM - vascular cell adhesion molecule  
VEGF - vascular endothelial growth factor

Chapter 1  
~ **Introduction** ~

# 1 Introduction

## 1.1 Breast cancer

### 1.1.1 Statistics & risk factors

Breast cancer is the most common form of female cancer in Britain. In 2003 there were 44,091 new cases (43,756 in women, 335 in men), equivalent to one in nine women developing breast cancer at some point in their life (Singletary 2003; Office for National Statistics). Breast cancer mortality rates peaked in the late 1980's, and since 1990 there has been a decrease in the mortality rate due to early detection (with mammographic screening introduced in 1988) and improved anti-hormonal and chemotherapeutic treatments (Jatoi and Miller 2003). However, breast cancer death remains a significant problem as in Europe there were 132,000 breast cancer related deaths in 2006 (Ferlay *et al.*, 2007).

Although breast cancer is essentially a sporadic disease (only up to ~10% of cases are familial), there are risk factors that can increase the chance that a person will develop breast cancer. The strongest of these factors is age, with a very low incidence before the age of 30, but this increases following the age of 30 until the age of 80 (Singletary 2003). There have been links with increased alcohol intake resulting in a moderately increased risk of breast cancer (Lash and Aschengrau 2000), as well as geographical residence (with highest risk in developed western countries) (McPherson *et al.*, 2000). However, the single

factor of overriding importance to breast cancer risk is gender, where less than 1% of all breast cancer is found in men, a finding which is highly supportive of a role for the female steroid hormone oestrogen in the development and subsequent growth of this disease (Glordano *et al.*, 2002).

### 1.1.2 Oestrogens & breast cancer

In 1896 George Beatson discovered that the ovaries contributed to the growth of breast cancer, since oophorectomy performed in post menopausal breast cancer patients resulted in a regression of the cancer (Jensen and Jordan 2003). The active component of the ovaries involved in breast cancer growth is oestrogen. It is now known that approximately 70% of breast cancers over-express the target receptor for this steroid hormone, the oestrogen receptor (ER), and rely on oestrogen for tumour growth through the ER signalling pathway (Gee *et al.*, 2004). The importance of oestrogen is further reflected in many of the risk factors for breast cancer, where these invariably contribute to increased exposure to oestrogen throughout an individual's life time. These risk factors include: early menarche (before aged twelve), late menopause (after aged fifty-five) and late first pregnancy (after the age of thirty). Obesity in postmenopausal women moderately increases the risk of breast cancer, due to adipose tissue becoming a continued source for low levels of endogenous oestrogens, despite cessation of ovarian function, after the menopause (McPherson *et al.*, 2000). There is also evidence that exogenous oestrogens can increase the risk of breast cancer. As such the oral contraceptive pill has been

found to slightly increase the breast cancer risk in recent and current users, although 10 years after ceasing to take the contraceptive pill the risk is no higher than if it had never been taken (Johnson and Millard 1996). Moreover, hormone-replacement therapy (HRT) has also been shown to increase the risk of breast cancer as well as reducing the detection sensitivity of mammograms (Carney *et al.*, 2003). The increased breast cancer relative risk with oestrogen only or oestrogen/progesterone combination HRT is 1.30 and 2.0 respectively in current users over never users. However, the increased risk is again reversible on cessation of use (Beral 2003).

#### 1.1.2.1 Oestrogen receptor

##### 1.1.2.1.1 Oestrogen receptor Structure

The ER is a member of the nuclear steroid receptor superfamily of transcription factors. Other members of this nuclear receptor family include receptors for glucocorticoid, progesterone or androgen (Chen *et al.*, 2002). Two ER proteins (as well as various splice variants) have been identified, ER $\alpha$  and ER $\beta$ , which are encoded by separate genes. The ER $\alpha$  gene is located on chromosome 6q 25.1 and contains 8 exons. The encoded protein is 595 amino acids in length and has a molecular weight of 66kDa (MacGregor and Jordan 1998). The ER $\alpha$  protein (Figure 1.1) has six functional domains A-F. The A/B domain at the N-terminus of the ER $\alpha$  protein modulates transcription through its activation function-1 (AF-1) region, which bears key phosphorylation sites, notably serine 118 and 167, and is regulated in a ligand independent manner. Domain

C is a highly conserved DNA binding domain (DBD) that contains two zinc fingers, which mediate binding to the oestrogen response element (ERE) sequence found in the promoter of oestrogen responsive genes. Domain D forms the variable hinge region, which is essential for dimerization and heat shock protein (Hsp) binding. Domain E bears the ligand binding domain (LBD) which contains a hydrophobic 'pocket' that binds oestrogen, along with the helix 12 region that is responsible for hormone binding and the conformational change that seals oestrogen into the pocket. Domain E also contains activation function-2 region (AF-2) again responsible for activation of transcription, in this instance in a ligand dependent manner. Finally, domain F is found at the carboxy terminus and modulates transcriptional activation and dimerization (Klinge 2001). The most recently discovered of the two ERs is ER $\beta$ . ER $\beta$  is a protein of 485 amino acids with a molecular weight of 54.2kDa. However, ER $\alpha$  is thought to be the predominant mediator of the effect of oestrogens in breast cancer (Fuqua *et al.*, 2003).

#### 1.1.2.1.2 Classic genomic mechanism of oestrogen/oestrogen receptor action

The most potent and predominant oestrogen in women is 17 $\beta$ -oestradiol (E2, Figure 1.2), which acts via its binding of ER $\alpha$  to cause transcription of oestrogen-regulated genes. Oestrogens are lipophilic molecules that can freely diffuse across the plasma membrane of cells, where they can bind to the ER in the nuclei. The classical genomic mechanism of nuclear oestrogen action subsequently initiated is illustrated in Figure 1.3. Genes known to be regulated

by this classical mechanism include pS2 and vitellogenin (Hall *et al.*, 2002) where in general, E2-promoted gene expression is able to drive breast cancer cell proliferation and survival. In detail, Figure 1.3 shows that when oestrogen binds to the hydrophobic 'pocket' in the ER there is a conformational change in the receptor so that the helix 12 region seals the pocket, this leads to the activation of AF-2, displacement of heat shock chaperone proteins from the ER and subsequent dimerization of E2-bound ER (Pearce *et al.*, 2003). The E2:ER dimer is then able to bind to EREs, which are 13 base pair palindromic DNA sequences located in the 5' promoter region of E2 responsive genes. The conformational change in ER $\alpha$  following E2 binding not only activates AF-2 but generates a platform for co-activator binding, so that after binding to the DNA the E2:ER complex recruits co-activators, while co-repressors are generally displaced (Gruber *et al.*, 2002). The ligand independent AF-1 is activated by phosphorylation of key serine residues 118 and 167, and in order for there to be full transcriptional activation of ER $\alpha$  both AF-1 and AF-2 are required to be synergistically activated (Metivier *et al.*, 2001; Bentrem *et al.*, 2003).

Co-activators interact with ER $\alpha$  and enhance gene transcription by modulating the structure of chromatin and/or promoting further protein recruitment (Klinge 2000a). Many co-activators are able to remodel chromatin structure through their histone acetyl-transferase (HAT) activity, which acetylates the lysine residues on the N-terminus of histones 3 and 4 to result in a more 'open' chromatin structure which facilitates transcriptional activation. The 'open'

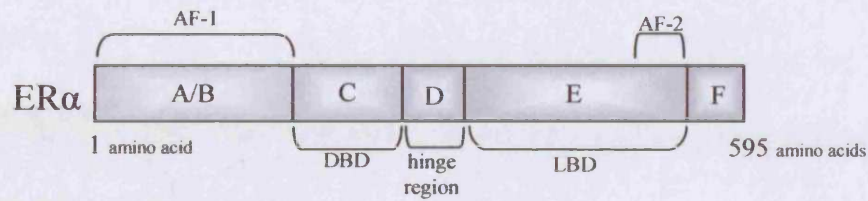


**Figure 1.1 Structure of ER $\alpha$**

The diagram illustrates the location of the transactivation domains AF-1 and AF-2 within the ER $\alpha$  protein. Also indicated are DNA binding domain (DBD), variable hinge region and ligand binding domain (LBD).

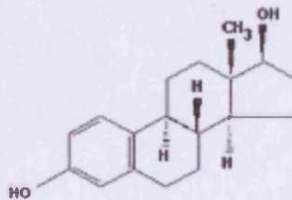


**Figure 1.2 Chemical structure of 17- $\beta$  oestradiol**

Shown is the chemical structure of 17- $\beta$  oestradiol, which is the most potent and predominant oestrogen in women and acts via its binding of ER $\alpha$  to cause transcription of oestrogen-regulated genes.

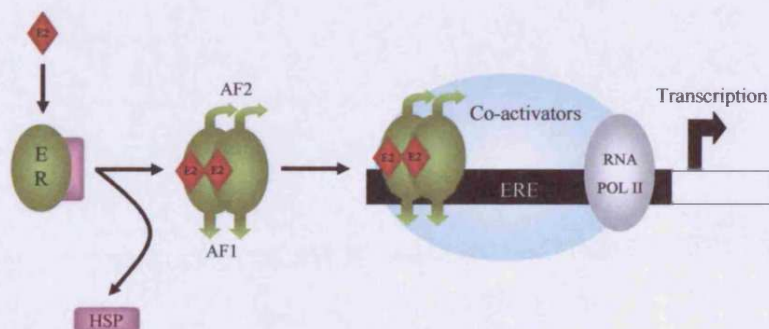


**Figure 1.3 Classical mechanism of oestradiol action**

The diagram shows the classical mechanism of E2 action. E2 binds to the ER and displaces Hsp and activates both AF-1 and AF-2. The E2:ER complex translocates to the nucleus where it binds to an ERE sequence in the promoter region of E2 responsive genes. This is followed by binding of co-activators and transcriptional machinery which results in gene transcription. Adapted from Howell *et al* (2000).



structure of chromatin, following recruitment of further co-activators to the oestrogen-occupied ER, allows for pre-initiation complex binding (PIC, containing general transcription factors and RNA polymerase II). Gene transcription can then commence once the transcription initiation complex is complete (Klinge 2000b). There are several classes of co-activators recruited to the ER $\alpha$ . The first group comprises of the p300 and CREB binding protein (collectively called p300/CBP), transcriptional intermediary-2 (TIF-1) class, which promote the histone and thus chromatin remodelling that is required for transcriptional activation. The second group comprises of the SRB and mediator-protein containing complex, thyroid-hormone-receptor-associated protein and vitamin-D-receptor-interacting protein (SMCC/TRAP/DRIP) family. These co-activators do not contain HAT activity but are important in allowing recruitment of the PIC, providing a direct bridge to the general transcriptional initiation complex (Metivier *et al.*, 2001). The third class of co-activators are the steroid receptor co-activator (SRC) family. This family of proteins have the capability of recruiting further co-activators through an activation domain (AD) as well as altering the structure of the chromatin. SRC-3 (also known as AIB1, ACTR, RAC3 or TRAM1) has been shown to be over-expressed or amplified in several breast cancer cell lines and was highly expressed in 64% of clinical primary breast tumours (Katzenellenbogen and Katzenellenbogen 2000; Klinge 2000b).

Co-repressors, such as silencing mediator of retinoic acid receptor (SMRT) and nuclear receptor co-regulator (NCoR), are responsible for the silencing of

genes, generally being recruited to ER $\alpha$  in the absence of E2 and in turn being displaced on E2:ER binding (Klinge 2000b). Several ER $\alpha$  co-repressors have been discovered, including repressor of ER $\alpha$  activity (REA) which competes with co-activators for the ligand binding domain. Ligand-dependent Co-repressor (LCoR) and the SMRT/histone deacetylase 1 (HDAC1)-associated repressor protein SHARP both recruit HDAC complexes, an event that results in condensed chromatin which impairs the access of transcription factors to the DNA and thus prevents gene expression in the absence of E2 (Dobrzycka *et al.*, 2003).

Alongside co-activators/co-repressors, transcriptional activity of ER $\alpha$  is also regulated by its phosphorylation status. ER $\alpha$  becomes hyperphosphorylated in the presence of E2 at several residues including serine 104, 106, 118, 167 and 294, all found in the AF-1 domain. This phosphorylation in the presence of oestrogen is mediated by the activity of kinases including cyclin A/CDK2 and TFIIH cyclin dependent kinase. Phosphorylation of ER $\alpha$  increases co-activator binding and therefore promotes E2:ER $\alpha$ -mediated transcription (Lannigan 2003). Interestingly, however, it has also been found that mitogen activated protein kinase (MAPK) is able to phosphorylate serine 118 in the AF-1 region to promote ER $\alpha$  transcriptional activity in a ligand-independent manner, driven by upstream growth factor signalling. Growth factor pathways such as EGFR and IGF1R are implicated, since phosphorylation can occur in response to epidermal growth factor (EGF) or phorbol 12-myristate 13-acetate (PMA) and IGFs (Joel *et al.*, 1998b; Chen *et al.*, 2002). In MCF-7 breast cancer cells, EGF

has been shown to induce phosphorylation of serine 167, and this is dependent on the involvement of p90 ribosomal S6 kinase (RSK) (Joel *et al.*, 1998a). Phosphorylation of serine 167 has also been noted by Akt via the PI3K pathway (Lannigan 2003). It is thought that ligand-independent activation of ER action becomes significant under conditions of resistance to anti-hormonal agents (see below; (Nicholson and Johnston 2005)).

#### 1.1.2.1.3 Non-classical, genomic mechanism of oestrogen receptor action

The ER has also been shown to be able to modulate the transcription of genes that do not contain an ERE. This is facilitated by direct protein-protein interaction of the nuclear ER $\alpha$  protein with other transcription factors such as Sp-1 and Activator Protein-1 (AP-1) that in turn interact with their own target promoter sequences to modulate gene transcription (Platet *et al.*, 2004). In the case of cyclin D1, for example, gene expression is thought to be regulated by ER $\alpha$  through its interactions with AP-1 via the cAMP response element (CRE) or Sp-1 site in the cyclin D1 promoter (Doisneau-Sixou *et al.*, 2003). It appears that the AP-1 sites linked with ER $\alpha$  also bind the Fos/Jun family of transcription factors which have recruited co-activators such as CBP/p300, p160 and SRC1 (Kushner *et al.*, 2000). Other genes regulated through this non classical genomic pathway include Hsp27, c-Myc and IGF-1 (Glidewell-Kenney *et al.*, 2005), where again such elements are believed to contribute significantly to regulation of breast cancer growth.

#### 1.1.2.1.4 Rapid, non-genomic mechanism of oestrogen/ER action

In addition to the transcriptional events initiated by nuclear ER $\alpha$  it has become apparent that steroid hormone stimulation can also trigger intracellular signalling events (e.g. kinase activation) within minutes, implying that not all action of E2 is through transcriptional mechanisms. These rapid events have been attributed to the presence of ER $\alpha$  at the plasma membrane, as first described by Pietras and Szego (1977) when the rapid generation of cyclic AMP (cAMP) was noted on E2 stimulation of cells. Membrane ER signalling has been associated with regulation of G-protein coupled receptors (GPCR), especially GPR30 (Filardo and Thomas 2005), in turn phosphorylating tyrosine kinases, MAPKs and Akt, which trigger cell membrane ion channels as well as activating adenylate cyclases (Simoncini and Genazzani 2003). In breast cancer membrane-localised ER is reported to cross-talk with EGFR, as well as insulin-like growth factor receptor (IGF-R) (Levin 2005). It is thought that the nuclear and membrane bound ER $\alpha$  is the same protein (Razandi *et al.*, 2004). The mechanism of translocation of ER $\alpha$  to the plasma membrane is unclear, but it seems likely to involve the growth factor signalling elements IGF-1R and Shc (Song *et al.*, 2004). Santen *et al.* (2005a) have shown that these non-genomic E2 effects result in elevated activation of the Elk-1 transcription factor, along with morphological changes in cell membranes of long-term E2 deprived cells (Santen *et al.*, 2005a).

While certainly detectable in breast cancer *in vitro* models such as MCF-7 (Santen *et al.*, 2005a), the part that this rapid non-genomic signalling plays in

breast cancer remains controversial and unclear (Nicholson and Johnston 2005). Indeed, only a very small percentage of total ER $\alpha$  generally resides at the plasma membrane, and to date it seems that this mechanism may only be a significant player in breast cancer cells when the growth factor signalling that can interact with membrane ER $\alpha$  is aberrantly over-expressed (for example, in anti-hormone resistance) (Schiff *et al.*, 2004).

### 1.1.3 Endocrine therapy

As described above, E2/ER signalling comprises a potent factor for driving growth of breast cancer cells, and indeed the majority (~70%) of breast cancers are ER positive (ER+ve). The remaining (~30%) breast cancers are ER negative (ER-ve), show dominance of growth factor pathways (e.g. EGFR/Her2) for their growth, and are also highly-aggressive and associated with a poorer patient survival, for the most part, compared to ER+ve disease (Rochefort *et al.*, 2003).

On presentation, primary breast cancer is treated by a combination of surgery with an adjuvant systemic therapy, where the aim of such management is to hopefully prevent relapse and thus cure the disease. Equally, systemic therapies are valuable in the advanced (inoperable) setting, in this instance with the aim of limiting further tumour growth, improving quality of life, and modestly improving survival (Gibson *et al.*, 2007). The systemic treatment of breast cancer is highly dependent on its ER status. Thus, while of no benefit in

patients without ER $\alpha$  (where chemotherapy is the agent of choice) (Piccart *et al.*, 2005), anti-hormonal therapy is the mainstay of breast cancer management for patients with ER+ve breast cancer through its ability to subvert E2/ER signalling (Goldhirsch *et al.*, 2006). Anti-hormones can be broadly classified into two main groups: firstly, anti-oestrogens that are either selective ER modulators (SERMs) or pure anti-oestrogens, and secondly oestrogen deprivation (ED) strategies. Simplistically, anti-oestrogens interfere with oestrogen/ER signalling by competitively inhibiting oestrogen binding to the ER $\alpha$  in breast cancer cells, and in the case of “pure” anti-oestrogens also having catastrophic effects on ER $\alpha$  protein level and activity. Oestrogen deprivation strategies aim to markedly deplete oestrogen production throughout the body (and hence oestrogen availability to the breast cancer cell) (Robertson 2001; McDonnell *et al.*, 2002; Johnston and Dowsett 2003).

### 1.1.3.1 Anti-oestrogens

#### 1.1.3.1.1 Selective oestrogen receptor modulators (SERMs)

The most frequently prescribed anti-oestrogen is the non-steroidal agent tamoxifen (Figure 1.4). This was initially investigated as a contraceptive but was abandoned due to its stimulatory effect on the reproductive tract (Jordan 2003). However in 1971 Cole *et al.* published on its ability to act as an anti-oestrogen on breast cancer (Cole *et al.*, 1971; Clarke *et al.*, 2003) and it was soon shown to be growth inhibitory in several *in vitro* and *in vivo* models of breast cancer, including the MCF-7 cell line, and in clinical ER $\alpha$  positive

disease (MacGregor and Jordan 1998). Over the last 25 years tamoxifen has been the gold standard treatment for ER+ve breast cancer, responsible for a 47% reduction in recurrence and a 26% reduced mortality in early breast cancer (Nicholson and Johnston 2005). In the clinic, tamoxifen can be used for primary ER+ve breast cancer in both premenopausal and postmenopausal patients following surgery (adjuvant) until relapse or for a maximum of 5 years. It is able to substantially delay (or even prevent) relapse and extend survival of approximately 70% of ER+ve patients in this setting (Fisher *et al.*, 2004). It is also beneficial in ~60% of advanced ER+ve breast cancer patients (Kuss *et al.*, 1997). In addition, Tamoxifen has proved useful as a chemopreventative agent, with clinical trials showing a 30-40% decrease in incidence when taken by postmenopausal, high risk women (Cuzick *et al.*, 2002).

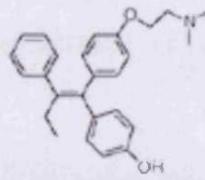
As indicated from initial studies described above, a key characteristic of a SERM is that they can display both anti-oestrogenic and oestrogenic effects according to the target ER+ve tissue. Thus, in the breast (and many breast cancers), tamoxifen acts as an antagonist, by competing with oestrogen for binding to the ER to inhibit growth. While such agents also have anti-oestrogenic activity in the brain (manifested as hot flushes), in the bone, liver, CVS and uterus, the binding of SERMs to ER results in an agonistic effect. As such tamoxifen has several clinical 'pros and cons' associated with its use. Its oestrogenic effects have been shown to lower levels of circulating cholesterol and to maintain bone density, while unfortunately increasing the risk of

thrombosis and, to some degree, endometrial cancer (O'Regan and Jordan 2002). Several further SERMS (e.g. Toremifene) have been developed in an attempt to eliminate the unwanted agonistic effects associated with tamoxifen (and to improve on its anti-oestrogenicity in breast cancer) but with little success, as all have retained their agonistic qualities (Nicholson and Johnston 2005).

#### 1.1.3.1.1.1 Molecular mechanism of actions of tamoxifen as a SERM

As an anti-oestrogen, tamoxifen is a competitive inhibitor of E2:ER binding. When E2 binds into the hydrophobic pocket it is sealed inside by Helix 12 and induces a conformational change with subsequent Hsp release and dimerization. When tamoxifen binds there is again a conformational change so Hsp's are still released and the tamoxifen-bound ER $\alpha$  proteins still dimerize, with subsequent binding to the ERE sequence in gene promoters (Figure 1.5). However, the bulky alkylaminoethoxy side-chain (and trans-configuration) of tamoxifen alters the ER $\alpha$  conformation such that Helix 12 cannot properly seal the pocket. This altered conformation prevents the binding of co-activators and allows recruitment of co-repressors to the ER, blocking AF-2 transcriptional activation function. However, the ligand independent function of AF-1 remains intact, allowing for its phosphorylation and co-activator recruitment in a ligand independent manner whenever the appropriate kinases and co-activators are present. Thus for genes that can be transcribed by an active AF-1 domain, tamoxifen acts as an agonist in an appropriate tissue context. Tissue selectivity





4-OH-tamoxifen

Figure 1.4 Chemical structure of 4-OH-tamoxifen

Shown is the chemical structure of 4-OH-tamoxifen, the active metabolite of tamoxifen.

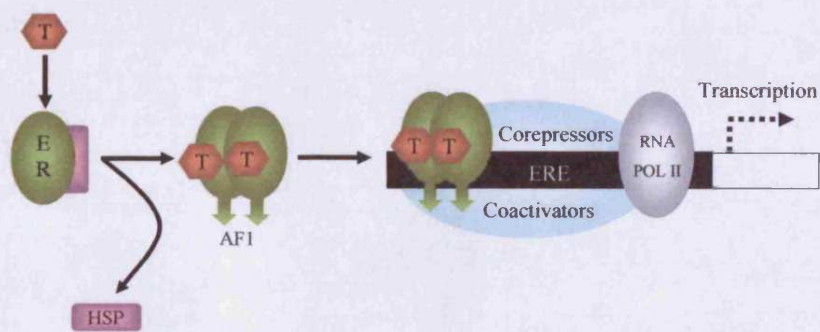


Figure 1.5 Mechanism of tamoxifen action

The diagram shows the mechanism of tamoxifen action. When tamoxifen binds to the ER, Hsp is displaced and AF-1 (but not AF-2) is activated. The tamoxifen:ER complex is translocated to the nucleus, where it binds to the ERE within the promoter region of E2 responsive genes. Co-activators and co-repressors bind allowing for the activation of AF-1 but not AF-2 which results in partial agonist activity of tamoxifen. Adapted from Howell *et al* (2000).

of tamoxifen in the human is therefore thought to be caused by the predominance of AF-1 (e.g. uterus) or AF-2 activated gene expression (e.g. breast) which is dependent on the local availability of kinases and co-activators (McDonnell *et al.*, 2002; Ring and Dowsett 2004). This leads to the understanding of the use of tamoxifen as an anti-oestrogen in breast cancer where it depletes expression of growth-related genes, and also to the modest increase in endometrial cancer associated with agonistic activity in this tissue (Fisher *et al.*, 1994).

#### 1.1.3.1.2 Pure anti-oestrogens

Pure anti-oestrogens do not display the same mixed agonistic/antagonistic qualities as SERMs: they act purely as E2/ER $\alpha$  antagonists (Wakeling and Bowler 1992). These agents are exemplified by the steroidal pure anti-oestrogen faslodex (fulvestrant, ICI 182,780, Figure 1.6) that is clinically administered monthly as an intramuscular injection. Faslodex competitively inhibits E2 binding to the ER with a binding affinity 100 times that of tamoxifen (Robertson 2001). Moreover, in contrast to tamoxifen, faslodex is also able to deplete levels of ER $\alpha$  and so has been referred to as a selective oestrogen receptor downregulator (SERD). *In vitro* studies on faslodex in ER+ve MCF-7 breast cancer cells have shown that it is a more potent inhibitor of cell growth than tamoxifen (Dowsett *et al.*, 2005). The drug was also a superior inhibitor of growth in hormone responsive ER+ve breast cancer xenograft models (Osborne *et al.*, 1995). Faslodex has shown much promise in

the clinic and is approved as a second line therapy for advanced breast cancer, showing anti-tumour activity following relapse with other endocrine treatments including tamoxifen. This indicates that there is no cross resistance between tamoxifen and faslodex in breast cancer and that there is a retained role for ER $\alpha$  in the tamoxifen resistant state (Howell *et al.*, 2000). A phase III study comparing first line treatment with tamoxifen or faslodex in postmenopausal women with ER+ve advanced breast cancer found that they had similar efficacies (Howell *et al.*, 2004), but there remains much clinical interest in improving dosage/delivery of pure anti-oestrogens in order to achieve their maximal anti-oestrogenic potential in this setting (Howell *et al.*, 2004; Robertson *et al.*, 2007). Interestingly, faslodex does not cross the blood brain barrier so hot flushes associated with other anti-oestrogens are not observed. Also, as a pure anti-oestrogen, faslodex treatment results in none of the oestrogenic effects seen with SERM treatment, as such endometrial cancer and thrombosis for example. Equally, of course, it would be expected that there are no beneficial agonistic effects (bone density maintenance and decreased blood lipids), but to date clinical studies do not indicate any adverse effect on these parameters with this agent.

#### 1.1.3.1.2.1 Mechanism of faslodex action

As stated above, faslodex is a steroidal agent and is a 7 $\alpha$ -alkylsulphinyl analogue of E2 that acts as a potent competitive inhibitor of E2 binding to the ER. When faslodex binds to the ER there is a severe conformation change

(distinct from the change induced by either E2 or tamoxifen) which severely disrupts the protein along with both the AF-1 and AF-2 domains, due to the long faslodex sidechain. The change in conformation prevents Hsp loss and receptor dimerization and hence nuclear localisation. Retained in the cytoplasm, the half-life of the ER protein is greatly reduced resulting in proteasomal degradation of the ER, and hence a decrease in the total cellular levels of ER (Figure 1.7) (Dowsett *et al.*, 2005). Faslodex thus efficiently inhibits the transcription of ER-regulated genes which promote breast cancer proliferation, and modestly promotes apoptosis (Howell *et al.*, 2000). In addition to efficiently reducing the E2-induced expression of pS2 and progesterone receptor (PR), Ki67 (a proliferation marker) and the cell survival gene Bcl-2 are depleted to a greater extent than with tamoxifen (McClelland *et al.*, 1996; Howell *et al.*, 2000; Dowsett *et al.*, 2005). There is also evidence for changes in such genes alongside significant depletion of the ER $\alpha$  protein, from studies performed in clinical breast cancer samples taken prior to and during treatment with faslodex (Robertson *et al.*, 2007).

#### 1.1.3.2 Oestrogen deprivation

As stated, anti-oestrogens that competitively inhibit E2/ER $\alpha$  binding (along with additional catastrophic effects on ER $\alpha$  in the case of pure anti-oestrogens) comprise one class of anti-hormones valuable in breast cancer. However an alternative strategy is to inhibit E2 synthesis from androgens throughout the body and thus deplete breast cancer cells of their ligand input. The ethos



**Figure 1.6 Chemical structure of faslodex**

Shown is the chemical structure of faslodex, which is also known as ICI 182,780 and fulvestrant.

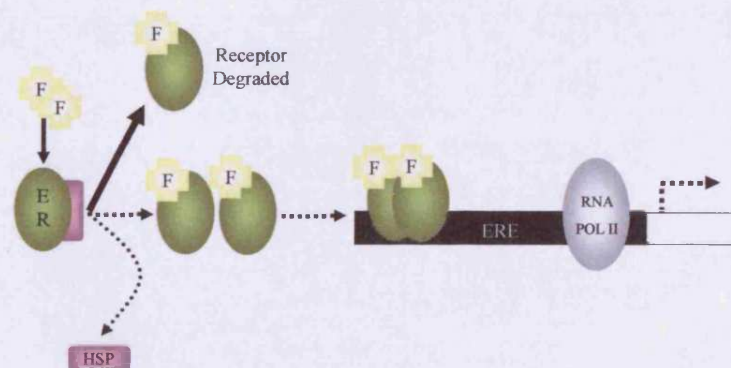


**Figure 1.7 Mechanism of faslodex action**

The diagram shows the mechanism of faslodex action. Faslodex binds to the ER and inhibits the displacement of Hsp, this is followed by the rapid degradation of ER. This results in decreased levels of faslodex:ER heterodimers and nuclear translocation, there is therefore reduced binding of faslodex occupied ER binding to ERE in the promoter region of E2 responsive genes resulting in reduced transcription. Adapted from Howell *et al* (2000).

behind such a strategy of E2 depletion aims to achieve a state of unoccupied ER $\alpha$  in breast cancer cells (with associated co-repressor recruitment), hence blocking ER-regulated transcription and thereby depleting growth. There are two strategies for E2 deprivation used in the treatment of breast cancer:

#### 1.1.3.2.1 Aromatase inhibitors

Following the very first studies with agents such as aminoglutethimide, third generation aromatase inhibitors (AIs) have now been developed to efficiently halt the synthesis of E2 from aromatisation of androgens through their selective targeting of the cytochrome P450 enzyme aromatase. While inappropriate for use in premenopausal patients, AIs are used in ER+ve postmenopausal breast cancer patients, where aromatase generates E2 in peripheral tissues and in the breast cancer itself despite the ovaries no longer producing E2. AIs subvert aromatase activity, dramatically lowering the levels of circulating E2 resulting in E2 deprivation and hence promoting a high level of unoccupied ER. This in turn means there is a reduced level of transcription of E2 regulated genes through the ER, resulting in an anti-proliferative effect (Johnston and Dowsett 2003). Since AIs act to remove E2 activity, there is no associated oestrogenic activity and so no increased risk of endometrial cancer or thrombosis. However there is an increased risk of joint disorders and fractures due to the lack of E2-like action on bone and equally, it remains to be seen if in long-term use AIs can adversely influence blood lipids. AIs can be separated into two main categories, type 1 or type 2.

Type 1 AIs are steroidal and considered to be aromatase inactivators. They are able to compete with androgen for binding to aromatase and once bound are metabolised into a reactive intermediate that irreversibly binds to the active site of the enzyme, thus inactivating the enzyme and profoundly suppressing oestrogen production. The main steroidal AI in current use is the third generation orally administered agent exemestane (Aromasin, Pfizer) (Johnston and Dowsett 2003). Exemestane has shown promise as both a first line and second line therapy following disease progression on other endocrine treatments in postmenopausal advanced ER+ve breast cancer. It is also emerging as valuable as an adjuvant treatment in primary breast cancer in postmenopausal patients, notably following 2-3 years of tamoxifen treatment (Coombes *et al.*, 2007).

The non steroidal type 2 AIs (where the prototype was aminoglutethimide) competitively and reversibly bind to the haem region of the aromatase enzyme reversibly blocking aromatase activity to again profoundly suppress oestrogen level (Carpenter and Miller 2005). The AIs anastrozole (Arimidex, AstraZeneca) and letrozole (Femara, Novartis) are both currently used in a clinical setting and are set to take over from tamoxifen as the gold standard treatment for breast cancer in ER+ve postmenopausal patients. Such agents are valuable in ER+ve postmenopausal advanced disease and when tamoxifen fails (Buzdar *et al.*, 1998). Moreover, several trials, notably the 'Arimidex, tamoxifen alone or in combination' (ATAC) clinical trial in breast cancer have revealed that such AIs are more effective than tamoxifen both in terms of

disease free survival and tolerability in the adjuvant postmenopausal setting (Baum *et al.*, 2003). As such, AIs are now approved as an alternative to, or following completion of, tamoxifen treatment (Buzdar 2004). Letrozole has also been licensed for use as a neoadjuvant therapy as it was more successful at shrinking tumours before surgery than tamoxifen (Carpenter and Miller 2005). Interestingly, there have been reports of a lack of cross resistance observed between the type 1 and type 2 AIs in advanced breast cancer following relapse (Lonning 2004).

#### 1.1.3.2.2 Luteinizing hormone-releasing hormone agonists

In premenopausal women, luteinizing hormone-releasing hormone (LH-RH) is produced by the hypothalamus, and via LH-RH receptors controls the secretion by the pituitary gland of follicle stimulating hormone (FSH) and luteinizing hormone (LH) which act on the ovaries to stimulate the synthesis of E2 by ovarian aromatases. The use of an LH-RH agonist results in an initial increase in FSH and LH, but this is followed by a substantial decrease in these gonadotrophins resulting in inhibition of ovarian aromatase activity and profound suppression of E2 level. LH-RH agonists are valuable in premenopausal breast cancer patients as they can reversibly reduce E2 levels equivalent to an ovariectomy (Spicer and Pike 2000). In the clinic the LH-RH agonist Zoladex (goserelin) has been used in premenopausal breast cancer patients both in primary and advanced ER+ve disease; it has also been used in combination with tamoxifen (Klijn *et al.*, 2001).



#### 1.1.4 Anti-hormone resistance & growth factor signalling

As described above, anti-hormones such as tamoxifen are of immense value in the management of ER+ve breast cancer. Unfortunately, however, along with all ER-ve patients, approximately 40% of ER+ve patients fail to respond to tamoxifen on presentation (*de novo* resistance), while many patients who do respond to tamoxifen eventually develop resistance (acquired resistance) and relapse, requiring further treatment options. Unfortunately, the development of tamoxifen resistance can also be associated with a more aggressive and invasive breast cancer phenotype in model systems (Hiscox *et al.*, 2004; Hiscox *et al.*, 2006a), while in the clinic relapse during treatment can be hallmarked by increased metastatic capacity and reduced patient survival, and *de novo* resistant ER+ve or ER-ve disease also has a poorer outlook (Platet *et al.*, 2004; Dunnwald *et al.*, 2007).

The molecular mechanisms underlying resistant growth and progression remain poorly defined, but in ER-ve disease aberrant growth factor signalling has been heavily-implicated. Equally, increased growth factor signalling has been linked to ER+ve *de novo* and acquired tamoxifen resistance, in this instance potentially cross-talking with the AF-1 domain of the retained ER, as demonstrated by several groups including our own (Schiff *et al.*, 2004; Shou *et al.*, 2004; Nicholson *et al.*, 2005; Britton *et al.*, 2006). In addition to acquired resistance to tamoxifen, *de novo* and acquired resistance is also noted with faslodex treatment or oestrogen deprivation, although the mechanisms underlying such events are less well characterised. Acquired faslodex

resistance has been studied *in vitro*, where in several laboratories faslodex resistant MCF-7 cells were found to have lost expression of the ER $\alpha$  protein and also have reduced levels of ER $\alpha$  mRNA, compared with faslodex sensitive MCF-7 cells. Continued exposure to faslodex *in vitro* ultimately promoted complete loss of ER gene expression (Sommer *et al.*, 2003; Nicholson *et al.*, 2005). *In vitro* studies of resistance to E2 deprivation from several groups have shown this can involve development of oestrogen hypersensitivity (Santen *et al.*, 2005b). In both instances, altered growth factor signalling has again been implicated in resistant growth (Sommer *et al.*, 2003; Nicholson *et al.*, 2005; Santen *et al.*, 2005b; Staka *et al.*, 2005).

Gene transfer studies, examination of *in vitro* and *in vivo de novo* and acquired resistant breast cancer models (McClelland *et al.*, 2001; Shou *et al.*, 2004; Nicholson *et al.*, 2005; Schiff *et al.*, 2005), and immunohistochemical analysis of clinical breast cancer material (Gee *et al.*, 2005) are cumulatively implicating several different growth factor ligands, their receptors and downstream elements in anti-hormone failure (Nicholson and Johnston 2005), but of particular prominence is the ErbB receptor family and its signalling.

#### 1.1.4.1 ErbB receptor signalling

EGFR (also termed ErbB1), was the first tyrosine kinase receptor to be characterised (Nahta *et al.*, 2003), and was found to be a member of a family of transmembrane tyrosine kinase receptors termed the ErbB receptors, a sub

family of the receptor tyrosine kinases (RTK). Other members of the ErbB family include ErbB2 (also termed Her2), ErbB3 and ErbB4 (Hynes and Lane 2005). EGFR has been reported to be expressed in 14 – 91% of breast cancers and had been linked to an aggressive tumour phenotype with increased potential for metastasis and invasiveness. EGFR positivity is associated with an increased risk of *de novo* resistance to tamoxifen, in part due to an inverse relationship between levels of ER and EGFR in breast cancer cells (Agrawal *et al.*, 2005). Also noted is the increased levels of Her2/EGFR signalling seen in clinical samples of *de novo* and acquired resistance to tamoxifen, along with ER-ve disease (Gee *et al.*, 2005). Additionally, overexpression of various ErbB ligands notably EGF, transforming growth factor alpha (TGF $\alpha$ ) and heregulins have also been implicated in resistance (Nicholson *et al.*, 1994; Shou *et al.*, 2004).

In our laboratory the levels of EGFR and Her2 in emerging tamoxifen resistant MCF-7 cells *in vitro* were found to be significantly increased over levels in parental MCF-7 cells, contributing to an increase in their growth rate, motility, and invasiveness (Hiscox *et al.*, 2004; Nicholson *et al.*, 2005). MCF-7 cells with acquired tamoxifen resistance also showed increased EGFR/Her2 heterodimerisation and phosphorylation (Knowlden *et al.*, 2003; Gee *et al.*, 2005). Increased levels of activated erk 1/2 MAP kinase (p-MAPK), a vital component of the plasma membrane to nucleus cascade for EGFR/HER2 signal transduction, were apparent in the tamoxifen resistant cell line, and have also been reported in the ~80% of ER+ve tamoxifen resistant tumours which also

displayed increased TGF- $\alpha$ /EGFR signalling (Gee *et al.*, 2001; Nicholson *et al.*, 2001). Increases in p-MAPK (Gee *et al.*, 2005) and in activity of further MAPK family members, such as p38 MAPK, have also been associated with acquired resistance in clinical breast cancer (Gutierrez *et al.*, 2005). Elevated phosphorylation of Akt was also apparent in the tamoxifen resistant MCF-7 cells compared with their parental cells. Akt is a serine/threonine kinase which is activated following stimulation of PI3K via RTKs such as ErbB receptors or G-protein coupled receptors. It has been linked to increased cell proliferation and cell survival. Both p-MAPK and Akt activity are elevated further in response to the EGFR ligands EGF and TGF $\alpha$  in acquired tamoxifen resistant cell lines, indicating that increased Akt activation is driven by the increased EGFR in tamoxifen resistance cells alongside the MAPK signalling pathway (Jordan *et al.*, 2004). We have shown that activated Akt and MAPK cross-talk with the AF-1 region of nuclear ER in tamoxifen resistant cells by phosphorylating residues Ser118 and Ser167. This in turn promotes co-activator recruitment to re-instate transcription of ER-regulated genes, including the EGFR ligand amphiregulin, to complete an EGFR autocrine growth signalling loop in tamoxifen resistant cells promoting their growth and invasion (Hiscox *et al.*, 2004; Britton *et al.*, 2006). In addition, ligand-independent promotion of the ER regulated gene IGF2 re-activates IGF-1R within tamoxifen resistant cells which further enhances EGFR signalling via a cross-talk mechanism involving c-Src (Knowlden *et al.*, 2005). Interestingly, increased levels of Akt, PI3K and MAPK activation, erbB receptors, IGF-1R and c-Src have also been implicated in resistance to oestrogen deprivation,

where there is again evidence of cross-talk with ER in either a genomic or non-genomic manner (Johnston and Dowsett 2003; Martin *et al.*, 2005b; Santen *et al.*, 2005b; Staka *et al.*, 2005). Finally, FASR cells can also exhibit increased EGFR that is again growth contributory (McClelland *et al.*, 2001).

#### 1.1.4.2 Inhibition of growth factor signalling in resistance & its limitations

The importance of EGFR signalling in tamoxifen resistant cells is evidenced by their increased growth sensitivity to the small molecule EGFR tyrosine kinase inhibitor (TKI) Gefitinib (Iressa, ZD1839) both *in vitro* and *in vivo* (Nicholson *et al.*, 2001; Knowlden *et al.*, 2003; Agrawal *et al.*, 2005; Schiff *et al.*, 2005). As such, EGFR blockade has been proposed for the treatment of anti-hormone resistance, and through clinical trials gefitinib has been shown to be of some value in acquired or *de novo* ER-ve, tamoxifen resistant breast cancer (Agrawal *et al.*, 2005; Johnston 2005a; Polychronis *et al.*, 2005). Further agents targeting aspects of the EGFR/HER2 autocrine signalling loop are also inhibitory in the resistant models and are entering clinical trials (Johnston 2006), including inhibitors of Her2 and other erbB family members (Agrawal *et al.*, 2005; Johnston and Leary 2006), their downstream kinases or IGF-1R (Gee *et al.*, 2005; Nicholson *et al.*, 2005). Such agents can also be inhibitory in further anti-hormone resistant models, including gefitinib in faslodex resistant MCF-7 cells (McClelland *et al.*, 2001), and inhibitors of Her2, MAPK, AKT or IGF-1R have been shown to be active in resistance to oestrogen deprivation (Martin *et al.*, 2005a; Santen *et al.*, 2005a; Staka *et al.*, 2005). However, in all

instances, resistance to the anti-growth factor therapy ultimately emerges and in some instances this can be associated with a further gain in aggressive cellular behaviour in model systems (Jones *et al.*, 2005). Emerging data indicate that resistance to these anti-growth factors, both *de novo* and acquired, is also a significant clinical problem (Johnston 2005b).

It is thus evident that while treating anti-hormonal resistant states with anti-growth factors may have some value, benefits are likely to be short-lived. As such, there remains a need to prevent (or significantly delay) the emergence of anti-hormonal resistance and its associated undesirable phenotype if significant improvements in patient survival are to be made. In order for there to be resistant cell growth following anti-hormonal therapy, there must be cells that initially evade growth inhibition during early response where these subsequently permit resistance and progression. Indeed, ER+ve breast cancer model systems reveal that while anti-hormones can exert anti-proliferative effects, they promote only modest cell kill (Gee *et al.*, 2003). These already identified growth factors include EGFR/Her2, which are increased in breast cancer cells and provide survival mechanisms during initial response. If the “protective” mechanisms that limit maximal response in anti-hormone-treated cells could be more fully deciphered and appropriately targeted alongside anti-hormones, resistance could potentially be subverted. While as yet largely unexplored, it is feasible that the phenomenon of oestrogen repression of gene expression is relevant for study in this context:

### 1.1.5 Molecular mechanisms for oestrogen repression of gene expression

It is known that as well as genes being induced by E2 treatment by the mechanisms outlined above (sections 1.1.2.1.2 to 1.1.2.1.4), genes can also be repressed by this ligand and in turn induced by anti-hormonal treatment. The extent of this phenomenon was demonstrated by Frasor *et al.*, showing that upon E2 challenge almost 70% of E2 regulated genes were repressed in an ER+ve breast cancer model (Frasor *et al.*, 2003). It was later shown by this group that these repressive events could be antagonised by anti-oestrogens leading to gene induction, most notably with the pure anti-oestrogen faslodex (Frasor *et al.*, 2004). With the knowledge that some of the E2 repressed genes are anti-proliferative and pro-apoptotic (Frasor *et al.*, 2004), some of the anti-oestrogen induced genes may contribute to mediating their inhibition of breast cancer growth, for example TGF $\beta$  (Frasor *et al.*, 2003). However, it is also plausible that the E2-occupied ER represses, while in turn the anti-oestrogen occupied ER induces, expression of further signalling genes that may be able to promote proliferation and cell survival. If identifiable, such genes may be key in limiting maximal anti-tumour activity of anti-oestrogens in ER+ve breast cancer cells, allowing residual proliferation and cell survival in the presence of the drug (and perhaps even promoting emergence of other features of progression). Such genes may provide potential targets for novel therapies to increase the effectiveness of anti-oestrogens.

The underlying biology of oestrogen repression is poorly understood, despite the surprisingly frequent oestrogen inhibitory effect on gene expression

reported (Zubairy and Oesterreich 2005). However, four molecular mechanisms by which E2 can repress gene expression have been implicated to date, where there is emerging evidence that these are reversible by anti-oestrogens:

#### 1.1.5.1 Competition for co-activators by the oestrogen-bound ER $\alpha$ complex

It is thought that Her2 gene expression is repressed by E2 through a 409 base pair region in the first intron of the Her2 gene that acts as an E2 suppressible enhancer in ER+ve breast cancer cells. Competition for the co-activator SRC-1 occurs between the E2:ER complex and AP-2 transcription factor. When ER is occupied by E2, the AF-2 domain of the receptor provides a strong binding site for SRC-1, activating the E2 suppressible enhancer of Her2. However in the presence of anti-oestrogen occupied ER, SRC-1 is free to bind to AP-2, an event that promotes transcription of the Her2 gene (Newman *et al.*, 2000). Furthermore, there is evidence of competition for p300/CBP co-activator family members between ligand-bound steroid receptors and Fos/Jun proteins during transrepression of AP-1 sites in some gene promoters (Kamei *et al.*, 1996).

#### 1.1.5.2 Recruitment of co-repressors by the oestrogen bound ER $\alpha$ complex

Although at odds with classical E2 action, there is some evidence that the E2:ER complex is able to recruit co-repressors to the promoter region of some genes, an event that may occur according to cell context. For example, it



appears that folate receptor expression is repressed in the presence of E2 occupied ER, where over-expression of the co-repressor SMRT enhances the repression seen with E2 (Kelley *et al.*, 2003). Repression has also been noted for the E-cadherin gene in the presence of E2, this time linked to the overexpression of the co-repressor scaffold attachment factor B1 (SAFB1) (Oesterreich *et al.*, 2003). Interestingly, both of these suppressive events with E2 were reversed by tamoxifen or faslodex (Kelley *et al.*, 2003; Oesterreich *et al.*, 2003). In addition to this, a recently discovered novel co-repressor DEAD box RNA helicase, termed DP97, has been shown to act in a ligand-dependent manner with nuclear receptors to repress gene expression. E2 triggers recruitment of DP97 to the promoter of the Her2 gene blocking its expression. In turn, silencing DP97 reduced E2 repression of Her2 expression (Rajendran *et al.*, 2003).

#### 1.1.5.3 ER $\alpha$ protein/protein interactions sequestering other transcription factors

An example of this mechanism is the repression of interleukin-6 (IL-6) expression which activates osteoclasts that promote bone resorption by the E2-bound ER through its interplay with NF $\kappa$ B and C/EBP $\beta$ . NF $\kappa$ B or C/EBP $\beta$  alone are strong activators of IL-6; however it appears that the DNA binding domain of ER can directly interact with the NF $\kappa$ B Rel domain and the C/EBP $\beta$  bZIP region, reducing IL-6 promoter activity which is key to regulating bone density (Stein and Yang 1995). Further examples of

protein/protein interactions between transcription factors and the E2 bound ER can be drawn from the bone morphogenic protein (BMP) signalling pathway. The E2 bound ER has been shown to repress BMP gene expression through its direct binding of the transcription factor Smad in breast cancer cells. In addition, E2 was found to suppress TGF $\beta$ -induced activation of Smad3 (Matsuda *et al.*, 2001). Both of these inhibitory effects of E2 were reversed by tamoxifen (Matsuda *et al.*, 2001; Yamamoto *et al.*, 2002).

#### 1.1.5.4 Role for ER $\beta$ in oestrogen mediated repression of gene expression

Although the idea that ER $\beta$  could contribute to E2 mediated repression of genes has not been addressed substantially, there are findings that point to such a mechanism (Zubairy and Oesterreich 2005). These include reports that in the presence of E2, ER $\beta$  binds to the co-repressors N-CoR and SMRT to suppress gene expression both *in vitro* and *in vivo*. It has also been shown that while in response to E2 the ER $\alpha$  can enhance transcription of some genes with an AP-1 site in their promoters (e.g. cyclin D1), E2-bound ER $\beta$  is able to repress such events. In turn, it was noted that anti-oestrogens enhanced AP-1 activity through ER $\beta$  (Webb *et al.*, 2003). Montano *et al.* (1998) have also observed that activity of a reporter for the quinone reductase gene promoter could be increased by anti-oestrogen treatment and repressed by E2, where ER $\beta$  was seen to be a stronger activator of the quinone reductase gene in the presence of anti-oestrogens than ER $\alpha$  (Montano *et al.*, 1998).

### **1.1.6 Proof of principle that E2 suppresses growth regulatory genes that increase on anti-oestrogen treatment: targeting potential of epidermal growth factor receptor**

Based on proof of principle data for the EGFR gene, it appears that targeting of oestrogen repressed genes alongside anti-hormonal agents has potential to enhance inhibition of proliferation and substantially induce apoptosis (Gee *et al.*, 2003; Nicholson *et al.*, 2005). If such mechanisms are also seen *in vivo*, combination strategies may improve initial response and delay/prevent resistance to anti-hormones. E2/ER signalling has been shown to suppress EGFR levels in ER+ve breast cancer cells *in vitro* (Yarden *et al.*, 2001). Although not well defined, this is thought to be due to a negative regulatory element found in the first intron of the EGFR gene in ER+ve cells (Wilson and Chrysogelos 2002). While the levels of EGFR protein in MCF-7 cells treated with E2 are decreased, anti-hormones modestly increase EGFR protein levels during the drug-responsive phase, particularly the anti-oestrogens tamoxifen or faslodex (McClelland *et al.*, 2001; Gee *et al.*, 2003). MCF-7 cells treated with anti-oestrogens exhibit residual ER activity that is driven by kinases downstream of the modestly increased EGFR. These kinases maintain some phosphorylation of ser118/167 on the ER. This residual ER activity leads to low levels of anti-apoptotic genes and hence some cell survival during anti-oestrogen treatment. This is paralleled by incomplete anti-tumour effects of tamoxifen, which results in a 35% decrease in proliferation and 15% induction of apoptosis, together accounting for approximately 50% inhibition of growth (Gee *et al.*, 2003). The incremental increases in EGFR seen with tamoxifen and

faslodex treatment reach a maximum by the time of acquisition of resistance, where EGFR signalling is thought to provide the dominant growth mechanism (McClelland *et al.*, 2001; Knowlden *et al.*, 2003) alongside its heterodimer partner Her2 which is also induced during anti-oestrogen treatment (Newman *et al.*, 2000).

EGFR therefore appears to provide proof of principle that the induction of E2-repressed signalling elements can be important in the mechanism for promoting growth and cell survival during endocrine therapy and for the subsequent emergence of resistance. In agreement with this, our group has shown that the EGFR TKI, gefitinib, when used in combination with tamoxifen or faslodex to block the early protective effect of anti-oestrogen-induced EGFR enhances *in vitro* anti-tumour effects of the use of the anti-oestrogens alone (Gee *et al.*, 2003; Okubo *et al.*, 2004). Shou *et al.* (2004) have investigated the *in vivo* effects of tamoxifen in combination with gefitinib in MCF-7 xenografts and similarly found that the combination significantly delayed emergence of resistance (Shou *et al.*, 2004). Anti-hormone/anti-ErbB combination therapies are currently under clinical investigation in breast cancer (Johnston 2005a; Johnston 2006). However, the use of gefitinib in combination with anti-oestrogens does not result in the complete abolishment of cell growth, and moreover has a more limited anti-tumour effect *in vitro* when combined with E2 deprivation (Gee *et al.*, 2006). EGFR/Her2 increases also only occur in a proportion of patients during tamoxifen treatment (Nicholson *et al.*, 2001; Gee *et al.*, 2005). Thus there must be further as yet undefined 'compensatory'

factors induced by anti-oestrogens or oestrogen deprivation. Identification of the breadth of these compensatory factors could provide superior therapies for breast cancer in combination with anti-hormones.

## 1.2 Microarrays

### 1.2.1 Technology overview

In 1995 Schena *et al.* published the first paper detailing gene expression profiling using microarrays (Schena *et al.*, 1995). This relatively recent emergence of microarray technologies, together with the sequencing of the human genome, permits the expression analysis of hundreds to tens of thousands of genes at one time. Essentially microarrays are the opposite of northern blotting, where instead of separating the sample mRNA on a gel and probing for a gene with a specific labelled cDNA probe, a large number of cDNA sequences are immobilized on a surface and a labelled mRNA sample is hybridised. This results in the possibility of expression profiling large numbers of genes in a single experiment and the ability to compare the gene expression profiles under two or more conditions, for example a normal versus disease state. At present there are several different types of microarrays available that can be divided into two main groups: microarrays where the detection sequences are pre-synthesised in the form of cDNA before being immobilized onto a support, and microarrays where the synthesis of oligonucleotides takes place *in situ* on the support (Lyons 2003).

### 1.2.1.1 cDNA microarrays

The cDNA microarray group consists of arrays which use cDNA immobilized on a suitable platform. The cDNA sequences on the arrays are pure PCR products generated from cDNA and expressed sequence tag (EST) clones using either gene specific or vector specific primers (Schulze and Downward 2001). Such microarrays can be further sub-grouped depending on the type of support platform and method of detection:

#### 1.2.1.1.1 Two colour microarrays

Two colour microarrays use cDNA sequences (ranging from 100-800 base pairs) immobilised onto poly-1-lysine coated glass microscope slides. It is possible to array 50,000 cDNA sequences onto a glass slide using a robotic ink-jet based printer or mechanical microspotter (Murphy 2002). Two colour arrays allow for the comparative analysis of two conditions on one microarray. With the use of fluorescent labelling, mRNA for the two different conditions are reverse transcribed in the presence of either cy3-dUPT or cy5-dUPT dyes, resulting in fluorescent cDNA. The two labelled cDNA samples are then mixed and hybridised to a microarray, with the resulting fluorescent signal captured using a confocal laser scanner. Microarray results from this type of experiment are generated in the form of ratios between the samples along with a colour coded image where yellow represents a no change in expression between the samples and red (cy3) or green (cy5) represent an induction or repression in expression respectively (Figure 1.8).

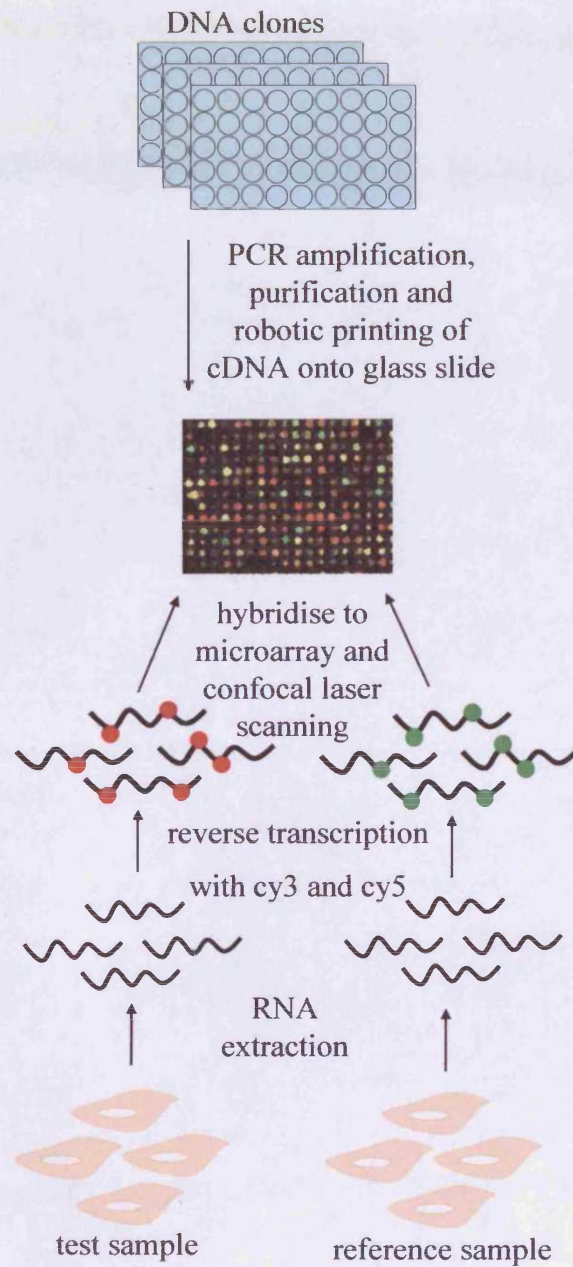


**Figure 1.8 Schematic of two colour microarray procedure**

The diagram shows an overview of the two colour microarray procedure. To generate the arrays, cDNA from DNA clones is robotically printed onto glass slides. RNA samples are extracted from a test and reference sample, the RNA is reverse transcribed in the presence of either cy3 or cy5 fluorescent label. The test and reference samples are then mixed and hybridised to the glass array. Following hybridisation the array is scanned by a confocal laser scanner at two different wavelengths to identify the cy3 and cy5 label.

#### 1.2.1.1.2 Nylon cDNA microarrays

These arrays comprise double stranded cDNAs (200-400 base pairs) immobilised on a nylon membrane. Nylon arrays are hybridized with mRNA from a sample which has been reverse transcribed to cDNA in the presence of radiolabelled nucleotides, typically  $^{32}\text{P}$  or  $^{33}\text{P}$ , which following hybridisation can be detected using autoradiography or phosphorimaging. Nylon cDNA arrays are sometimes referred to as macroarrays due to the generally lower density of genes represented (Figure 1.9).

#### 1.2.1.2 Oligonucleotide microarrays

Oligonucleotide arrays were first introduced by Affymetrix in 1996 (Lockhart *et al.*, 1996). Affymetrix arrays use short oligonucleotides (20-25mers) which are synthesised *in situ* by photolithography (Fodor *et al.*, 1991) onto a derivatized glass surface. This method makes it possible to produce high-density arrays with up to 250,000 spotted sequences on a  $1.28\text{cm}^2$  chip (Lipshutz *et al.*, 1999). Affymetrix 'Gene-Chips' are hybridised with biotinylated cRNA, which is reverse transcribed from mRNA of the sample under study using oligo-dT primers that contain the T7 polymerase promoter. The resulting sample cDNA is converted into double stranded DNA and this acts as a template to produce *in vitro* cRNA. The biotin labelled cRNA is stained by a streptavidin-phycoerythrin conjugate and detected using an Affymetrix microarray reader. To reduce cross-hybridisation and background levels and act as a control, Affymetrix Gene-Chips use mismatch pairs. Each gene is represented by 11 distinct pairs of oligonucleotides, where one of each



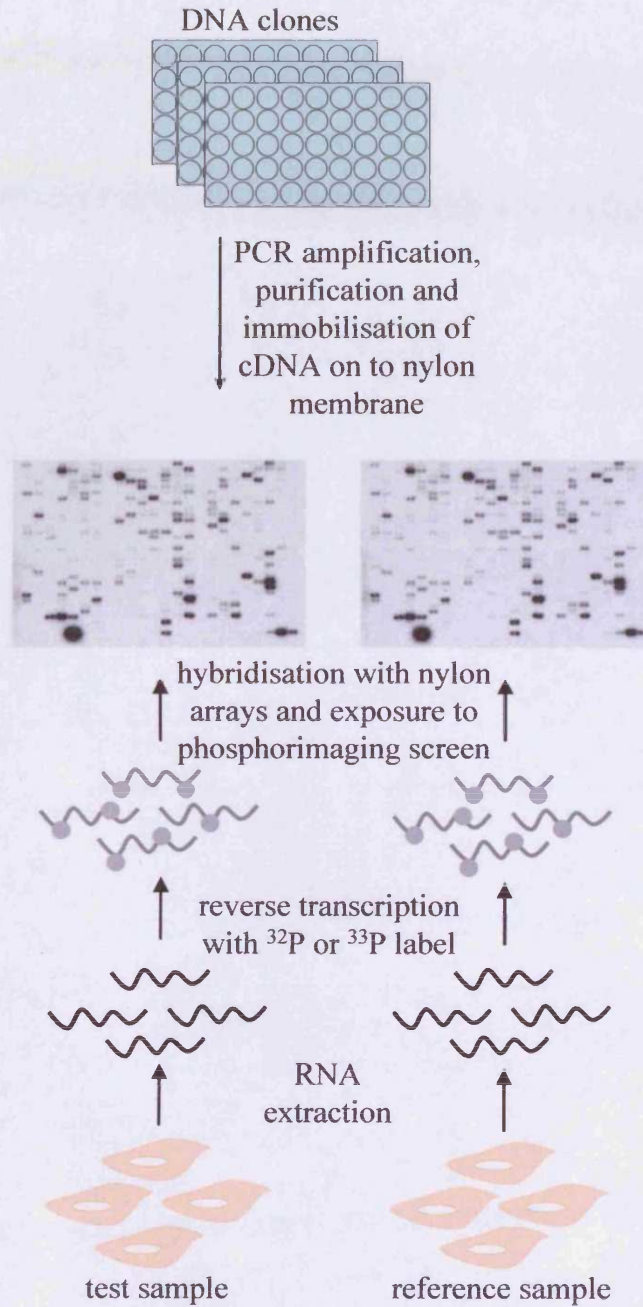


**Figure 1.9 Schematic of nylon microarray procedure**

Shown in the diagram is a schematic representation of the nylon microarray procedure. Arrays are generated by immobilising cDNA isolated from DNA clones onto a nylon membrane. RNA from test and reference samples is extracted and reverse transcribed in the presence of  $^{32}\text{P}$  or  $^{33}\text{P}$  radiolabelled nucleotides. Each sample is then hybridised to an array, following hybridisation the arrays are exposed to a phosphorimaging screen to generate an image for analysis.

pair is a 'perfect match' to the transcript sequence and the other has a change at the 13th base pair, making it a 'mismatch'. Since the development of the Affymetrix system, several other companies have developed similar systems including Amersham Life Sciences and Rosetta Inpharmatics. However, the oligonucleotides in these systems are not synthesised *in situ*, but pre-synthesised oligonucleotides are printed onto slides (Figure 1.10).

#### 1.2.1.3 Comparison of cDNA & oligonucleotide microarrays

There are several advantages and disadvantages associated with the use of the different arrays systems. The advantages of the two colour array system is that the equipment for producing arrays can be bought and used in house relatively inexpensively, along with the possibility of creating custom microarrays using cDNA libraries. However, due to the problem of differing efficiencies of dye incorporation, caused by the bulky dye molecules during reverse transcription, dye swap experiments need to be carried out using the test samples. Recent methods aim to overcome this by incorporating a tag during reverse transcription to which the dye molecule can be attached after reverse transcription has taken place.

Nylon arrays have the advantage of been commercially available from many companies that offer custom arrays and that they need no specialist equipment. Nylon arrays have been developed that allow researchers to focus on distinct gene groups, for example tumour-related sequences, avoiding the need for

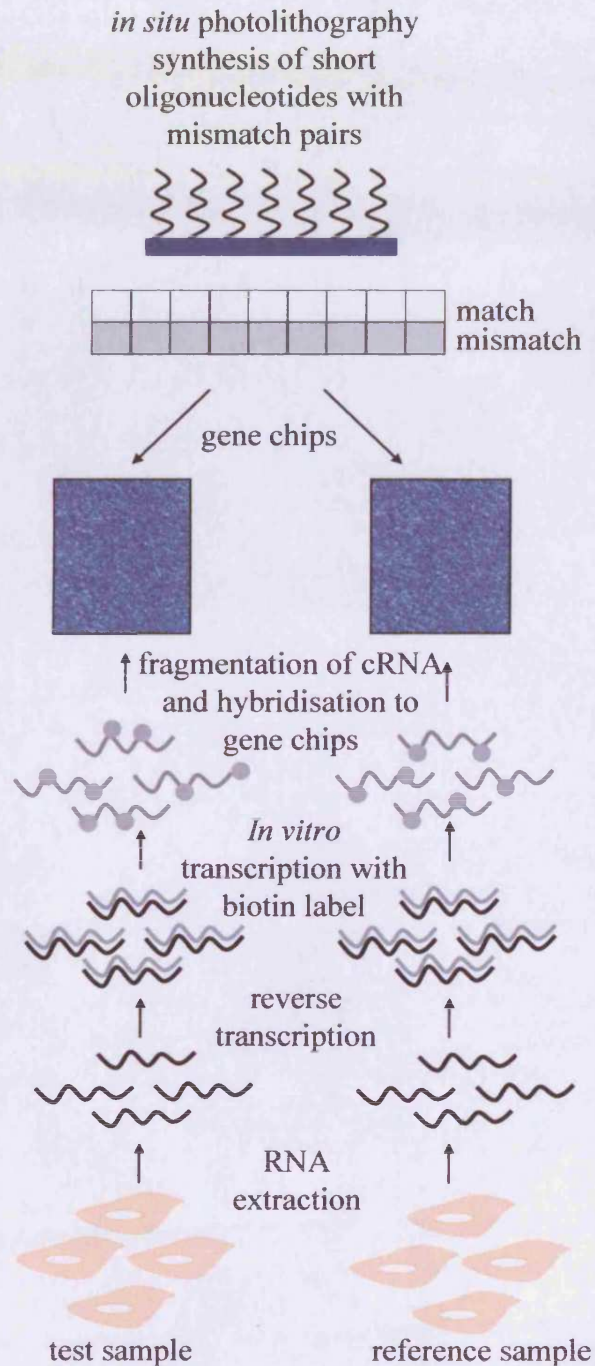


**Figure 1.10 Schematic of affymetrix microarray procedure**

Shown is a schematic representation of the affymetrix microarray procedure. The gene chip is generated by synthesising short oligonucleotides with match and mismatch pairs, *in situ* by photolithography onto a glass surface. RNA is extracted from test and reference samples and reverse transcribed. cDNA acts as a template for *in vitro* transcription with the incorporation of a biotin label. Each biotin labelled sample is hybridised to a gene chip, following hybridisation the signal is read with an Affymetrix microarray reader.

overly complex data analysis. Nylon arrays are also extremely cost effective as they can be stripped and re-probed, sometimes up to three or four times. However, nylon arrays are usually lower density and require careful analysis to avoid the known and accepted high background levels that are sometimes seen with this technique.

The main advantage of the Affymetrix system is the high level of specificity due to the perfect match/mismatch oligonucleotides. Oligonucleotides also have the advantage that they are all the same length and have very similar melting temperatures as well as C-G content, allowing for more consistent hybridisation conditions across the array. There are, however, several disadvantages, including chip cost, the need for expensive specialist equipment and the lack of custom arrays, as well as a requirement for more complex bioinformatics. While short oligonucleotides can also be less specific than longer cDNAs, the development of long oligonucleotides (50-100mers) has overcome this drawback (Schulze and Downward 2001).

### **1.3 Microarray technology in breast cancer research**

#### **1.3.1 Expression profiling in clinical samples**

In clinical breast cancer, arrays have been used to classify tumour types as reviewed by Cleator and Ashworth (Cleator and Ashworth 2004), as well as to begin to understand the impact of current therapies and signatures associated with drug resistance.

Three different array platforms have recently been used by Sorlie *et al.* (2001, 2006), to identify cell subtypes with distinct expression profiles that are present in clinical breast tumours. These include: luminal A, normal breast-like, Her2/neu-positive, and basal-like cell subtypes. The two main cell subtypes, luminal A and basal-like cells, have been shown to utilise the activation of different signalling pathways. Correlations between patient outcome and cell subtypes have also been noted with patients with luminal A cell containing tumours having a good prognosis, while women with basal-like cell tumours have a shorter disease-free and survival time (Sorlie *et al.*, 2001; Sorlie *et al.*, 2006). Similarly, West *et al.* (2001) analysed the expression profile of 49 primary breast cancers using Affymetrix GeneChips and found that the patterns of gene expression allowed for discrimination based on ER status and lymph node status (West *et al.*, 2001).

The possibility of using arrays as a predictive tool has also been investigated. Affymetrix GeneChips have been used to analyse the gene expression of 89 primary breast cancers and with approximately 90% accuracy predicted lymph node metastases and relapse (Huang *et al.*, 2003). van 't Veer *et al.* (2002) used two colour cDNA arrays representing 25,000 human genes to identify gene expression profiles associated with 'poor prognosis' (short interval to distant metastasis) and 'good prognosis' in 98 primary breast cancers. They concluded that gene expression profiling could be a powerful tool used to tailor treatment and reduce the number of lymph node negative patients unnecessarily treated with adjuvant chemotherapy (van 't Veer *et al.*, 2002). This has resulted in a

large randomised prospective MINDACT (microarray in node negative disease may avoid chemotherapy) trial using a 70 gene prognosis predictor signature. It is hoped that the gene signature can be used to select breast cancer patients that have a good prognosis and do not require adjuvant treatment and to identify gene signatures associated with optimal treatment strategies. Early indications show that the 70 gene signature is out-performing both the St. Gallen criteria and Nottingham prognostic index (NPI), however difficulties have arisen due to the need to use fresh frozen samples and the expertise required to hybridise samples to the prognostic arrays (Mauriac *et al.*, 2005; Bogaerts *et al.*, 2006; Gruvberger-Saal *et al.*, 2006). Importantly, only one study (Jansen *et al.*, 2005) has been carried out on clinical samples from patients who have developed anti-hormone resistance, primarily due to problems of sample collection. The study however, has shown that a 44 gene signature generated from an 18,000 gene cDNA array hybridised with tamoxifen responsive and resistant tumours, was able to predict response to anti-oestrogen therapy and time to disease progression in recurrent ER+ve breast cancers (Jansen *et al.*, 2005).

With respect to all clinical samples, the main problem associated with array studies stems from the notable heterogeneity of samples. Thus, as well as containing breast cancer cells, specimens can also contain varying levels of normal breast, stroma, lymphocytes and blood vessels which clearly will impact on the expression profiles observed. It is therefore preferable to employ microdissection to maximise the breast cancer cell content of samples (Cooper 2001).

Significantly, as well as looking at the overall expression profile of clinical samples, arrays have been employed to identify individual novel genes that may be contributory to a particular cancer phenotype. For example, Finlin *et al.* (2001) identified, using two colour cDNA arrays and 78 primary breast tumours, the unique gene RERG (ras-related and oestrogen-regulated growth inhibitor) which is thought to act as a negative growth regulator. The expression of this gene was found to be decreased or lost in primary breast cancers with poor prognosis, whilst high expression levels correlated with the less aggressive ER+ve tumour subgroup. The gene was subsequently shown to be an E2-induced and tamoxifen repressed gene in MCF-7 breast cancer cells (Finlin *et al.*, 2001). RERG over-expression in MCF-7 cells resulted in decreased tumour formation in nude mice and inhibited anchorage dependent and independent growth *in vitro* (Finlin *et al.*, 2001).

### 1.3.2 Microarrays in breast cancer cell lines & models systems

Arrays have been used to investigate overall gene expression patterns and to reveal individual genes associated with breast cancer growth and progression in several breast cancer cell model systems (Perou *et al.*, 1999; Ross *et al.*, 2000; Wang *et al.*, 2005; Kim *et al.*, 2006; Villeneuve *et al.*, 2006; Milde-Langosch *et al.*, 2007). Cell model systems are especially valuable in the study of drug treatment effects and resistance mechanisms due to the lack of equivalent clinical samples. They have the additional advantage of using homogenous populations of cells and as such have been used to study the effects of E2 and

anti-oestrogens on breast cancer growth. Importantly, publications are emerging that show array studies performed in models can reveal E2-regulated gene signatures of clinical relevance (Oh *et al.*, 2006).

Research into E2 responsive genes (and in turn impact of anti-oestrogens) has been carried out using various array platforms and breast cancer cell lines. For example, gene expression of ER+ve MCF-7 cells in the presence and absence of E2 was examined using custom two-colour 9000 cDNA gene arrays (Inoue *et al.*, 2002). The result of this study was the selection of 138 E2-responsive genes and the creation of custom cDNA arrays for these genes to monitor a time course of E2 treatment and anti-oestrogen treatment. This led to the identification of a series of novel E2-responsive genes that could identify early and late responses. Importantly, faslodex suppressed many of the E2 induced genes suggesting that the E2 induction indeed takes place through an ER-dependent mechanism. However the extent of suppression seen with tamoxifen was not as great as that seen with faslodex, probably relating to its known mixed agonistic/antagonistic activity (Inoue *et al.*, 2002). Novel genes which were direct targets of E2 during its growth promotion have also been revealed in a study of the ZR-75 breast cancer cell line treated with cyclohexamide, in this instance using Affymetrix GeneChips (Soulez and Parker 2001). The E2-induced genes could be divided into sub-groups according to their function, i.e. genes involved in proliferation (Tob, IGFBP4, IEX-1 and cyclin D1), adhesion/migration (Gap alpha 1) and enzymes involved in cell metabolism (G6PD and the cyt family), including cytochrome P450 gene which was the



most E2-sensitive gene in this model (Soulez and Parker 2001). Similarly, another study, using high-density two colour oligonucleotide arrays with ER+ve T47D cells has identified 89 genes that are direct ER targets (Lin *et al.*, 2004), while other E2-regulated genes have been identified with 8400 gene two colour cDNA microarrays in ZR-75 cells. In the latter instance, E2 treatment resulted in the differential expression of 344 genes which following hierarchical clustering fell into 8 clusters, three of which showed transient induction patterns related to the cell cycle, while two contained genes which showed continued activation by E2 up to 32 hours (Cicatiello *et al.*, 2004). The identification of early oestrogen-responsive genes by two colour microarrays has also been studied in ER+ve MCF-7 cells treated with E2 for between 0 - 48 hours (Wang *et al.*, 2004). This revealed eight previously unknown early oestrogen-induced genes, including EEIG1, which was suppressed by anti-hormone treatment in MCF-7 cells and was not expressed in an ER-ve breast cancer cell line (Wang *et al.*, 2004). Affymetrix arrays have also been used to select oestrogen-induced genes involved in breast cancer growth of three ER+ve cell lines (Rae *et al.*, 2005), and these identified GREB1 which was found to be induced by E2 in all three cell lines but not by tamoxifen or faslodex. Significantly, suppression of GREB1 was subsequently found to reduce E2 stimulated growth of the cell lines studied (Rae *et al.*, 2005).

Finally, several groups are also attempting to study gene expression changes that may underlie differences between anti-oestrogens. Among these, Levensen *et al.* (2002) have attempted to classify different types of anti-oestrogens

(including SERMs and pure anti-oestrogen) based on their gene expression profiles using Clontech nylon cDNA arrays for 588 genes (Levenson *et al.*, 2002). A more recent study has also been carried out by Scafoglio *et al.* (2006) investigating the gene expression profiles of E2 in the presence of either tamoxifen, faslodex or raloxifen. Expression profiles revealed that there was no clear-cut distinction between the treatments, with all showing agonistic and antagonistic actions (Scafoglio *et al.*, 2006).

It is noteworthy that in general, research in experimental models has tended to focus on identifying genes induced by E2 which are likely to promote growth and in turn whose repression could contribute to growth inhibitory response with anti-oestrogens. The exception to this is the study of Frasor *et al.* (2003, 2004) who identified, using Affymetrix gene chips, that substantial E2-repression of gene expression also exists. Such E2 associated gene repression and its reversal by anti-hormones is the subject of this thesis.

#### **1.4 Project Aims**

The aim of this project is to identify, using array technology, genes induced by anti-oestrogens (tamoxifen and faslodex) in breast cancer cells that may exert an early protective effect during treatment. It is hypothesised that such genes may allow a subset of cells to escape the pro-apoptotic and anti-proliferative effects of anti-hormonal treatments and thereby limit initial anti-tumour response and facilitate eventual development of resistance. Equally, some of

the drug-induced genes may contribute to the gain of further adverse features, notably invasive capacity that is subsequently maximised in the resistant state.

Using commercially available Clontech Nylon 1.2 Cancer arrays, genes will be identified that are induced by both a tamoxifen and faslodex-occupied ER compared to either an unoccupied ER (untreated control) and/or E2-occupied ER (E2 treated) in MCF-7 ER+ve breast cancer cells. Once candidate anti-oestrogen induced adverse genes have been selected following profiling and in depth ontological investigation, their array profiles will be verified using RT-PCR both on the original RNA and using an independent validation set of RNA. This approach will aid in the robust identification of genes differentially affected by anti-oestrogen-occupied ER versus unoccupied and E2 occupied ER, and will further clarify if the changes observed are generic or drug-specific. Where possible the protein products of these genes will then be investigated by immunocytochemistry and/or Western blotting in the presence or absence of the anti-hormone treatments or E2 treatment in MCF-7 cells. Such studies will be extended, where feasible, to MCF-7 cells that have acquired tamoxifen or faslodex resistance to address whether the gene changes observed are transient, or persist into (and may be supportive of) the resistant state. Functional and inhibitor studies will also be carried out on the drug-induced genes of most interest.

The goal of this project is to identify new therapeutic targets which may ultimately be inhibited alongside anti-hormonal treatments to delay or prevent the emergence of endocrine resistant growth.

Chapter 2  
~ **Materials and Methods** ~

## **2 Materials and Methods**

### **2.1 Materials and equipment**

Shown in Table 2.1 are the general reagents, chemicals, materials and equipment, along with their suppliers used throughout this project. Table 2.2 shows the antibodies used in this study along with their source and supplier.

**Table 2.1 Materials, Reagents, Equipment and Their Suppliers**

Detailed in this table are the materials, reagent and equipment that were used throughout this project in combination with the relevant supplier.

Product	Supplier
TransAM™ NFκB Family Transcription Factor Assay Kit	Active Motif, Rixensart, Belgium
<sup>32</sup> P labelled dCTP (10μCi/μl) <sup>32</sup> P labelled dATP(10μCi/μl) dNTPs G50 microspin columns Random hexamers Rainbow marker (10-250kDa)	Amersham Biosciences UK Ltd., Little Chalfont, England
Fulvestrant (faslodex, ICI 182,780) Iressa (Gefitinib, ZD1839)	AstraZeneca, Cheshire, UK
Bromophenol blue Glass cover slips (number 2, 22mm <sup>2</sup> )	BDH Chemicals Ltd, Poole, UK
BIOTAQ® DNA Polymerase Hyperladder IV	Biogenex, California, USA
Agarose	Bioline, London, UK
DC Protein Assay kit Cuvettes	BioRad Laboratories, Hemel Hempstead, UK
Atlas™ Human Cancer 1.2 Arrays Atlas™Image 2.7 ExpressHyb NucleoSpin Extraction Columns	Clontech (Takara Bio Inc.), California, USA
3,3'-diaminobenzidine tetrahydrochloride (EnVision DAB) EnVision secondary antibodies mouse anti-rabbit and rabbit anti-mouse antibody	DAKO, Cambridgeshire, UK
Eppendorf tubes	Elkay Laboratory Products Ltd, Basingstoke, UK
Acetone Cell scraper Choloroform Ethanol Formaldehyde Glycerol Hydrochloric acid (HCl) Isopropanol Methanol Xylene	Fisher Scientific, Loughborough, UK
MXB Autoradiography Film (blue sensitive 18cm x 24cm)	Genetic Research Instrumentation (GRI), Rayne, UK

RPMI 1640 medium Phenol-red free RPMI 1640 medium L-glutamine Penicillin/streptomycin Gentamycin Fungizone Dulbecco's phosphate buffered saline (PBS) Trypsin	Gibco Invitrogen Corporation, Paisley, UK
Normal human serum (NHS)	Golden West Biologicals Inc. California, USA
Custom primers	MWG Biotechnology, London, UK
Plasticware 12-24 well plates 60mm, 100mm, 150mm dishes 25cm <sup>2</sup> , 75cm <sup>2</sup> flasks 25ml universal containers 15ml, 50ml Falcon tubes 5ml bijoux tubes 5ml, 10ml, 200µl, 10µl tips	Nunc Invitrogen Corporation, Paisley, UK
Perbio Chemiluminescent Supersignal® West Pico, Dura and Femto Antibody detection systems	Pierce and Warriner Ltd, Cheshire, UK
Luciferase Assay system with reporter lysis buffer MMLV Prime-a-gene labelling system Recombinant RNasin® Ribonuclease inhibitor	Promega UK Ltd., Southampton, UK
RNeasy Mini Kit	Qiagen, Crawley, UK
Western Blocking reagent Herceptin (Transtuzumab)	Roche Diagnostics, Mannheim, Germany
Coulter counter cups and lids	Sarstedt AG and Co., Nümbrecht, Germany
Nitrocellulose membrane BA 85 (0.45µM) Nytran 0.45 nylon membrane Turboblotter	Schleicher and Schuell, Dussell, Germany
4-Hydroxytamoxifen (tamoxifen, ICI 46474) 17-β oestradiol (E2) Bovine serum albumin (BSA) C <sub>0</sub> t-1 DNA Dimethyl sulphide (DMSO) Ethylenediaminetetraacetic acid (EDTA)	Sigma-Aldrich, Dorset, UK

Ethylene glycol-bis (2-aminoethylether)-N,N,N',N' tetraacetic acid (EGTA) Foetal calf serum (FCS) Glycine dithiothreitol (DTT) 3-(N-morpholino) propanesulfonic acid (MOPS) N,N,N,N tetramethylethylenediamine (TEMED) Potassium chloride RNA loading buffer Sheared salmon testes DNA Sodium chloride (NaCl) Sodium dodecyl sulphate (SDS) Sodium molybdate (Na <sub>2</sub> MoO <sub>4</sub> ) Trisodium citrate Triton X-100 Trizma base Trizma-HCl Tween 20 TRI reagent Ethidium bromide Potassium chloride Magnesium chloride Tris-base Acetic acid Methyl green 5-bromo-4-chloro-3-indolyl-β-D- Galactopyranoside (X-Gal) 30% Acrylamide/Bis-acrylimide (29:1)	Sigma-Aldrich, Dorset, UK (cont.)
Filter paper (No. 4) Filter paper (grade 3, 460 x 370mm)	Whatman, Maidstone, UK
Developer (X-0-dev) Fixer (X-0-fix)	X-0-graph Imaging System, Tetbury, UK



**Table 2.2 Antibodies and Suppliers**

Shown are the antibodies that were used throughout this project along with their animal source and supplier.

<b>Antibody</b>	<b>Source</b>	<b>Supplier</b>
14-3-3 zeta (C-16)	Rabbit polyclonal	Santa Cruz Biotechnology (California)
$\beta$ -actin	Mouse monoclonal	Santa Cruz Biotechnology (California)
Bag-1	Mouse monoclonal	Chemicon International (California)
Delta catenin (C-20)	Goat polyclonal	Santa Cruz Biotechnology (California)
Hif-1 $\alpha$	Mouse monoclonal	BD Transduction Laboratories
NDR	Mouse monoclonal	Abnova Corporation (Taiwan)
NFkB p105/p50	Rabbit polyclonal	Cell Signaling Technology
NME3	Mouse polyclonal	Abnova Corporation (Taiwan)
RhoE	Mouse monoclonal	Upstate Cell Signaling Solutions (New York)

## 2.2 Cell Culture

The cell culture in this section was kindly performed by the Tenovus tissue culture staff.

The following media were used throughout the study:

Phenol red RPMI + 5% foetal calf serum (FCS): RPMI 1640 medium supplemented with whole foetal calf serum (5% v/v), penicillin/streptomycin (10 U/ml-10µg/ml), fungizone (2.5µg/ml) and L-glutamine (200µM).

Phenol red free RPMI + 5% stripped foetal calf serum (SFCS): phenol red free RPMI 1640 medium supplemented with charcoal stripped foetal calf serum (5% v/v), penicillin/streptomycin (10 U/ml-10µg/ml), 1ml fungizone (2.5µg/ml) and L-glutamine (200µM).

### 2.2.1 Routine Maintenance and Passaging of MCF-7 cells

All preparative work was carried out in a vertical circulating air class II biological safety cabinet (MDH Intermed Airflow, Bioquell, Andover, UK) under sterile conditions. The cultures were maintained in a BB16 Function Line incubator (Hanau, Germany).

MCF-7 cells (gift from AstraZeneca Pharmaceuticals) were grown as a monolayer in 75cm<sup>2</sup> flasks with phenol red RPMI + 5% FCS in a humidified atmosphere with 5% CO<sub>2</sub> at 37°C. The phenol red RPMI + 5% FCS was

renewed every 3 to 4 days. When approximately 70% confluency was reached the cells were passaged. To passage the cells they were incubated at 37°C with 5mls bovine trypsin (0.05% w/v) and EDTA (0.02% w/v) solution for 3 to 5 minutes, to detach the cells from the flask. The cells were subsequently transferred to a sterile universal container and the flask was washed out once with medium, this was then added to the universal container. The cells were pelleted at 168 x g for 5 minutes, the supernatant removed and the cells re-suspended in fresh medium. The cell solution was split and one tenth was used to re-seed (routinely at  $2 \times 10^5$  cells/cm<sup>2</sup>) each sterile flask which was incubated at 37°C with 5% CO<sub>2</sub> until required for experiments.

### **2.2.2 Experimental medium**

Due to the unwanted oestrogenic properties of the phenol red pH indicator present in standard RPMI medium and the presence of oestrogenic steroids in FCS, all cells for experimental purposes were grown in the presence of phenol red free RPMI media containing SFCS for 24 hours before the commencement of and for the subsequent duration of cell culture experiments. SFCS was prepared from foetal calf serum (FCS) by the following procedure. Norit A (charcoal, 11.1%) and Dextran C (0.06%) were diluted in distilled water to create a charcoal/dextran solution; this was then stirred vigorously for 1 hour. Meanwhile the pH of FCS was altered to 4.2 using 5M HCL, allowing it to equilibrate for 30 minutes at 4°C. To each 100ml aliquot of FCS, 5ml of charcoal/dextran solution (5% v/v) was then added. The mixture was incubated

at 4°C for 16 hours with gentle agitation. Following this the solution was centrifuged for 40 minutes at 12,000 x g and the supernatant removed and filtered with Whatman No 4 filter paper to remove trace charcoal. The pH was readjusted to 7.2 and the media sterilized by filtration through a 0.2µM membrane filter Supor Vacucap 60, which removed impurities and any contaminating micro-organisms.

### **2.2.3 Development of a tamoxifen and faslodex resistant cell line**

The tamoxifen and faslodex resistant cell lines were developed by continuously exposing parental MCF-7 cells to phenol red free RPMI + 5% SFCS supplemented with either tamoxifen (100nM, in ethanol carrier) or faslodex (100nM, in ethanol carrier) for a period of six months. The cells were passaged as necessary. The tamoxifen or faslodex supplemented media inhibited cell growth for the first two months, however, following this period the growth rate slowly increased to that of parental MCF-7 cells grown in non-supplemented medium. Once this growth rate was reached, the tamoxifen resistant MCF-7 (TAM-R) and faslodex resistant (FAS-R) cell lines were cultured for several months still in the presence of anti-oestrogens before experimental work took place.

## 2.3 RNA Extraction

### 2.3.1 Cell culture for RNA extraction

MCF-7 cells were seeded onto culture dishes (150mm) at a density of  $2 \times 10^5$  per  $\text{cm}^2$  in phenol red free RPMI + 5% SFCS. After 24 hours the following treatments were added to the media:

- Control (ethanol carrier)
- Oestradiol ( $10^{-9}\text{M}$  in ethanol carrier [0.05%])
- Tamoxifen ( $10^{-7}\text{M}$  in ethanol carrier [0.05%])
- Faslodex ( $10^{-7}\text{M}$  in ethanol carrier [0.05%])

The cells were maintained at  $37^\circ\text{C}$  in 5%  $\text{CO}_2$  and the media changed every 4 days. Cells were harvested after 4, 7 or 10 days growth for RNA isolation. This procedure was repeated to produce four full sets of independent replicates. Material from three of these sets was used in array hybridisations, one of which was also used for the initial RT-PCR profiling and the fourth for further RT-PCR validation.

### 2.3.2 Tri-Reagent extraction

Prior to RNA extraction the medium was removed and the cell monolayer washed with 5ml PBS, this was aspirated off and the commercial RNA extraction solution, Tri-Reagent (1ml per  $100\text{mm}^2$ ) was added to the plate. A sterile cell scraper was subsequently used to remove all of the cells from the bottom of the plate and the suspension was then transferred to 2ml

microcentrifuge tubes. At this point the cells were stored at  $-80^{\circ}\text{C}$  for a maximum of a month. On removal from the  $-80^{\circ}\text{C}$  freezer, cell lysates were allowed to thaw and then left for a further 5 minutes at room temperature. Chloroform ( $200\mu\text{l}$  per 1ml of Tri-Reagent used in lysis) was added to each of the samples which were then shaken vigorously for 15 seconds and left at room temperature for 15 minutes. Samples were centrifuged at  $12,000 \times g$  for 5 minutes at  $4^{\circ}\text{C}$ . The mixture separated into 3 distinct layers, an upper aqueous phase containing RNA, the interphase layer containing DNA and the lower organic phase containing protein. The upper aqueous phase was removed to a sterile microcentrifuge tube, taking care not to disturb the interphase layer and hence contaminate the RNA with DNA. To this aqueous phase, isopropanol ( $500\mu\text{l}$  per 1ml of initial Tri-Reagent) was added, mixed and allowed to stand at room temperature for 10 minutes. The samples were vortexed and microcentrifuged at  $12,000 \times g$  for 10 minutes at  $4^{\circ}\text{C}$ , forming a pellet on the side of the tube. The supernatant was carefully removed and the pellet washed with ethanol (75% v/v made up with sterile RNase/DNase free  $\text{H}_2\text{O}$ , using 1ml per 1ml Tri-Reagent used in lysis) prior to vortexing and then microcentrifugation at  $7500 \times g$  for 5 minutes at  $4^{\circ}\text{C}$ . The supernatant was carefully removed and the pellet air-dried for 10 minutes. The RNA pellet was finally re-dissolved in sterile, RNase/DNase free  $\text{H}_2\text{O}$  ( $25\mu\text{l}$  per 1ml of initial Tri-Reagent) and stored at  $-80^{\circ}\text{C}$  until required.

### 2.3.2.1 Measurement of total RNA concentration

The concentration and purity of the RNA was determined using a spectrophotometer (CECIL 2000 series, Cambridge UK). The RNA was diluted 1/500 in sterile H<sub>2</sub>O and the absorbance measured at two wavelengths; A<sub>260</sub>nm and A<sub>280</sub>nm. The concentration of the RNA (µg/ml) was calculated by multiplying the absorbance at 260nm by the extinction coefficient of single stranded RNA which is 40µg/ml and the dilution factor, i.e.

$$\text{RNA conc}^n (\mu\text{g/ml}) = [\text{A}_{260\text{nm}}] \times [\text{dilution factor}] \times [\text{extinction coefficient}]$$

Furthermore, the A<sub>260</sub>nm:A<sub>280</sub>nm ratio gives an indication of the purity of the RNA; a desired ratio of between 1.8 and 2.0 was required.

### 2.3.2.2 Agarose gel electrophoresis of total RNA

Gel electrophoresis was performed using a 2% agarose gel made with 1 x TAE (Tris-acetate [40mM], EDTA [1mM], at pH 8.0) and ethidium bromide solution (stock 10mg/ml) to give a final concentration of 0.2mg/ml. The gel was placed in Sub-Cell Agarose Electrophoresis System (Biorad laboratories, Ltd, Hemel Hempstead, UK) apparatus and submerged in 1 x TAE buffer. The gel was loaded with 1µg of RNA sample diluted five times with loading buffer which comprised of sucrose (40%) and bromophenol blue (BPB; 0.25% w/v) made up in sterile pure water. The gel was run at 70v until the BPB dye front had progressed to two thirds the length of the gel. The RNA was visualised on a UV trans-illuminator (FotoDyne Incorporation, USA) to check the integrity of the RNA.

### 2.3.3 DNase Treatment and RNA purification

The RNA samples to be hybridised with the arrays were DNase treated to remove any genomic contamination. To a final volume of 200µl in sterile RNase/DNase free H<sub>2</sub>O, 100µg of RNA was incubated with 20µl 10 x DNase buffer and 10µl DNase I (1 unit/µl), for 30 minutes at 37°C. The RNA was re-extracted and purified using RNeasy columns according to the manufacturer's instructions. The RNA was eluted in 50µl RNase/DNase free H<sub>2</sub>O and stored at -80°C until required. The post-DNase treated concentration and purity was assessed by spectrophotometry and its integrity by gel electrophoresis as stated previously.

## 2.4 Northern Blotting

Primers used to produce cDNA for northern blotting:

pS2 forward primer: 5'-CATGGAGAACAAGGTGATCTG-3'

pS2 reverse primer: 5'-CAGAAGCGTGTCTGAGGTGTC-3'

β-Actin forward primer: 5'-GGAGCAATGATCTTGATCTT-3'

β-Actin reverse primer: 5'-CCTTCCTGGCATGGAGTCCT-3'

### 2.4.1 Use of ionising radiation

Ionising radiation was used in accordance with the Ionising Radiations Regulations 1999 (IRR99) and Radioactive substances Act 1993 (RSA93).



Appropriate training was carried out before using radiation. Use of radiation was limited to restricted areas and local rules were followed.

#### **2.4.2 Formaldehyde Gel Electrophoresis**

1.2g of agarose was dissolved in 84.6ml sterile RNase/DNase free H<sub>2</sub>O, 5.4ml formaldehyde (0.66M, 37%), 10ml 10 x MOPS (0.4M MOPS, 0.1M Sodium acetate, 0.01M EDTA). The agarose gel was allowed to cool slightly before adding 2µl ethidium bromide solution (stock 10mg/ml) and the gel cast. Once the gel had solidified it was equilibrated by immersion in 1 x MOPS for 15 minutes. Samples of RNA (15µg) were dried under vacuum centrifugation (Savant DNA 120 SpeedVac) and resuspended by vortexing in 10µl of RNA loading buffer. The samples were then denatured by heating to 65°C for 10 minutes to ensure RNA was single stranded, placed on ice for 2 minutes and then pulse microcentrifuged and loaded onto the formaldehyde-agarose gel. Electrophoresis was performed at 150v for approximately 2 hours, the gel was subsequently immersed 3 times for 5 minutes in sterile RNase/DNase free H<sub>2</sub>O to remove formaldehyde. The RNA was transferred from the gel onto Nytran 0.45 nylon membrane in 20 x SSC (3M NaCl, 0.3M trisodium citrate) by passive blotting using turboblotter. The RNA was cross-linked to the membrane by exposure to UV light for 10 minutes. The position of the wells and RNA marker bands was marked on the membrane and a photograph was taken of the gel and ruler using a polaroid DS-34 camera and polaroid 665 positive/negative black and white film (Polaroid Corporation, Cambridge, UK);

this enable the positions and size of subsequent bands to be determined from the autoradiograph. The membrane was sealed in saran wrap and stored at  $-20^{\circ}\text{C}$  until use.

### 2.4.3 Probe Production

Northern blot membranes were probed for pS2 and  $\beta$ -Actin using Promega Prime-a-Gene kit according to manufacturers instructions. 25ng of each cDNA probe (generated by RT-PCR section 2.7) was added to sterile  $\text{H}_2\text{O}$  to make a volume of  $30\mu\text{l}$ . The cDNA probe was denatured at  $100^{\circ}\text{C}$  for 5 minutes, and chilled on ice for 2 minutes. To the denatured probe  $2\mu\text{l}$  unlabelled dNTPs (20mM each),  $2\mu\text{l}$  nuclease free BSA ( $400\mu\text{g}/\text{ml}$ ),  $5\mu\text{l}$   $\alpha^{32}\text{P}$  dCTP ( $10\mu\text{Ci}/\mu\text{l}$ ),  $1\mu\text{l}$  DNA polymerase I ( $100\text{u}/\text{ml}$ ) and  $10\mu\text{l}$  of labelling buffer were added and the samples incubated at room temperature for 60 minutes. Unincorporated nucleotides were removed by microcentrifugation through a G50 microspin column and then the purified probe placed on ice until required.

### 2.4.4 Hybridization

The northern blot membranes were pre-hybridized in 15ml commercially prepared hybridisation fluid (ExpressHyb) with  $140\mu\text{l}$  denatured sheared salmon testes DNA (stock:  $10\text{mg}/\text{ml}$ ) by rotation in a hybridisation oven (Techne, UK) for 30 minutes at  $65^{\circ}\text{C}$ . To the labelled probe,  $5\mu\text{l}$   $\text{C}_{\text{ot}}\text{-1}$  DNA,  $15\mu\text{l}$  sheared salmon testes DNA (stock:  $10\text{mg}/\text{ml}$ ),  $50\mu\text{l}$   $20 \times \text{SSC}$ , and  $105\mu\text{l}$  sterile  $\text{H}_2\text{O}$  were added. The probe mix was added to the pre-hybridization

solution and membranes were rotated in a hybridization oven (Techne, UK) overnight at 65°C.

After hybridization, the northern blot membranes were washed twice with a solution of 1 x SSC, SDS (1%) and then once with a solution of 0.1 x SSC, SDS (0.1%), each for 20 minutes at 65°C. The levels of radioactivity were monitored using a hand Geiger counter. The membranes were sealed in Saran wrap and placed into autoradiography film cassettes with intensifying screens and used to expose autoradiography film at -80°C for the length of time predicted by the Geiger counter (24 hours - 72 hours). The films were processed using an X-O-graph compact X2 film developer (X-O-graph imaging systems Ltd, Gloucestershire, UK) and bands scanned using a GS-700 densitometer (Biorad Laboratories, Hercules, USA).

#### **2.4.5 Removal of Radioactivity from Membranes**

After acceptable film images had been obtained from labelled membranes it was possible to reuse membranes. The residual radiolabelled probe was removed by immersing the membrane in SDS (0.1%) at 100°C for 10 minutes. The hand Geiger counter was used to check that radioactivity had been removed; the membranes were also used to expose autoradiography film which confirmed this. Membranes were then stored at -20°C until they were re-probed.

## 2.5 cDNA Atlas Array Procedure

### 2.5.1 Probe Synthesis from Total RNA

A master mix was made up using the following reagents (all included in the Atlas Expression array kit except radioactivity); 4 $\mu$ l 5 x reaction buffer (250mM Tris HCl pH 8.3, 375mM KCl, 15mM MgCl<sub>2</sub>), 2 $\mu$ l 10 x dNTP mix (5mM each dCTP, dGTP, dTTP), 1 $\mu$ l DTT (100mM), and 5 $\mu$ l  $\alpha^{32}$ P dATP (10 $\mu$ Ci/ $\mu$ l) for each labelling reaction. The RNA was reverse transcribed using a thermo cycler (Biometra PCR machine) by incubating 7 $\mu$ g sample RNA with 2 $\mu$ l CDS primers (a mixture of forward and reverse primer sequences specific to each of the 1184 genes represented on the array) at 70°C for 2 minutes to denature. The temperature was then reduced to 50°C for 2 minutes, during which time 2 $\mu$ l reverse transcriptase enzyme moloney murine leukemia virus (200 units/ $\mu$ l, MMLV) was added to the master mix. The master mix (13 $\mu$ l) was then added to each RNA/CDS primer sample and incubated for 25 minutes at 50°C.

### 2.5.2 Column Chromatography

Removal of unincorporated nucleotides from the above reaction was then performed. All reagents, buffers and columns involved were included in the NucleoSpin Extraction Kit and used according to manufacturer's instructions. The probe synthesis reaction was diluted to a final volume of 200 $\mu$ l with NT2 buffer. The samples were placed onto NucleoSpin Extraction Spin columns and microcentrifuged at 11,000 x g for 1 minute. The supernatant was discarded,

and 400µl of NT3 buffer was added to each column and the sample was microcentrifuged at 11,000 x g for 1 minute. This was repeated twice more to ensure all unincorporated nucleotides were removed. To elute the cleaned probe, 100µl of NE buffer was added to each column and allowed to stand for 2 minutes before centrifugation at 11,000 x g for 1 minute. The eluted probe was kept on ice until hybridization. The radioactive levels of the probe were monitored using the Geiger hand counter.

### **2.5.3 Pre-hybridization of nylon arrays**

30ml ExpressHyb solution was preheated to 68°C. 280µl sheared salmon testes (stock: 10mg/ml) DNA was denatured by heating to 100°C for 5 minutes then chilled on ice for 2 minutes before mixing with the ExpressHyb solution. The arrays were secured within the hybridization bottles (Techne, UK) by filling the bottles with distilled H<sub>2</sub>O and inserting the arrays, then pouring off the H<sub>2</sub>O making sure there was no overlap of membranes. This ensured that the arrays adhered to the inside wall of the hybridisation bottles without any air pockets. Immediately 7ml of pre-hybridization solution (ExpressHyb and sheared salmon testes DNA) was added to the bottles, and they were rotated in a hybridisation oven at 68°C for at least 30 minutes.

### **2.5.4 Hybridization**

11µl 10x denaturing solution (1M NaOH, 10mM EDTA) was added to the purified probe and incubated at 68°C for 20 minutes. 5µl C<sub>0</sub>t-1 DNA and 115µl

2x neutralizing solution (1M NaH<sub>2</sub>PO<sub>4</sub>) was added to the denatured probe and incubated for a further 10 minutes at 68°C. The denatured probe (~230µl) was then added directly to the pre-hybridization solution and the arrays rotated overnight at 68°C.

### 2.5.5 Washing

After hybridization the arrays were washed twice in low stringency washing solution 1 (2x SSC, 1% SDS) at 68°C for 30 minutes and the levels of radioactivity checked using the hand Geiger counter. If the residual signal was approximately 10 counts per second (CPS) and appeared to be localized, no further washing was performed; otherwise a further wash was performed with washing solution 1 at 68°C for 30 minutes. If there was still an apparent non-specific background level of radioactivity a high stringency wash was performed with washing solution 2 (0.1x SSC, 0.5% SDS) at 68°C for 5 minutes. The arrays were then sealed in plastic film, taking care to remove all air bubbles and wrinkles, and placed in a β-shielded autoradiography cassette with a phosphorimaging screen (Amersham, Little Chalfont, UK) for the amount of time indicated by the radioactivity of the arrays using a Geiger counter. After this time the phosphorimaging screen was scanned with the phosphorimager (Typhoon, Amersham, Little Chalfont, UK) to produce an image with densitometric information.

### **2.5.6 Stripping Arrays for Re-hybridization**

Following successful phosphorimage capture, arrays were stripped for reuse. To remove the radioactivity from the arrays they were incubated at 100°C in SDS (0.05%) for 10 minutes. They were then checked with the Geiger counter, wrapped in plastic and placed with autoradiography film overnight at -80°C to check all radioactivity (and probe) was removed. The arrays were stored at -20°C until re-probing. Arrays were stripped and reused a maximum of three times.

## **2.6 Array Analysis**

### **2.6.1 AtlasImage 2.7™**

To analyse the arrays, densitometric values reflecting hybridisation signal intensity were needed for each 'spot' on the arrays. AtlasImage 2.7™ software is affiliated with the Clontech 1.2 cancer arrays, which allows for spot alignment and basic analysis. The phosphorimage produced from the arrays was opened in AtlasImage and the appropriate template aligned with the spots. The background calculation varied for each spot depending on the signal; there were three different background calculations in AtlasImage and the most appropriate was selected to calculate the background:

1. Default External: the background is calculated as the median intensity of the blank areas of the arrays. This was suitable for arrays that had low, even background.

2. Custom External: the background was calculated as the median intensity of a user defined area. This was suitable if the background was uneven as it allowed the selection of an appropriate area of background.
3. Local: the background was calculated based on the median intensity of the space directly surrounding the gene spot. This method was useful if there was signal bleed from a neighbouring spot, but it could not be used for genes which produced an intense signal that bled into the surrounding area, as this would result in an underestimation of the signal intensity.

The densitometric value was exported from AtlasImage as a text file to be used for further software analysis.

### **2.6.2 GeneSifter™**

GeneSifter is a web-based array analysis software programme. GeneSifter was used after the arrays had been aligned in AtlasImage. A densitometric value for each gene on each array was uploaded into GeneSifter for analysis.

#### **2.6.2.1 Normalisation and log transformation**

Log transformation and normalisation took place prior to all array analysis. Log transformation within GeneSifter is carried out by  $\text{Log}_2$ ; this gave the data a more normal distribution for analysis. The data was also median normalised, normalisation of the array data meant that differences in intensities not due to



time point or treatment were minimised. These differences could be due to differences in labelling efficiency, hybridisation/washing and image exposure. Median normalisation is a two round normalisation. The first step is to divide the intensity of each gene by the median of all the genes on each array, followed by step two, where the intensity for each gene is divided by the median of the same gene on all the arrays. This resulted in one log transformed, normalised intensity for each gene on each array.

#### 2.6.2.2 Box plots and Scatter plots

Box plots were generated in GeneSifter which encompassed all the array data over the three time points and four treatments. Scatter plots were also generated by comparing one of the treatment array replicate sets to the untreated control array set. The mean log of the replicates was plotted against each other to produce a log-log scatter plot.

#### 2.6.2.3 Pairwise comparison

Pairwise analysis was used to identify genes expressed (mRNA) differentially between two groups of data. The results were a list of genes up and down regulated between the two conditions. The method was used to produce lists of genes up regulated at least 1.5 fold between all the treatments, at the three time points. These lists were subsequently manually combined to identify genes up regulated by just one treatment, two treatments or even three treatments compared to the other.

#### 2.6.2.4 Hierarchical clustering

Hierarchical clustering was carried out across data from the relevant treatments. The hierarchical clustering output was in the form of a heatmap with associated tree diagram.

#### 2.6.2.5 Statistical Array Analysis

During the initial selection for array genes induced at least 1.5 fold there were no statistical tests applied to maximise the amount of genes selected.

### 2.7 Semi quantitative RT-PCR

#### 2.7.1 Reverse Transcription (RT)

The RT-master mix was prepared to synthesise first strand complementary DNA (cDNA) from total RNA with the following reagents; random hexamers (10 $\mu$ M), 0.625mM of each deoxy nucleotide triphosphate (dNTPs), 1 x PCR buffer (Tris-HCL; 10mM pH 8.3, potassium chloride [KCl]; 50mM), magnesium chloride (MgCl<sub>2</sub>; 1.5mM), gelatine (0.001% v/v) and DTT (0.01M) with 1 $\mu$ g RNA in 7 $\mu$ l of sterile RNase/DNase free H<sub>2</sub>O. This reaction mix was denatured at 95°C for 5 minutes followed by cooling on ice. After this, reverse transcriptase enzyme MMLV (200 units) and Recombinant RNasin ribonuclease inhibitor (25 units) were added to give a final volume of 20 $\mu$ l. The Reaction mix was incubated at 22°C for 10 minutes (annealing), and then at 42°C the RT extension took place for 40 minutes. To terminate the reaction

the mix was incubated at 95°C for 5 minutes. The cDNA samples produced by this process were stored at -20°C until required.

### **2.7.2 Semi-Quantitative Polymerase chain reaction (PCR)**

The reverse transcribed cDNA samples were subsequently subject to semi-quantitative PCR using the primers and optimised cycle numbers shown in Table 2.3.  $\beta$ -actin expression was used as an internal control and for normalisation purposes. A 'master mix' was made with the following reagents; sterile RNA/DNase free H<sub>2</sub>O, 1 x PCR buffer, dNTPs (200 $\mu$ M), Taq DNA polymerase enzyme (2 units), forward primers (0.5 $\mu$ M), reverse primers (0.5 $\mu$ M) and if a co-amplification was to be performed then  $\beta$ -actin forward and reverse primers (0.125 $\mu$ M) were also added. A total volume of 24.5 $\mu$ l, i.e. 24 $\mu$ l of 'master mix' and 0.5 $\mu$ l of sample cDNA (equivalent to 0.025 $\mu$ g), was used to perform amplification. Amplification took place in a PTC-100 thermocycler (Genetic Research Instrumentation Ltd, Essex, UK), using the following parameters shown in Table 2.4. 5 $\mu$ l of PCR product was visualised on a 2% agarose gel (see section 2.3.2.2) alongside a 100bp DNA marker ladder.

**Table 2.3 Primer sequences, cycle number, annealing temperature and size**

Shown in Table 2.3 are the forward and reverse primer sequences, cycle number, annealing temperature and product size for the genes that were validated.

Gene	Forward Sequence (5'→3')	Reverse Sequence (5'→3')	Cycles/ Annealing	Size (bp)
14-3-3 $\zeta$ ^	GAGAAAATTGAGACG GAGCTAAGAG	AGCCACCTCAAGATG AAAACAGATAAC	25/55°C	707
$\beta$ -Actin	GGAGCAATGATCTTG ATCTT	CCTTCCTGGCATGGA GTCCT	Up to 28/55°C	204
$\beta$ -Actin (large)	CTACGTCGCCCTGGA CTTCGAGC	GATGGAGCCGCCGAT CCACACGG	Up to 28/55°C	385
Amphiregulin *	GGACTTTTCCCCACA GGTC	TCCTCGGAGACATGA C	29/55°C	350
Bag-1 *	AATGAGAAGCACGAC CTTCATGTTACC	GGATTCCAGTAAGCT CTTTATTCAACTC	28/55°C	319
CD59 *	CTGTCTTCTGCCATTC AGGTCATAGC	GGTGTGACTTAGGG ATGGCTCC	25/55°C	347
$\delta$ -catenin ^	CAGCTTCACCTCGGG AAATGATCAG	ACCTGGTTGTGTTTG ATGTCTTCAGC	28/55°C	119
Dvl-1 *	TCACCATCGCCAATG CCGTCATCG	TGGAGCCACTGTTGA GGTTCAGGG	28/55°C	228
Hif-1 $\alpha$ *	TCACCACAGGACAGT ACAGGATGC	CCAGCAAAGTTAAAG CATCAGGTTCC	25/55°C	303
NDR ^	ATTCGTGCGGAGCGT GACATTCTAG	AGAGTCTATGGCTAA TACTGTTTCTGC	28/55°C	207
NF $\kappa$ B *	CCTACGATGGAACCA CACCCCTGC	TCCACCAGCTCTCTG ACTGTACCC	28/55°C	475
NME3 ^	GCGGCTGGTGGGCGA GATTGTG	GGTTCGTGGCTCCGA TGAGCGC	28/55°C	233
Rac1 *	GACGGAGCTGTAGGT AAAACCTGC	CAAATGATGCAGGAC TCACAAGGG	28/55°C	241
Rac2 *	GCAAGACCTGCCTTC TCATCAGC	CTCGATGGTGTCCCTT GTCGTCCC	28/55°C	205
RhoC *	AGGTCCGCAAGAACA AGCGTCG	CGGGGCTAGAAAACA ATGCAGTCC	25/55°C	196
RhoE *	GAATAGAGTTGAGCC TGTGGGACAC	GAGCATTCGATATAA GTAGCTGCTCC	28/55°C	325

\* run as co amplification with actin 204 base pairs

^ run as co-amplification with large actin 385 base pairs

**Table 2.4 Polymerase chain reaction programme**

Shown is the standard PCR programme, the number of cycles (n) and annealing temperature\* were optimised for each set of primers used.

PCR Program			
Cycle 1	Denaturing	95°C	120 seconds
	Annealing	55°C	60 seconds
	Extension	75°C	300 seconds
Cycle 2 (x n)	Denaturing	95°C	60 seconds
	Annealing	55-60°C*	30 seconds
	Extension	72°C	60 seconds
Cycle 3	Denaturing	94°C	60 seconds
	Annealing	55°C	60 seconds
	Extension	60°C	300 seconds
	Finish	4°C	∞

## 2.8 Protein isolation

### 2.8.1 Cell Culture for western blotting

In order to obtain whole cell lysate, cells cultured as a monolayer were resuspended by trypsinisation and seeded onto 60mm dishes ( $\sim 1 \times 10^5$  cells/dish) and allowed to adhere to the dishes for 24 hours before the standard medium was replaced with experimental media containing either:

- Control (ethanol carrier)
- Oestradiol ( $10^{-9}$ M in ethanol carrier [0.05%])
- Tamoxifen ( $10^{-7}$ M in ethanol carrier [0.05%])
- Faslodex ( $10^{-7}$ M in ethanol carrier [0.05%])

Cells were grown for 7 days before lysis took place, with media being replenished on day 4.

To investigate protein levels in resistant cell lines, TAM-R, FAS-R and parental MCF-7 cells were seeded onto 60mm dishes ( $\sim 1 \times 10^5$  cells/dish) in phenol red free RPMI + 5% SFCS in the presence of tamoxifen or faslodex where appropriate. Cells were grown until approximately 70% confluency was reached, with the media being replaced every 4 days.

### 2.8.2 Cell lysis

After 7 days of treatment or when confluency was reached, the medium was removed and the dishes were washed three times with PBS, this was removed by aspiration. 250 $\mu$ l of ice cold lysis buffer [Tris (hydroxymethyl) aminomethane (Trizma) base (50mM), Ethyleneglycol-*bis*( $\beta$ -aminoethyl)-N,N,N',N'-tetraacetic Acid (EGTA; 5mM), sodium chloride (NaCl; 150mM), Triton X 100 (1% v/v), distilled water, pH 7.5 with a cocktail of protease and phosphatase inhibitors added to give a final concentration of sodium orthovanadate (Na<sub>3</sub>VO<sub>4</sub>; 2mM), sodium fluoride (NaF; 200mM), phenylmethyl sulfonylfluoride (PMSF; 1mM), phenylarsine oxide (20 $\mu$ M), sodium molybdate (10mM), leupeptin (10 $\mu$ g/ml), aprotinin (10 $\mu$ g/ml)] was then added to each of the dishes and the cells removed from the surface of the dish using a cell scraper. The dishes were subsequently incubated on ice for 10 minutes before the cell lysates were transferred into microcentrifuge tubes and microcentrifuged at 14,000 x g for 15 minutes at 4°C. The supernatant was removed, aliquoted and stored at -20°C until required.

### 2.8.2.1 Lowry Protein Concentration Assay

The protein content in each cell lysate was determined by the Lowry method (1951) using the BioRad protein assay according to manufacturer's instructions. All samples were prepared in disposable spectrophotometry cuvettes. In brief, a standard curve of known concentrations (0, 0.25, 0.5, 0.75, 1.0 and 1.45 mg/ml) of bovine serum albumin (BSA) was created using 50µl of lysis buffer (see section 2.8.2) in duplicate. The protein samples (12.5µl) were diluted in lysis buffer (37.5µl). To each of the BSA standards and diluted lysates proteins, 250µl Reagent A (containing 5µl reagent S for detergent compatibility) and 2ml of reagent B was added. After mixing the colour was allowed to develop at room temperature for a minimum of 15 minutes before the optical density was read at 750nm on a spectrophotometer (CECIL 2000 series). A standard curve was produced from the BSA standard concentrations and the concentrations of the unknown proteins deduced from this.

## 2.9 Sodium Dodecyl Sulphate - Polyacrylamide Gel

### Electrophoresis (SDS-PAGE)

SDS-PAGE was carried out using a Mini-Protein Slab II Electrophoresis Cell (BioRad Labs) as per manufacturer's directions. The resolving gel (7.5% acrylamide, 375mM lower buffer (pH8.8), 0.1% (v/w) SDS, 0.1% (w/v) APS and 70µM TEMED) and stacking gel (5% acrylamide, 125mM upper buffer (pH6.8), 0.1% (v/w) SDS, 0.05% (v/w) APS, 116µM TEMED) were prepared as described in Table 2.5. The lower resolving gel was pipetted into the

assembled plates to within 1.5cm of the top of the inner glass plate and water layered above this to eliminate air bubbles. The gel was allowed to polymerise for approximately 30 minutes. When set the water was removed, an upper stacking gel was pipetted on top of the resolving gel and a well-forming comb was immediately inserted into the stacking gel. Following polymerisation of the stacking gel, the gels were submerged in an electrophoresis tank containing 1 x running buffer (final concentration: 250mM Trizma base, 2M glycine, 40mM SDS, in distilled water, pH 8.3) and the combs were removed. The protein samples (20-40µg) were combined with the same volume of 2 x Laemmli loading buffer comprising of SDS (4% v/v), glycerol (0.4% v/v), Tris-HCL (120 mM pH 6.8), bromophenol blue (BPB); (0.01% w/v), DTT (1.54% w/v) and distilled water; the samples were heat denatured at 100°C for 10 minutes. The samples were loaded onto the gel along with a rainbow protein marker set (5µl, 10-250kDa). Electrophoresis was carried out at 150 volts until the BPB dye front reached the bottom of the gel.

Table 2.5 Resolving and stacking gel components

Shown in the table are the components that make up the resolving and stacking gel of polyacrylamide gels

Gel component	7.5% (w/v) Resolving gel	5% (w/v) Stacking gel
dH <sub>2</sub> O	4.8ml	6.1ml
0.5M upper buffer	-	2.5ml
1.5M lower buffer	2.5ml	-
Acrylamide (30%)	2.5ml	1.25ml
10% (w/v) APS	100µl	100µl
10% (w/v) SDS	100µl	50µl
TEMED	6µl	10µl



## 2.10 Western Blotting

The Trans-Blot Electrophoretic Transfer cell (Bio-Rad) apparatus was used according to manufacturer's instructions to carry out western blotting. Transfer buffer (0.2M glycine, 25mM Trizma base, 20% (v/v) methanol and distilled water, pH8.3) was used to soak a nitrocellulose membrane (0.45 $\mu$ m), two pieces of Whatman filter paper (grade 3) and two transfer blot fibre pads, all cut to the size of the gel. The proteins separated in the gel were transferred onto a nitrocellulose membrane by placing it in a transfer cassette in the following order: fibre pad, filter paper, gel, nitrocellulose membrane, filter paper, fibre pad. The cassette was placed in a transfer tank which contained transfer buffer and an ice block. Transfer was achieved electrophoretically by passing an electric current through the cassette for 1 hour at 100 volts.

After transfer the membranes were incubated in the protein stain, Ponceau S, to check the transfer had been a success and that equivalent amounts of protein had been loaded. Membranes were briefly immersed in Ponceau S solution (Ponceau S; 1% w/v made up in 5% v/v acetic acid in water) until the protein bands were visible, to remove the stain the membranes were washed three times for 5 minutes with Tris buffered saline buffer (TBS)-Tween (0.05% v/v) [Trizma base (10mM) pH 7.6, NaCl, (100mM), Tween 20 (0.05% v/v)]. Following this the nitrocellulose membranes were immersed in a 5% w/v solution of non-fat dried milk made up in TBS-Tween (0.05% v/v) at room temperature for 1 hour on a platform rocker STR6 (Stuart Scientific Bibby Sterilin Ltd, Stone, UK) to prevent non-specific antibody binding. Specific

antibodies to proteins of interest (Table 2.6) were then used to probe the membrane. The primary antibodies were diluted in 5% v/v Western Blocking Reagent in TBS Tween (0.05% v/v) and incubated with the membrane for an appropriate length of time (primary antibody concentrations and duration of incubations are shown in Table 2.7). After incubation with the primary antibody the membrane was washed with TBS-Tween (0.05% v/v) for three x 5 minutes before incubation with the secondary IgG horse radish peroxidase labelled antibody (see Table 2.7), diluted 1/10,000 in Western Block Reagent (5% v/v)/TBS Tween (0.05% v/v), which took place for 1 hour on a rocking platform at room temperature.

### **2.10.1 Detection and analysis**

After incubation with the secondary antibody the membrane was washed for 5 minutes in TBS-Tween (0.05% v/v) and the process repeated 4 more times. The washed membrane was placed into a plastic folder where a chemiluminescent substrate was applied for 5 minutes. Three substrates were used: Femto, for maximal signal enhancement; Dura, for moderate signal enhancement and Pico for less intense signal enhancement. The plastic folder including the membrane was placed into an autoradiography cassette and used to expose an autoradiography film until a satisfactory exposure level had been obtained (usually between 1-60 minutes). An X-O-graph compact X2 film developer was then used to develop the film. Densitometry results were obtained by scanning the film with a BioRad GS-690 Imaging Densitometer.

**Table 2.6 Primary antibody concentrations and durations of incubations**

Shown in the table are the antibodies used for western blotting, along with the concentrations and secondary antibody used. Also shown is the expected size of band and the detection conditions used.

Primary antibody	Concentration	Duration	Secondary antibody	Size	Detection
14-3-3 zeta	1:2000	Overnight 4°C	Anti-rabbit	30kDa	Pico 1:1 10 minutes
β-actin	1:10,000	Overnight 4°C	Anti-mouse	42kDa	Dura 1:1 10 seconds
NFκB p50/p105	1:1000	Overnight 4°C	Anti-rabbit	50kDa 105kDa	Dura 1:1 30 seconds
RhoE	1:1000	Overnight 4°C	Anti-mouse	29kDa	Femto 1:1 10 seconds

## 2.11 Immunocytochemistry

### 2.11.1 Optimisation

The ICC procedure for each protein under investigation was optimised to give the best staining results. For each antibody, several different antigen retrieval methods and primary antibody concentrations were used. Unfortunately RhoE did not give satisfactory results with pellet cell arrays and antigen retrieval, therefore a coverslip assay was performed with optimisation of fixation method and primary antibody concentration. Additionally, it was not possible to optimise ICC conditions for Hif-1α even after two different antibodies and many different antigen retrievals. The following sections detail the successfully optimised ICC procedures used for each primary antibody.

### 2.11.2 RhoE Coverslip assay

#### 2.11.2.1 Coverslip cell culture

70% confluent MCF-7 cells were trypsinised, removed from the flask and re-suspended in phenol red free RPMI + 5% SFCS. The cells were subsequently seeded onto 22mm<sup>2</sup> 3-aminopropyltriethoxysilane (APES)-coated glass coverslips (~8 x 10<sup>4</sup> cells/coverslip) contained in 35mm culture dishes. Cells were allowed to adhere to the coverslips for 24 hours before the following treatments were added in phenol red free RPMI + 5% SFCS:

- Control (ethanol carrier)
- Oestradiol (10<sup>-9</sup>M in ethanol carrier [0.05%])
- Tamoxifen (10<sup>-7</sup>M in ethanol carrier [0.05%])
- Faslodex (10<sup>-7</sup>M in ethanol carrier [0.05%])

The media was replenished on day 4 and the cells were fixed for immunocytochemistry after 7 days.

#### 2.11.2.2 Paraformaldehyde/vanadate fix for RhoE

The experimental medium was removed from the culture dishes and replaced with 2% paraformaldehyde/vanadate (PFV). The PFV was prepared by dissolving paraformaldehyde (0.25g) in PBS (3ml) with gentle agitation and heating at 60°C. The solution was cleared by the addition of 10µl NaOH (1M) followed by 9.5ml PBS. Finally 10µl HCl (1M) was added before the pH was adjusted to 7.4. Immediately prior to fixation, 2% sodium orthovanadate

( $\text{NaVO}_4$ , 100mM) was added. The cells were fixed in the PFV for 20 minutes before being washed three times for 5 minutes with PBS. The coverslips were stored in sucrose storage medium at  $-20^\circ\text{C}$ . The use of coverslips and PFV fixation procedure was for the detection of RhoE only.

### 2.11.2.3 RhoE ICC Assay

The coverslips were removed from sucrose storage solution and washed twice for 5 minutes in PBS. Blocking to prevent non-specific binding was performed using PBS-Tween (0.02% v/v) for 3 minutes before the primary RhoE antibody, diluted 1:100 in PBS, was applied and incubated overnight at room temperature. Coverslips were then washed three times for 3 minutes in PBS, followed by a PBS-Tween (0.02% v/v) rinse. The appropriate (primary antibody specific) enVision peroxidase labelled polymer secondary antibody was subsequently applied for 1 hour before the coverslips were again washed three times for 3 minutes with PBS. Coverslips were rinsed with PBS-Tween (0.02% v/v) before the addition of  $10\mu\text{l}$  diaminobenzidine tetrahydrochloride and hydrogen peroxide (DAB) chromagen substrate for 10 minutes. To remove the DAB, the coverslips were rinsed in distilled water three times for 3 minutes before an aqueous methyl green solution (0.02% v/v) counterstain was added to the coverslips for 30 seconds. The excess counterstain was washed off with distilled water, the coverslips were air dried and mounted onto glass slides using a xylene soluble mountant.

### **2.11.3 Use of Cell pellet arrays**

Cell pellet arrays were prepared by technical staff as described in the appendix (section 7).

#### **2.11.3.1 De-wax sections**

Slides with paraffin sections containing the cell arrays were de-waxed prior to immunochemical assay. Slides were placed in a slide rack, immersed and transferred through the following baths:

1. xylene (2 x 7 minutes)
2. 100% alcohol (2 x 2 minutes)
3. 90% alcohol (2 x 2 minutes)
4. 70% alcohol (2 x 2 minutes)
5. distilled water (2 x 5 minutes)

#### **2.11.3.2 Immunocytochemistry Assay**

Following the above process, the slides were removed from the rack and a 3% aqueous solution of hydrogen peroxidase was applied to each section for 5 minutes at room temperature. After being washed in distilled water for 2 minutes, the slides were then subject to an antigen retrieval process which varied according to the antigen being retrieved. Antigen retrieval exposes antigens that have become masked during the fixation process and previous processing.

### 2.11.3.3 Pronase retrieval

Slides were placed in pre-warmed PBS and then kept at 37°C for 10 minutes. The slides were transferred into the 37°C pre-warmed 0.02% pronase solution in PBS for 5 minutes. To stop the enzyme reaction the slides were placed under running tap water for 5 minutes.

### 2.11.3.4 Pressure cooking retrieval

The slides were immersed in sodium citrate (10mM, pH 6) in a pressure cooker. The pressure cooker was heated until full pressure (~100kPa) was reached. The slides were kept at full pressure for 1 minute before the pressure was slowly released and running tap water applied to the slides for 10 minutes.

### 2.11.3.5 Microwave retrieval

Microwave retrieval was undertaken in 11 sodium citrate (10mM, pH 6) or 11 citric acid (10mM, pH 6). Slides were transferred to a plastic microwaveable rack; the rack was submerged in either the sodium citrate or citric acid and covered with saran wrap. This was then microwaved at 950W for 1 minute then 560W for 9 minutes. Following this the slides and solution were allowed to cool for 20 minutes *in-situ* before being placed under running tap water for 5 minutes.

After the retrieval step the slides were immersed in distilled water for 2 minutes. Following removal of the water a peroxidase anti-peroxidase (PAP)

pen was used to outline the cell array area on the slide, enabling the localisation of subsequent solutions. The slides were then immersed in PBS-Tween (0.02% v/v) for 2 minutes before 50µl primary antibody diluted in PBS was applied (concentrations and durations used in the various assays are shown in Table 2.8). After the appropriate time, the sections were washed for 3 minutes in PBS, followed by two 5 minute washes in PBS-Tween. The relevant secondary antibody detection system was then applied for either 1 or 2 hours (see Table 2.7). The secondary antibody was drained from the slides and a 3 minute PBS wash and two 5 minute PBS-Tween (0.02% v/v) washes applied. After this procedure, 50µl DAB chromagen substrate was added for 10 minutes, followed by two distilled water washes for 2 minutes. A methyl green (0.02% v/v) counterstain was applied for between 1 and 5 minutes depending on the retrieval procedure (1 minute pronase, 5 minutes pressure cook/microwave); finally distilled water was used to wash the slides until the water was clear. The slides were left to air dry before a coverslip was mounted over the cell array with DPX soluble mountant. This was also left to air dry at room temperature.



**Table 2.7 Immunocytochemistry conditions according to antibody**

Shown in the table are the immunocytochemical conditions including antigen retrieval method and primary antibody concentration used for the optimal visualisation of proteins.

Assay	Retrieval	Block	Concentration	Duration	Secondary
14-3-3	Pronase 5 minutes	0.02% Tween	1/5000	Overnight	Rabbit 1 hour
Bag-1	No retrieval	0.02% Tween	1/200	Overnight	Mouse 2 hours
$\delta$ - catenin	Pressure cook 2 minutes	20% normal human serum	1/50	3 hours	Goat (1/100) 2 hours
NFkB	Microwave citric acid 30 minutes	0.02% Tween	1/50	Overnight	Rabbit 1 hour
NME3	Microwave citric acid (1+9)	0.02% Tween	1/4000	Overnight	Mouse 2 hours

#### 2.11.4 Immunocytochemistry Analysis

The assessment of immunocytochemical staining took place on a dual viewing Olympus BH-2 light microscope at x20 and x40 magnification by two people. For each area of cells being viewed the percentage of positively stained cells and the intensity were estimated. Semi quantitative H-scoring on a scale of 0-300 was used to visualise the results. The H-score is calculated using the following equation:

$$\begin{aligned}
 & \Sigma \text{ of } (\% \text{ weakly stained cells} \times 1) \\
 & \quad + (\% \text{ moderately stained cells} \times 2) \\
 & \quad + (\% \text{ strongly stained cells} \times 3) \\
 & = \text{H-score}
 \end{aligned}$$

### 2.11.5 Statistical Analysis

To statistically analyse the immunocytochemical H-scores, the Mann-Whitney 'U' test for non-parametric data was used and displayed in as a boxplot. Outliers (○) and extreme values (\*) are as defined by SPSS. For a difference to be considered significant the P values had to be less than 0.05.

## 2.12 TransAM Assay

### 2.12.1 Cell Culture for TransAM assay

MCF-7 cells were seeded onto 150mm dishes ( $\sim 3 \times 10^9$  cells/dish) containing phenol red free RPMI + 5% SFCS and allowed to adhere for 24 hours. After 24 hours the medium was replaced with experimental media containing the following:

- No treatment (control, ethanol carrier)
- Oestradiol ( $10^{-9}$ M in ethanol carrier [0.05%])
- Tamoxifen ( $10^{-7}$ M in ethanol carrier [0.05%])
- Faslodex ( $10^{-7}$ M in ethanol carrier [0.05%])

The medium was replaced on day 4 and the cells harvested after 7 days.

TAM-R, FAS-R and parental MCF-7 cells were also seeded onto 150mm dishes ( $\sim 3 \times 10^9$  cells/dish) in phenol red free RPMI + 5% SFCS in the presence of tamoxifen or faslodex where appropriate. The medium was replenished every 4 days and the cells harvested when approximately 70% confluency was reached.

### 2.12.2 Preparation of whole cell extract

Whole cell extracts were produced according to the Active Motifs manufacturer's instructions using reagents from the TransAM kit. In outline, the media was aspirated from the dish and ice cold PBS/phosphatase inhibitor solution (5ml, Table 2.9) was added as a wash, before a further 3ml of PBS/phosphatase inhibitor was applied to the cells. The cells were then removed from the dish with a cell scraper and the PBS/phosphatase inhibitor and cell suspension transferred to a pre chilled conical tube (15ml). The cell suspension was microcentrifuged at 500 rpm for 5 minutes at 4°C. The supernatant was then discarded and the cell pellet kept on ice until it was re-suspended in a complete lysis buffer (300µl, Table 2.8) and vortexed for 10 seconds. The suspension was incubated on ice on a rocking platform (150 rpm) for 10 minutes, vortexed for 30 seconds and centrifuged for 20 minutes at 14,000 x g at 4°C. The supernatant containing the whole cell extract was removed to a pre-chilled microcentrifuge tube and stored at -20°C until use. The concentration of protein in the whole cell extract was determined using the method previously described (section 2.8.2.1 Protein concentration assay).

**Table 2.8 Components of PBS/phosphate inhibitor and complete lysis buffer from the TransAM kit**

Reagent	Components	Per 150mm dish
PBS/phosphatase inhibitor	10X PBS	1.6 ml
	Distilled water	13.6 ml
	Phosphatase inhibitors	0.8 ml
	Total required	16.0 ml
Complete lysis buffer	10 mM DTT	90.0 $\mu$ l
	Lysis buffer	801.0 $\mu$ l
	Protease inhibitor cocktail	9.0 $\mu$ l
	Total required	900 $\mu$ l

### 2.12.3 NF $\kappa$ B Transcription factor assay

#### 2.12.3.1 Binding of NF $\kappa$ B isoforms to the NF $\kappa$ B consensus sequence

NF $\kappa$ B transcription factor assays were carried out according to the manufacturer's instructions. The appropriate number of microwells needed was determined (one well per sample plus positive, negative and blank controls). The microwells were pre-coated with an NF $\kappa$ B consensus binding site oligonucleotide, to bind NF $\kappa$ B protein. The complete lysis buffer, complete binding buffer, 1x washing buffer and 1x antibody binding buffer were prepared as shown in Table 2.9. Complete binding buffer (30 $\mu$ l) was placed in each well being used. To the experimental wells a further 7 $\mu$ g of protein sample diluted in 30 $\mu$ l of complete lysis buffer was applied. To the positive control wells 5 $\mu$ g of Raji (human Burkitts lymphoma cell line) nuclear cell extract in 20 $\mu$ l of complete lysis buffer was added. To the negative wells 20 $\mu$ l of complete lysis buffer only was used. The wells were covered with a plastic seal and incubated for 1 hour at room temperature on a rocking platform (100

rpm). Following this procedure each well was washed three times with 200 $\mu$ l 1x washing buffer, draining each time by ‘flicking’ the inverted plate and tapping three times onto absorbent paper towels.

**Table 2.9 Amounts and components of reagents required for TransAM NF $\kappa$ B transcription factor assay**

Reagent	Components	For 1 Well
Complete lysis buffer	DTT	0.11 $\mu$ l
	Protease inhibitor cocktail	0.23 $\mu$ l
	Lysis buffer AM2	22.2 $\mu$ l
	Total required	22.5 $\mu$ l
Complete binding buffer	DTT	0.07 $\mu$ l
	Herring sperm DNA	0.34 $\mu$ l
	Binding buffer AM3	33.4 $\mu$ l
	Total required	33.8 $\mu$ l
1x Washing Buffer	Distilled water	2.025ml
	10X Washing buffer AM2	225 $\mu$ l
	Total required	2.25ml
1x Antibody binding buffer	Distilled water	202.5 $\mu$ l
	10x Ab binding buffer AM2	22.5 $\mu$ l
	Total required	225 $\mu$ l
Developing solution	Total required	112.5 $\mu$ l
Stop solution	Total required	112.5 $\mu$ l

### 2.12.3.2 Binding of primary antibody

Antibodies to the NF $\kappa$ B family proteins; p50, p65, C-Rel or p52 were diluted 1:1000 in 1x antibody binding buffer. 100 $\mu$ l of the antibody to the NF $\kappa$ B family member of interest was added to each well being used. The plate was covered and incubated for 1 hour at room temperature without agitation. The wells were then washed three times as described previously.

### 2.12.3.3 Binding of secondary antibody

Horseradish peroxidase (HRP) conjugated antibody was diluted 1:1000 in 1x antibody binding buffer and 100µl was added to each well. The plate was covered and incubated at room temperature for 1 hour without agitation. Following this interval the plate was washed with 200µl 1x washing buffer three times as described above.

### 2.12.3.4 Colorimetric reaction

A developing solution (100µl) was added to each well and was incubated, protected from direct light, for between 2-10 minutes until the positive control turned a medium blue. At this point 100µl of stop solution was added to each well turning the solution yellow. The concentration of NFκB binding activity is directly proportional to the absorbance of the solution in each well and this was determined within 5 minutes at 450nm using a plate reading spectrophotometer.

## 2.13 NFκB Transient transfection assays

### 2.13.1 Cell culture and transfection

Stock cultures of MCF-7 cells growing in phenol red free RPMI + 5% SFCS were dispersed by trypsinisation, re-suspended in experimental medium and seeded into 12-well plates ( $\sim 2.5 \times 10^5$  cells/well). The cells were allowed to adhere to the wells for 24 hours. On the following day a transfection mixture

was prepared as follows; tube A containing Lipofectin reagent (3 $\mu$ l/well) plus serum free/phenol red free DCCM medium (60 $\mu$ l/well) with L-glutamine (400mM). A second tube B contained NF $\kappa$ B plasmid DNA (400ng per well), a luciferase reporter construct or 'control' construct and 700ng per well carrier plasmid DNA in serum free/phenol red free DCCM (60 $\mu$ l/well). Both tubes were shaken to mix and left to equilibrate at 37°C for 45 minutes. After 45 minutes the mixture containing Lipofectin and the plasmid DNA were combined and re-incubated at 37°C for a further 15 minutes. Into another tube were aliquoted 380 $\mu$ l DCCM containing L-glutamine (400mM) and 5 $\mu$ l DMSO per well (for example 10 wells - 10 x 380 $\mu$ l = 3.8ml DCCM and 10 x 5 $\mu$ l = 50 $\mu$ l DMSO). A final mix for transfection was then created by combining the Lipofectin/plasmid DNA mixture with the DCCM which contained DMSO to create a final transfection medium. The overnight cell culture medium was removed from the wells by aspiration and a DCCM wash applied, this was also aspirated and 0.5 ml of transfection medium applied to each well. The plate was incubated at 37°C in 5% CO<sub>2</sub> for 6 hours. The transfection medium was then removed; cells were washed with medium before treatment medium was added. Phenol red free RPMI + 5% SFCS plus L-glutamine with no treatment, oestradiol (10<sup>-9</sup>M) faslodex (10<sup>-7</sup>M) or gefitinib (1 $\mu$ M) all in the presence and absence of parthenolide (3 $\mu$ M) was added to triplicate wells. Plates were incubated at 37°C for 18 hours.

### 2.13.2 Cell Lysis

After the 18 hours of treatment the medium was removed, the cells washed with PBS and 200 $\mu$ l of 1x Promega Reporter lysis buffer (diluted from 5x stock lysis buffer with sterile water) was added. Any remaining cells were gently scraped from the wells using the plunger from a 1 ml syringe and the lysates transferred to 1.5ml microcentrifuge tubes. The lysates were kept on ice for at least 10 minutes before being frozen at -80°C.

### 2.13.3 Luciferase Assay

The Promega single (firefly) luciferase reporter assay kit was prepared and used according to the manufacturers instructions to determine NFkB-activated luciferase activity. The frozen transfected cell lysates were thawed and 100 $\mu$ l samples were added to an equivalent volume of reporter assay buffer. The resulting solution was read over 10 seconds using a Lumat LB 9507 luminometer (GC+C Wallac, UK).

### 2.13.4 *In-situ* $\beta$ -Galactosidase Fixation, Staining and Quantification

As a control to determine transfection efficiencies, several wells were transfected (as described before) with a construct containing the  $\beta$ -Galactosidase gene. These wells were washed with 1 ml PBS. The cells were then fixed with a 0.5% glutaraldehyde solution in PBS (1 ml per well) for 15 minutes. Following this the cells were washed with 1 ml PBS and X-gal



staining solution [3.125  $\mu$ l of X-gal (40 mg/ml) per ml of 1.0% potassium ferricyanide (300 mM/ 130 mM  $MgCl_2$  in PBS) and 1.0% potassium ferrocyanide (300 mM/ 130 mM  $MgCl_2$  in PBS) in PBS] was applied. Staining was allowed to develop overnight at 37°C. The percentage of  $\beta$ -Galactosidase positive stained (transfected) cells was determined by cell counting at x40 magnification. This was used as a control for consistency in transfection efficiency.

#### **2.14 Parthenolide Growth Inhibition Assay**

Log-phase growth MCF-7 cells and FAS-R cells in phenol red free RPMI + 5% SFCS were trypsinised, re-suspended in experimental medium and seeded into 24-well plates ( $\sim 4 \times 10^4$  cells/well). The cells were allowed to adhere to the wells for 24 hours, after which time the media was replaced with phenol red free RPMI + 5% SFCS with and without faslodex ( $10^{-7}$ M in an ethanol carrier) to a 0.01% final volume and parthenolide (0, 0.5, 1, 3, and 5  $\mu$ M in DMSO) in triplicate. The media was replenished on day 4. After 7 days the media was aspirated and 1 ml trypsin (0.05% w/v) and EDTA (0.02% w/v) solution was added to each of the wells for between 3 and 5 minutes until cells were detached from the well. The detached cells were drawn up and down a 5ml syringe with a 25G<sup>5/8</sup> 0.5 x 16 needle to separate the cells into a single cell suspension, which was collected in the syringe. Isoton (1ml) was then added to the well and also drawn up into the syringe, this was repeated twice more. The suspension in the syringe was added to 6ml of isoton, giving a final volume of

10 ml. The solution was inverted twice before the number of cells in the solution was counted twice using the Coulter counter Multisizer II (Beckman Coulter UK Ltd, High Wycombe, UK). The average cell number from the two replicates was multiplied by a dilution factor of 20 to derive the number of cells per well. These experiments were repeated three times each.

## Chapter 3

**~ Results ~**

## 3 Results

### 3.1 Array Analysis

#### 3.1.1 Clontech Atlas™ Human 1.2 Nylon arrays

RNA was extracted from triplicate cultures of MCF-7 cells treated with vehicle or vehicle plus E2, tamoxifen or faslodex for 4, 7 or 10 days. The growth promoting effects of E2 treatment were visible in these cultures by day 7 and the growth inhibition effects of tamoxifen and particularly faslodex by day 10. The RNA was subject to DNase treatment and re-extraction using Qiagen RNeasy columns. Figure 3.1 shows 1µg of the DNase treated RNA separated on an agarose gel (2%) for each treatment and time point from an example replicate set. The 18s and 28s ribosomal RNA bands are clearly visible with an intensity ratio of approximately 1:2 as expected. As there was no degraded RNA (i.e. very low molecular weight bands) or genomic DNA contamination (i.e. very high molecular weight bands), this indicated that the extracted RNA was of high quality and integrity. The removal of residual DNA was essential for successful array performance as otherwise it would have resulted in extremely high background and non-specific binding to the nylon cDNA arrays. The DNase treated RNA was subsequently verified as appropriate for further detailed analysis of E2-regulated gene expression by northern blotting for pS2, a known E2-regulated gene. As predicted the MCF-7 cell preparations used were representative of hormone responsive cells, with an induction of pS2 by E2, and depletion with the anti-hormones tamoxifen and faslodex. A

representative pS2 blot and graph showing the mean of three replicates after actin normalisation can be seen in Figure 3.2. It clearly shows a trend across the time points of an increase in pS2 levels with E2 treatment, and decrease with anti-hormonal treatment. Day 7 shows the best pS2 profile, with E2 treatment resulting in a significant increase of 493% ( $p < 0.001$ ), along with a 14% ( $p < 0.001$ ) and 57% ( $p < 0.001$ ) decrease in pS2 levels with tamoxifen and faslodex treatment respectively compared to the untreated control.

The validated RNA was reverse transcribed with the incorporation of  $^{32}\text{P}$  and hybridized overnight to the Clontech Atlas™ Human Cancer 1.2 nylon arrays. Altogether, 36 arrays (3 time points, 4 treatments in triplicate) were created and the signals captured by phosphorimaging. A representative phosphorimage of four matched, day 7 MCF-7 cell arrays (untreated control, E2, tamoxifen and faslodex) can be seen in Figure 3.3. Several different length exposures of the phosphorimage were taken to ensure the full range of low to high gene expression levels were captured. A phosphorimage for each set of arrays was selected which showed the lowest background with no saturated gene signals and a good overall level of signal for the majority of the gene spots on the arrays. Such images were then used for spot densitometry and subsequent gene analysis.

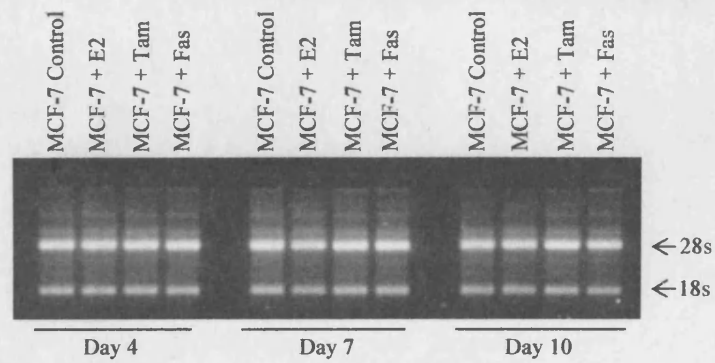


**Figure 3.1** DNase treated RNA from MCF-7 cells

This figure shows an example of Tri-reagent extracted day 4, 7 and 10 RNA, after DNase treatment. The RNA ( $1\mu\text{g}$ ) has been visualised by gel electrophoresis, and the 28s and 18s bands can be clearly seen, with a ratio of 2:1 indicating good quality.

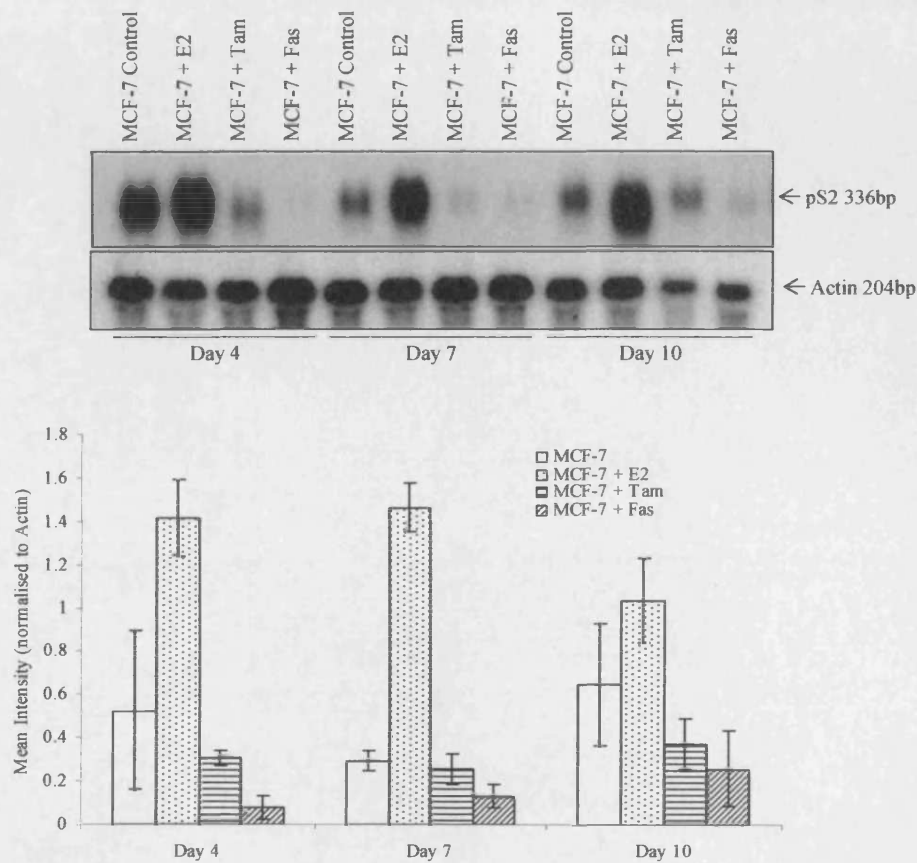
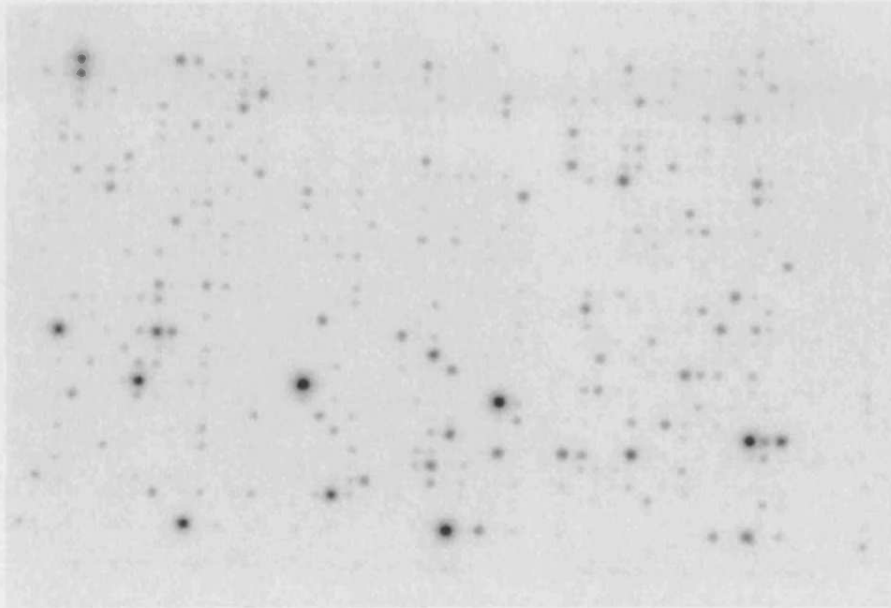


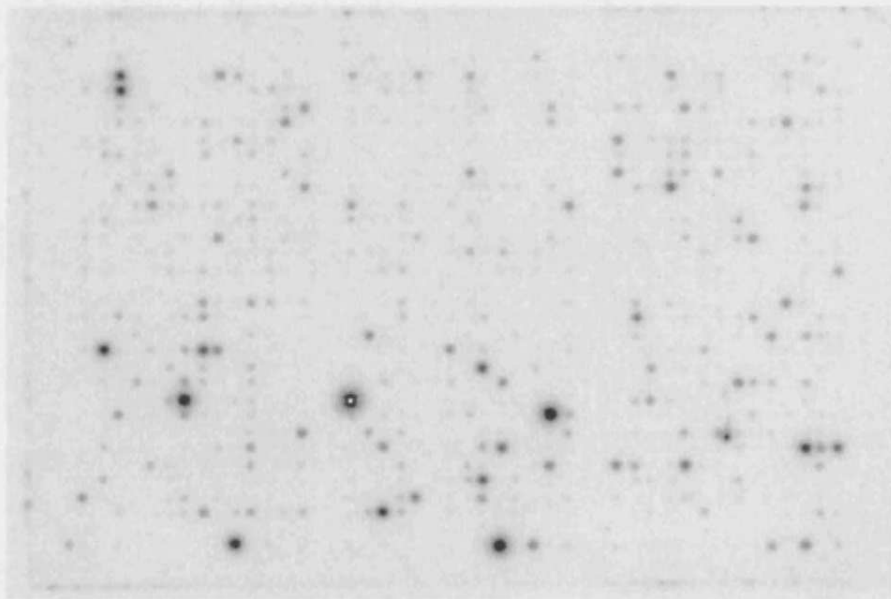
**Figure 3.2.** RNA verification of MCF-7 cell preparations by northern blot for pS2

Northern blotting was carried out on RNA extracted from MCF-7 at days 4, 7 and 10, either untreated or treated with E2 ( $10^{-9}$ M), tamoxifen ( $10^{-7}$ M) or faslodex ( $10^{-7}$ M). Blotted membranes were probed for pS2 and  $\beta$ -actin with radio-labelled cDNA. The graph illustrates the mean densitometric intensities of pS2 bands after  $\beta$ -actin normalisation  $\pm$  SEM from 3 independent experiments and across the three time points. Day 7 shows the most consistent profile and data was statistically analysed and significant differences were found at day 7 between MCF-7 control and MCF-7 + E2 ( $p < 0.001$ ), MCF-7 + E2 and MCF-7 + Tam ( $p < 0.001$ ) and MCF-7 + E2 and MCF-7 + Fas ( $p < 0.001$ ). Day 4, 7 and 10 all show this same trend.

a



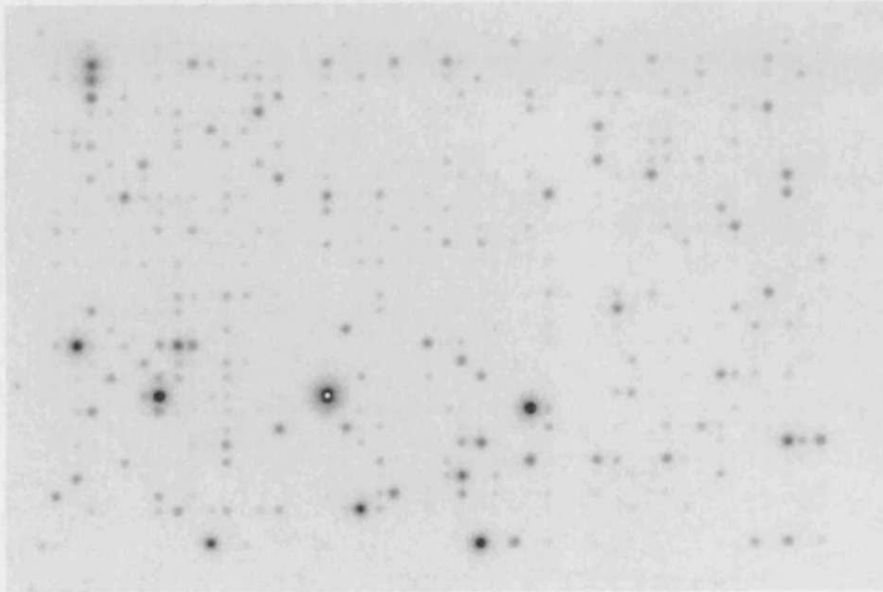
b



Continued.....



d



c

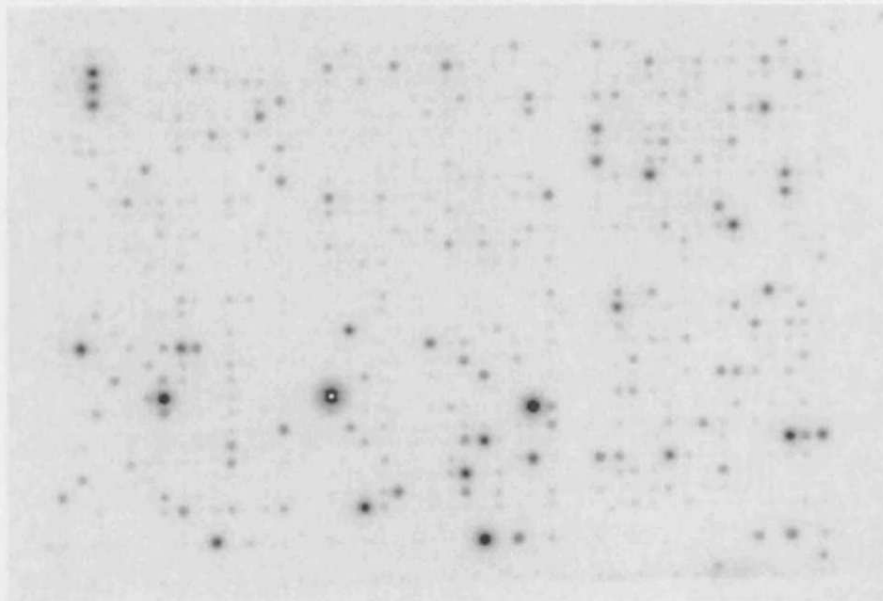


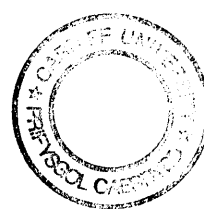
Figure 3.3 Clontech Cancer 1.2 Nylon arrays of MCF-7 cell preparations

A representative set of 4 Clontech arrays from the 36 that were generated by sample hybridisation is shown. Day 7 MCF-7 cell RNA (a) in the absence of or treated with (b) E2 ( $10^{-9}$ M), (c) tamoxifen ( $10^{-7}$ M) or (d) faslodex ( $10^{-7}$ M) was radio-labelled and hybridized to the nylon arrays. Images were generated by an 8 day exposure to a phosphorimaging screen.

### 3.1.2 Array analysis software: data log transformation & normalisation

The spot densitometry was subsequently carried out using the Clontech AtlasImage™ software package (as described in Chapter 2 Materials and Methods: section 2.6).

There were several different types of software assessed during this project to carry out the subsequent array analysis (Table 3.1). These included Clontech Atlas Navigator™, Clusfavor 6.0, GenMAPP 2 and GeneSifter™. The software found to provide the most user friendly interface and extensive analytical options was GeneSifter™. GeneSifter was therefore chosen to perform all the array analysis. Before any analysis was carried out, the spot densitometric values were log transformed and normalised. Boxplots of the data prior to log transformation and normalisation from the arrays can be seen in Figure 3.4. The median densitometric value for each of the replicates per treatment proved to be different, as were the minimum and maximum values. The data thus needed to be normalised and the medians brought to a comparative level to account for differences in exposure, labelling efficacy and hybridisation. Figure 3.5 shows the array data post log transformation and normalisation where the median for all arrays have been equalised. Normalisation was carried out by dividing the densitometric value for each gene on a particular array by the median densitometric value for all signals in that array, followed by dividing the resultant densitometric value of each gene by the median densitometric value for that gene across all the arrays. The resultant minimum and maximum gene values are also similar, except for the



day 4 array R1 and R2 replicates, which had a lower maximum and lower minimum value compared to the other arrays (Figure 3.5). This indicated that there may have been under performance with two of the three day 4 replicates that was not fully rectified by log transformation or normalisation. Indeed low densitometric levels were seen consistently in two out of the three replicates. However such observations may also indicate lower levels of expression for many genes at this earlier time point.

### **3.1.3 Scatter plots to validate array profiles & performance**

Scatter plots were subsequently generated to compare the spread of the expression data from the arrays and to overview the broad numbers of induced and suppressed genes between treatments after log transformation and normalisation. The scatter plots in Figures 3.6 to 3.14 show the mean log intensities for each gene on the array in group 1 (i.e. MCF-7+E2, tamoxifen or faslodex), plotted against the mean log intensities for the same gene in group 2 (untreated MCF-7 control) at each time point.

In each scatter plot the diagonal line denotes a no-change in gene expression (1:1 ratio in expression); the majority of genes are found around this line in the plots. The distance genes lie from the diagonal line reflects the level of induction or suppression of expression by treatment versus untreated control. Genes found at the top of the diagonal line are highly expressed, and included for example, the housekeeping gene GAPDH which is highly expressed in all

the arrays. Genes at the bottom of the graph are expressed at very low levels. The different distribution of spots on the scatter plot reveals information about the overall expression of genes on the arrays. For day 4 (Figures 3.6, 3.7 and 3.8) many of the gene spots are clustered at the bottom of the graph (below a log intensity of 1), suggesting many of the changes occur in very low intensity genes. Indeed, log intensities of  $<0.1$  were quite frequent for either treated or untreated control samples at this time point, and a large number of genes in the day 4 scatter plots are at a much lower intensity than the genes in the day 7 (Figures 3.9, 3.10 and 3.11) and day 10 (Figures 3.12, 3.13 and 3.14) scatter plots, where log intensities of  $<0.1$  were not observed in any treatment group. This again may indicate that either there is a problem with the performance of arrays at day 4 or that genes are at a very much lower level of expression after only 4 days of growth. The day 4 profiles for E2, tamoxifen and faslodex versus untreated MCF-7 control are also similar, indicating small gene changes in general with the biggest changes being in the very lowly expressed genes. Other observations made from the various scatter plots include the spread of data with different treatments at days 7 and 10. When comparing untreated MCF-7 control and E2 treated samples (Figures 3.9 and 3.12) the genes are in general clustered closer to the diagonal line than when comparing the untreated MCF-7 control with tamoxifen (Figures 3.10 and 3.11) or faslodex (Figures 3.13 and 3.14) treated samples. There therefore appeared to be more induced (red) and suppressed (green) genes as a consequence of anti-oestrogen treatment. This phenomenon was particularly obvious with higher intensity genes where more genes are apparently anti-oestrogen induced versus

untreated MCF-7 control (10-1,000 log intensity range). The genes of most potential interest with regard to this project are to be found in Figures 3.10, 3.11, 3.13 and 3.14 above a log intensity of 1 that are persistently induced by anti-oestrogens at days 7 and 10, i.e. where such changes are likely to be more reliable than those achieved at lower intensity.

This low level of expression levels in the day 4 data coupled with the differing data spread in two of the three replicates led to the exclusion of day 4 array data from substantial array analysis and associated gene selection on the grounds of potentially poorer array performance. However, since there was no evidence of any problems with the actual quality of the day 4 RNA used to produce the arrays (see Figure 3.1), the RNA samples were still deemed relevant for subsequent RT-PCR studies of inducible genes.

**Table 3.1 Results of array analysis software assessment**

The table shows the 7 arrays analysis software packages that were assessed for suitability to analyse nylon array data in this project. From the table it is evident that GeneSifter is the most appropriate software in this instance.

Software	Operating System	Affordable	User friendly	Array type
Clementine	Linux	Yes	No	Cy3/Cy5
ClontechAtlas Navigator	Windows	Yes	No	One colour
ClusFavor 6.0	Windows	Yes	No	All
GeneSifter	Web-based	Yes	Yes	All
GeneSpring	Windows	No	No	All
GenMAPP 2	Windows	Yes	No	All
MatArray Toolbox	Windows	Yes	No	All

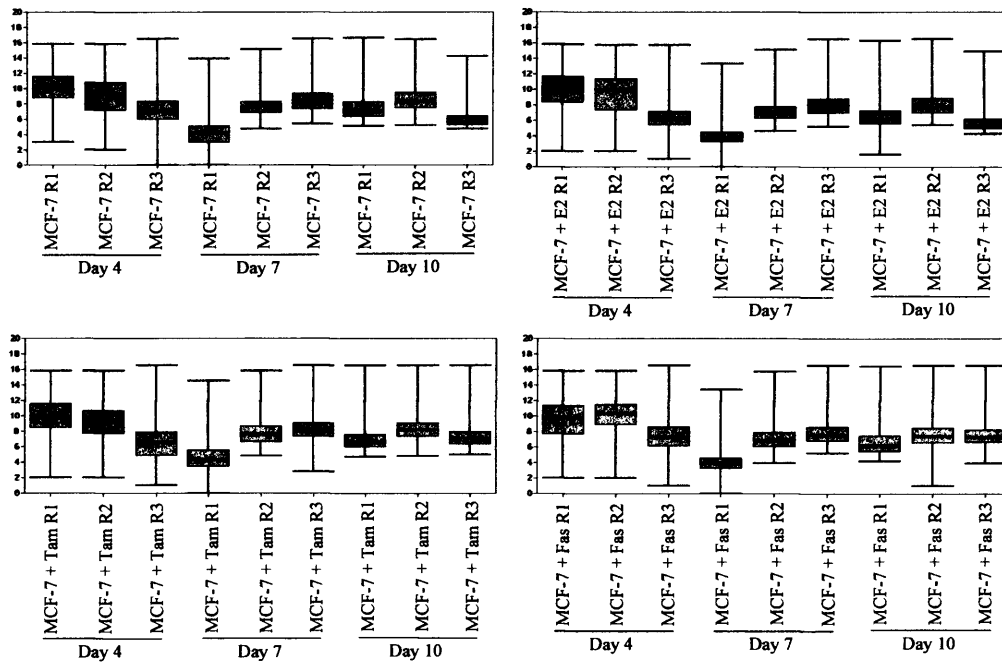


**Figure 3.4** Boxplots of MCF-7 treatment data prior to log transformation and normalisation from the arrays

Box plots were generated in GeneSifter™. For each set of treatments, i.e. untreated control, E2 ( $10^{-9}$ M), tamoxifen ( $10^{-7}$ M) and faslodex ( $10^{-7}$ M) the replicates (e.g. R1, R2 or R3) have been grouped together for each time point. The boxplots show the median, 1st and 3rd quartiles and minimum and maximum values for each data set.

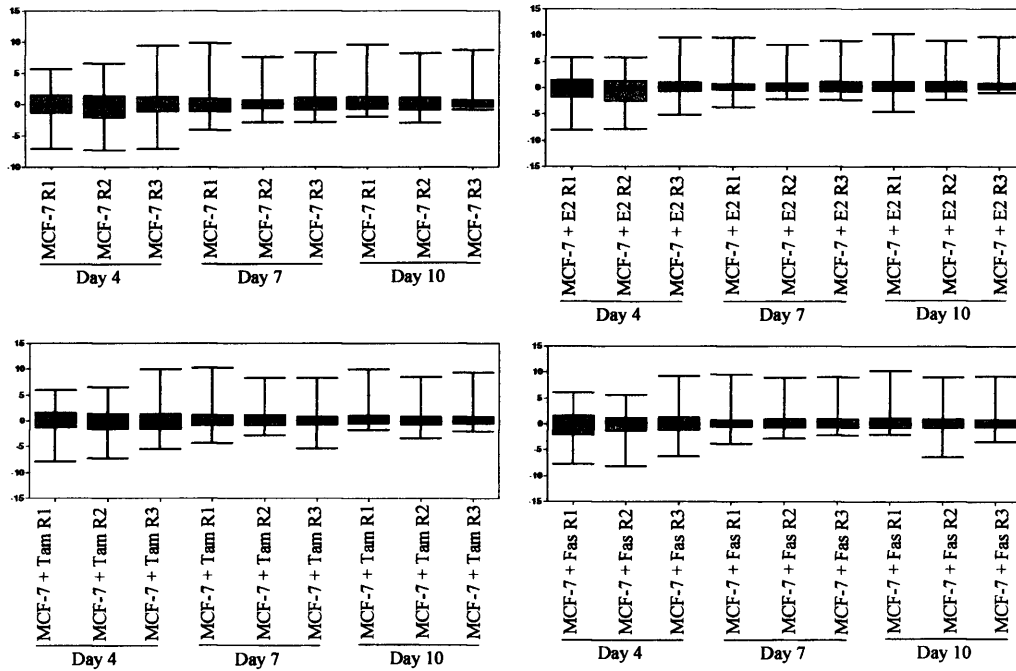


**Figure 3.5** Boxplots of log transformed and normalised MCF-7 treatment data from arrays

Boxplots were been generated in GeneSifter™ after array data had been log transformed and normalised ready for analysis. For each set of treatments, i.e. untreated control, E2 ( $10^{-9}$ M), tamoxifen ( $10^{-7}$ M) and faslodex ( $10^{-7}$ M) the replicates (e.g. R1, R2 or R3) have been grouped together at each time point. The boxplots show the median, 1st and 3rd quartiles, minimum and maximum values for each data set.



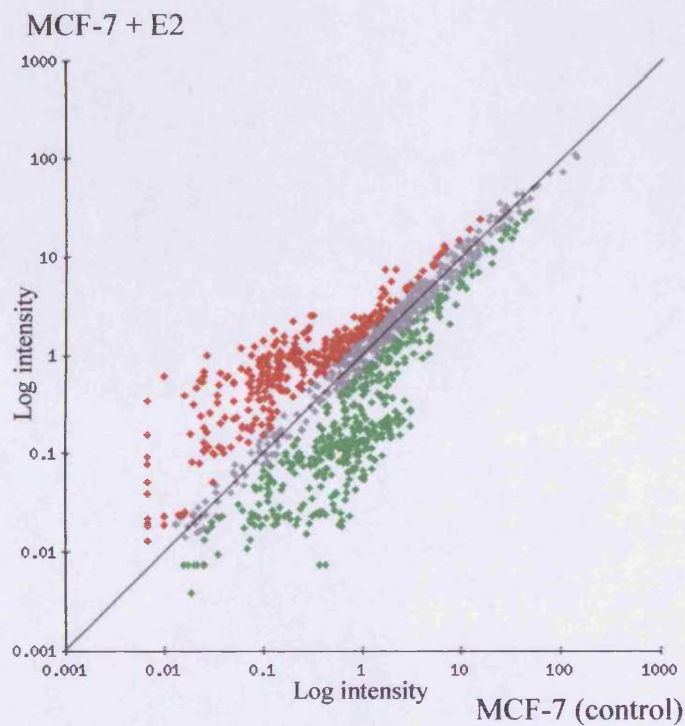


Figure 3.6 Day 4 MCF-7 + E2 vs. MCF-7 (control) gene expression scatter plot

The scatter plot has been generated in Genesifter™ for day 4. The mean log intensity for the untreated MCF-7 data has been plotted for each gene against the mean log intensity for MCF-7 + E2 ( $10^{-9}$ M) data. Each of the 1184 genes on the array are represented. The red spots represent genes that are upregulated by  $\geq 1.5$  fold or more in MCF-7 cells treated with E2 verses untreated MCF-7 cells. The green spots represent genes that are downregulated by  $\geq 1.5$  fold in E2 treated MCF-7 cells compared with untreated MCF-7 cells. The grey spots are genes that are not either upregulated or downregulated  $\geq 1.5$  fold.

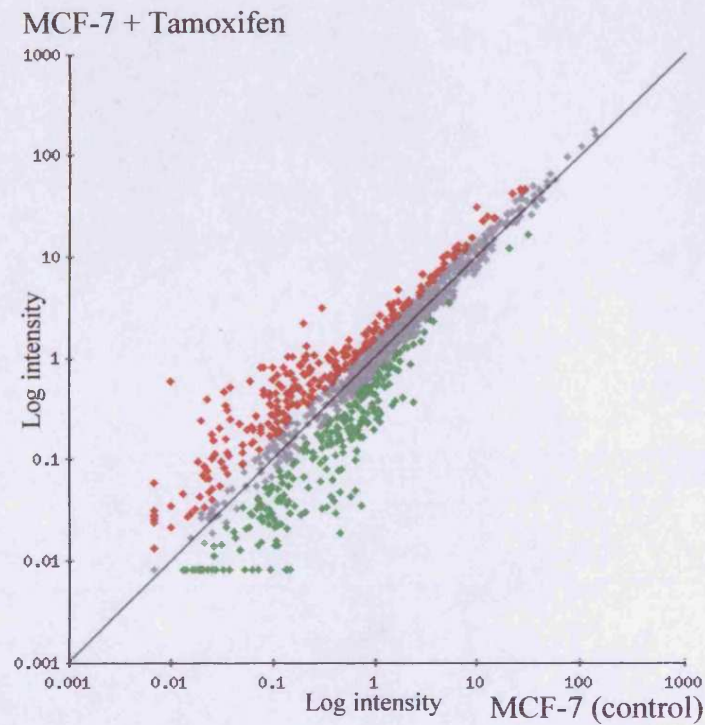


Figure 3.7 Day 4 MCF-7 + Tamoxifen vs. MCF-7 (control) scatter plot

Shown is the scatter plot generated in Genesifter™ for day 4. The mean log intensity for the untreated MCF-7 data has been plotted against the mean log intensity for MCF-7 + tamoxifen ( $10^{-7}$ M) data. Each of the 1184 genes on the array are represented. The red spots represent genes that are upregulated by  $\geq 1.5$  fold or more in MCF-7 cells treated with tamoxifen versus untreated MCF-7 cells. The green spots represent genes that are downregulated by  $\geq 1.5$  fold in tamoxifen treated MCF-7 cells compared with untreated MCF-7 cells. The grey spots are genes that are not either upregulated or downregulated  $\geq 1.5$  fold.

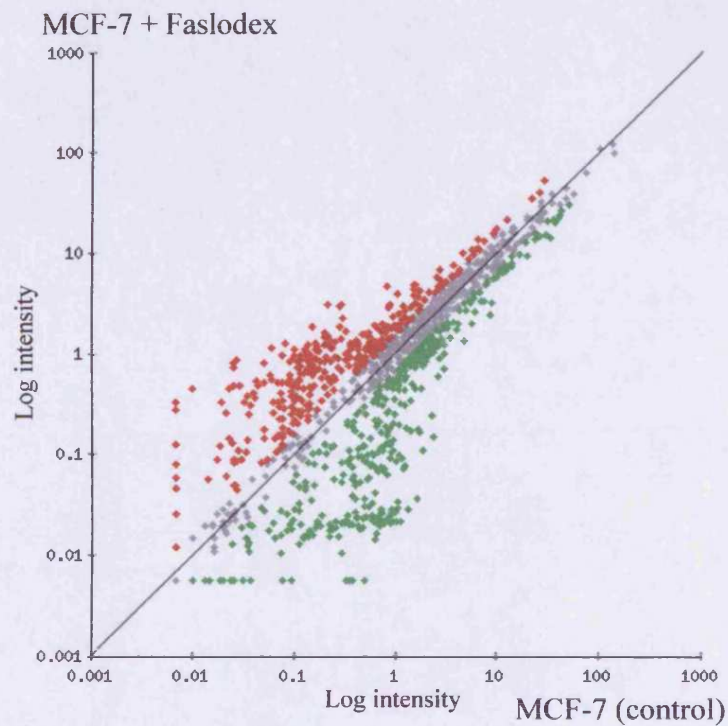


Figure 3.8 Day 4 MCF-7 + Faslodex vs. MCF-7 (control) scatter plot

Shown is the scatter plot generated in Genesifter™ for day 4. The mean log intensities for the untreated MCF-7 data has been plotted against the mean log intensities for MCF-7 + faslodex ( $10^{-7}$ M) data. Each of the 1184 genes on the array are represented. The red spots represent genes that are upregulated by  $\geq 1.5$  fold or more in MCF-7 cells treated with faslodex versus untreated MCF-7 cells. The green spots represent genes that are downregulated by  $\geq 1.5$  fold in faslodex treated MCF-7 cells compared with untreated MCF-7 cells. The grey spots are genes that are not either upregulated or downregulated  $\geq 1.5$  fold.

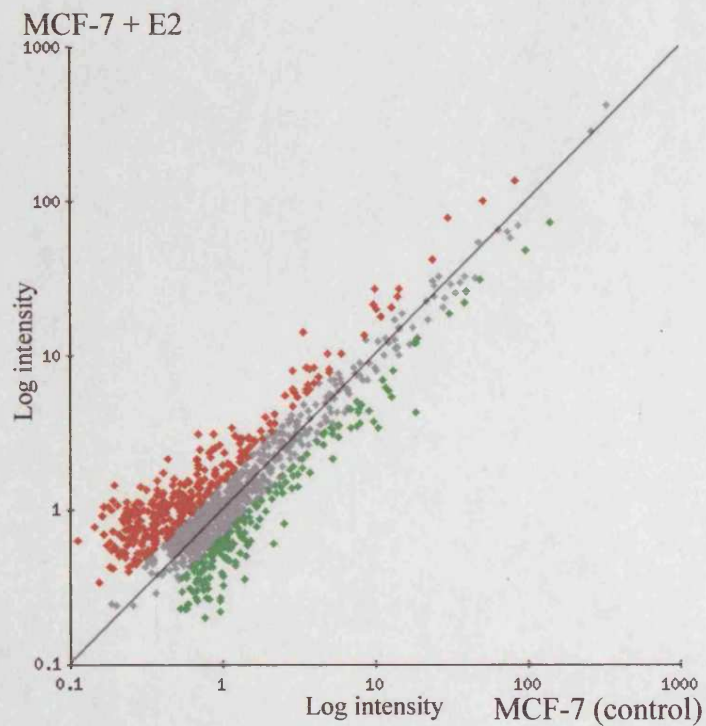
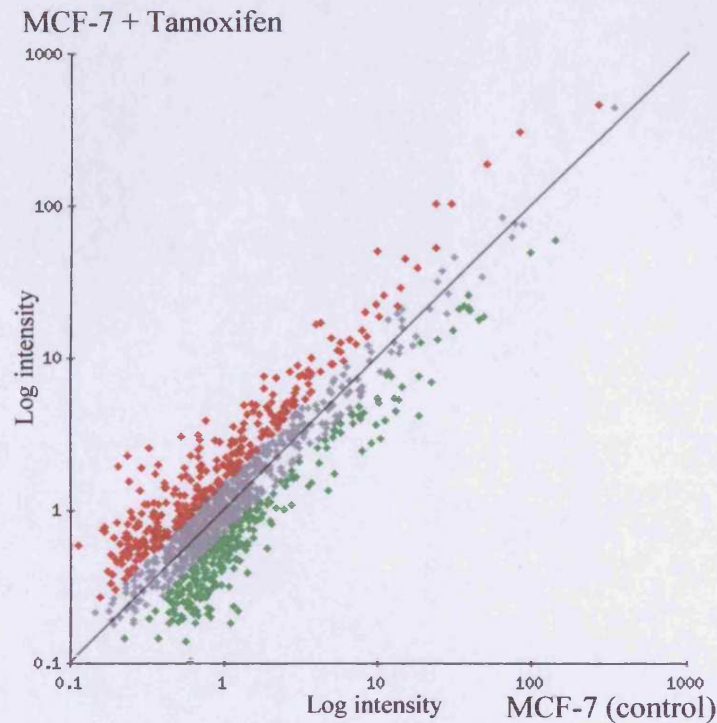


Figure 3.9 Day 7 MCF-7 + E2 vs. MCF-7 (control) scatter plot

Shown is the scatter plot generated in Genesifter™ for day 7. The mean log intensities for the untreated MCF-7 data has been plotted against the mean log intensities for MCF-7 + E2 ( $10^{-9}$ M) data. Each of the 1184 genes on the array are represented. The red spots represent genes that are upregulated by  $\geq 1.5$  fold or more in MCF-7 cells treated with E2 than untreated MCF-7 cells. The green spots represent genes that are downregulated by  $\geq 1.5$  fold in E2 treated MCF-7 cells compared with untreated MCF-7 cells. The grey spots are genes that are not either upregulated or downregulated  $\geq 1.5$  fold.



### 3.10 Day 7 MCF-7 + Tamoxifen vs. MCF-7 (control) scatter plot

Shown is the scatter plot generated in Genesifter™ for day 7. The mean log intensities for the untreated MCF-7 data has been plotted against the mean log intensities for MCF-7 + tamoxifen ( $10^{-7}$ M) data. Each of the 1184 genes on the array are represented. The red spots represent genes that are upregulated by  $\geq 1.5$  fold or more in MCF-7 cells treated with tamoxifen versus untreated MCF-7 cells. The green spots represent genes that are downregulated by  $\geq 1.5$  fold in tamoxifen treated MCF-7 cells compared with untreated MCF-7 cells. The grey spots are genes that are not either upregulated or downregulated  $\geq 1.5$  fold.

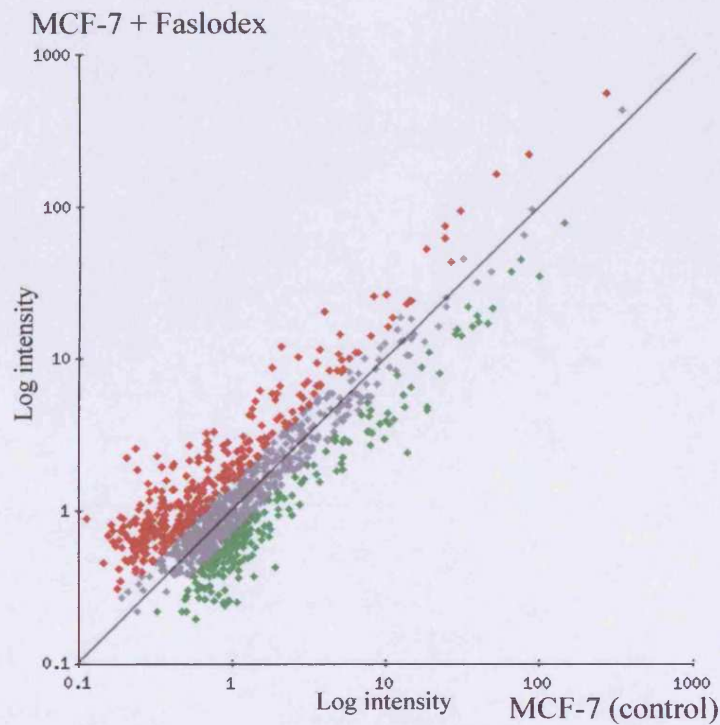


Figure 3.11 Day 7 MCF-7 + Faslodex vs. MCF-7 (control) scatter plot

Shown is the scatter plot generated in Genesifter™ for day 7. The mean log intensities for the untreated MCF-7 data has been plotted against the mean log intensities for MCF-7 + faslodex ( $10^{-7}$ M) data. Each of the 1184 genes on the array are represented. The red spots represent genes that are upregulated by  $\geq 1.5$  fold or more in MCF-7 cells treated with faslodex verses untreated MCF-7 cells. The green spots represent genes that are downregulated by  $\geq 1.5$  fold in faslodex treated MCF-7 cells compared with untreated MCF-7 cells. The grey spots are genes that are not either upregulated or downregulated  $\geq 1.5$  fold.

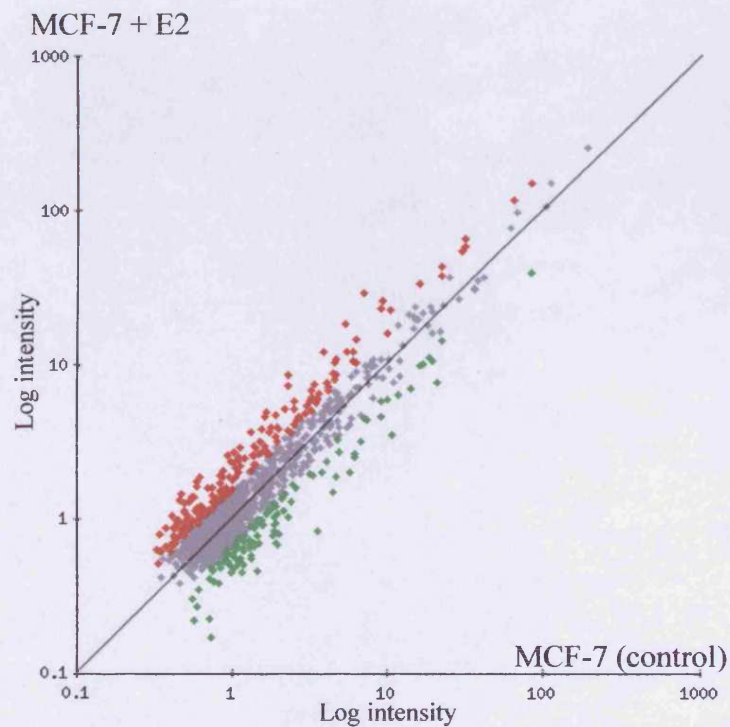
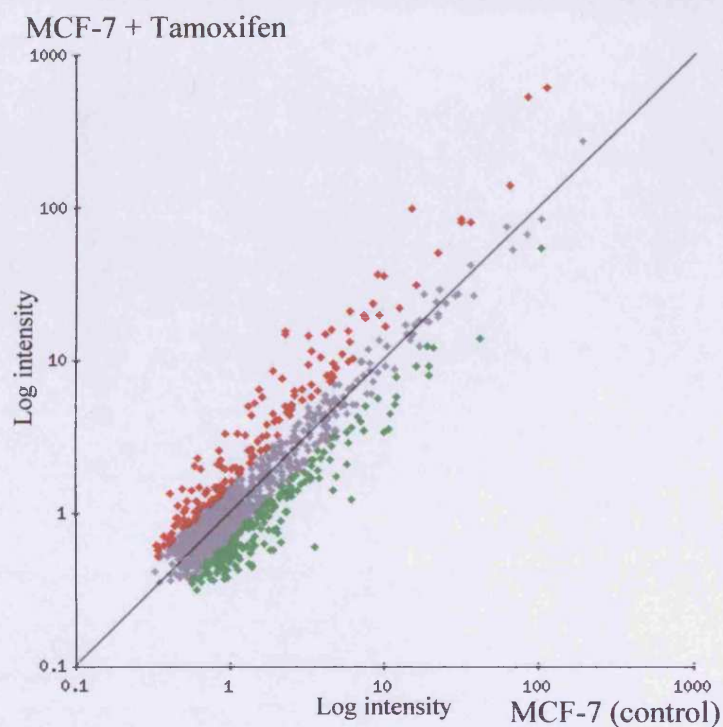


Figure 3.12 Day 10 MCF-7 + E2 vs. MCF-7 (control) scatter plot

Shown is the scatter plot generated in Genesifter™ for day 10. The mean log intensities for the untreated MCF-7 data has been plotted against the mean log intensities for MCF-7 + E2 ( $10^{-9}$ M) data. Each of the 1184 genes on the array are represented. The red spots represent genes that are upregulated by  $\geq 1.5$  fold or more in MCF-7 cells treated with E2 verses untreated MCF-7 cells. The green spots represent genes that are downregulated by  $\geq 1.5$  fold in E2 treated MCF-7 cells compared with untreated MCF-7 cells. The grey spots are genes that are not either upregulated or downregulated  $\geq 1.5$  fold.



**Figure 3.13** Day 10 MCF-7 + Tamoxifen vs. MCF-7 (control) scatter plot

Shown is the scatter plot generated in Genesifter™ for day 10. The mean log intensities for the untreated MCF-7 data has been plotted against the mean log intensities for MCF-7 + tamoxifen ( $10^{-7}$ M) data. Each of the 1184 genes on the array are represented. The red spots represent genes that are upregulated by  $\geq 1.5$  fold or more in MCF-7 cells treated with tamoxifen versus untreated MCF-7 cells. The green spots represent genes that are downregulated by  $\geq 1.5$  fold in tamoxifen treated MCF-7 cells compared with untreated MCF-7 cells. The grey spots are genes that are not either upregulated or downregulated  $\geq 1.5$  fold.



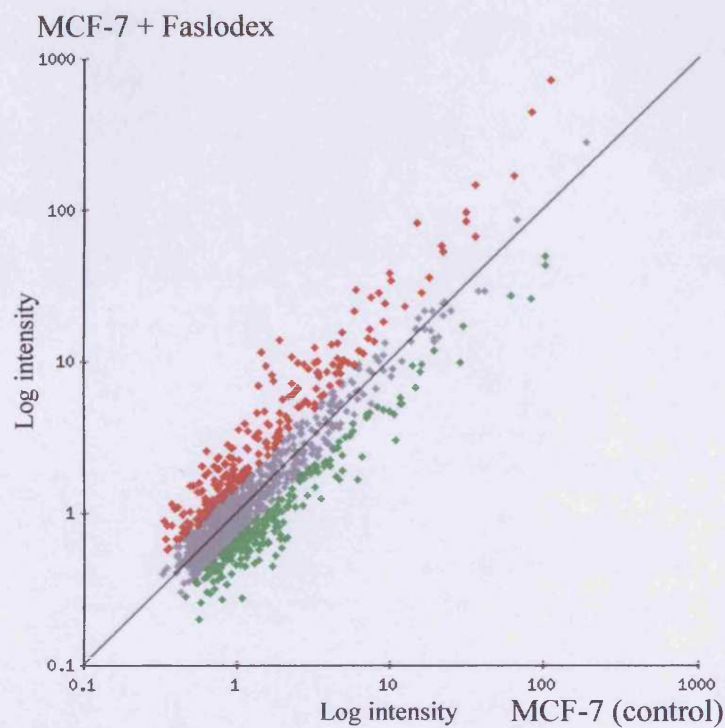


Figure 3.14 Day 10 MCF-7 + Faslodex vs. MCF-7 (control) scatter plot

Shown is the scatter plot generated in Genesifter™ for day 10. The mean log intensities for the untreated MCF-7 data has been plotted against the mean log intensities for MCF-7 + faslodex ( $10^{-7}$ M) data. Each of the 1184 genes on the array are represented. The red spots represent genes that are upregulated by  $\geq 1.5$  fold or more in MCF-7 cells treated with faslodex versus untreated MCF-7 cells. The green spots represent genes that are downregulated by  $\geq 1.5$  fold in faslodex treated MCF-7 cells compared with untreated MCF-7 cells. The grey spots are genes that are not either upregulated or downregulated  $\geq 1.5$  fold.

### 3.1.4 Detailed evaluation of array performance for day 7 & 10 samples

Once the arrays had been generated, the data extracted, log transformed and normalised and general expression pattern overviewed using scatter plots, the day 7 and 10 arrays were explored for their ability to successfully reveal known E2-regulated genes as a further indicator of their performance prior to gene discovery. The genes initially considered for such evaluation were EGFR and pS2 that have been established as E2-repressed/anti-oestrogen-induced and E2-induced/anti-oestrogen-repressed genes respectively in MCF-7 cells. Unfortunately however, EGFR was not expressed at a high enough level on the arrays for reliable observations to be made and pS2 was not represented on these small format arrays. The genes therefore selected were firstly CD59 (Rushmere *et al.*, 2004), a further known E2-suppressed/anti-oestrogen-induced gene in MCF-7 cells. This gene is also expressed in clinical breast cancer and is linked with immune surveillance and known to limit anti-oestrogen inhibitory effect. The second gene chosen was amphiregulin, an E2-induced/anti-oestrogen suppressed gene (Martinez-Lacaci *et al.*, 1996). In parallel with using Genesifter to extract the array profile for these genes, RT-PCR analysis was performed on the RNA used to create the arrays to verify profiles across the treatment groups.

The array profile is largely in agreement with the known E2-suppressed, anti-oestrogen-induced profile for CD59 which can be seen in Figure 3.15. CD59 is a readily detectable gene in MCF-7 cells (log intensity >0). The day 7 array profile shows a very slight decrease in CD59 with E2 treatment together with a

substantial increase in expression with tamoxifen or faslodex treatment compared to both untreated and E2 treated MCF-7 cells. Although the day 10 array profile did not show a prominent tamoxifen induction of CD59, there was an obvious faslodex induction coupled to a small E2-suppression. This acceptable array profile for CD59 in general shows a similar profile to that obtained by subsequent RT-PCR (Figure 3.16) on the samples, in that there was again some indication of E2-suppression and anti-oestrogen-induction. It can be seen that tamoxifen induction was apparent at day 4 and 7 versus untreated control (28%, 20%), while faslodex also showed a more substantial increase at these earlier time points (80%, 57%). Interestingly untreated control levels increased with time, increasing by 120% by day 10. Indeed at 10 days, untreated control levels were elevated such that they were equivalent to the high levels achieved with anti-oestrogen treatment. Following the E2 profile over days 4, 7 and 10, it can be seen that the E2 suppression versus untreated control becomes more substantial (8%, 30%, 65% respectively) with increased treatment time. Thus the control data appeared to reflect E2 depletion of the MCF-7 cells under untreated control conditions.

The array profile for the classically E2-induced/anti-oestrogen-suppressed gene amphiregulin can be seen in Figure 3.17. This was a lowly expressed gene (log intensity <0), however day 7 treatment was able to reveal the expected decrease in amphiregulin levels with tamoxifen and faslodex, compared to both untreated control and E2 treatment. By day 10 the level of amphiregulin had reached slightly higher levels in the E2 versus untreated control, with lower

levels again with tamoxifen or faslodex treatment. The parallel RT-PCR profile for amphiregulin is shown in Figure 3.18. The gene was again very lowly expressed, and in this instance only the E2-induction was detectable by RT-PCR reaching a maximum increase of 70% by days 7 and 10. Because of the low levels of amphiregulin in the untreated control samples, no suppression of this gene was observed with anti-oestrogen treatment.

In summary, when the general trend of these profiles is looked at there is a broad correlation between the array profiles and RT-PCR. The arrays have successfully shown some E2-suppression and anti-oestrogen-induction for CD59, and slight E2-induction with anti-oestrogen-suppression for amphiregulin as previously reported. There was also a correlation between the general expression level detected with the arrays and RT-PCR, where the readily detectable levels of CD59 on the arrays (log intensity >0) is mirrored by a low associated cycle number of 25 required for optimal PCR signal. In contrast, the log intensity levels of amphiregulin were low on the arrays (log intensity <0) and the RT-PCR required a higher cycle number of 29 for optimal signal.

These findings indicate the day 7 and 10 arrays should be appropriate to reveal anti-oestrogen-induced genes, although subsequent RT-PCR verification over days 4 to 10 was required to evaluate if there is an equivalent effect of E2 deprivation (ED) under the control conditions.

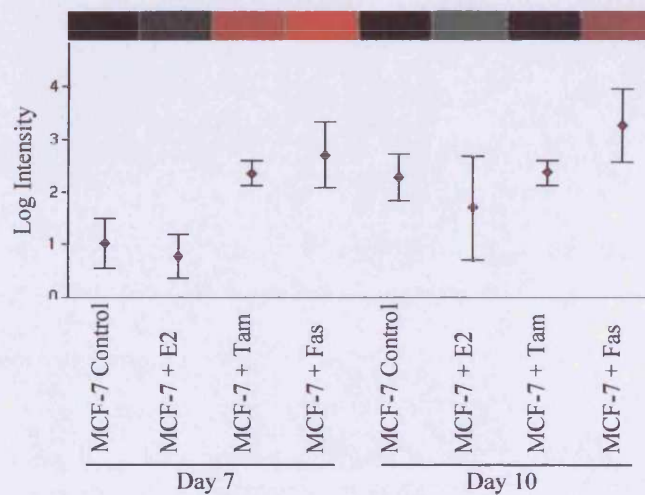


**Figure 3.15** CD59 array heatmap and expression profile at days 7 and 10

The array heatmap and log intensity profile for CD59 in untreated control, E2 ( $10^{-9}$ M), tamoxifen ( $10^{-7}$ M) or faslodex ( $10^{-7}$ M) treated MCF-7 RNA preparation after 7 and 10 days are illustrated. In the heatmap, red denotes an increase in CD59 expression and green a decrease compared to the control which is shown in black, as is a no change in expression levels compared to the untreated control. Also shown is the log intensity array profile, after median normalization and log transformation of three independent sets of replicate densitometric data  $\pm$  SEM.

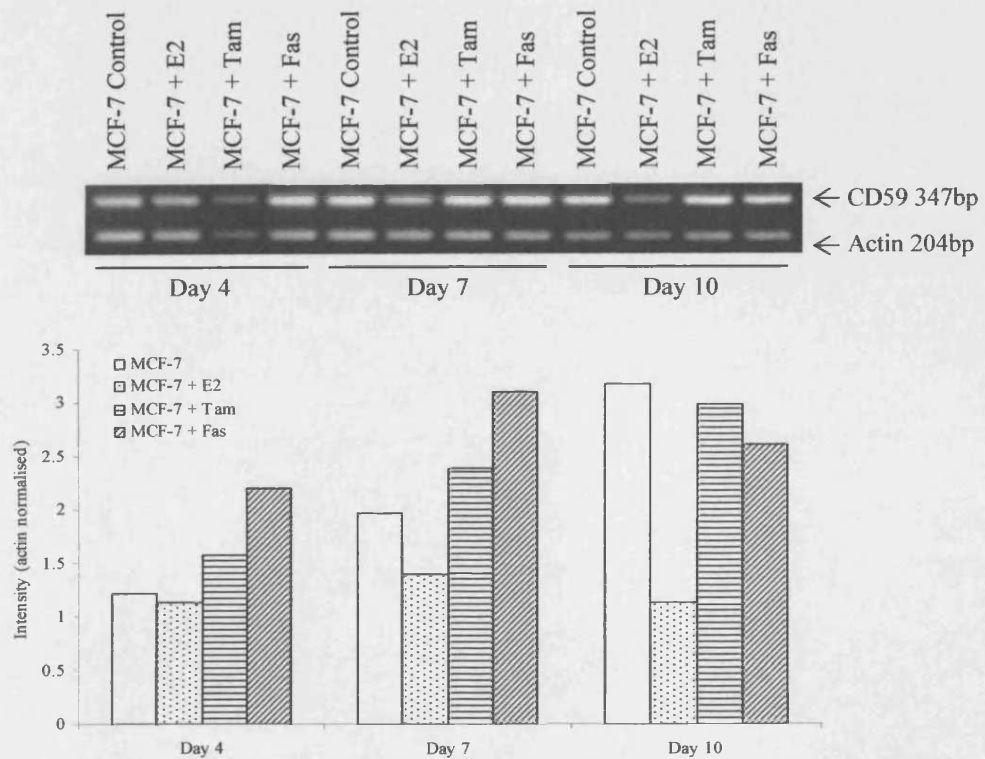


**Figure 3.16** Levels of CD59 mRNA in treated MCF-7 cells by RT-PCR in day 4, 7 and 10 array samples

MCF-7 cells were grown for 4, 7 and 10 days either untreated, treated with E2 ( $10^{-9}$ M), tamoxifen ( $10^{-7}$ M) or faslodex ( $10^{-7}$ M). RNA extracted from these cells was subject to RT-PCR using CD59 and  $\beta$ -actin specific primers, to parallel array analysis on these samples. The graph represents CD59 mRNA levels after  $\beta$ -actin normalization, with a representative PCR gel displayed.

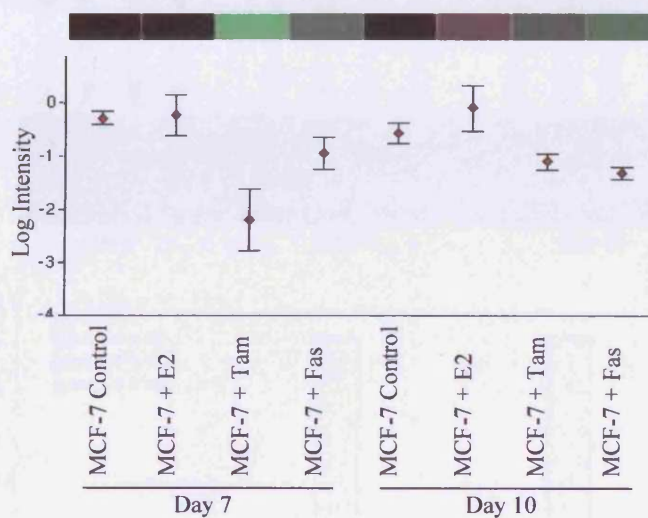
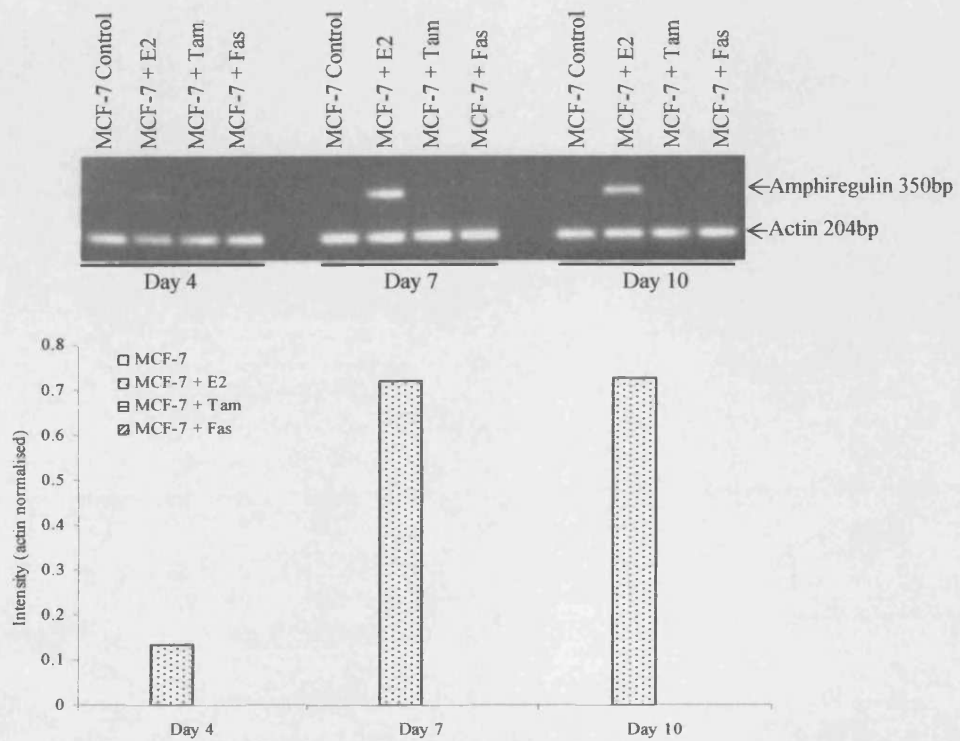


Figure 3.17 Amphiregulin array heatmap and expression profile at days 7 and 10

Illustrated is the array heatmap and log intensity profile for amphiregulin in untreated MCF-7 RNA preparations, or after 7 or 10 days of treatment with E2 ( $10^{-9}$ M), tamoxifen ( $10^{-7}$ M) or faslodex ( $10^{-7}$ M). Annotation information for this data is given in figure 3.15.



**Figure 3.18** Levels of amphiregulin mRNA in treated MCF-7 cells by RT-PCR in day 4, 7 and 10 array samples

The mRNA from MCF-7 cells either untreated, or treated with E2 ( $10^{-9}$ M), tamoxifen ( $10^{-7}$ M) or faslodex ( $10^{-7}$ M) for 4, 7 or 10 days was subject to RT-PCR with amphiregulin and  $\beta$ -actin specific primers to parallel array analysis on these samples. The graph represents the mRNA amphiregulin levels after  $\beta$ -actin normalization, with a representative PCR gel displayed.



### 3.1.5 Anti-oestrogen induced gene selection by expression profiling

#### 3.1.5.1 Venn diagrams

Scatter plots show the general distribution of all the genes on the arrays together with their levels of expression, and allow a broad estimation of induced and decreased genes to be made, such displays do not easily allow for detailed comparison at a gene number level, or across more than two treatments or time points to select robustly, persistently anti-oestrogen induced genes. To ensure that no genes were overlooked in the search for anti-oestrogen induced genes, selection took place versus both the untreated control and E2 treated MCF-7 cells separately and in combination. Such comparisons were made using Venn diagrams, as can be seen in Figures 3.19 to 3.21. A relatively modest  $\geq 1.5$  fold increase in gene expression was selected as a cut off for this project, as a strategy to capture potentially small differences in expression due to treatment effects being examined within a single cell line (as opposed to between markedly different breast cancer models or clinical samples) (Levenson *et al.*, 2002).

##### 3.1.5.1.1 Genes induced at both day 7 & 10 versus untreated control

A Venn diagram showing the distribution of the 204 genes revealed to be persistently induced (i.e. both at days 7 and 10) according to treatment compared to the untreated control can be seen in Figure 3.19. The number on the periphery of each circle shows the total number of genes induced  $\geq 1.5$  fold at both days 7 and 10 by a particular treatment. As may be seen from the

diagram, tamoxifen treatment resulted in an increase in expression of 89 (44%) genes; E2 increased 90 (44%), while faslodex gave the largest increases at 127 (62%).

The total number of genes induced versus untreated control can be divided into three groups:

1. Genes that were induced at least 1.5 fold by a single treatment: 23 (11%) of the genes were induced by tamoxifen alone, 63 (31%) by faslodex alone and 43 (21%) by E2 alone.
2. Genes that were induced by two of the treatments: 28 (14%) of the genes were induced by 1.5 fold by both tamoxifen and faslodex, 11 (5%) by both tamoxifen and E2, and 9 (4%) by both faslodex and E2 compared to untreated control.
3. Genes that were induced by all three treatments, 27 (13%) of the genes induced  $\geq 1.5$  fold fell into this category.

#### 3.1.5.1.2 Genes induced at both day 7 & 10 versus oestradiol

Figure 3.20 shows that 116 genes were induced  $\geq 1.5$  fold at day 7 and 10 for tamoxifen, faslodex or control compared to the E2 treated sample. There are 37 (32%) of these induced with tamoxifen, 67 (58%) with faslodex and 44 (38%) increased in the untreated control compared to E2 treatment. Again, these genes can be divided into three groups.

1. Genes induced at least 1.5 fold by single treatments: 11 (9%) of the genes were induced with tamoxifen, 38 (33%) with faslodex and 37 (32%) by untreated control versus E2.
2. There were 23 (20%) genes induced by both tamoxifen and faslodex, 1 (1%) by both tamoxifen and untreated control, and 4 (3%) by both faslodex and untreated control.
3. Genes that were induced by all three treatments. There were 2 (2%) genes of all induced genes upregulated by tamoxifen, faslodex and untreated control compared to E2 treated cells.

#### 3.1.5.1.3 Anti-oestrogen induced genes

From the two Venn diagrams (Figures 3.19 and 3.20) the anti-oestrogen induced genes of greatest interest in this project fell into four groups:

1. The 28 genes induced by both tamoxifen and faslodex compared with untreated control.
2. The 27 genes induced by tamoxifen, faslodex and E2 compared to untreated control.
3. The 23 genes induced by both tamoxifen and faslodex compared with E2 treated cells.
4. The 2 genes induced by tamoxifen, faslodex and untreated control compared to the E2 treated cells.

This resulted in a total of 55 genes induced by anti-oestrogens versus untreated control samples and 25 genes induced versus E2 treated cells. The Venn diagram subsequently created to view this subset of genes can be seen in Figure 3.21, and shows a total of 60 unique genes induced by tamoxifen and faslodex at both day 7 and 10. The Venn diagram shows the 35 (58%) genes (listed in Table 3.2) induced by tamoxifen and faslodex compared to only the untreated control (fold change range 1.51-6.55), while 20 (33%) genes (listed in Table 3.3) are induced by tamoxifen and faslodex compared to both untreated and E2 treatment (fold change range 1.5-10.57). Only 5 (8%) genes (listed in Table 3.4) were induced versus E2 treatment alone (fold change range 1.51-7.72). These 60 genes were analysed in detail by pattern analysis using hierarchical clustering across days 7 and 10, subsequently investigating their ontology to further select a sub-set of anti-oestrogen induced genes that may feasibly limit growth inhibitory response to these agents for subsequent RT-PCR and protein verification.

#### 3.1.5.2 Hierarchical clustering to further explore gene profiles

Hierarchical clustering allowed for the complete expression profile of the 60 selected genes to be viewed across all four conditions and both day 7 and 10 time points, unlike the Venn diagrams. Figure 3.22 shows the hierarchical clustering by Genesifter™ and associated heatmaps across all groups for the 35 genes that are induced  $\geq 1.5$  fold by both tamoxifen and faslodex at days 7 and

10 compared to the untreated control. This software showed that the genes cluster into four main anti-oestrogen induced sub-groups:

- Group 1 contains 3 anti-oestrogen induced genes that showed a different profile over the day 7 and 10 time points, where at day 7 the level of expression was lower than at day 10 even though there is still a  $\geq 1.5$  fold increase in tamoxifen and faslodex compared with the untreated control. E2 also induced these genes by day 10 with only a barely detectable induction at day 7.
- Group 2 contains 7 genes that generally showed induction not only with tamoxifen and faslodex but also to some degree with E2 at both time points compared to the untreated control. Again with some evidence of a larger induction at day 10 than day 7.
- Group 3 contains 12 genes that are similar to group 2, except that the anti-oestrogen induced fold changes at day 7 and 10 are similar, and interestingly for several genes the E2 levels remained very low, (especially NME3/F11e by day 10).
- Group 4 contains a cluster of 13 genes that were induced to a higher level with faslodex compared to tamoxifen, but also induced (sometimes quite substantially) with E2.

Figure 3.23 illustrates the heatmap and clustering for the 5 genes that were induced 1.5 fold by tamoxifen and faslodex compared to lower levels with E2 treatment at days 7 and 10. These 5 genes split into two groups.

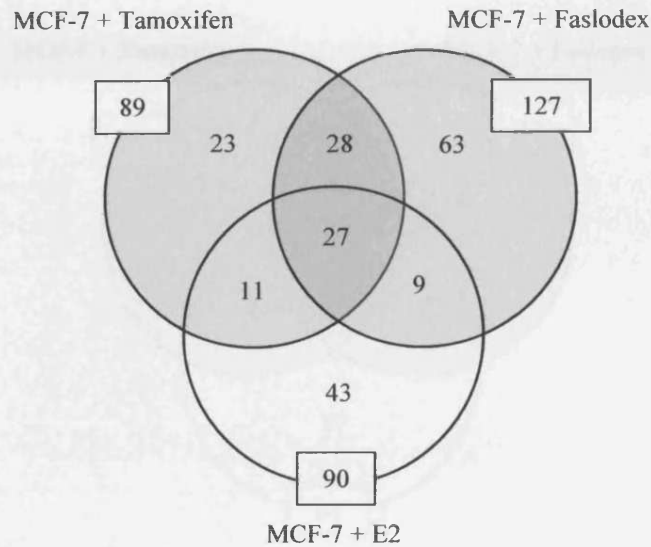
- Group 1 contains a single gene that showed a modest induction in the untreated control, as well as in tamoxifen and faslodex treated cells versus E2; this pattern was most obvious at day 7.
- Group 2 encompasses genes with a more obvious anti-oestrogen increase, particularly with faslodex after a day 10 treatment period. There is evidence of E2-suppression: Included in this cluster of 4 genes is CD59 (E111), the reported anti-oestrogen induced/E2 suppressed gene used to verify the arrays. It showed a slight induction by control versus E2 but never as large as faslodex treatment at day 10.

Figure 3.24 shows the heatmap and clustering for the 20 genes that are induced 1.5 fold by tamoxifen and faslodex compared to both the untreated control and E2 treated MCF-7 cells over both the days 7 and 10 time points. The genes have been hierarchically clustered into three further sub-groups:

- Group 1 the majority of the genes in this cluster generally showed the largest difference in expression between the untreated control/E2 treatment and tamoxifen/faslodex treatment by day 10, although increases were also seen at day 7. There were low levels in both untreated control and E2 treated samples.
- Group 2 genes in this cluster showed generally a larger difference at day 7 than day 10, particularly versus the untreated control where very low levels are achieved.

- Group 3 genes show roughly equivalent increases with tamoxifen and faslodex treatment at both days 7 and 10, with lower levels in both the untreated control and E2 treated samples.

Of all the genes in the three heatmaps, the ones of most interest to this project (i.e. anti-oestrogen induced) are those that are induced by tamoxifen and faslodex versus the untreated control and versus E2 treatment (where they may be suppressed further). The majority of these genes are obviously found in Figure 3.24, but some are also recorded from Figure 3.23 (cluster 2) and Figure 3.22 (cluster 3). However, it is noteworthy that anti-oestrogen induced genes may also be worthy of further study if their reported ontology is interesting in the context of limiting therapeutic response, even if their profiles were weaker. Therefore ontological deciphering of 60 genes was performed.



**Figure 3.19 Venn diagram showing the 204 genes upregulated by treatment at both day 7 & 10 versus untreated control**

The Venn diagram show the number of genes that were upregulated  $\geq 1.5$  fold at both the day 7 and day 10 time points when MCF-7 cells were treated with tamoxifen ( $10^{-7}\text{M}$ ), faslodex ( $10^{-7}\text{M}$ ) or E2 ( $10^{-9}\text{M}$ ) compared with untreated control. Sub-sectors show the number of genes upregulated by both tamoxifen and faslodex, by both tamoxifen and E2, and by both faslodex and E2, as well as the number of genes upregulated by all treatments when compared to untreated MCF-7 control. The number in the box on the edge of the circle shows the total number of genes upregulated by the treatment.



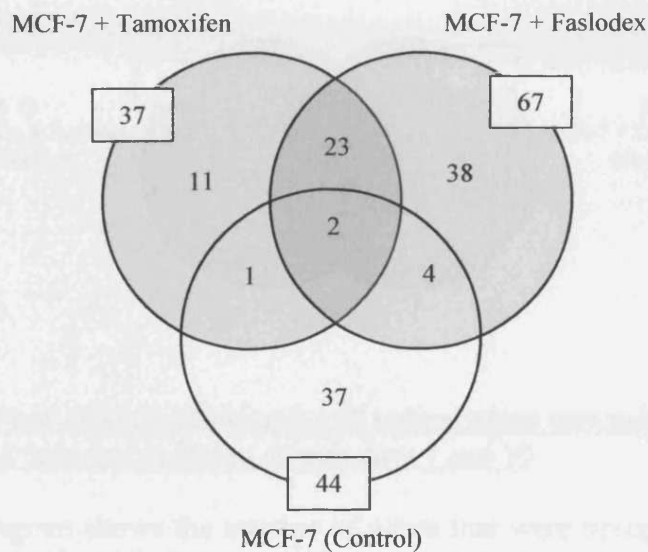


**Figure 3.20 Venn diagram showing the 116 upregulated genes by treatment at both Day 7 & 10 versus E2 treatment**

The Venn diagram show the number of genes that were upregulated  $\geq 1.5$  fold at both the day 7 and day 10 time points when MCF-7 cells were either untreated (-E2), treated with tamoxifen ( $10^{-7}$ M) or faslodex ( $10^{-7}$ M) compared with MCF-7 cells treated with E2 ( $10^{-9}$ M). Sub-sectors are as shown in figure 3.19 but compared with E2 treatment.

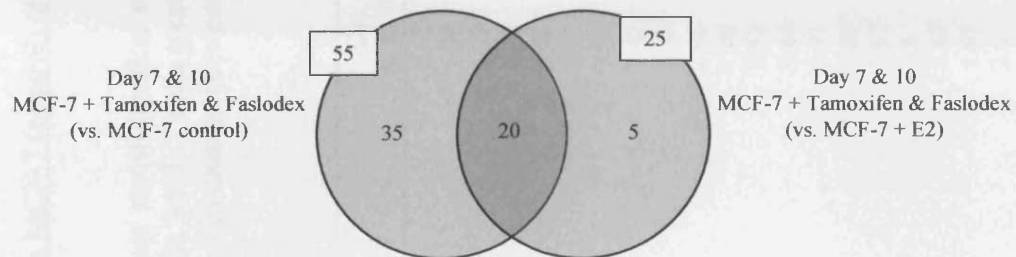


**Figure 3.21** Venn diagram showing the 60 unique genes upregulated by both tamoxifen and faslodex treatment at both days 7 and 10

The Venn diagram shows the number of genes that were upregulated by both tamoxifen ( $10^{-7}$ M) and faslodex ( $10^{-7}$ M) treatment compared to either untreated control or E2 ( $10^{-9}$ M) treated MCF-7 cells at both the day 7 and 10 time point. Also shown are the number of genes that are common to both of these anti-oestrogen induced groups. The number in the box is the total number of genes upregulated by a condition.

**Table 3.2 Fold changes of genes upregulated >1.5 fold in MCF-7 + Tam and MCF-7 + Fas versus MCF-7 (control) at both day 7 and 10 (n=35)**

Upregulated genes were selected from the arrays by profile after median normalisation and log transformation of intensity data in GeneSifter™. Shown in the table are the fold changes of the 35 genes that are  $\geq 1.5$  fold higher in MCF-7 cells treated with tamoxifen ( $10^{-7}$ M) or faslodex ( $10^{-7}$ M) compared with untreated MCF-7 cells over both 7 and 10 days. The fold change between untreated MCF-7 cells and for each gene at the two time points and with different treatments is shown.

Gene ID	Gene Name	Accession	Day 7 Fold Change		Day 10 Fold Change	
			C vs. T	C vs. F	C vs. T	C vs. F
A071	Ink4D	NM_079421	1.95	1.89	2.12	2.57
B01k	Cytchesin-1	NM_017456	1.73	1.54	1.99	1.88
B04f	Rho C	NM_005168	2.62	2.86	1.74	2.25
B05i	PP6	NM_002721	1.54	1.97	1.57	2.03
B071	S100A4	NM_002961	2.25	2.18	6.55	3.09
B08m	Dishevelled	NM_004421	2	1.68	3.91	1.97
B12f	MST-1	NM_006282	1.66	1.96	3.61	2.86
B12j	Rac 2	NM_002872	1.8	1.52	3.41	2.64
B13h	PPEF2	NM_006239	1.57	1.76	3.27	2.68
C04k	NF-kB	NM_003998	3.22	3.99	2.46	2.71
C08g	Mutl protein homolog	NM_000249	1.51	1.73	1.66	1.78
D06b	HMGN2	NM_005517	3.05	2.14	2.53	3.2
E02g	Taxilin alpha	NM_175852	1.93	1.62	3.44	2.85
E14g	Ephrin-B1 precursor	NM_004429	1.63	1.56	3.71	2.39
F01k	Ribosomal protein L10	NM_006013	4.84	2.56	1.88	1.68
F02i	LySP100	NM_007237	1.55	1.96	3.37	3.39
F03i	Haemoglobin alpha 1	NM_000558	1.63	2.06	1.6	2.2
F03j	NCBP1	NM_002486	2.5	1.95	1.67	1.95
F04k	60s ribosomal protein L5	NM_000969	5.66	4.93	1.91	2.35
F05k	RPL32	NM_000994	4.21	3.02	2.6	2.99

F06b	Aldehyde oxidase	NM_001159	1.69	2.62	1.6	2.62
F06i	THOC1	NM_005131	2.44	2.96	1.84	2.97
F06j	PPAP2B	NM_003713	2.11	3.16	1.53	3.03
F06k	elf-2B	NM_003908	3.57	3.12	1.51	3.27
F07h	RAN	NM_006325	2.79	3.45	1.57	1.95
F07k	elf-2A	NM_004094	2.68	5.43	2.07	2.92
F10h	AKAP1	NM_003488	3.44	3.38	1.57	2.89
F10j	Supp. for yeast mutant 1	NM_001536	1.89	2.53	1.93	1.64
F11e	NME3	NM_002513	2.55	2.2	1.71	2.2
F11j	elf-4E	NM_001968	4.98	4.25	2.28	2.33
F12i	Ribonuclease 6 precursor	NM_003730	3	3.66	2.02	2.76
F12j	EFl alpha	NM_001402	3.62	3.15	2.08	2.5
F14i	DEAD box polypeptide	NM_006773	4.12	4.07	3.53	2.82
F14j	RPS16	NM_001020	3.31	2.95	2.47	2.55
G15	HGPR1	NM_000194	1.78	1.7	1.66	3.94

C = untreated MCF-7, T = MCF-7 + tamoxifen, F = MCF-7 + Fastodex

**Table 3.3 Fold change of genes upregulated >1.5 fold in MCF-7 + Tam and MCF-7 + Fas versus both MCF-7 (control) and MCF-7 + E2 at both day 7 and 10 (n=20)**

Upregulated genes were selected from the arrays after median normalisation and log transformation in GeneSifter™. Shown in the table are the fold changes of the 20 genes that are ≥1.5 fold higher in MCF-7 cells treated with tamoxifen (10<sup>-7</sup>M) or faslodex (10<sup>-7</sup>M) compared with both untreated MCF-7 cells and MCF-7 cells treated with E2 (10<sup>-9</sup>M) at both 7 and 10 days.

Gene ID	Gene Name	Accession	Day 7 Fold Change				Day 10 Fold Change			
			C vs. T	C vs. F	E2 vs. T	E2 vs. F	C vs. T	C vs. F	E2 vs. T	E2 vs. F
B01m	LAT	NM_014387	2.46	2.77	1.71	1.9	4.1	5.9	1.71	2.47
B05h	NDR protein kinase	NM_007271	2.99	2.94	2.61	2.57	1.6	2.3	1.52	2.19
B13i	Rac 1	NM_006908	4.14	4.76	2.63	3.03	3.1	4.86	2.81	4.41
C02c	Bag-1	NM_004323	3.61	3.39	1.71	1.61	1.86	1.97	2.08	2.2
C06d	SUMO-1	NM_003352	3.24	3.92	2.26	2.73	1.8	4.16	1.86	4.29
C06m	PNRC2	NM_017761	2.61	3.02	1.65	1.92	4.31	7.13	3.21	5.31
C13i	HIF-1alpha	NM_001530	2.35	2.61	2.15	2.39	1.59	2.39	1.82	2.73
D02j	TKA	NM_002529	2.81	2.27	1.98	1.6	2.9	3.43	1.51	1.79
D07g	CAPR	NM_004389	2.13	2.54	1.73	2.05	6.21	5.14	4.18	3.46
E01f	FGF5	NM_033143	1.88	1.72	1.89	1.73	3.49	3.06	2.21	1.94
E01g	Interleukin 13	NM_002188	1.66	2.04	1.6	1.97	5.36	6.37	4.08	4.86
E02i	CD9 antigen	NM_001769	2.33	2.99	2.86	3.67	1.56	3.25	1.76	3.67
E07n	COL2A1	NM_001844	3.1	3.96	1.65	2.11	2.19	2.57	1.88	2.21
E14a	TGF-beta2	NM_003238	3.33	3.11	3.09	2.89	1.9	2.03	2.2	2.35
E14c	GMF-beta	NM_004124	9.47	10.57	2.02	2.25	1.61	3.03	1.63	3.08
F05j	Sialyltransferase 1	NM_003032	7.72	6.92	2.61	2.34	2.05	2.03	1.8	1.78
F07i	HNRNPK	NM_002140	4.08	4.98	2.01	2.45	2.56	3.55	1.83	2.54
F09h	TRAM	NM_014294	2.68	5.64	1.9	3.98	3.5	7.79	3.46	7.72
F11i	CstF 3	NM_001326	6.23	7.55	2.06	2.5	2.97	2.83	1.71	1.63
G13	14-3-3 zeta	NM_145690	1.56	1.7	1.69	2.14	1.5	4.74	1.84	5.78

C = Untreated MCF-7, E2 = MCF-7 + E2, T = MCF-7 + tamoxifen, F = MCF-7 + faslodex

**Table 3.4 Fold change of genes upregulated >1.5 fold in MCF-7 + Tam and MCF-7 + Fas versus MCF-7 + E2 at both day 7 and 10 (n=5)**

Upregulated genes were selected from the arrays after median normalisation and log transformation in GeneSifter™. Shown in the table are the fold changes of the 5 genes that are ≥1.5 fold higher in MCF-7 cells treated with tamoxifen (10<sup>-7</sup>M) or faslodex (10<sup>-7</sup>M) compared with MCF-7 cells treated with E2 (10<sup>-9</sup>M) over both 7 and 10 days.

Gene ID	Gene Name	Accession	Day 7 Fold change		Day 10 Fold Change	
			E2 vs. T	E2 vs. F	E2 vs. T	E2 vs. F
B10j	RhoE (RND3)	NM_005168	2.18	4.76	1.75	2.68
D02h	Delta catenin	NM_001332	2.08	2.65	1.55	2.76
D05k	PTK7 protein kinase 7	NM_002821	1.66	1.54	1.58	2.05
E01h	Ephrin-B2	NM_004093	1.85	3.16	2.84	3.44
E11i	CDS9	NM_203331	2.95	3.79	1.6	2.94

E2 = MCF-7 + E2, T = MCF-7 + tamoxifen, F = MCF-7 + faslodex

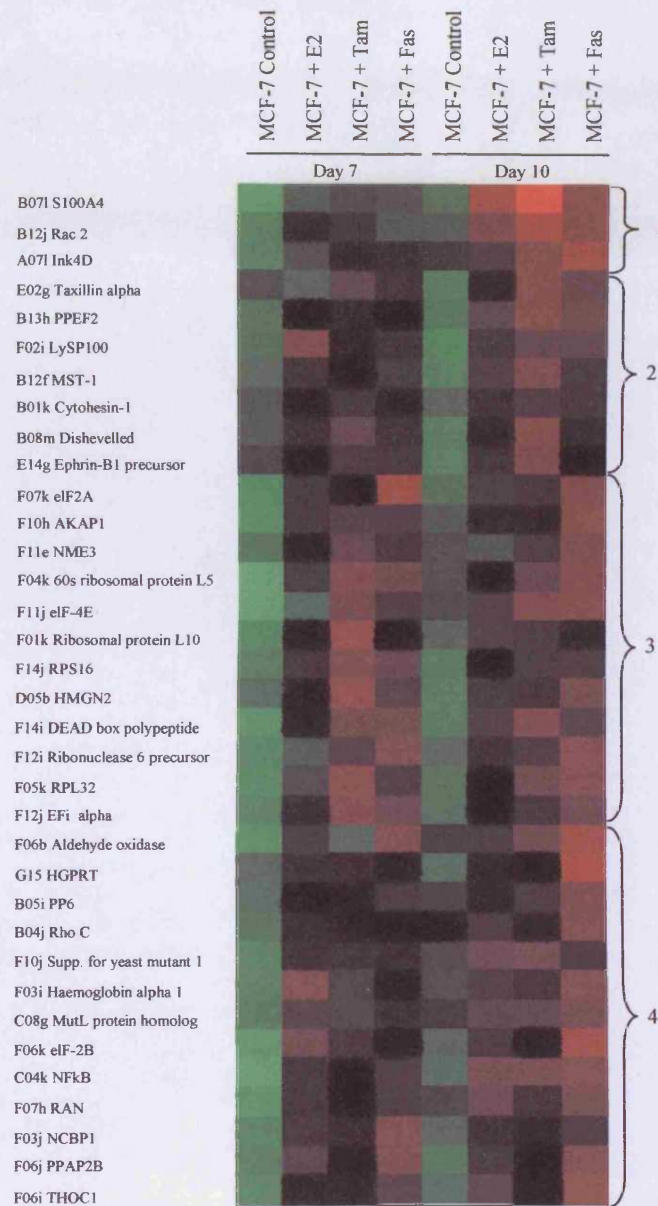


**Figure 3.22** Clustered heatmap of the 35 genes upregulated by tamoxifen and faslodex when compared with untreated control MCF-7 cells

The clustered heatmap for the 35 genes along with their name and Clontech ID's is shown. The genes upregulated  $\geq 1.5$  fold by both tamoxifen ( $10^{-7}$ M) and faslodex ( $10^{-7}$ M) compared to untreated MCF-7 cells at both day 7 and 10 are illustrated including the E2 arm. The red represents an increased expression level and the green a decrease, the brighter the shade the larger the increase or decrease. Also shown is the hierarchical clustering of the genes, the four main clusters have been numbered 1 to 4.

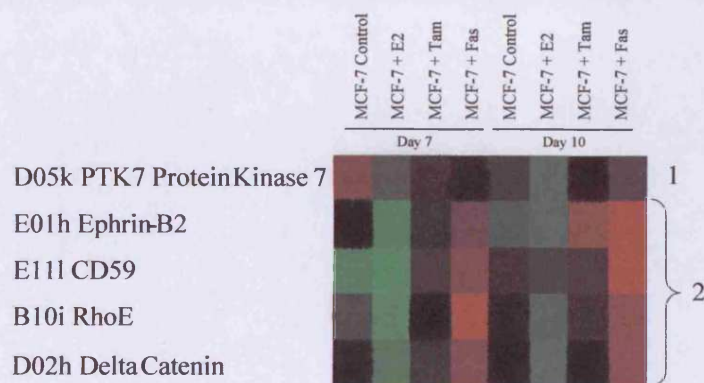


**Figure 3.23** Clustered heatmap of the 5 genes upregulated by tamoxifen and faslodex when compared with E2 treated MCF-7 cells

The clustered heatmap for the 5 genes that are upregulated  $\geq 1.5$  fold by both tamoxifen ( $10^{-7}\text{M}$ ) and faslodex ( $10^{-7}\text{M}$ ) compared to E2 ( $10^{-9}\text{M}$ ) treated MCF-7 cells at both day 7 and 10 is shown, including the untreated control arm. The two main clusters have been numbered 1 and 2. Annotation information is as overviewed in figure 3.22.



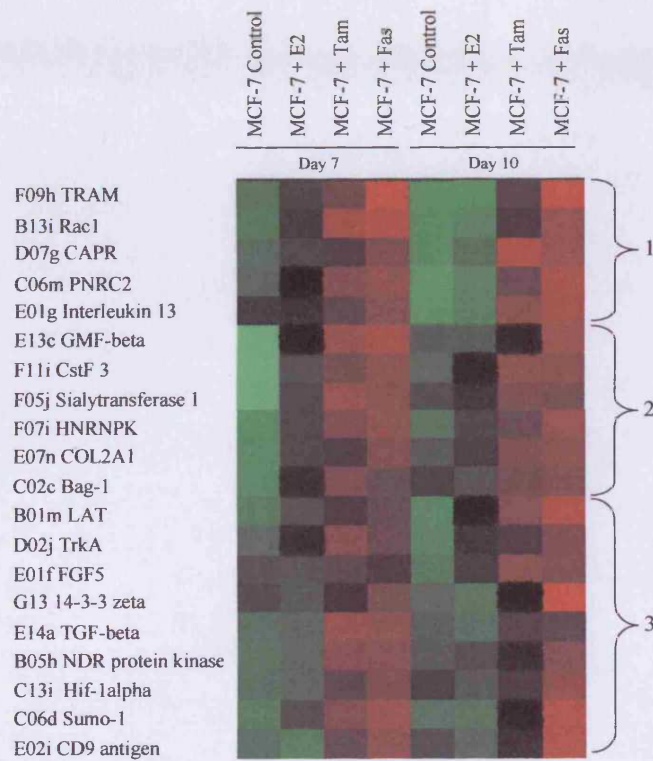


**Figure 3.24** Clustered heatmap of the 20 genes upregulated by tamoxifen and faslodex when compared with both untreated control and E2 treated MCF-7 cells

The clustered heatmap for the 20 genes that are upregulated  $\geq 1.5$  fold by both tamoxifen ( $10^{-7}$ M) and faslodex ( $10^{-7}$ M) compared to both untreated control and E2 ( $10^{-9}$ M) treated MCF-7 cells at both day 7 and 10 is shown. The three main clusters have been numbered 1-3. Annotation information is as stated in figure 3.22.

## **3.2 Detailed ontological analysis of the 60 anti-oestrogen induced genes & selection for verification**

### **3.2.1 Broad profiling of molecular function & cancer related ontology for the anti-oestrogen induced genes**

Following detailed array profiling across all conditions, ontology reports for the 60 genes induced by tamoxifen and faslodex (compared to untreated and/or E2 treated MCF-7 cells at day 7 and 10) were created in GeneSifter™ to aid in gene selection for verification. A pie chart can be seen in Figure 3.25, showing molecular functional ontologies (where some of the induced genes fall into more than one category). Binding function accounted for 50% of the induced genes, catalytic activity 19%, signal transduction 12%, structural molecular activity 8%, transcriptional regulation activity 4%, translational regulation activity 4%, enzyme regulation activity 1%, transporter activity 1% and finally unknown gene function at only 1%, in keeping with the generally well characterised genes represented on this type of array.

As well as investigating the general ontology of the induced genes, their ontologies in relation to cancer were investigated by extensive literature review in this project utilising Pubmed. Figure 3.26 shows the cancer related ontologies of the 60 genes. In keeping with the established anti-tumour effect of anti-oestrogens, the induced genes had been linked negatively to cell survival (pro-apoptotic 7%), proliferation (anti-proliferative 7%), halting of cell cycle (3%) or invasion (anti-invasive 2%, i.e. 19% in total). Interestingly

however, genes were also induced that were anti-apoptotic (12%), involved in immune escape (8%), pro-proliferative (7%), pro-angiogenic (5%) and invasion promoting (5%, i.e. 37% in total). There were also 13% of genes that had conflicting ontologies, where depending on cell line or phosphorylation state for example, they displayed different inhibitory/stimulatory properties, in some instances being able to promote adverse behaviour. There was also a large percentage (31%) of genes that were cancer-related, but with no specific function being defined. However, in general, considerable gene ontological evidence suggested that a significant percentage of the 60 identified genes induced by anti-oestrogens could potentially limit response or promote further aggressive features in the presence of these agents. From the cancer related ontology pie chart there are several categories that are of particular interest in this regard. For example, genes that fall into the anti-apoptotic, pro-proliferative and pro-invasive categories may aid cells to overcome the growth inhibitory effects of the anti-oestrogens and allow a subset of cells to persist and progress.

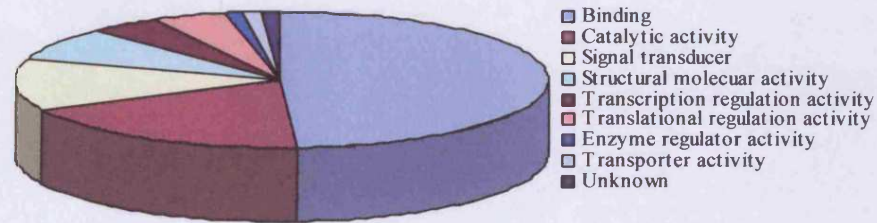


Figure 3.25 Molecular ontologies of the 60 anti-oestrogen upregulated genes

The Genesifter generated pie chart shows the molecular ontologies of the 60 tamoxifen and faslodex upregulated genes, where some of the genes fall into more than one category.

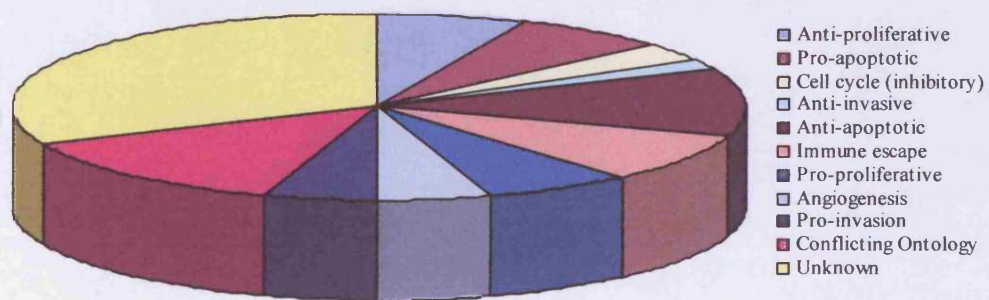


Figure 3.26 Cancer-related ontologies of the 60 anti-oestrogen upregulated genes

The pie chart shows the cancer related ontologies of the 60 genes upregulated 1.5 fold by tamoxifen and faslodex compared to untreated MCF-7 cells and/or E2 treated MCF-7 cells at both days 7 and 10.

### 3.2.2 Anti-oestrogen induced genes selected for verification

In order to finally select genes for verification it was imperative to draw together the detailed ontological and profile findings for the 60 genes. For this purpose, ontology and profile summary sheets were designed and compiled for each of the 60 anti-oestrogen induced genes. The resultant summary sheets for each gene aided in the elimination of unsuitable genes for verification based on the following criteria:

1. Poor array profile. Even though all 60 genes were anti-oestrogen induced compared with untreated control and/or E2 treatment, the size of SEM bars was not taken into account until this point in the selection procedure. Genes with large overlapping SEMs were eliminated to reduce the number of genes that required in-depth ontological analysis. Many genes were also eliminated from the group of 35 genes that were induced by tamoxifen and faslodex compared to untreated control where there was evidence of substantial E2 induction. This encompassed many of the genes found in Figure 3.22: cluster 4. NME3 (Flle) was retained from cluster 3 where E2 was suppressed at day 10.
2. Genes with strong anti-proliferative or pro-apoptotic properties. For example, cyclin dependent kinase 4 inhibitor D (Ink4D, A071) and transforming growth factor  $\beta$  (TGF $\beta$ , E14a) were excluded.
3. Genes with a poor ontological rationale or means of investigating further. This also included genes for which further validation would be difficult due to the lack of available antibodies or inhibitors, and genes

with poor future selective targeting potential (e.g. due to localisation or lack of regulatable activity).

RhoE (B10i) and  $\delta$ -catenin (D02h) were subsequently selected from the 5 genes up regulated by tamoxifen and faslodex compared to the E2 treatment in cluster 2 (Figure 3.23), and were each induced  $\sim 2$  fold with anti-oestrogens by day 10 (Table 3.4). The 4 genes subsequently selected from the 20 genes up regulated with tamoxifen and faslodex compared to both untreated control and E2 treatment were Bag-1 (C02c) found in cluster 2 and 14-3-3 $\zeta$  (G13), NDR protein kinase (B05h) and Hif-1 $\alpha$  (C13i) found in cluster 3 after hierarchical clustering of the genes (Figure 2.24). Bag-1, NDR and Hif-1 $\alpha$  were induced  $\sim 2$  fold by anti-oestrogens by day 10, but 14-3-3 $\zeta$  reached a  $\sim 5$  fold induction with faslodex by this time point (Table 3.3). The 2 genes subsequently selected from the 35 genes up regulated by tamoxifen and faslodex compared to the untreated control can be seen in Table 3.6. NME3 (F1le) was found in cluster 3, and NFkB1 (C04k) in cluster 4 after hierarchical clustering with both showing a  $\sim 2$  fold induction by day 10 (Figure 3.22). Even though the heatmap profile of NFkB1 showed an increase with E2 compared to the untreated control (Figure 3.22), the ontology results indicated that the gene was of particularly significant interest and so this gene was retained for study. The following sections detail the ontological results supportive of further study of these 8 genes, and subsequently their associated array profiles, RT-PCR verification, and protein investigation.

### 3.2.3 Ontological results of the 8 genes selected for verification

#### 3.2.3.1 RhoE

Ontological investigation revealed that RhoE is part of the Rnd subfamily of the Ras superfamily. The Rnd family also contains Rnd1, Rnd2 as well as RhoE which is also known as Rnd3. As part of the Ras family, the Rnd proteins are unusual as they show no detectable GTPase activity. The localization of RhoE is thought to be dependent on its phosphorylation state, however it has been found both at the plasma membrane and in the cytoplasm, particularly in the trans-golgi network (Riento *et al.*, 2003). RhoE has been shown to undergo post-translational modification by farnesylation which is the addition of a membrane attachment moiety (Riento *et al.*, 2005). The main regulatory function of RhoE appears to be in the actin cytoskeleton where its expression leads to lack of actin stress fibres, promoting cell rounding (Nobes *et al.*, 1998) and in the cell cycle. RhoE over-expression has been shown to induce cell migration due to the increased plasticity of focal adhesions and actin filaments (Chardin 2006). If RhoE is indeed increased in cells during anti-hormone treatment it may help to explain the increased invasive potential subsequently observed in the MCF-7 cell acquired tamoxifen and faslodex resistant models (Hiscox *et al.*, 2006). However, there is also evidence that RhoE can block cell cycle progression by inhibiting cyclin D1, leading to decreased proliferation (Villalonga *et al.*, 2004). This gene may therefore have dual function during anti-oestrogen treatment suppressing cell proliferation, while increasing their potential for invasiveness and motility.



### 3.2.3.2 Delta Catenin

The ontological analysis of  $\delta$ -catenin revealed that it belongs to the p120-catenin (p120<sup>ctn</sup>) protein family, a group of proteins characterized by the presence of ten Armadillo (ARM) repeat domains which allows binding of these proteins to the juxtamembrane segment of the classical cadherins. Through this binding, catenins can regulate cadherin function at the cell surface and thus modulate transmembrane cell-cell adhesion. Catenins also influence transcription through interactions with TCF/LEF where catenins play a key role in the development, morphogenesis and metastasis of tumours. The p120<sup>ctn</sup> subfamily can be further subdivided into two groups depending on their similarity to p120<sup>ctn</sup> and localization.  $\delta$ -catenin, which is also known as neural plakophilin-related Arm-repeat protein (NPRAP) or neurojungin, belongs to the group with most (>45%) homology to p120<sup>ctn</sup> (Anastasiadis and Reynolds 2000). Although  $\delta$ -catenin was thought to be a protein normally expressed almost exclusively in the nervous system, Burger *et al.* (2002) identified  $\delta$ -catenin as a potential marker for prostate cancer, indicating that its expression is not limited to the nervous system. The group also showed that  $\delta$ -catenin overexpression altered cell morphology and promoted growth factor-induced cell spreading, but did not increase cell proliferation (Burger *et al.*, 2002). As such, it is feasible that its increase by anti-oestrogens may again contribute to progression during treatment of breast cancer cells. Interestingly,  $\delta$ -catenin has also been shown to interact with the signalling molecule 14-3-3, an isoform of which has also been identified for further study in this project, through a

potential 14-3-3 binding site at the C-terminus of the  $\delta$ -catenin protein. The biological impact of this  $\delta$ -catenin/14-3-3 interaction is not yet known (Mackie and Aitken 2005).

### 3.2.3.3 Bag-1

Ontological deciphering revealed BCL-2 associated anthanogene (Bag-1) exists as four protein isoforms (p36, p46, p50 and p29) generated by the use of different transcription start sites from one gene. These different isoforms are localised to different regions within the cell (e.g. p50 in the nucleus and p36, p46, p29 in the cytoplasm) and interact with a vast array of molecular targets and modulate several regulatory pathways, including apoptosis, signalling, proliferation, cell motility and transcription. Interestingly it has been shown that Bag-1 can regulate or interact with several nuclear hormone receptors, for example, the ER. It is thought that this is mediated through interplay with heat shock protein 70 (Hsp70) (Townsend *et al.*, 2002). Bag-1 has also been identified, due to its association with BCL-2, as an anti-apoptotic molecule in several different cell types when over expressed. The expression of Bag-1 has been seen to suppress apoptosis induced by several different stimuli, including serum withdrawal, chemotherapy, radiation and heatshock (Townsend *et al.*, 2005). In addition to this it has been reported that increased cytoplasmic (p36) and nuclear (p50) Bag-1 in ZR-75-1 breast cancer cells accelerated cell growth and enhanced cell survival during growth factor deprivation (Kudoh *et al.*, 2002). Bag-1 levels have also been associated controversially with breast

cancer patient survival. High levels of Bag-1 in the cytoplasm were associated with increased patient survival in stage I and II disease and high nuclear levels were associated with decreased survival in stage I -IV disease (Tang *et al.*, 1999). Contrary to this, however there have been studies in early breast cancer that showed increased cytoplasmic Bag-1 levels had a positive effect on patient prognosis and that prior to, and during therapy, nuclear expression correlated with a less malignant phenotype (Krajewski *et al.*, 1999; Turner *et al.*, 2001).

#### 3.2.3.4 14-3-3 zeta

Ontological investigation of the anti-oestrogen induced 14-3-3 $\zeta$  gene revealed that the 14-3-3 family of cytoplasmic proteins regulate many different cellular processes, including apoptosis and proliferation. In the human 14-3-3 family there are 7 genes that encode for the highly conserved proteins,  $\beta$  (beta),  $\gamma$  (gamma),  $\epsilon$  (epsilon),  $\eta$  (eta),  $\sigma$  (sigma),  $\tau$  (tau) and  $\zeta$  (zeta). 14-3-3 proteins have been defined as phosphoserine-binding proteins that bind to consensus motifs to regulate cell signalling (Dougherty and Morrison 2004). More than one hundred proteins bind to 14-3-3 in a phosphorylation-dependent manner, including receptor proteins (e.g. insulin like growth factor 1 and glucocorticoid receptors), protein kinases (e.g. Raf1, MEK kinases and P13K), cell cycle control proteins (e.g. cdc25, p53, p27 and wee1), cytoskeletal proteins (e.g. vimentins and keratins), proteins involved in apoptosis (e.g. BAD) and proteins involved in transcriptional control (e.g. histone acetyltransferase and TATA box binding proteins). There are also several proteins that bind 14-3-3 in a

phosphorylation-independent manner, including the apoptosis regulator BAX (Mhawech 2005). 14-3-3 isoforms have been found at increased levels in several different cancers, including 14-3-3 $\zeta$  in lung cancer, oral squamous cell carcinomas, stomach and breast cancers (Tzivion *et al.*, 2006). In lung cancer cells the over-expression of 14-3-3 $\zeta$  has also been linked to poorer radioresponse via an interaction with CDC25C (Qi and Martinez 2003).

One of the most interesting features of 14-3-3 proteins (including zeta) in relation to this project is their role in apoptosis. 14-3-3 $\zeta$  has been linked to binding with both Bad and apoptosis signal-regulating kinase 1(ASK1), which are pro-apoptotic proteins. Bad belongs to the Bcl-2 family, other members including the pro-apoptotic elements BID and BAX and the anti-apoptotic Bcl-2 and Bcl-X<sub>L</sub>. When Bad is phosphorylated by Akt it becomes disassociated from Bcl-2 which is then able to move to the mitochondrial membrane and suppress apoptosis. 14-3-3 binds phosphorylated BAD, thus accelerating Bcl-2 disassociation to promote cell survival (Rosenquist 2003). Significantly, Masters *et al.* (2002) confirmed that Bad-induced apoptosis could be inhibited by 14-3-3 over-expression. There is also evidence that 14-3-3 can inhibit cell death induced via ASK1, a serine/threonine kinase. It has been reported that over-expression of 14-3-3 $\zeta$  inhibited wild type ASK1-induced apoptosis, but was without effect in cells bearing a mutated form of ASK1 where the phosphoserine binding motif was altered (Masters 2002). The anti-apoptotic properties of 14-3-3 $\zeta$  were particularly important when selecting it as an anti-oestrogen induced gene to study in further detail in this project.

Importantly, 14-3-3 is also linked to one of the other selected genes of interest within this project - NF $\kappa$ B. It is known that several 14-3-3 isoforms ( $\zeta$ ,  $\beta$ ,  $\eta$  and  $\epsilon$ ) can bind to the zinc finger protein A20 (Vincenz and Dixit 1996), whose expression is regulated by the apoptosis suppressing NF $\kappa$ B. The binding of A20 and 14-3-3 has been found to mediate interactions with c-Raf kinase, indicating the involvement of 14-3-3 in the link between signal transduction and apoptosis (Rosenquist 2003). It has also been reported that 14-3-3 $\zeta$  can interact directly with EGFR through an activation-dependent mechanism (Oksvold *et al.*, 2004). This is interesting since EGFR levels are also increased in MCF-7 cells treated with, and resistant to, anti-oestrogens (Gee *et al.*, 2003; Knowlden *et al.*, 2003; Nicholson *et al.*, 2005). There are reported links between 14-3-3 and insulin-like growth factor receptor (IGF-1R), a receptor which is associated with both tamoxifen sensitive and tamoxifen resistant cell growth (Gee *et al.*, 2005). IGF-1R appears to interact directly with 14-3-3 where interplay is dependent on phosphorylation of serines in the C-terminus of IGF-1R (Peruzzi *et al.*, 1999). It is thought that IGF-1R has an anti-apoptotic effect via three different intracellular pathways, all of which end with the phosphorylation of Bad, which as stated previously also interacts with 14-3-3 to promote cell survival.

One of the most studied 14-3-3 isoforms is 14-3-3 $\sigma$ , which is thought to control carcinogenesis through multiple mechanisms. Lui *et al.* (2006) identified, using functional proteomic analysis, that 14-3-3 $\sigma$  contributes to multi-drug resistance (MDR) in MCF-7 breast cancer cells resistant to both mitoxanthrone and

Adriamycin (Liu *et al.*, 2006). However, it has also been reported that p53 induces 14-3-3 $\sigma$  expression upon DNA damage, which arrests the cell in the G2/M phase of the cell cycle by binding to Cdc2-cyclinB complexes and sequestering them to the cytoplasm, thus acting as a tumour suppressor (Laronga *et al.*, 2000). Induced levels of 14-3-3 $\sigma$ , however, are very low in breast cancer due to the methylation of the 14-3-3 $\sigma$  promoter (Zhang *et al.*, 2004), and hence the release of the alternative isoform remains controversial. In total the 14-3-3 $\zeta$  isoform may feasibly contribute to cell survival signalling during anti-oestrogen treatment.

#### 3.2.3.5 Hif-1 $\alpha$

Ontological searching showed that Hypoxia-inducible factor alpha (Hif-1 $\alpha$ ) is a nuclear transcription factor whose expression is dependent on oxygen (O<sub>2</sub>) levels (Kimbrow and Simons 2006). Under hypoxic conditions Hif-1 $\alpha$  induces the transcription of over 60 genes, including vascular endothelial cell growth factor (VEGF). The protein products of many of these genes are involved with promotion of angiogenesis and erythropoiesis which increase the O<sub>2</sub> availability to cells, thereby promoting cell survival and invasive behaviour (Lee *et al.*, 2004). Hif-1 $\alpha$  has recently been linked to therapeutic resistance (Generali *et al.*, 2006) and as such its induction by anti-oestrogens may equally promote adverse behaviour. Before Hif-1 $\alpha$  can induce transcription it has to form a dimer with Hif-1 $\beta$ , which is also known as aryl hydrocarbon receptor nuclear translocator (ARNT). Hif-1 $\beta$  is constitutively expressed in the nucleus

regardless of O<sub>2</sub> levels, unlike Hif-1 $\alpha$  (Lee *et al.*, 2004). The protein stability of Hif-1 $\alpha$  is directly dependent on the levels of O<sub>2</sub>. The von Hippel-Lindau tumour suppressor (pVHL) mediated ubiquitin-proteasome pathway, after the post-translational hydroxylation of proline (Pro402/564), is responsible for the rapid degradation of Hif-1 $\alpha$  under normoxic conditions (Lee *et al.*, 2004). It has also been reported that several growth factors and cytokines can stabilise Hif-1 $\alpha$  such as EGF, TGF $\alpha$ , PDGF, IGF-1 and interleukin-1 $\beta$ , although the precise mechanism by which they do this is not yet fully understood (Zelzer *et al.*, 1998; Hellwig-Burgel *et al.*, 1999; Richard *et al.*, 2000; Pore *et al.*, 2006). In addition, Hif-1 $\alpha$  protein translation can be induced by growth factors regardless of the O<sub>2</sub> levels via the PI3K and MAPK signalling pathways (Lee *et al.*, 2004). In cancer there is often an increase in angiogenesis and vascularisation of tumours and many different cancers have been shown to have increased levels of Hif-1 $\alpha$  protein, including invasive breast cancer (Zhong *et al.*, 1999).

#### 3.2.3.6 NME3

Relatively little is known about the anti-oestrogen induced gene 'Protein expressed in Non-metastatic cells 3' (NME3), compared to the other members of the nm23 family. NME3, which is also known as DR-nm23, belongs to a family of five nm23 genes: nm23-H1, nm23-H2, NME3, nm23-H4 and nm23-H5. The most studied of these are nm23-H1 and nm23-H2 which have been defined as metastasis-supressor genes. All members of the nm23 family are

cytoplasmic and possess nucleoside diphosphate kinase (NDPK) activity which is associated with differentiation, proliferation and tumour progression (Negroni *et al.*, 2000). The few studies that have taken place on NME3 have been conflicting, indicating that a positive or negative effect of NME3 is dependent on cellular context. Venturelli *et al.* (1995) found that NME3 over-expression in 32Dcl3 cells resulted in apoptosis (Venturelli *et al.*, 1995). Contradicting this, Negroni *et al.* (2000) discovered that in neuroblastoma cells, NME3 over-expression protected cells from serum deprivation induced apoptosis (Negroni *et al.*, 2000). Thus, while its ontology is conflicting, induction of NME3 by anti-oestrogens could possibly facilitate breast cancer cell survival during treatment.

#### 3.2.3.7 NFkB1

Ontological analysis of NFkB1 has revealed that it is a member of a family of transcription factors key to several cellular processes, including proliferation, regulation of cell survival and differentiation, as well as controlling immune response and inflammation (Bours *et al.*, 2000). There are five members of the NFkB family in humans: NFkB1 (p50/p105), p65 (RelA), RelB, c-Rel, and NFkB2 (p52/p100), all characterised by the presence of a conserved 300 amino acid Rel homolog domain (RHD) at the N terminus of the protein. The RHD is responsible for DNA binding and dimerization of these transcription factors along with interactions with inhibitor of kB (IkB). The five NFkB family members exist either as homodimers or family heterodimers, which are bound



to I $\kappa$ B (e.g. Bcl-3, I $\kappa$ B $\alpha$ , I $\kappa$ B $\beta$ , I $\kappa$ B $\epsilon$  and I $\kappa$ B $\gamma$ ) proteins in unstimulated cells. The NF $\kappa$ B gene identified within this project as induced by anti-oestrogens was NF $\kappa$ B1, which encodes an I $\kappa$ B like protein precursor, p105. This protein undergoes proteolysis following phosphorylation by I $\kappa$ B kinase (IKK) complex (IKK $\alpha$ , IKK $\beta$  and IKK $\gamma$ ) to become the active form p50. The processed p50 subunit either forms a homodimer or heterodimer with other members of the NF $\kappa$ B family, where the most abundant dimer is reported to be p50/p65 (Karin *et al.*, 2002; Zhou *et al.*, 2005a).

I $\kappa$ B binding prevents NF $\kappa$ B translocation to the nucleus by masking its nuclear localisation sequence (NLS), thereby maintaining its cytoplasmic, transcriptionally-inactive state (Hayden and Ghosh 2004). However, phosphorylation of I $\kappa$ B by IKK causes its rapid ubiquitin-mediated proteasomal degradation, allowing a predominantly nuclear localisation for NF $\kappa$ B. The nuclear NF $\kappa$ B dimers are able to subsequently bind to specific DNA sequences, termed  $\kappa$ B sites (GGGRNNYYCC N=any base, R=purine and Y=pyrimidine), that are found in the promoter region of at least 150 target genes, enhancing their transcription. These include genes involved in inflammation, such as cytokines (e.g. IL-6 and TNF $\alpha$ ) and chemokines (eg IL-8 and RANTES); adhesion molecules (e.g. VCAM-1 and E-selectin); proliferation/cell survival associated genes (including cyclin D1, c-MYC, Bcl-2, Bcl-xL and IAPs) and also angiogenesis related genes (e.g. VEGF) (Magnani *et al.*, 2000; Karin *et al.*, 2002; Bonizzi and Karin 2004; Hayden and Ghosh 2004; Wu and Kral 2005). The activity of the NF $\kappa$ B dimer is normally

regulated by two main pathways. Firstly, the canonical (classical) NF $\kappa$ B activation pathway is activated in response to infection and proinflammatory cytokines which serve to activate the IKK complex. Interestingly, there is also evidence that growth factor signalling (e.g. EGFR) can activate the canonical NF $\kappa$ B pathway (Biswas and Iglehart 2006). The IKK complex phosphorylates the I $\kappa$ B protein, which in turn leads to its polyubiquitination and subsequent degradation by the 26S proteasome. This degradation of the I $\kappa$ B reveals the NF $\kappa$ B protein NLS, allowing it to translocate to the nucleus and initiate transcription. While all NF $\kappa$ B proteins can be regulated by this pathway, the most commonly regulated is the p50/RelA heterodimer (Bonizzi and Karin 2004). In contrast, the second pathway specifically affects IKK $\alpha$  and its interplay with NF $\kappa$ B2. Members of the tumour-necrosis factor (TNF) cytokine family activate both IKK $\alpha$  and NF $\kappa$ B-inducing kinase (NIK). Rather than acting on the I $\kappa$ Bs, IKK $\alpha$  and NIK directly initiate the phosphorylation-dependent proteolytic removal of the I $\kappa$ B like C-terminal of NF $\kappa$ B2 itself, to form the active p52 via polyubiquitination and proteasome degradation. The p52 protein preferentially forms a heterodimer with RelB, which translocates to the nucleus where it initiates transcription of genes thought to be involved in organogenesis (Karin *et al.*, 2002; Bonizzi and Karin 2004). A particularly interesting aspect of NF $\kappa$ B signalling in relation to breast cancer is its apparent negative regulation by E2 occupied ER, where ER can block NF $\kappa$ B activity by acting at several levels. Thus, E2 occupied ER has been shown to inhibit IKK activity, inhibit degradation of I $\kappa$ B, block DNA binding of NF $\kappa$ B, compete

with NFkB for binding to its co-activators, and bind to DNA-bound NFkB to inhibit its transcriptional activity (Kalaitzidis and Gilmore 2005).

As stated above NFkB has been associated with tumourigenesis through its ability to promote expression of genes involved in proliferation and survival of cancer cells as well as those that serve to increase metastatic and invasive potential (Bours *et al.*, 2000; Karin *et al.*, 2002). Perhaps not surprisingly, NFkB is thought to be a prominent factor in chemoresistance, through the induction of cell survival pathways. The strongest evidence that NFkB acts as a survival factor stems from studies in chemoresistant myeloma, which is caused by an accumulation of B-cells due to constitutively active NFkB. In addition to this, NFkB activity had been shown to be induced with chemotherapy treatment (e.g. daunorubicin, doxorubicin and paclitaxel), resulting in the initial expression of survival genes reducing the effectiveness of chemotherapy (Cusack 2003). Interestingly, NFkB has also been linked to development of anti-hormone resistant growth in breast cancer cells. Zhou *et al.* (2005) have shown that the level of NFkB binding activity is significantly increased in tamoxifen-resistant (ER-positive/ErbB2-positive) breast cancer cells compared with tamoxifen-sensitive (ER-positive/ErbB2-negative) MCF-7 cells, and is also elevated in clinical samples that demonstrate early tamoxifen relapse (Zhou *et al.*, 2005b). The PI3/Akt pathway has been shown to protect breast cancer cells from tamoxifen-induced apoptosis and promote resistance, including via activation of NFkB signalling. Tamoxifen-resistant MCF-7 cells with constitutively active Akt have significantly higher levels of NFkB DNA

binding and transcription-promoting activity as well as increased levels of phosphorylated I $\kappa$ B compared with the responsive control MCF-7 cells (deGraffenried *et al.*, 2004). Mouse mammary gland tumours engineered to over-express Her2 exhibit constitutive induction of NF $\kappa$ B downstream of PI3/Akt that promotes degradation of I $\kappa$ B $\alpha$ . E2-independent, ER<sup>+</sup> breast cancer cells have also been shown to have elevated NF $\kappa$ B activity along with elevated Bcl-3, this NF $\kappa$ B activity consisted primarily of p50 homodimers (with low levels of p50/p65). As well as acting as an I $\kappa$ B, Bcl-3 can act as transcriptional co-activator for p50 and p65 hetero/homodimers (Pratt *et al.*, 2003). Thus there is significant evidence that ER<sup>+</sup> anti-hormone resistance in breast cancer is in part dependent on the activation of NF $\kappa$ B. In addition, NF $\kappa$ B activation has also been observed in both *in vitro* and *in vivo* ER<sup>-ve</sup> breast cancers that over-express Her2, and is thought to be contributory to their proliferation and increased cell survival (Biswas *et al.*, 2004).

Given the emerging importance for NF $\kappa$ B in cancer, there are now several classes of NF $\kappa$ B pharmacological inhibitors available, where some are under investigation in clinical cancer trials. IKK inhibitors act by inhibiting the phosphorylation of I $\kappa$ B and hence the activation and nuclear translocation of NF $\kappa$ B. For example, the non-steroidal anti inflammatory drug salicylic acid (aspirin) inhibits IKK $\beta$ . However at present one of the most promising IKK inhibitors is parthenolide (isolated from the herb Feverfew), which binds to and inhibits IKK $\beta$  (Ravi and Bedi 2004). Parthenolide is currently in phase I clinical trials in cancer patients and has been well tolerated with no dose-

limiting toxicity. Purification of parthenolide, however, to achieve higher plasma concentrations is still required (Curry *et al.*, 2004). In addition, proteasome inhibitors, such as bortezomib (Velcade) or dipeptidyl boronic acid, can decrease ubiquitin-mediated degradation of I $\kappa$ B and hence block activation of p50 NF $\kappa$ B1 from p105 and p52 NF $\kappa$ B2 from p100 resulting in decreased overall levels of activated NF $\kappa$ B (Ravi and Bedi 2004). Bortezomib has been shown to have anti-tumour activity in several tumour types both alone and in combination with standard chemotherapeutic treatments (Olivier *et al.*, 2006). The treatment of refractory myeloma with bortezomib is currently being explored in phase III clinical trials, while trials in other cancer types (notably including breast cancer) are in their early stages (Cusack 2003; Ravi and Bedi 2004).

#### 3.2.3.8 NDR1 protein Kinase

Ontological results showed that NDR1 is a member of the nuclear DBf2-related (NDR) family of serine/threonine kinases, which is a subfamily of the AGC kinases (protein kinases A, G and C). Relatively little is known about the nuclear NDR1 protein kinase, but it is thought to participate in cell proliferation, tumour progression and cell morphology (Stegert *et al.*, 2005) and as such may be an interesting anti-oestrogen induced gene. Most studies on NDR1 have taken place in lower eukaryotes, such as *S. cerevisiae* (budding yeast) and *S. pombe* (Fission yeast). Cbk1, Dbf2 and Dbf20 are NDR1 homologues in *S. cerevisiae*, where all three proteins have been implicated in

the cell cycle. In *S. pombe*, the closest NDR1 homologue is Orb6 which is involved in cell morphogenesis (Tamaskovic *et al.*, 2003). The few studies that have taken place in mammalian cells have shown that NDR1 can be activated by S100B, which is a member of the S100 calcium-binding protein family and has been reported as over-expressed in over 80% of metastatic melanomas, and by Mps One Binder (Mob1), which has also been implicated in several different types of cancer (Devroe *et al.*, 2004). NDR1 was also identified by Adeyinka *et al.* (2002) using cDNA microarrays as one of several genes with greater expression levels in higher-grade ductal breast carcinoma *in situ* (DCIS), than low-grade tumours (Adeyinka *et al.*, 2002).

### **3.3 Full RNA Array profiles & PCR Validation for the 8 selected genes**

Genesifter was used to reveal the mean log intensity array profiles across the day 7 and 10 treatment periods for the eight selected genes. The genes were also subjected to an initial RT-PCR on the 3rd replicate set of array RNA samples (due to the limited quantity of RNA available from other replicates), with second-round validation RT-PCR on a single independent set of RNA across day 4, 7 and 10 time points. The day 4 RNA samples were included in all RT-PCR analysis as there was no evidence to suggest it was of an inferior quality. Importantly, in this section comparisons are made between:

- I. the oestrogen treated and untreated control/ED arms
- II. oestrogen and anti-oestrogen treated arms
- III. untreated control/ED and anti-oestrogen treated arms

For these reasons the second-round RT-PCR validation results present the untreated control MCF-7 cell arm as an oestrogen deprived (ED) condition in comparison with the anti-oestrogens and E2 treated samples. In this way it was hoped that similarities and dissimilarities between E2/ED and anti-oestrogens would be identified, as well as those associated with receptor occupancy by oestrogens and anti-oestrogen ligands.

### 3.3.1 RhoE

#### 3.3.1.1 Summary

Overall, the gene expression profiles revealed:

- I. a slight induction of RhoE upon E2 deprivation compared with E2
- II. an obvious anti-oestrogen induction of RhoE versus E2 treatment
- III. a faslodex induction of RhoE versus the untreated/ED arm, with no equivalent effect of tamoxifen

#### 3.3.1.2 Array profile

RhoE (B10j) was one of the 5 genes that was induced at least 1.5 fold by anti-oestrogen treatment compared with E2 at both day 7 and 10. When the 5 genes were hierarchically clustered, RhoE fell into cluster 2 of this gene set with some evidence of E2-suppression (Figure 3.23). Shown in Figure 3.27 is the array log intensity profile (and heatmap) generated for RhoE. The profile and heatmap show that at day 7 there was a decrease with E2 treatment, with some increase with tamoxifen, but a larger increase with faslodex treatment versus E2 (and to a lesser extent versus the untreated control). A similar result is seen at day 10, although the anti-oestrogen increases are more modest versus E2 or untreated control.

#### 3.3.1.3 RT-PCR profile with array RNA

The subsequent RT-PCR results for RhoE can be seen in Figure 3.28. The day 4 RT-PCR profile shows a decrease in RhoE levels with E2 treatment by 22%



compared with the untreated control. Tamoxifen treatment showed no marked difference versus E2 treatment and a modest decrease versus untreated control. However, faslodex treatment resulted in a large increase of 114% versus E2, and 68% versus untreated control. The day 7 results showed a very similar profile, but with a greater (54%) decrease with E2 treatment compared to the day 7 untreated control, and greater anti-oestrogen induction, particularly with faslodex, versus E2 treated. Expression levels with anti-oestrogens only exceeded untreated control with faslodex at this time point. At day 10, maximal suppression with E2 treatment is seen with a decrease of 66% compared to the day 10 untreated control. The anti-oestrogens significantly increased expression versus E2 treatment (i.e. tamoxifen 117% and faslodex 181%). At this time point the level of expression of the untreated control had increased by 65% compared to day 4 and so is largely the equivalent of faslodex treatment at this time point.

#### 3.3.1.4 RT-PCR Validation profile

Second round RT-PCR results are illustrated in Figure 3.29 and again showed E2-suppression and anti-oestrogen induction versus E2 at all time points. The RT-PCR results at day 4 were able to show a superior 192% and substantial 415% increase with tamoxifen and faslodex treatment respectively versus E2 treatment, and also increased with faslodex versus ED. Days 7 and 10 showed a similar E2-suppressed, anti-oestrogen induced profile versus E2 treatment. Removal of E2 from the medium promoted a continuous increase in RhoE

levels across day 4, 7 and 10 (217%, 93% and 113% respectively compared to E2 treatment), suggesting that ED was behaving as an anti-hormonal strategy largely comparable with anti-oestrogens by days 7 and 10.

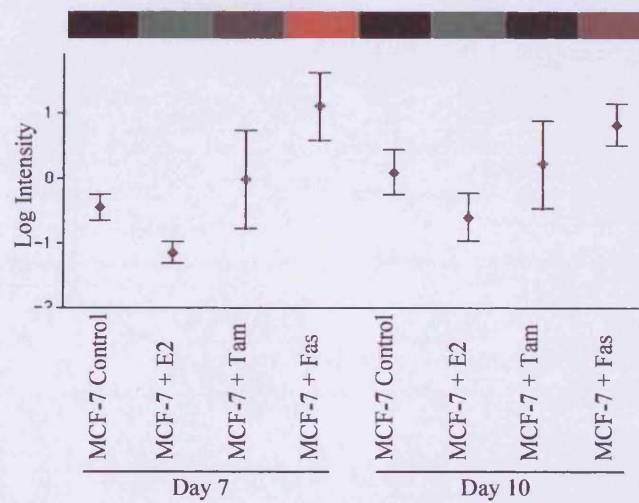
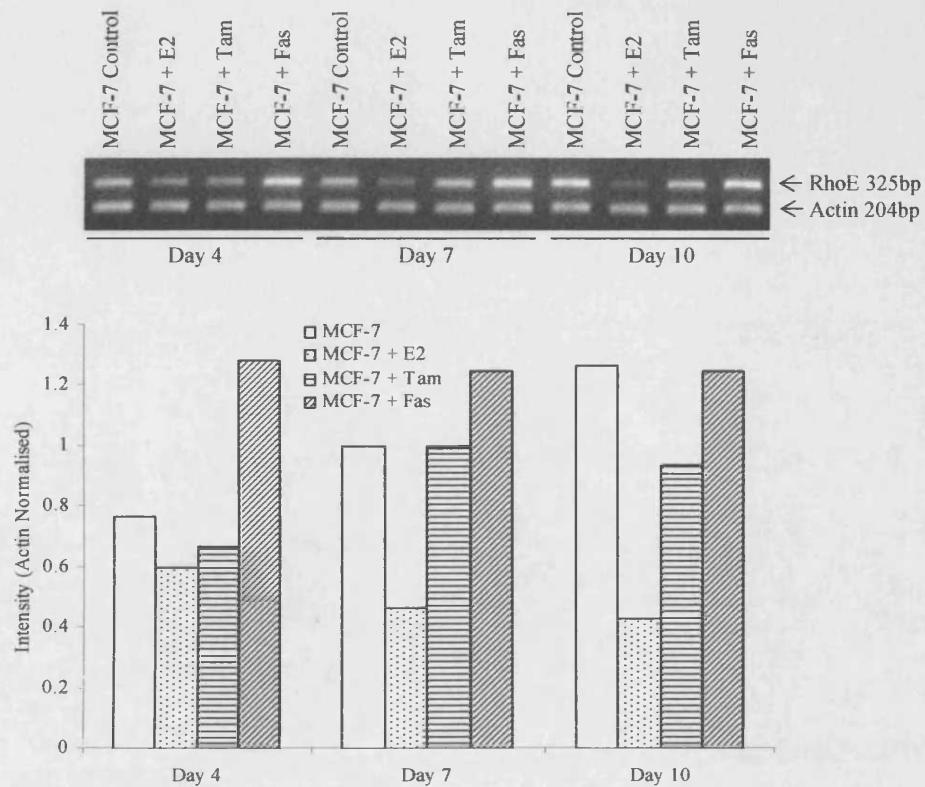


Figure 3.27 RhoE array heatmap and log intensity profile at days 7 and 10

Red indicates an increase and the green a decrease in mRNA levels with black indicating no change versus the MCF-7 control (also black). The RhoE array profile represents the mean of 3 independent replicates after median normalization and log transformation  $\pm$  SEM.



**Figure 3.28** RT-PCR analysis of RhoE mRNA in a sample set used to create arrays

RT-PCR was carried out on the mRNA (3rd set) used to create the arrays. Specific primers for RhoE and  $\beta$ -actin were used for amplification before size fractionation on an agarose gel. The graph represents the mRNA levels of RhoE after  $\beta$ -actin normalization at days 4, 7 and 10, with the associated PCR gel.

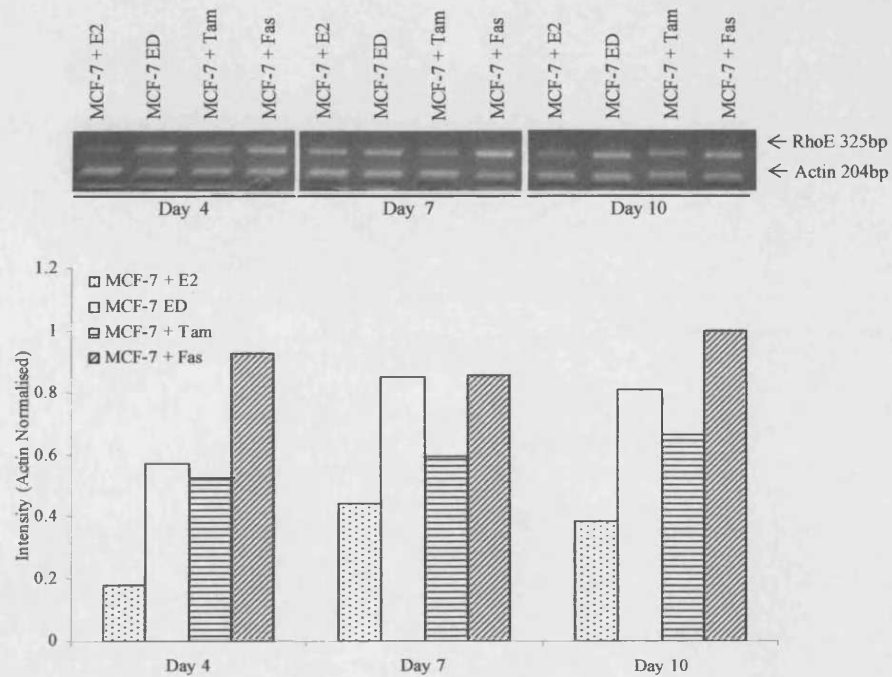


Figure 3.29 RT-PCR second round validation of RhoE

A validation set of RNA was prepared from MCF-7 cells untreated (ED) or treated with E2, tamoxifen or faslodex at days 4, 7 and 10. The mRNA was subject to RT-PCR using primers specific to RhoE and  $\beta$ -actin where the amplification products were size fractionated on an agarose gel. The graph represents the mRNA levels of RhoE after  $\beta$ -actin normalization at days 4, 7 and 10 with the associated PCR gel.

### 3.3.2 $\delta$ -catenin

#### 3.3.2.1 Summary

Overall the gene expression profiles revealed:

- I. an induction of  $\delta$ -catenin with ED compared to E2 treatment
- II. an induction with anti-oestrogens of  $\delta$ -catenin compared to E2 treatment
- III. the array profile showed faslodex but not tamoxifen as inducing  $\delta$ -catenin over ED, however in the RT-PCR neither anti-oestrogens were induced over ED

#### 3.3.2.2 Array profile

$\delta$ -catenin (D02h) was selected from the 5 genes that were induced by anti-oestrogens by at least 1.5 fold compared to E2 treated MCF-7 cells, found in cluster 2 after hierarchical clustering with some evidence of a modest E2 suppression (Figure 3.23). Figure 3.30 shows the heatmap and log intensity profile for  $\delta$ -catenin. The day 7 data showed a small decrease in  $\delta$ -catenin levels with E2 treatment versus untreated control, while tamoxifen treatment resulted in a modest increase and faslodex treatment a slightly larger increase versus E2 treatment, with much smaller increases versus untreated control. Day 10 shows a very similar profile with E2 treatment causing suppression of  $\delta$ -catenin versus untreated control, and faslodex treatment causing an increase in expression versus E2 treatment and to a lesser extent versus untreated control. Tamoxifen had no effect on the levels of  $\delta$ -catenin at day 10 relative to the untreated day 10 control but was again increased slightly versus E2 treatment.

### 3.3.2.3 RT-PCR profile with array RNA

RT-PCR analysis for  $\delta$ -catenin was carried out on the same third RNA sample set that was used to create the arrays to establish if the profiles were consistent. The RT-PCR profiles achieved for day 4, 7 and 10 (Figure 3.31) were very similar to each other and to the heatmaps. Significantly, E2 treatment decreased levels by approximately 50% versus untreated control. There was induction by anti-oestrogens versus E2 treatment at day 4 (tamoxifen 129%, faslodex 84%), day 7 (tamoxifen 80%, faslodex 191%) and day 10 (tamoxifen 136%, faslodex 114%). However the untreated control, tamoxifen and faslodex treated samples were all within 30% of each other, with no further induction by anti-oestrogens versus the untreated control.

### 3.3.2.4 Validation RT-PCR profile

RT-PCR for  $\delta$ -catenin was carried out on a second validation set of RNA. The results (Figure 3.32) were largely comparable with the initial RT-PCR results showing anti-oestrogen induction versus E2 treatment, and E2-suppression versus ED. At day 4, there was an increase in  $\delta$ -catenin levels with all three anti-hormonal strategies (ED 87%, tamoxifen 70% and faslodex 98%) compared with E2 treatment. This was mirrored across the day 7 and 10 time points. Again, there was a further induction by anti-oestrogens versus ED.

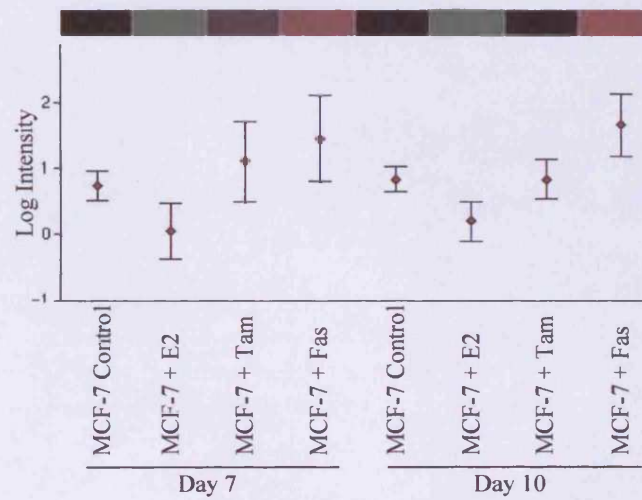


**Figure 3.30.**  $\delta$ -catenin array heatmap and log intensity profile at days 7 and 10

Array heatmaps and profiles were generated for  $\delta$ -catenin in GeneSifter<sup>TM</sup>. In the heatmap, red represents an increase, green a decrease and black a no change in mRNA levels of  $\delta$ -catenin relative to the MCF-7 untreated control level (also black). The log intensity profile shows the mean of 3 independent experiments after median normalization and log transformation  $\pm$  SEM.



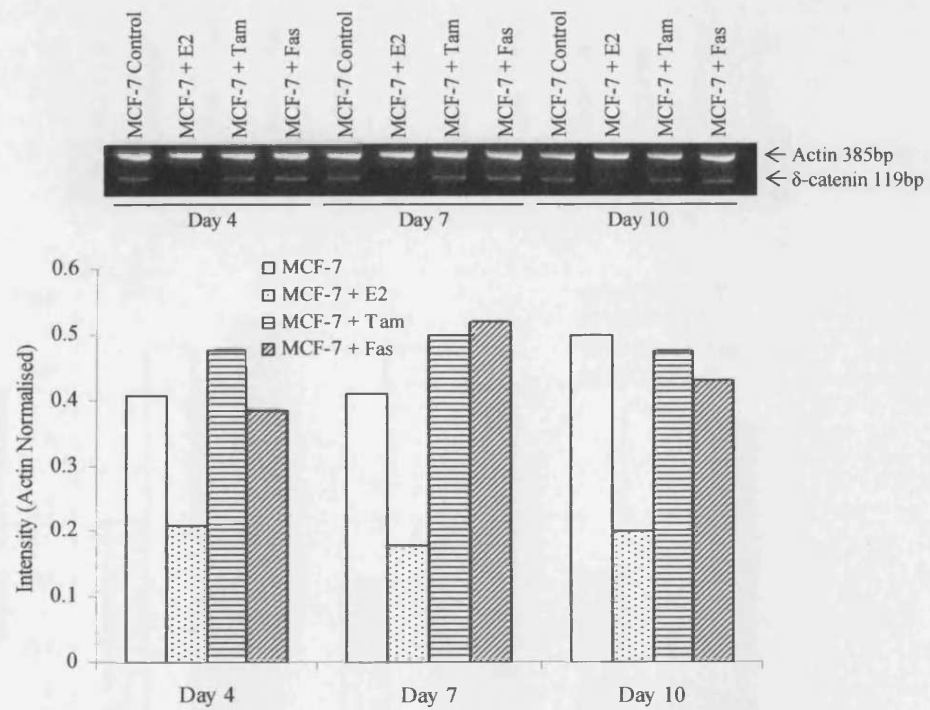


**Figure 3.31** RT-PCR analysis of  $\delta$ -catenin mRNA in a sample set used to create arrays

The mRNA 3rd set samples used to create the arrays were subject to RT-PCR analysis using specific primers for  $\delta$ -catenin and  $\beta$ -actin. The amplified products were size fractionated on an agarose gel. The graph shows the densitometric intensity representative of the mRNA levels of  $\delta$ -catenin after  $\beta$ -actin normalisation, with the associated PCR gel also shown.

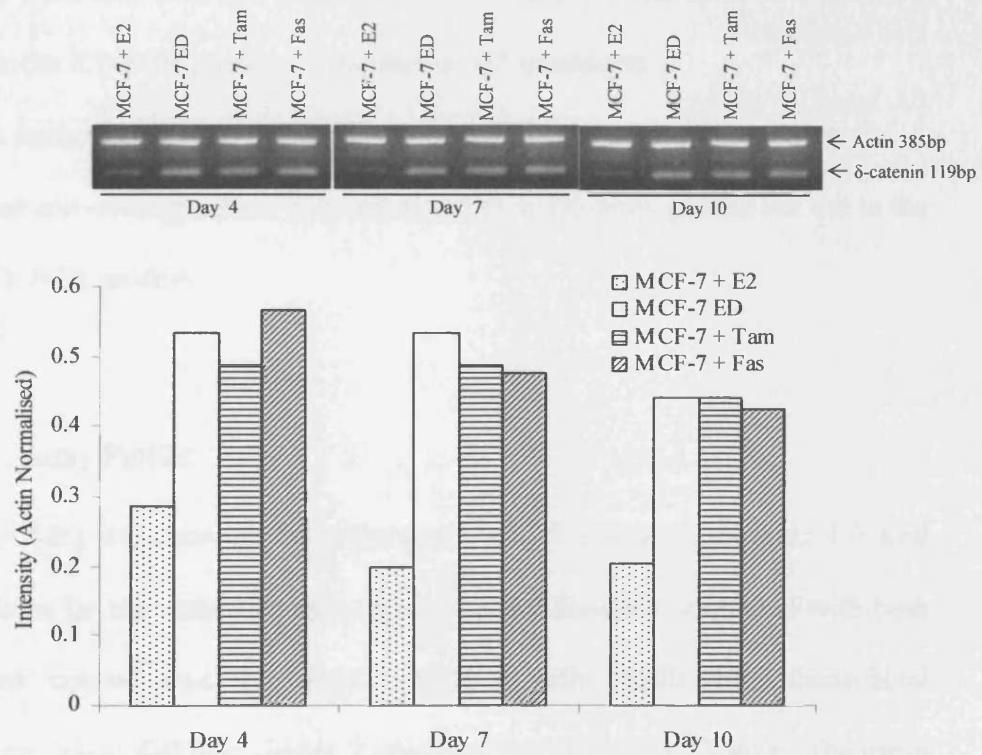


Figure 3.32 RT-PCR second round validation of  $\delta$ -catenin

A validation set of RNA was prepared from MCF-7 cells, either untreated (ED), treated with E2, tamoxifen or faslodex for 4, 7 and 10 days. This RNA was subject to RT-PCR using specific primers for  $\delta$ -catenin and  $\beta$ -actin. Amplified products were size fractionated on an agarose gel. The graph represents the mRNA levels of  $\delta$ -catenin after  $\beta$ -actin normalization, with the associated PCR gel shown.

### 3.3.3 Bag-1

#### 3.3.3.1 Summary

Overall the gene expression profiles revealed:

- I. no induction of Bag-1 with ED for the array profile, there was however for the RT-PCR profiles, compared to E2 treatment.
- II. an induction of Bag-1 with the anti-oestrogens versus E2 treatment
- III. that anti-oestrogens are induced over ED in the array profile but not in the RT-PCR profiles

#### 3.3.3.2 Array Profile

Bag-1 (C02c) was selected from the group of 20 genes which were 1.5 fold upregulated by the anti-hormones tamoxifen and faslodex compared with both untreated control and E2 treated MCF-7 cells. Following hierarchical clustering, Bag-1 fell into cluster 2 (Figure 3.24). Figure 3.33 shows the mean log intensity profile and intensity array heatmap, with obvious persistent anti-oestrogen induction of expression at days 7 and 10 versus untreated control and E2 treatment. While at day 7 there was an increase in Bag-1 levels after E2 treatment, there was an even larger increase with tamoxifen and faslodex treatment versus untreated control, and also versus E2 treatment. The day 10 profile showed that the untreated control and E2 treated samples had approximately the same levels of Bag-1, with anti-oestrogen treatment inducing gene levels versus both untreated control and also versus E2 treatment.

### 3.3.3.3 RT-PCR profile with array RNA

Based on the convincing anti-oestrogen induced profile and ontology, further RT-PCR analysis for Bag-1 was carried out to verify its anti-oestrogen induced expression. The detailed results are shown in Figure 3.34. The day 4 RT-PCR profile showed a marginal increase in expression with E2 (31%) and tamoxifen (12%) versus untreated control but this was much more obvious for faslodex versus untreated control (77%) and versus E2 treatment (34%). Compared to the day 7 untreated control, E2 treatment resulted in a 30% decrease. Tamoxifen and faslodex treatment caused a 41% and 12% increase respectively versus untreated control, and versus E2 treatment increase of 112% with tamoxifen and 68% with faslodex treatment. By day 7 the untreated control had increased by 45%, and after 10 days had further increased by 118% compared to the day 4 untreated control, revealing a substantial suppression by E2 treatment at this time point. The levels of Bag-1 in tamoxifen and faslodex treated cultures by day 10 were largely similar to those seen in untreated control and increased substantially versus E2 treatment.

### 3.3.3.4 Validation RT-PCR profile

Figure 3.35 shows the results from the RT-PCR validation, which was largely comparable with the initial RT-PCR by 10. Thus, Bag-1 profiles by day 10 revealed an induction with anti-oestrogens, as well as with ED when compared to the substantial suppression with E2 treatment, making this an interesting gene for further study.

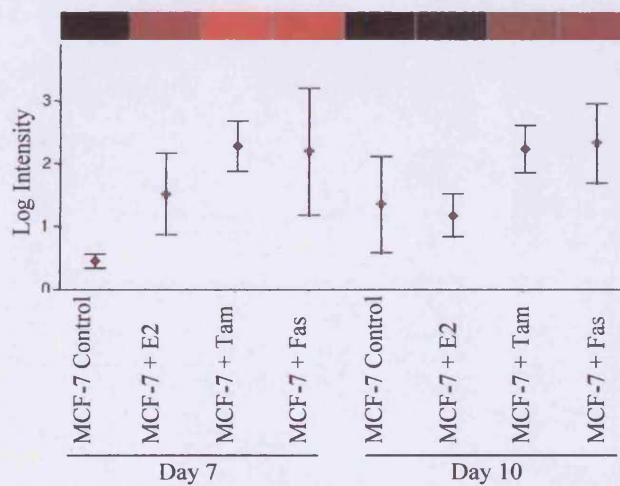
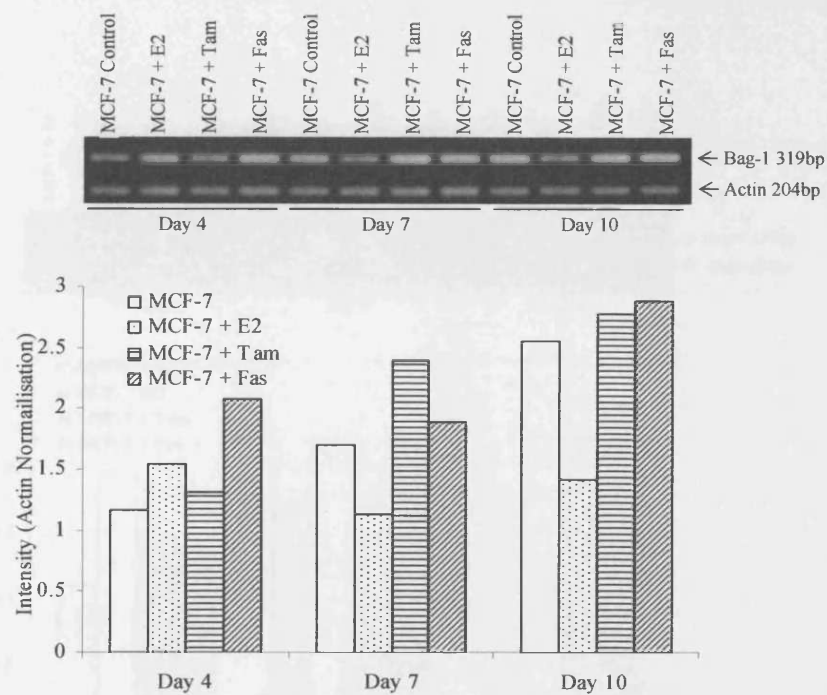


Figure 3.33 Bag-1 array heatmap and log intensity profile at days 7 and 10

Red on the heatmap indicates an increase and black a no change in the mRNA levels compared to MCF-7 untreated control (also black). The array log intensity profile shows the mRNA levels of 3 independent experiments after median normalization and log transformation  $\pm$  SEM.



**Figure 3.34** RT-PCR analysis of Bag-1 mRNA in a sample set used to create arrays

RT-PCR was carried out on the same mRNA (3rd set) used to create the arrays using specific primers to Bag-1 and  $\beta$ -actin. Amplified products were separated using agarose gel electrophoresis. The graph shows the densitometry for mRNA levels of Bag-1 after normalization to  $\beta$ -actin at days 4, 7 and 10, with the associated PCR gel.

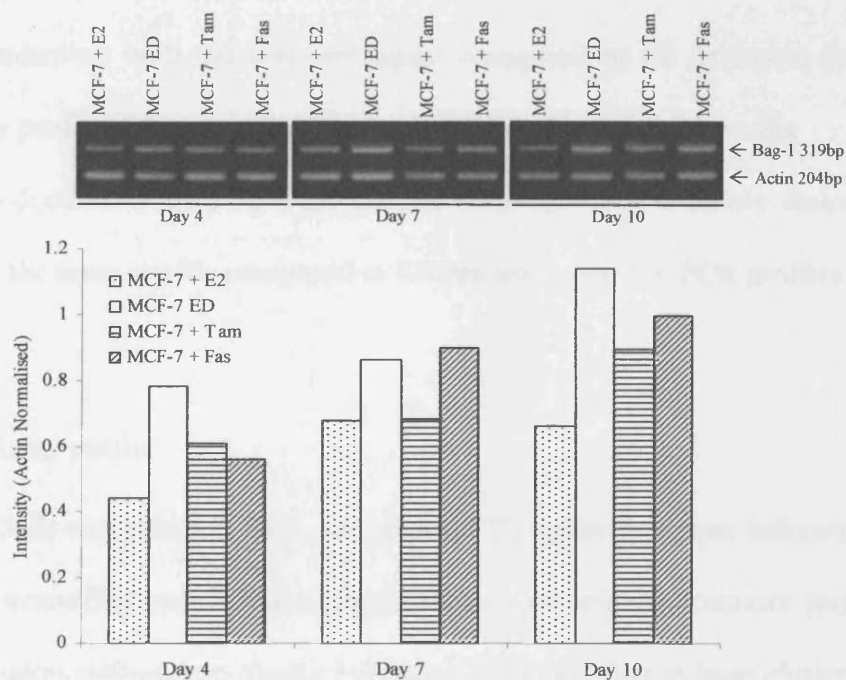


**Figure 3.35** RT-PCR second round validation of Bag-1

For validation purposes RNA was prepared from MCF-7 cells, either untreated (ED), or treated with E2, tamoxifen or faslodex at days 4, 7 and 10. The mRNA was subject to RT-PCR using primers specific to Bag-1 and  $\beta$ -actin. The amplified products generated were size fractionated on an agarose gel. The graph represents the mRNA levels of Bag-1 after  $\beta$ -actin normalization, with the associated PCR gel.

### 3.3.4 14-3-3 $\zeta$

#### 3.3.4.1 Summary

Overall the gene expression profiles revealed:

- I. no induction of 14-3-3 $\zeta$  under ED compared with E2 treatment until the later time point of the RT-PCR
- II. an induction with the anti-oestrogens compared to E2 treatment in the array profile, this was not consistently seen in the RT-PCR profile
- III. an induction of 14-3-3 $\zeta$  with the anti-oestrogens, particularly faslodex, with the array profile compared to ED but not in the RT-PCR profiles

#### 3.3.4.2 Array profile

14-3-3 $\zeta$  (G13) was selected from the group of 20 genes that were induced 1.5 fold with tamoxifen and faslodex compared to both untreated control and E2 treated samples, falling into cluster 3 (Figure 3.24) after hierarchical clustering. The 14-3-3 $\zeta$  array heatmap and log intensity profile can be seen in Figure 3.36 and shows a persistent induction by anti-oestrogens at days 7 and 10. The day 7 data showed that there was no expression change between E2 treatment and untreated control, but a small increase with anti-oestrogen treatment versus both E2 and untreated control. This profile became more prominent by day 10. At this time point there was also a slight decrease with E2 treatment versus untreated control, alongside the small increase with tamoxifen and substantial increase with faslodex treatment compared to the untreated control and also versus E2 treatment.



### 3.3.4.3 RT-PCR profile with array RNA

RT-PCR analysis for 14-3-3 $\zeta$  (Figure 3.37) was initially carried out to verify the anti-oestrogen induced expression profile over the 4 to 10 day course. At day 4 there were few changes in expression, with high levels in all treatments, the most convincing effect being a 43% increase for faslodex compared to the untreated control (and a smaller % versus E2 treatment). After 7 days of treatment there was a marginal decrease in 14-3-3 $\zeta$  levels with E2 treatment compared to the untreated control. The anti-oestrogens exhibited a small induction effect of 14% with tamoxifen and 26% with faslodex compared with the day 7 untreated control, where again these were also increased slightly versus E2 treatment. The level of suppression seen with E2 was more substantial by day 10, with a 72% decrease compared with the untreated control. At day 10 the anti-oestrogens tamoxifen and faslodex increased 14-3-3 $\zeta$  expression by 158% and 143% respectively versus E2 treatment. However, by day 10 the untreated control level had increased by 23% compared to the untreated control at day 4 so there was a substantial E2 suppression. Indeed, the levels of tamoxifen and faslodex were lower than those achieved by the day 10 untreated control.

### 3.3.4.4 Validation PCR profile

The validation RT-PCR at day 4 (Figure 3.38) revealed very little difference between the E2 or faslodex treated and ED samples, and also depleted levels (60%) with tamoxifen treatment compared to E2 treatment or ED. However, by

day 7 this decrease with tamoxifen treatment was largely lost and there was also an increase of 32% with faslodex versus E2 treated and also versus ED. By day 10, the profile showed that the levels of 14-3-3 $\zeta$  with E2 treated were suppressed substantially by 57% compared to the day 4 E2 level. The validation RT-PCR revealed a small increase (20-25%) with the anti-oestrogens compared to E2 treated at this time point. However there was a larger increase of 128% with ED compared to E2 treatment. Thus, as in the first RT-PCR run, the level of 14-3-3 $\zeta$  with tamoxifen or faslodex treatment decreased by 45% and 50% respectively versus the day 10 ED/untreated control.

When comparing both the RT-PCR profiles with the array profile at day 7 they were similar, both showing some evidence of a modest anti-oestrogen induction versus E2 treated or ED. At day 10, there was some evidence of induction with anti-oestrogens versus E2 treatment in both the arrays and RT-PCR. However, the day 10 profiles differed due to the high levels of 14-3-3 $\zeta$  achieved in ED and more profound E2 suppression in the RT-PCR profile, so no induction with anti-oestrogens versus ED was seen in contrast to the arrays. The obvious E2-suppression and high levels of 14-3-3 $\zeta$  expression with ED, tamoxifen and faslodex revealed by RT-PCR continued to convince that this was an interesting gene for further study.

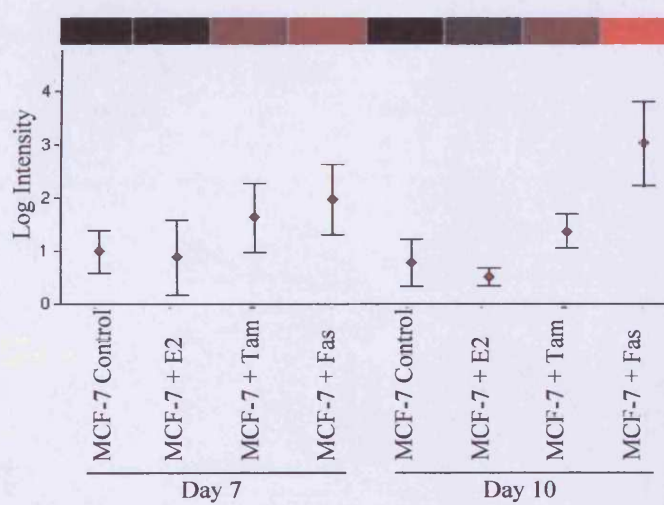


**Figure 3.36** 14-3-3 $\zeta$  array heatmap and log intensity profile at days 7 and 10

The heatmap shows an increase in red, decrease in green and no change in black of mRNA expression level compared to the untreated MCF-7 control (also black). The array log intensity profile shows the mean values for 14-3-3 $\zeta$  after median normalisation and log transformation of 3 independent replicates  $\pm$  SEM.

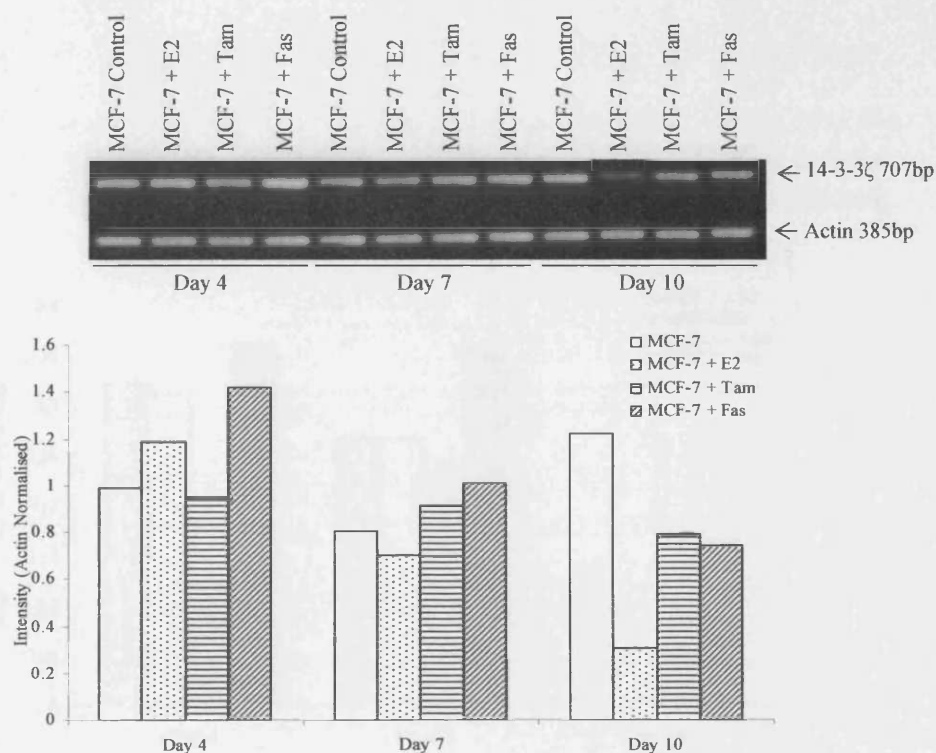


**Figure 3.37** RT-PCR analysis of 14-3-3 $\zeta$  mRNA in a sample set used to create arrays

RT-PCR was carried out on the mRNA (3rd replicate) used to create the arrays. Specific primers to 14-3-3 $\zeta$  and  $\beta$ -actin were used for amplification, and the products were then run on an agarose gel to size fractionate and visualise. The graph represents the densitometry for mRNA levels of 14-3-3 $\zeta$  after  $\beta$ -actin normalization at days 4, 7 and 10, with the associated PCR gel.

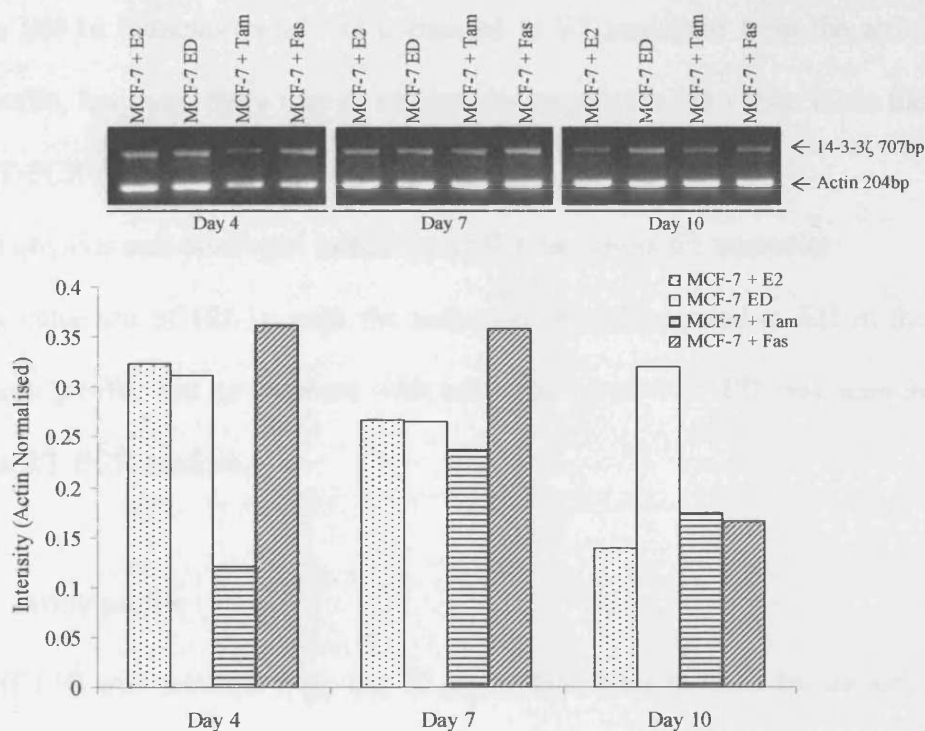


Figure 3.38 RT-PCR second round validation of 14-3-3 $\zeta$

For validation purposes RNA was prepared from MCF-7 cells, either untreated (ED), or treated with E2, tamoxifen or faslodex at days 4, 7 and 10. The mRNA was subject to RT-PCR using primers specific to 14-3-3 $\zeta$  and  $\beta$ -actin. The amplified products generated were size fractionated on an agarose gel. The graph represents the mRNA levels of 14-3-3 $\zeta$  after  $\beta$ -actin normalization, with associated PCR gel.

### 3.3.5 Hif-1 $\alpha$

#### 3.3.5.1 Summary

Overall the gene expression profiles revealed:

- I. no Hif-1 $\alpha$  induction with ED compared to E2 treatment from the array profile, however, there was an obvious increase with ED versus E2 in the RT-PCR profile
- II. an obvious anti-oestrogen induction of Hif-1 $\alpha$  versus E2 treatment
- III. an induction of Hif-1 $\alpha$  with the anti-oestrogens compared to ED in the array profile, but no increase with anti-oestrogens over ED was seen in the RT-PCR profiles.

#### 3.3.5.2 Array profile

Hif-1 $\alpha$  (C13i) was selected from the 20 genes that were induced by the anti-oestrogens tamoxifen and faslodex compared to both untreated control and E2 treated samples and after hierarchical clustering was found in cluster 3 (Figure 3.24). The array heatmap and mean log intensity profile for Hif-1 $\alpha$  at day 7 and 10 can be seen in Figure 3.39. At both time points, treatment with the anti-oestrogens tamoxifen and faslodex resulted in an increase in gene expression either versus E2 treated or untreated control. The day 10 data only showed a modest decrease in Hif-1 $\alpha$  levels with E2 treatment compared to the untreated control.

### 3.3.5.3 RT-PCR profile with array RNA

The RT-PCR with array samples is shown in Figure 3.40. At day 4, the untreated control, E2 and tamoxifen samples all lie within 14% of each other. However, the faslodex treated sample revealed increased levels (67%) versus the untreated control and versus E2 treated. At day 7, E2 treatment resulted in a 34% decrease in Hif-1 $\alpha$  levels versus ED. The anti-oestrogens tamoxifen and faslodex causing a 39% and 25% increase respectively, compared to the day 7 untreated control and more substantially versus E2 treatment. By day 10 there was maximal suppression in the levels of Hif-1 $\alpha$  in the presence of E2 treatment, where the levels were reduced to just 11% of the day 10 untreated control levels. At this time point, anti-oestrogen treatment markedly induced gene expression versus E2 treatment (tamoxifen 778%, faslodex 517%), although the anti-oestrogen treated levels were not obviously different to the untreated control.

### 3.3.5.4 Validation RT-PCR profile

The validation RT-PCR (Figure 3.41) at day 4 showed a 76% increase with tamoxifen and with faslodex treatment an increase of 131%, compared to E2 treatment. There was a 129% and 142% increase with tamoxifen and faslodex respectively compared to E2 treated by day 7, and similarly at day 10 there was an increase of 147% and 134% respectively. ED showed a similar induction to the anti-oestrogens at each time point, being induced by 50% (day 4), 107%

(day 7) and 122% (day 10) versus E2 treatment, thus revealing substantial E2 suppression of Hif-1 $\alpha$ .



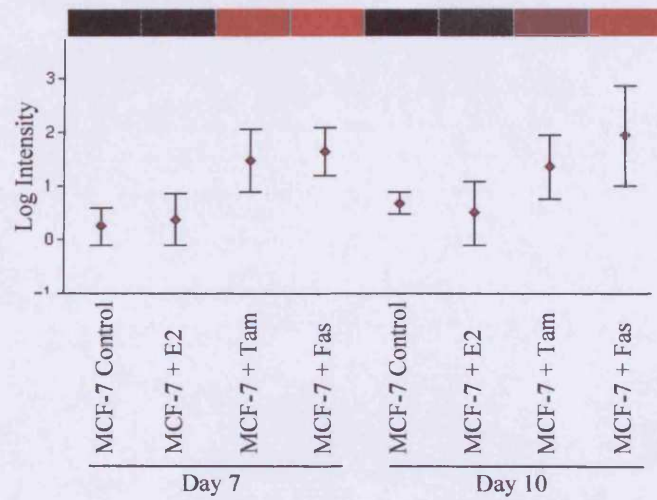


**Figure 3.39** Hif-1 $\alpha$  array heatmap and log intensity profile at days 7 and 10

In the heatmap, an increase in mRNA expression is represented by red and a decrease by green with no change in black compared to the untreated control (also black). The array log intensity profile for Hif-1 $\alpha$  represents the mean of 3 experiments after median normalization and log transformation  $\pm$  SEM.

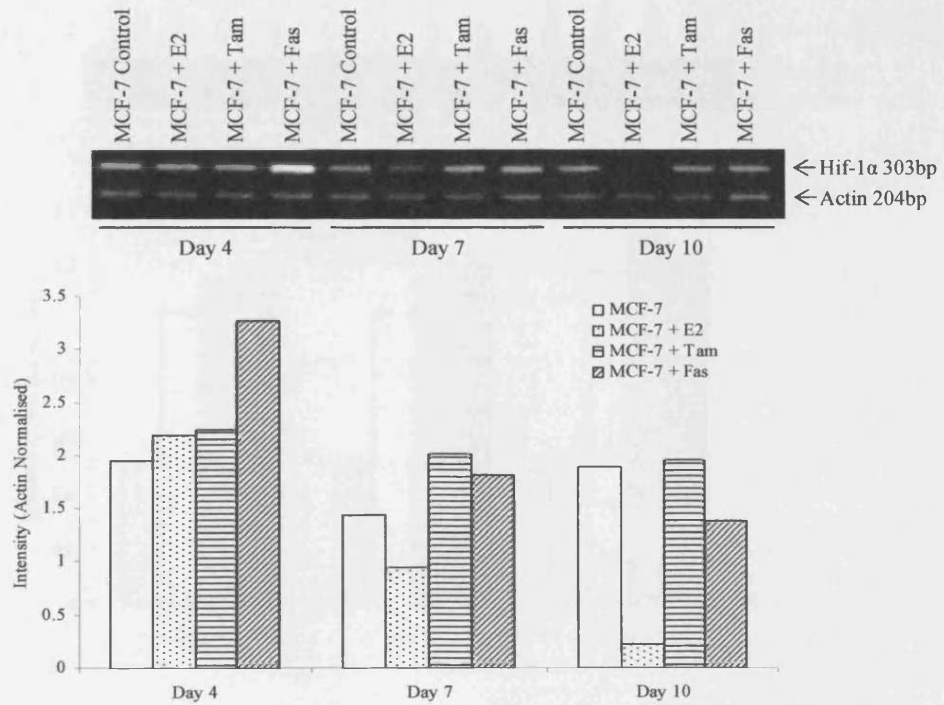


**Figure 3.40** RT-PCR analysis of Hif-1 $\alpha$  mRNA in a sample set used to create arrays

RT-PCR using specific primers for Hif-1 $\alpha$  and  $\beta$ -actin was carried out on the 3rd RNA set and after amplification the PCR products were size fractionated on an agarose gel. The graph represents the mRNA levels of Hif-1 $\alpha$  after normalization to  $\beta$ -actin at days 4, 7 and 10, with associated PCR gel.

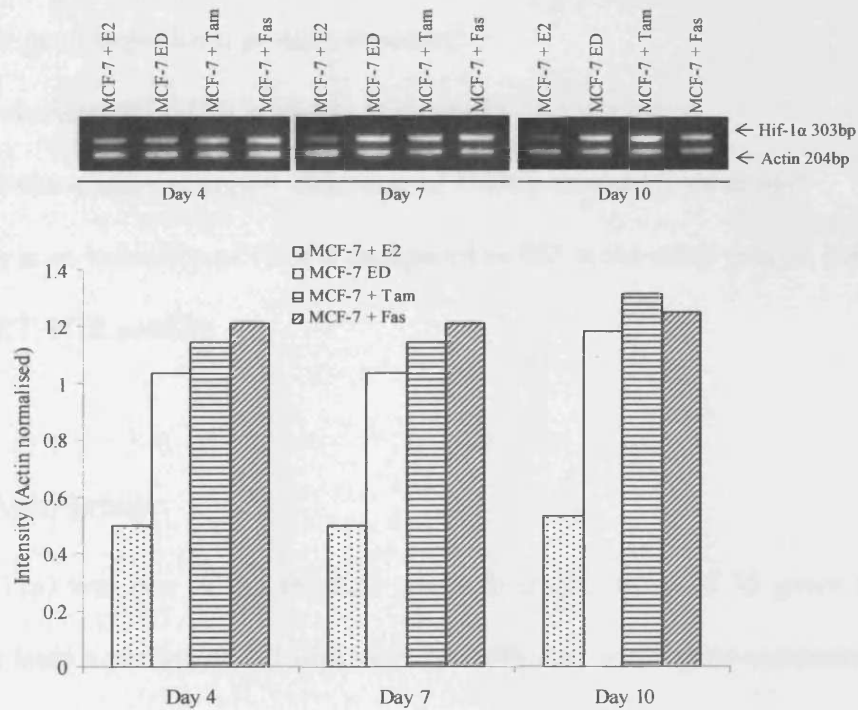


**Figure 3.41** RT-PCR second round validation of Hif-1 $\alpha$

RNA was prepared from a validation set of MCF-7 cells either untreated (ED) or treated with E2, tamoxifen or faslodex. RT-PCR was performed using primers specific to Hif-1 $\alpha$  and  $\beta$ -actin with the PCR products size fractionated on an agarose gel. The graph represents the mRNA levels of Hif-1 $\alpha$  after normalization to  $\beta$ -actin, with the associated PCR gel.

### 3.3.6 NME3

#### 3.3.6.1 Summary

Overall the gene expression profiles revealed:

- I. an induction of NME3 with ED compared to E2 treatment
- II. an obvious anti-oestrogen induction of NME3 versus E2 treatment
- III. there is an induction of NME3 compared to ED in the array profile, but not RT-PCR profiles

#### 3.3.6.2 Array profile

NME3 (F11e) was one of the selected genes from the group of 35 genes that showed at least a persistent 1.5 fold increase with anti-oestrogens compared to the untreated control. Following hierarchical clustering of the 35 genes, it lay in cluster 3 (Figure 3.22). Shown in Figure 3.42 are the array heatmap and mean log intensity profile for NME3. At day 7 the profile and heatmap showed an increase with tamoxifen and faslodex and also E2 treatment compared to the untreated control alone. There was still a persistent increase with anti-oestrogens by day 10, but no detectable increase with E2 treatment where levels remained low. Thus, at this time point there was an increase with both anti-oestrogens relative to the untreated control (and also at this time point versus E2 treatment).

### 3.3.6.3 RT-PCR profile with array RNA

Shown in Figure 3.43 is the RT-PCR for NME3 in the array samples. At day 4 there were clear increases with the anti-hormones tamoxifen (38%) and faslodex (70%) compared with both untreated control and E2 treatment. By days 7 and 10 the levels of NME3 in the untreated control had increased by 40% and 100% respectively, with the levels with E2 treatment suppressed by between 40% and 60% versus the untreated control. Thus, tamoxifen and faslodex treated samples showed an increase in expression at both days 7 and 10 versus E2 treatment, but not versus the untreated control.

### 3.3.6.4 Validation RT-PCR Profile

Figure 3.44 shows the RT-PCR results for NME3 on the second validation set of RNA. The profile shows that at day 4 there was an increase with the anti-oestrogens tamoxifen and faslodex of 26% and 75% respectively versus E2 treatment. E2-suppression was already apparent, with ED increasing expression by 68% versus E2 treatment and so the levels with anti-oestrogens were not increased versus ED. The day 7 profile was similar, although the level of NME3 present with E2 treatment had further reduced between day 4 and 7 by 36%, so there were more substantial increases with the anti-oestrogens or ED versus this treatment. This pattern persists at day 10, again with obvious anti-oestrogen induction versus E2 treated but not versus ED.

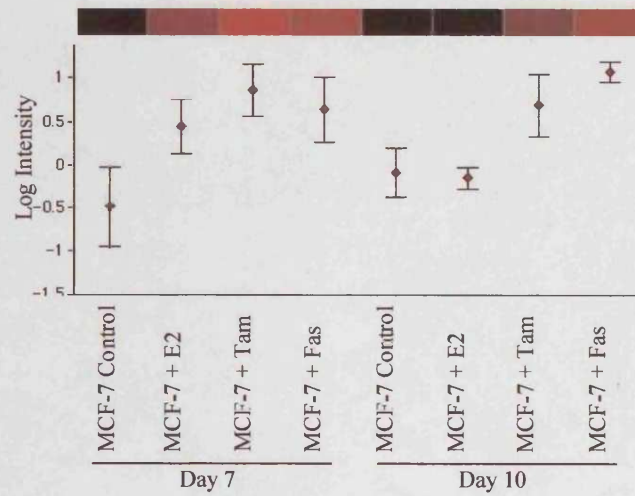
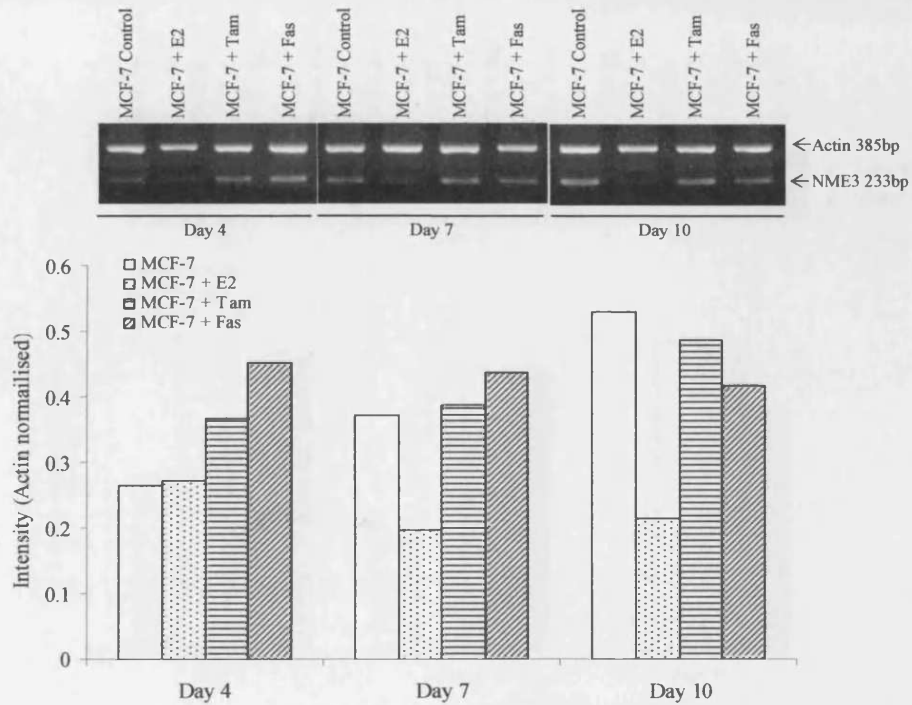


Figure 3.42 NME3 array heatmap and log intensity profile at days 7 and 10

The heatmaps show increases in red and control/no change in black of NME3 mRNA levels compared to the untreated MCF-7 (also black). The array profile shows the mean values of NME3 in 3 independent experiments after median normalization and log transformation  $\pm$  SEM



**Figure 3.43** RT-PCR analysis of NME3 mRNA in a sample set used to create arrays

RT-PCR on the 3rd set of array samples was performed using primers specific to NME3 and  $\beta$ -actin and the amplification products were size fractionated on an agarose gel. The graph represents the mRNA levels of NME3 after normalization to  $\beta$ -actin as densitometric intensity at days 4, 7 and 10, with the associated PCR gel.

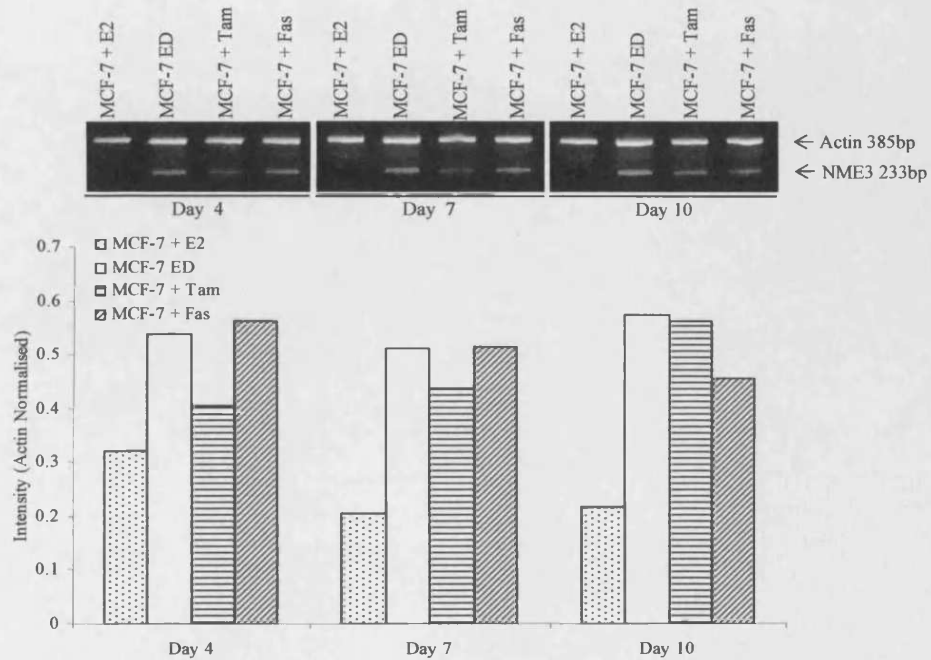


**Figure 3.44** RT-PCR second round validation of NME3

RNA was prepared from a validation set of MCF-7 cells either untreated (ED) or treated with E2, tamoxifen or faslodex. RT-PCR was performed using primers specific to NME3 and  $\beta$ -actin with the PCR products size fractionated on an agarose gel. The graph represents the mRNA levels of NME3 after normalization to  $\beta$ -actin, with the associated PCR gel.



### 3.3.7 NFkB1

#### 3.3.7.1 Summary

Overall the gene expression profiles revealed:

- I. a suppression of NFkB1 with ED with the array profile, however there was an induction in the RT-PCR profiles compared to E2 treatment
- II. an anti-oestrogen induction of NFkB1 compared to E2 treatment in the RT-PCR profiles
- III. there was no anti-oestrogen induction of NFkB1 compared with ED in the array profile, however the RT-PCR profiles showed an obvious induction with anti-oestrogen treatment

#### 3.3.7.2 Array profile

NFkB1 (C04k) was one of the genes selected from the 35 that showed a persistent 1.5 fold increase with the anti-oestrogens tamoxifen and faslodex compared with the untreated control only. Following hierarchical clustering it fell into cluster 4 (Figure 3.22), which also exhibited some E2 induction. The ontology of this gene linking it with therapeutic resistance is strong and hence NFkB1 was retained despite the E2 inductive effect. The array heatmap and mean log intensity profile can be seen in Figure 3.45. At both days 7 and 10 the heatmap and log intensity profile confirms an increase in gene levels with tamoxifen and faslodex, and also with E2 treatment versus the untreated control.

### 3.3.7.3 RT-PCR profile with array RNA

The RT-PCR profile is shown in Figure 3.46. While day 4 showed that the levels of NFkB1 in the untreated control, E2 and tamoxifen treated samples were very similar (100%, 83% and 106% respectively), there was a 113% increase with faslodex, compared to the untreated control and also versus E2 treatment. However, the day 7 and 10 profiles differed substantially from the day 4 profile. At these time points, anti-oestrogen treatment had little effect on the levels of NFkB1 versus untreated control, which had increased expression by 66% by day 10. However, there was a progressive E2-suppression (57% at day 7, 90% at day 10) versus untreated control, and so the anti-oestrogens were stimulatory on NFkB1 expression versus E2 treatment at these time points.

### 3.3.7.4 Validation RT-PCR profile

The second validation RT-PCR results are shown in Figure 3.47. At day 4, the greatest increase was again seen with faslodex treatment, at 62% versus ED and 84% compared to the E2 treated sample. There was also an obvious tamoxifen increase of 38% versus ED and 59% versus E2 treatment. This profile was also seen at day 7 both versus E2 treated and ED. By day 10 however, there was a substantial induction with tamoxifen, faslodex and also with ED of 60% compared with the day 10 E2 treated sample, confirming the gene was anti-hormone induced and E2-suppressed.

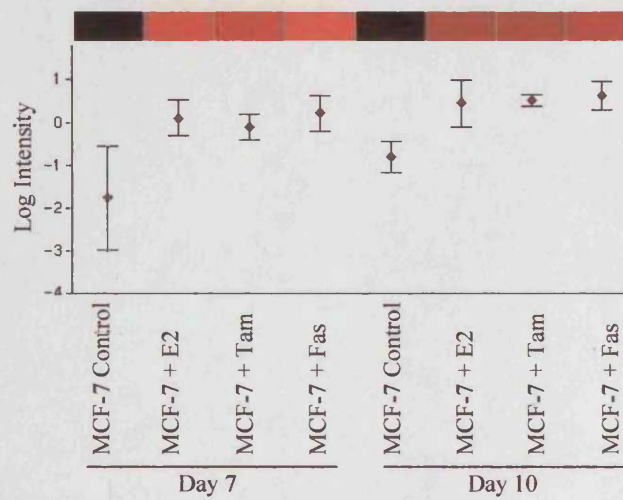
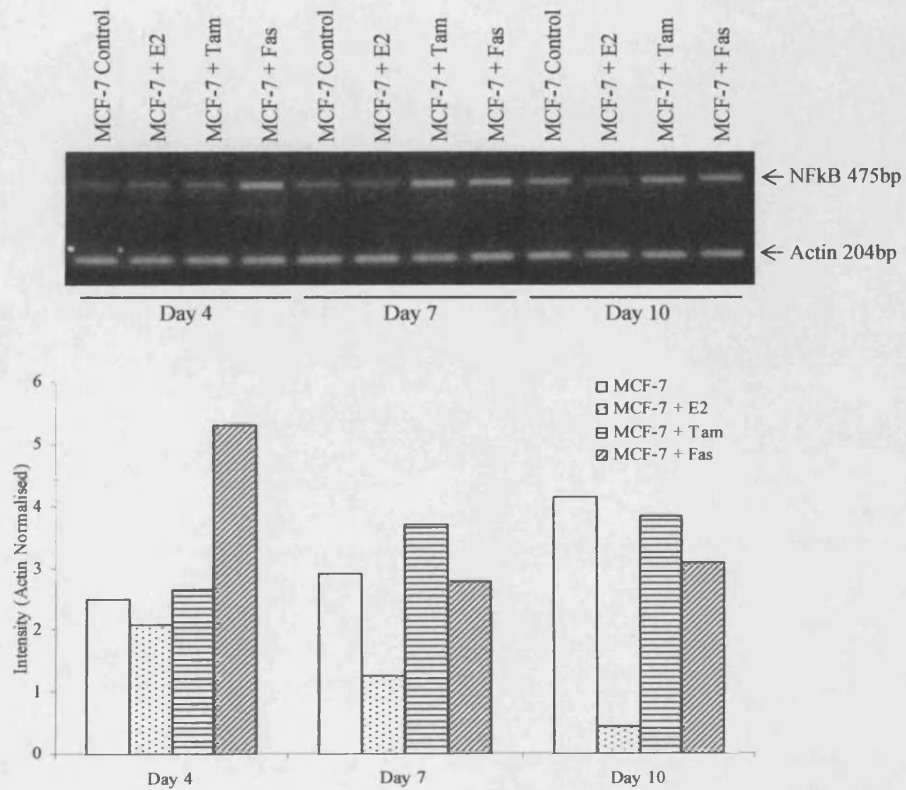


Figure 3.45 NFkB1 array heatmap and log intensity profile at days 7 and 10

The heatmap represents the mRNA levels of NFkB1; the red indicates an increase, versus the black control level. The array log intensity profile shows the level of NFkB from 3 independent replicates after median normalization and log transformation  $\pm$  SEM.



**Figure 3.46** RT-PCR analysis of NFκB1 mRNA in a sample set used to create arrays

RT-PCR on the 3rd set array sample set was performed using primers specific to NFκB1 and β-actin and the amplification products were size fractionated on an agarose gel. The graph represents the mRNA levels of NFκB1 after normalization to β-actin as densitometric intensity at days 4, 7 and 10, with the associated PCR gel.

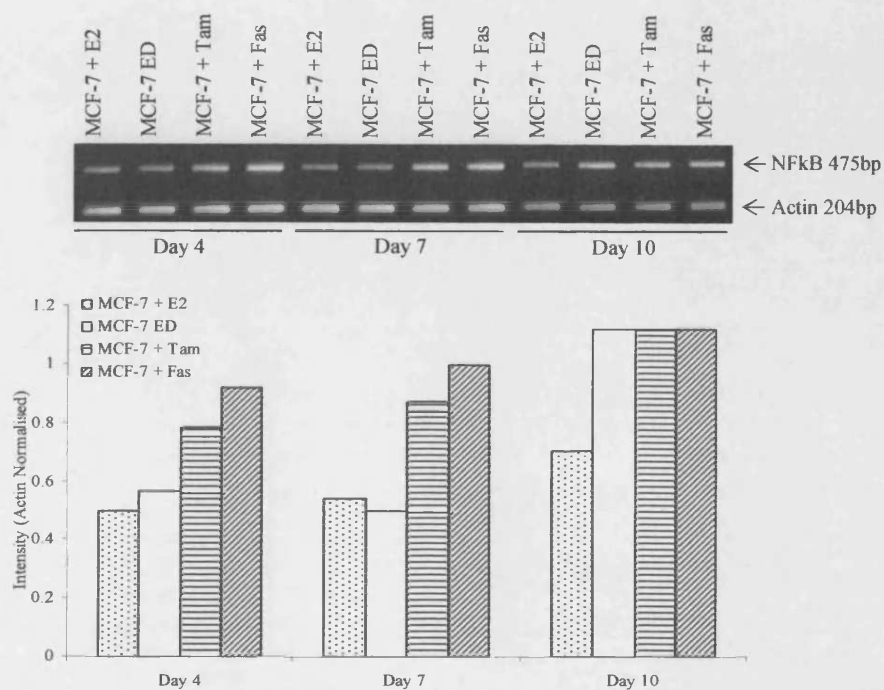


**Figure 3.47** RT-PCR second round validation of NFkB1

A validation RT-PCR was performed on RNA prepared from MCF-7 cells either untreated (ED) or treated with E2, tamoxifen or faslodex for 4, 7 and 10 days. Primers specific to NFkB and  $\beta$ -actin were used, with the resulting products size fractionated on an agarose gel. The graph represents the mRNA levels of NFkB after  $\beta$ -actin normalization, with the associated PCR gel.

### 3.3.8 NDR

#### 3.3.8.1 Summary

Overall the gene expression profiles revealed:

- I. induction of NDR with ED in the RT-PCR profile but not array profile compared to E2 treatment
- II. an obvious anti-oestrogen induction of NDR versus E2 treatment
- III. an anti-oestrogen induction of NDR versus ED in the RT-PCR profile only

#### 3.3.8.2 Array profile

NDR protein kinase (B05h), was selected from the list of 20 genes that were induced at least 1.5 fold with anti-oestrogens compared with both untreated control and E2 treated MCF-7 cells. Following hierarchical clustering it was found in cluster 3 (Figure 3.24). The array heatmap and mean log intensity profile can be seen in Figure 3.48. At days 7 and 10 the profile and heatmap showed that while the levels of NDR protein kinase present in the untreated control and E2 treated samples were very similar and low, both tamoxifen and faslodex treatment resulted in an increase in gene level versus E2 treatment and untreated control.

### 3.3.8.3 RT-PCR profile with array PCR

The day 4 RT-PCR results (Figure 3.49) showed an increase with faslodex (72%) compared with the untreated control, but this was not apparent with tamoxifen. There were no increases with the anti-oestrogens at this time point versus E2 treatment. Indeed, E2 treatment appeared to stimulate NDR protein kinase expression versus untreated control at this single time point. By day 7, however, there was a 45% decrease in NDR protein kinase expression with E2 treatment. Thus, alongside 13% and 35% increases with tamoxifen and faslodex treatment respectively compared to the untreated control, there was also a very obvious induction by anti-oestrogens versus the E2 treated group. The day 10 profile showed a maximal E2-suppression at 84%. The levels of NDR protein kinase with anti-oestrogens were largely comparable to the untreated control but again elevated versus E2 treatment. Unfortunately limited quantities of RNA meant it was not possible to complete the validation RT-PCR profile for NDR protein kinase in this project.

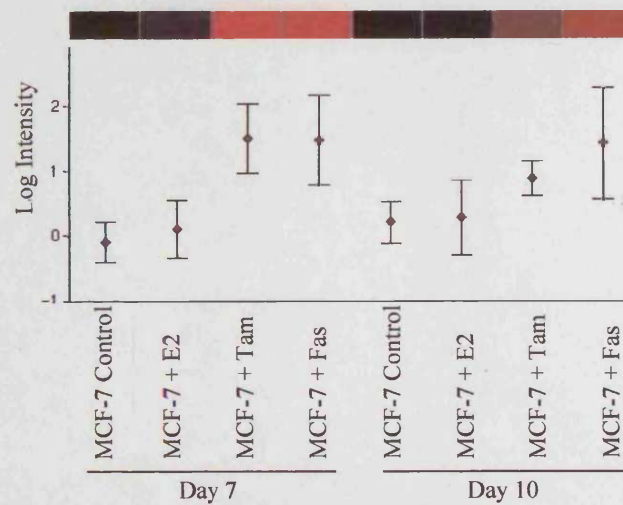
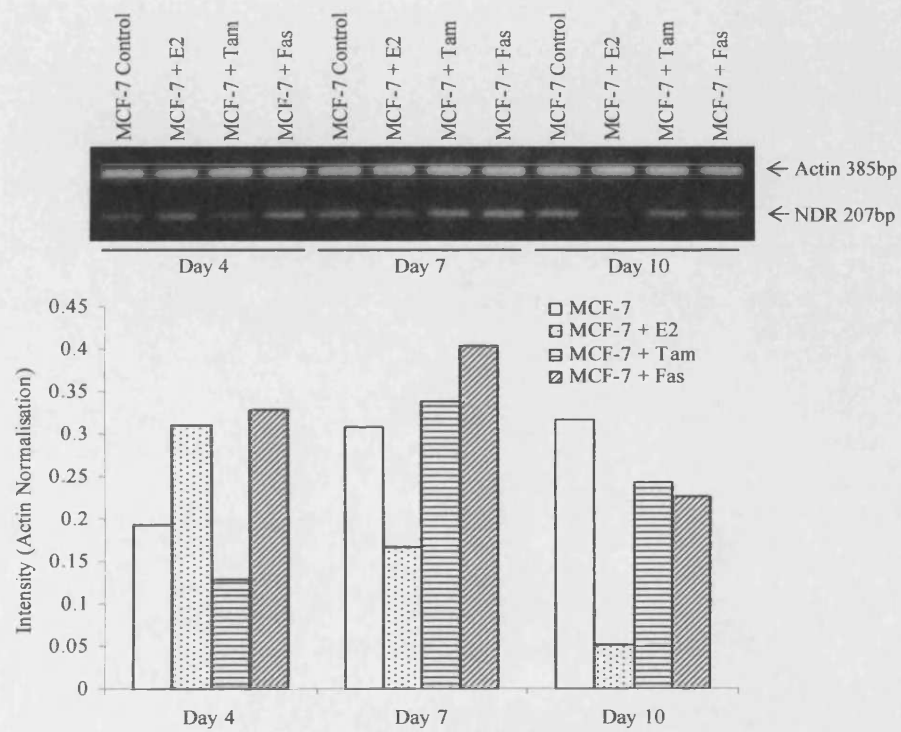


Figure 3.48 NDR protein kinase array heatmap and log intensity profile at days 7 and 10

In the heatmap the red indicates an increase in mRNA levels, with black indicating a no change compared to the untreated control level (also black). The array log intensity profile shows the mean of 3 experiments after median normalization and log transformation  $\pm$  SEM as analysed in GeneSifter™.





**Figure 3.49** RT-PCR analysis of NDR protein kinase mRNA in a sample set used to create arrays

RT-PCR was performed on the 3rd set of array samples using specific primers to NDR protein kinase and  $\beta$ -actin and amplified products were size fractionated on an agarose gel. The graph represents the mRNA levels of NDR protein kinase after  $\beta$ -actin normalization at day 4, 7 and 10, with the associated PCR gel.

### **3.4 Investigation at a protein level**

Following the mRNA level validation, the gene products of the selected genes were investigated by ICC and/or western blotting to examine if evidence of anti-hormone-induction and E2-suppression persisted at a protein level. This was performed using cell pellet array sections, coverslips of cells in monolayer culture or cell lysates from MCF-7 cells treated with E2, tamoxifen, faslodex or under ED conditions. In addition, where possible, protein expression was evaluated in cell preparations from the acquired anti-oestrogen resistant MCF-7 cell lines (TAM-R and FAS-R), to address if anti-hormone induction was transient during the drug responsive phase or sustained into the resistant state.

The following sections document the protein results for delta catenin, RhoE, Bag-1, 14-3-3 $\zeta$ , NME3 and NFkB1. Unfortunately time constraints, together with experimental difficulties (e.g. poor primary antibody performance), meant it was not possible to investigate the protein levels of NDR protein kinase in cells challenged with E2 and anti-hormonal treatments, or for 14-3-3 $\zeta$  and NME3 in the acquired anti-oestrogen resistant cell lines.

### 3.4.1 RhoE

#### 3.4.1.1 Oestradiol and anti-hormonal treatments

##### 3.4.1.1.1 Immunocytochemistry

A RhoE specific antibody was used to visualise the levels and localisation of RhoE in paraformaldehyde fixed MCF-7 cells grown on coverslips under ED conditions or treated with E2, tamoxifen or faslodex for 7 days. Due to experimental difficulties (i.e. antigen destruction in pellet processing), paraformaldehyde-fixed cells on coverslips were used. Figure 3.50 shows the localisation of RhoE in faslodex treated MCF-7 cells, which was predominantly cytoplasmic with occasional weak nuclear staining. In comparison with the lack of staining following antibody omission, RhoE immunostaining was heterogeneous across the MCF-7 cell population. Shown in Figure 3.51 both photographically and graphically, is the RhoE staining across the four treatment arms. Although nuclear staining remained low throughout, cytoplasmic staining showed a significant increase of 80% ( $p=0.004$ ) under ED conditions and 125% ( $p=0.004$ ) and 165% ( $p=0.004$ ) with tamoxifen and faslodex treatment respectively, compared to E2 treated samples. Significantly, further increases were observed in tamoxifen (19%,  $p=0.07$ ) and faslodex (40%,  $p=0.009$ ) treated cells versus ED conditions at this time point.

#### 3.4.1.1.2 Western blotting

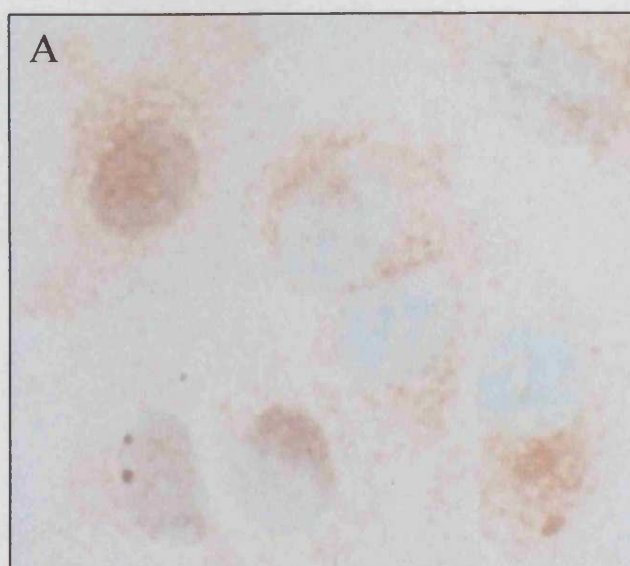
Western blotting was also carried out for RhoE and  $\beta$ -actin at day 7 and the results can be seen in Figure 3.52. The results showed the same profile as the ICC with an increase in RhoE with both ED and anti-oestrogen treated cells versus E2 treatment, this was particularly evident for the anti-oestrogens. Thus, ED resulted in a 420% increase in RhoE protein, while tamoxifen and faslodex treatment produced 500% and 602% increases respectively compared to the E2 treated MCF-7 cells, with some further increases with tamoxifen (85%) and faslodex treatment (180%) versus ED at this time point.

The profile revealed by both the ICC and western blotting broadly confirms the anti-hormonal-induction and E2-suppression seen at day 7 at the mRNA level. Protein studies revealed a graded response, with ED showing the smallest increase in RhoE expression, followed by tamoxifen, with faslodex showing the largest increase in expression versus E2 treatment. The results confirmed that RhoE is an anti-hormone-induced, E2-suppressed gene.

#### 3.4.1.2 Resistance

##### 3.4.1.2.1 Western blotting

Figure 3.53 shows the levels of RhoE in tamoxifen or faslodex resistant cell lines compared to parental MCF-7 cells by western blotting. While there was no obvious increase in RhoE in TAM-R cells, a large increase of 363% was observed in FAS-R cells.



Localisation of RhoE immunostaining



Omission of primary antibody

Figure 3.50 RhoE immunocytochemistry with omission of primary antibody control in MCF-7 cells treated with faslodex for 7 days

Faslodex treated MCF-7 cells were paraformaldehyde fixed and RhoE detected with a specific primary antibody followed by DAB detection. As a control the primary RhoE antibody was omitted. Photograph A shows the nuclear and cytoplasmic localisation of RhoE staining, while the photograph B (original magnification x40) shows the lack of staining with omission of primary antibody.

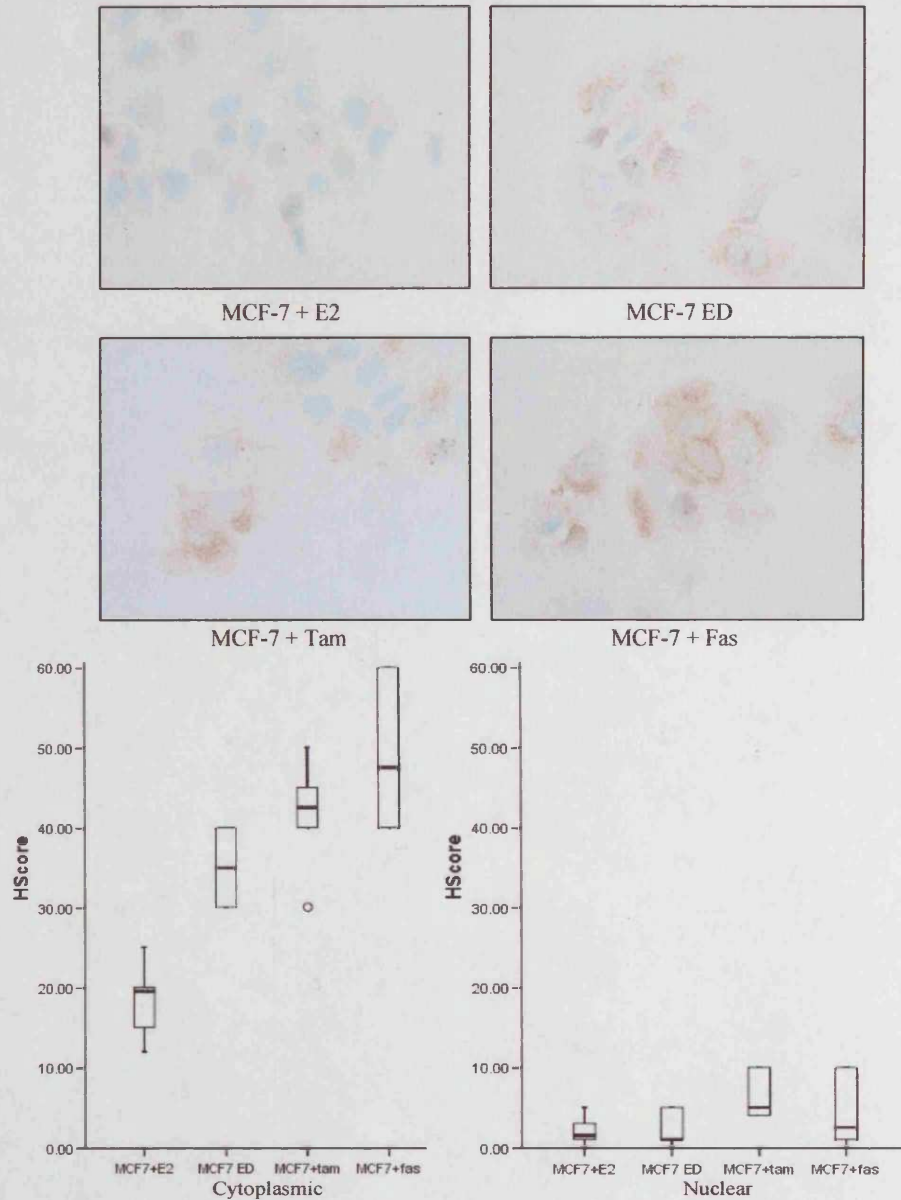


**Figure 3.51 Immunocytochemical staining of RhoE levels in MCF-7 cells treated with/without oestradiol or anti-oestrogens**

MCF-7 cells were grown on coverslips in the absence of (ED), or in media containing E2, tamoxifen or faslodex for 7 days. Cells were then paraformaldehyde fixed and stained using an antibody specific to RhoE, secondary antibody and DAB detection. Coverslips were photographed at an original magnification of x40. The graph represents the H scores  $\pm$  SEM. The data was analysed by Mann-Whitney testing (n=6), circle indicates outliers. There are significant differences between E2 treated and ED in the cytoplasm ( $p=0.004$ ); E2 and tamoxifen treatment in the cytoplasm ( $p=0.004$ ) and nucleus ( $p=0.015$ ); E2 and faslodex treatment in the cytoplasm ( $p=0.004$ ); ED and tamoxifen treatment in the nucleus ( $p=0.05$ ) and between ED and faslodex treatment in the cytoplasm ( $p=0.009$ ).

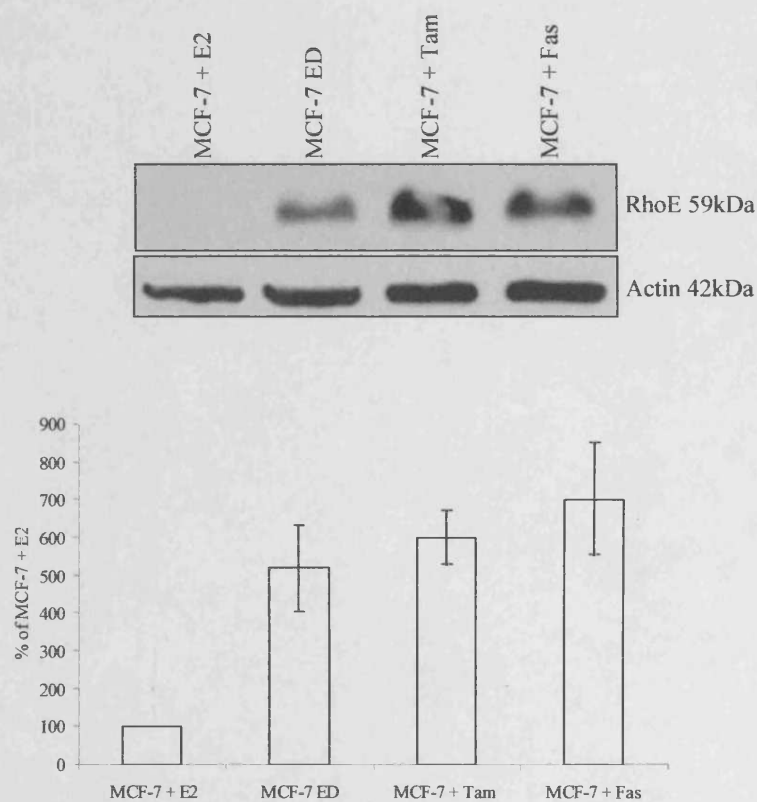


**Figure 3.52** Levels of RhoE protein by western blotting in MCF-7 cells with/without 7 days treatment with oestradiol or anti-oestrogens

Whole cell extracts from MCF-7 cells either ED or treated with E2, tamoxifen or faslodex for 7 days were subject to western blot analysis. RhoE and  $\beta$ -actin specific antibodies were used to probe the blotted membranes. The Graph shows  $\beta$ -actin normalised, mean RhoE levels from 3 independent experiments  $\pm$  SEM and expressed as a percentage of E2 treated levels (n=3).

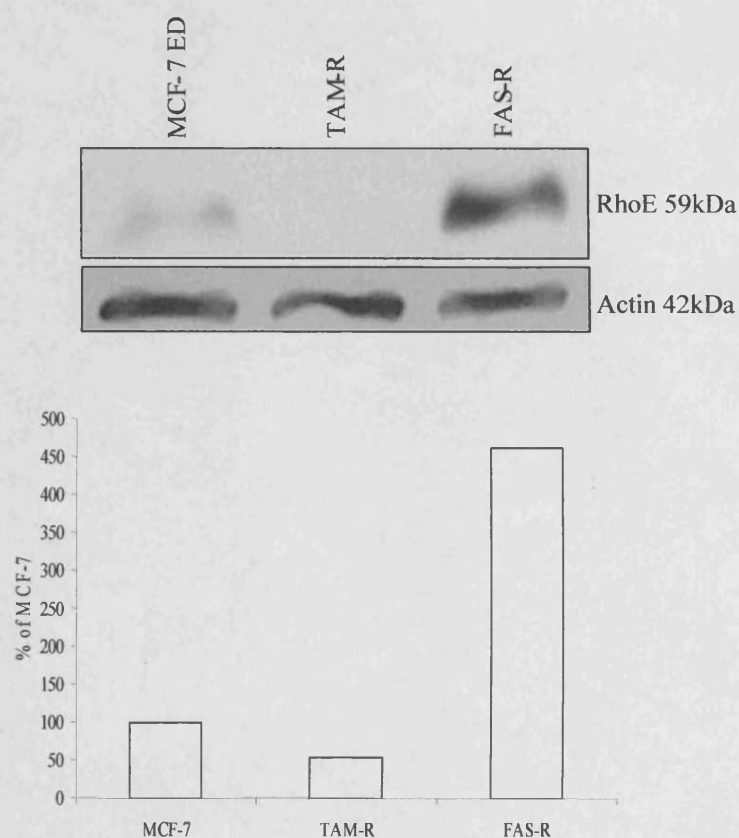


**Figure 3.53** Levels of RhoE protein by western blotting in MCF-7 ED, TAM-R and FAS-R cells

Whole cell extracts from day 7 MCF-7, TAM-R or FAS-R cells were subject to western analysis. RhoE and  $\beta$ -actin specific antibodies were used to probe the blotted membranes, as shown. The Graph shows the levels of RhoE present in the samples, normalised to  $\beta$ -actin and expressed as a percentage of MCF-7 data (n=1).



## 3.4.2 $\delta$ -catenin

### 3.4.2.1 Oestradiol and anti-hormonal treatments

#### 3.4.2.1.1 Immunocytochemistry

Paraffin sections of an MCF-7 treatment cell pellet array were re-hydrated and stained using a specific antibody for  $\delta$ -catenin, followed by a goat secondary antibody with DAB detection.  $\delta$ -catenin staining was predominantly homogenous throughout the cytoplasm with heterogenous plasma membrane staining. At the day 10 time point in the faslodex treated cells there was also very occasional nuclear staining (Figure 3.54). In general, most changes in staining were seen at the plasma membrane, whereas cytoplasmic staining remained low across the time points and treatments, with the exception of faslodex treatment at later time points (days 7 and 10). Also shown in Figure 3.54 is the lack of staining seen in the omission of primary antibody control. Day 4 preparations (Figure 3.55) revealed that  $\delta$ -catenin membrane staining increased significantly with tamoxifen by 324% ( $p=0.003$ ) compared to E2 treatment, and 47% ( $p=0.008$ ) compared to ED conditions. Faslodex treatment significantly increased membrane levels by 987% ( $p=0.003$ ) compared to E2 treatment, and 278% ( $p=0.008$ ) compared to ED conditions. There was also a smaller, although still significant increase of 187% ( $p=0.004$ ) in membrane staining with ED conditions compared with E2 treatment. The day 7 (Figure 3.56) staining followed a similar profile, with a significant 196% ( $p=0.005$ ) increase in membrane staining with ED conditions compared to E2 treatment. However, larger increases were seen in the presence of anti-oestrogens;

tamoxifen treatment produced a significant 696% ( $p=0.003$ ) versus E2 treatment and 168% ( $p=0.003$ ) versus ED, while faslodex showed 1066% ( $p=0.004$ ) versus E2 treatment and 293% ( $p=0.003$ ) versus ED. At this point the inductive effect of faslodex on cytoplasmic staining became evident with a significant 120% ( $p=0.032$ ) and 150% ( $p=0.019$ ) increase versus E2 treatment and ED respectively. At day 10 (Figure 3.57) there were further significant increases in membrane staining with the anti-oestrogens. Tamoxifen treatment resulted in a 358% ( $p=0.002$ ) and 587% ( $p=0.003$ ) increases versus E2 treatment and ED conditions respectively, while faslodex treatment resulted in 433% ( $p=0.002$ ) and 700% ( $p=0.003$ ) increases versus E2 treated and ED respectively. As seen at day 7, there was also a 170% ( $p=0.003$ ) and 92% ( $p=0.003$ ) increase in cytoplasmic staining with faslodex compared to E2 treated and ED respectively. At this day 10 time point the occasional occurrence of nuclear staining was observed with faslodex treatment (as in Figure 3.54b). However, ED showed no increase versus E2 at this time point, in fact there was a small but significant 34% ( $p=0.019$ ) decrease in membrane staining.

These results convincingly showed that there was an anti-oestrogen inductive effect on the levels of  $\delta$ -catenin at the plasma membrane and with faslodex in the cytoplasm and nucleus at the later time points. Tamoxifen and faslodex increased  $\delta$ -catenin staining level versus both E2 treatment and ED. Comparison of the three time points suggests that while the tamoxifen increases were gradual over the time course, faslodex levels increased more

rapidly. Only at the early time points was there some evidence of a small increase in membrane staining of  $\delta$ -catenin under ED conditions compared to E2 treatment. Thus the protein profile most closely resembles the mRNA array profile in that it is primarily anti-oestrogen induced (but marries to a lesser extent with the RT-PCR profiles where there was more obvious induction with ED).

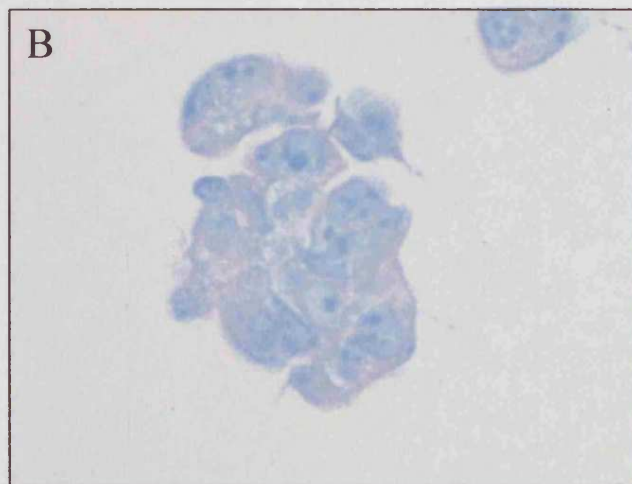
### 3.4.2.2 Resistance

#### 3.4.2.2.1 Immunocytochemistry

Levels of  $\delta$ -catenin in parental MCF-7 cells and acquired tamoxifen and faslodex resistant cell lines are shown in Figure 3.58. There was no change in the levels of staining in TAM-R cells at either the plasma membrane or in the cytoplasm, indicating that the increases seen with tamoxifen treatment are transient during drug treatment and not sustained through to acquired resistance. Unlike the faslodex treated cells at day 10, there was no evidence of nuclear staining in the FAS-R cells. However, results revealed that there was a significant staining increase of 133% ( $p=0.004$ ) in the cytoplasm and 678% ( $p=0.002$ ) in the plasma membrane in FAS-R cells compared to MCF-7 cells. This showed that the increases seen in  $\delta$ -catenin levels during faslodex treatment are sustained and probably further increased in acquired faslodex resistance, since the H-scores obtained in FAS-R cells exceeded those following 10 days of faslodex treatment of MCF-7 cells (Figure 3.57)



Localisation of  $\delta$ -catenin immunostaining



Omission of primary antibody

Figure 3.54  $\delta$ -catenin immunostaining and omission of primary antibody in MCF-7 cells treated with faslodex for 10 days

Photograph A shows the brown staining localisation of  $\delta$ -catenin, which is found homogenously through the cytoplasm with variable membrane staining and at day 10 evidence of occasional nuclear staining (arrow). Photograph B (original magnification x40) shows that there is no staining with omission the of the  $\delta$ -catenin primary antibody control.

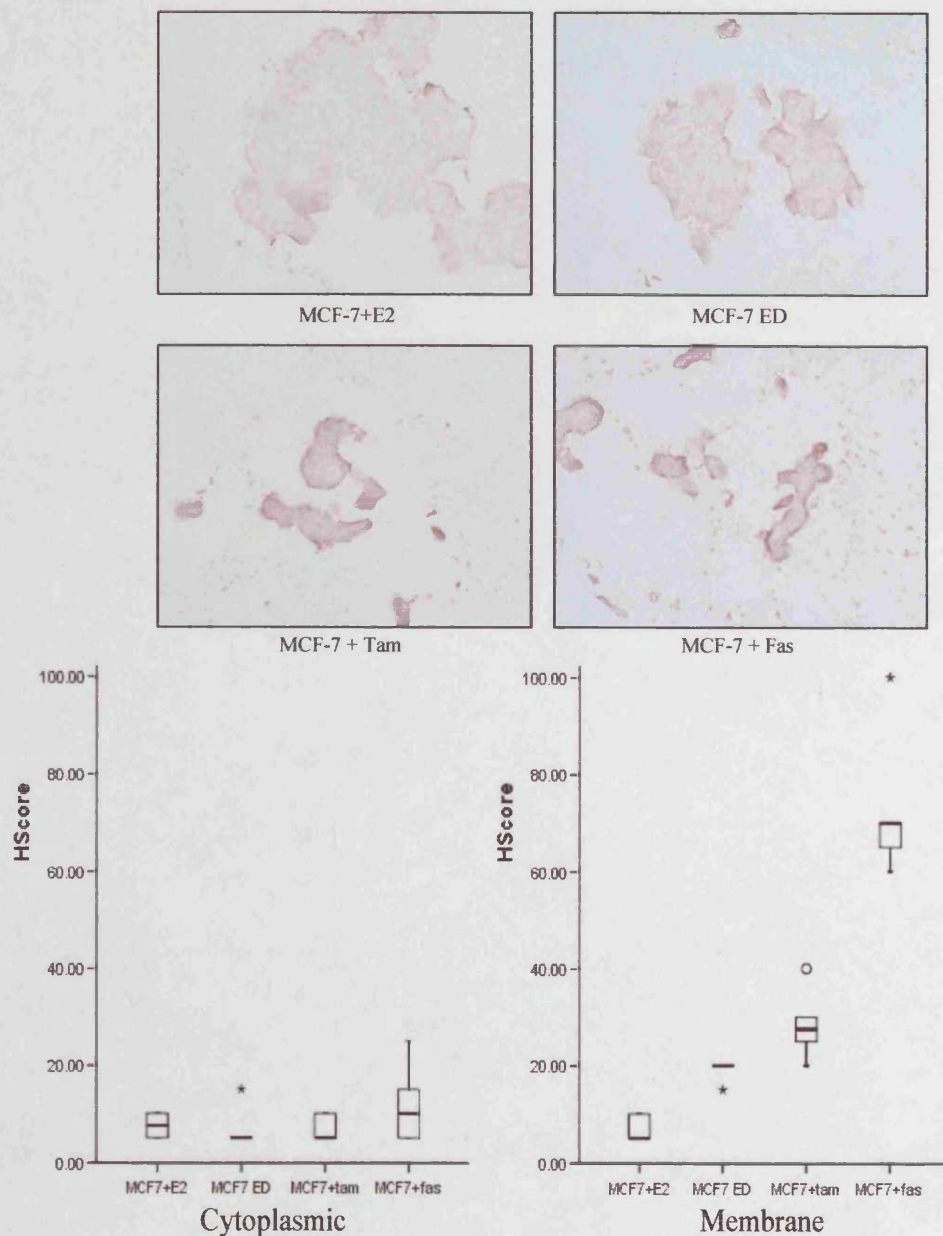


**Figure 3.55** Immunocytochemical staining of  $\delta$ -catenin in MCF-7 cell pellet preparations after 4 days with/without oestradiol or anti-oestrogen treatment

Day 4 MCF-7 cell pellet treatment arrays were re-hydrated and stained for  $\delta$ -catenin with a specific antibody. Array cell pellets were photographed at an original magnification of  $\times 40$ . The H-score data was analysed by Mann-Whitney testing ( $n=6$ ) and represented in boxplots where outliers are represented by a circle (o) and extreme values by a star (\*). There are significant staining differences between E2 and tamoxifen treatment in the membrane ( $p=0.003$ ); E2 and faslodex treatment in the membrane ( $p=0.003$ ); ED and tamoxifen treatment in the membrane ( $p=0.008$ ); ED and faslodex treatment in the membrane ( $p=0.003$ ) and between ED and E2 treatment in the membrane ( $p=0.002$ ).

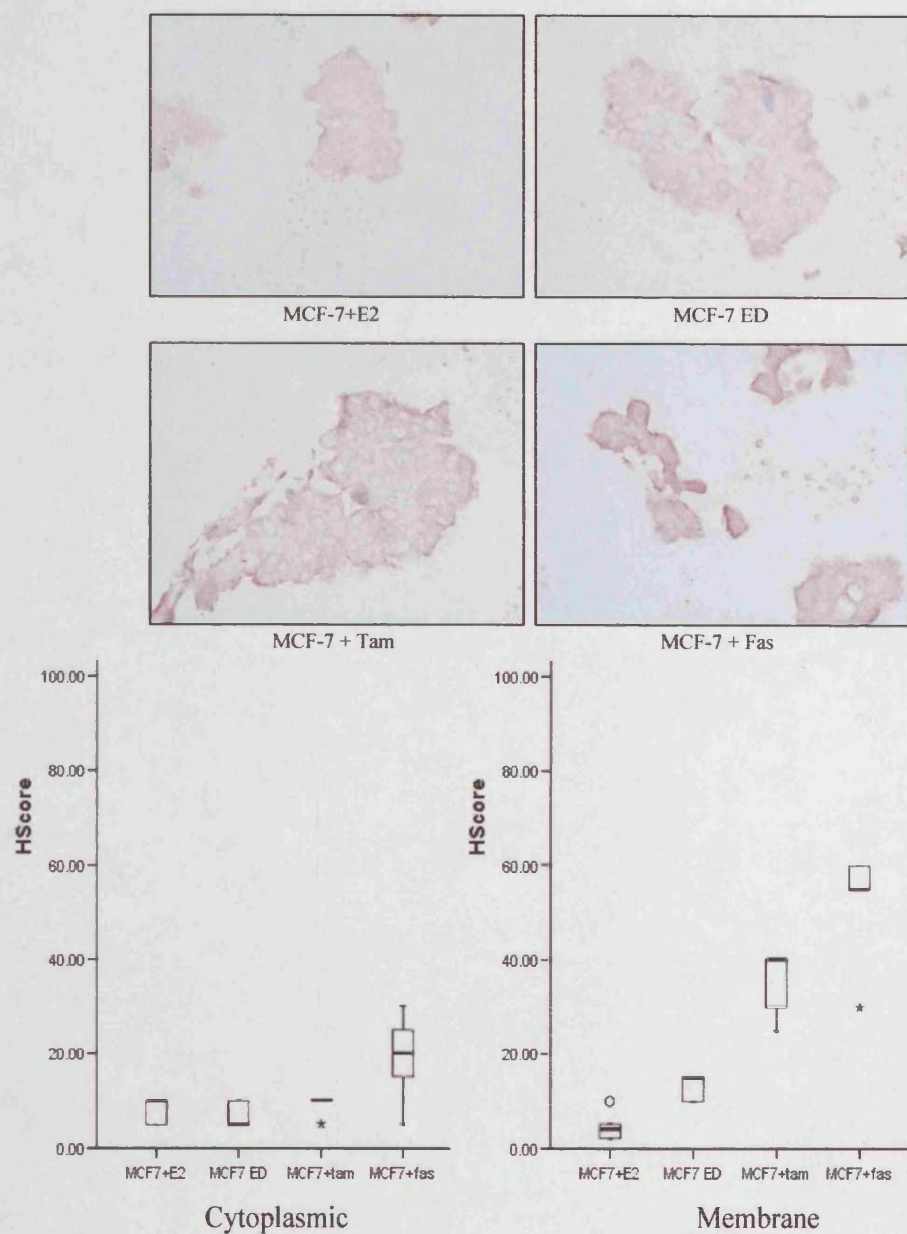


**Figure 3.56** Immunocytochemical staining of  $\delta$ -catenin in MCF-7 cell pellet preparations after 7 days with/without oestradiol or anti-oestrogen treatment

Day 7 MCF-7 cell pellet treatment arrays were re-hydrated and stained for  $\delta$ -catenin. Annotation is as in Figure 3.55. There are significant differences between E2 and tamoxifen treatment in the membrane ( $p=0.003$ ); E2 and faslodex treatment in the cytoplasm ( $p=0.032$ ), membrane ( $p=0.004$ ); ED and tamoxifen treatment in the membrane ( $p=0.003$ ); ED and faslodex treatment in the cytoplasm ( $p=0.019$ ), membrane ( $p=0.003$ ) and between ED and E2 treatment in the membrane ( $p=0.005$ ).

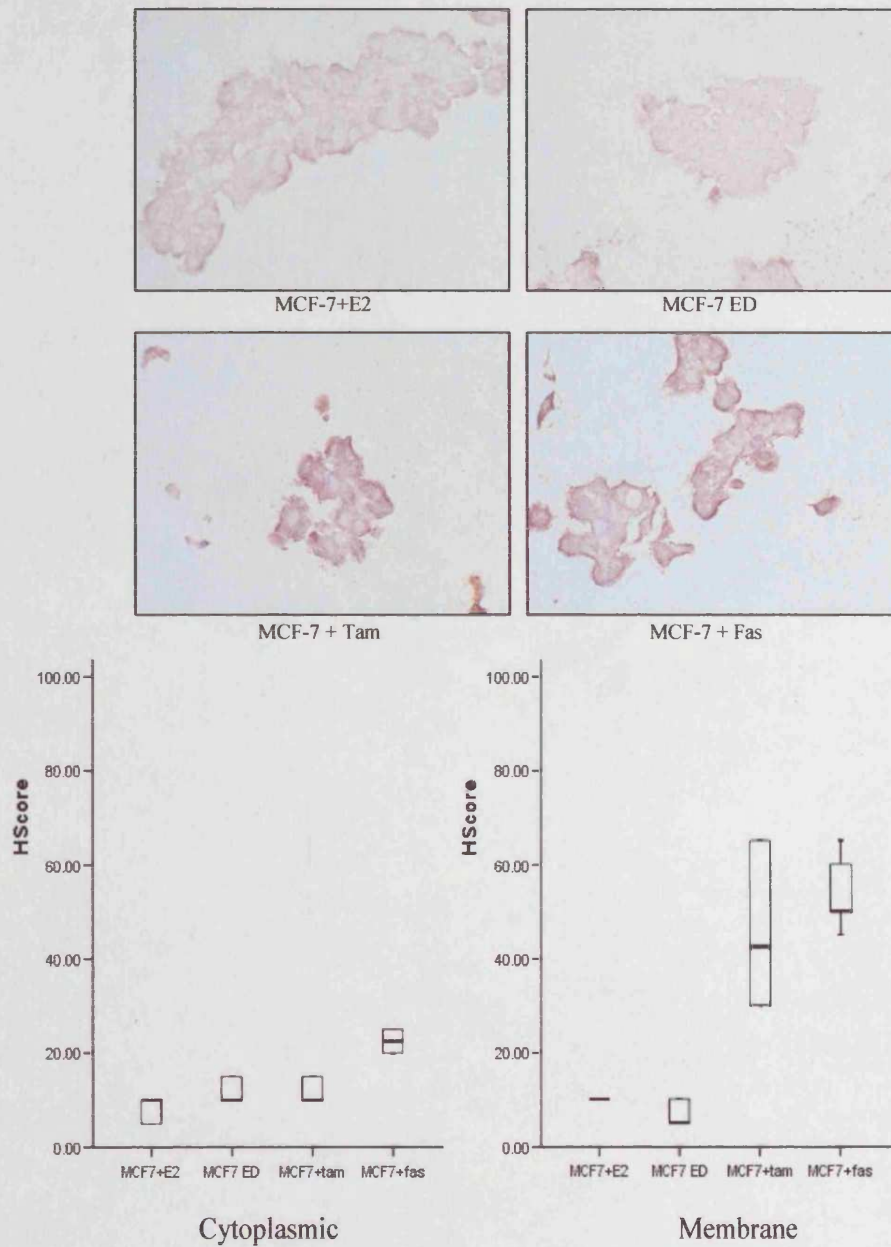


**Figure 3.57** Immunocytochemical staining of  $\delta$ -catenin in MCF-7 cell pellet preparations after 10 days with/without oestradiol or anti-oestrogen treatment

Day 10 MCF-7 cell pellet treatment arrays were re-hydrated and stained for  $\delta$ -catenin. Annotation is as in Figure 3.55. There are significant differences between E2 and tamoxifen treatment in the membrane ( $p=0.002$ ); E2 and faslodex treatment in the cytoplasm ( $p=0.003$ ) and membrane ( $p=0.002$ ); ED and tamoxifen treatment in the membrane ( $p=0.003$ ); ED and faslodex treatment in the cytoplasm ( $p=0.003$ ) and membrane ( $p=0.003$ ) and between ED and E2 treatment in the membrane ( $p=0.019$ ).

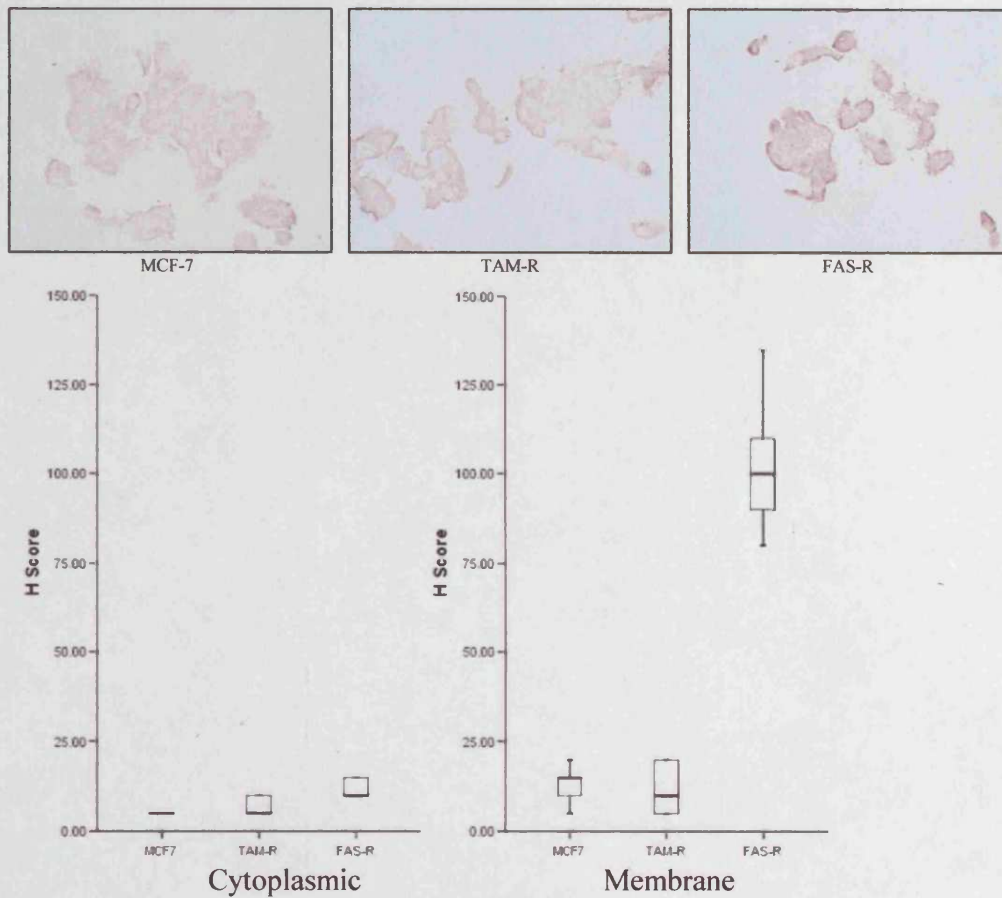


**Figure 3.58** Immunocytochemical staining of  $\delta$ -catenin levels in MCF-7, TAM-R and FAS-R cell pellet preparations

Resistant cell line arrays were stained for  $\delta$ -catenin. Annotation is as in Figure 3.55. Shown here are the staining levels in MCF-7 cells, acquired tamoxifen resistant (TAM-R) and faslodex resistant (FAS-R) cells. There is only a significant difference between the MCF-7 and FAS-R cells at the cytoplasmic ( $p=0.004$ ) and membrane ( $p=0.002$ ) level.



### 3.4.3 Bag-1

#### 3.4.3.1 Oestradiol and anti-hormonal treatments

##### 3.4.3.1.1 Immunocytochemistry

Staining for Bag-1 with a specific antibody resulted in heterogeneous nuclear staining with only very low levels of cytoplasmic staining, the latter remaining relatively constant throughout treatment. An example of Bag-1 staining can be seen in Figure 3.59, which shows low cytoplasmic and substantial nuclear staining. Figure 3.59 also shows that there was no staining in the omission of primary antibody control. At all time points there were no significant changes in protein levels (cytoplasmic or nuclear) between the E2 treated and ED group. However, at day 4 (Figure 3.60) there was a small non-significant increase of 54% ( $p=0.08$ ) and larger significant 111% ( $p=0.027$ ) increase in nuclear staining with the anti-oestrogens tamoxifen and faslodex respectively compared with E2 treatment. Furthermore, when compared to ED there was a significant 61% ( $p=0.049$ ) increase with tamoxifen and 121% ( $p=0.022$ ) with faslodex treatment. At day 7 (Figure 3.61) the Bag-1 nuclear staining promoted by the anti-oestrogens was increased relative to day 4. Tamoxifen resulted in a significant increase of 150% ( $p=0.004$ ) versus E2 treatment, and with an increase of 100% ( $p=0.003$ ) versus ED. Faslodex treatment showed a large significant increase of 265% ( $p=0.004$ ) versus E2 treatment and a 195% ( $p=0.003$ ) increase versus ED. Day 10 (Figure 3.62) nuclear staining for tamoxifen showed a significant 76% ( $p=0.013$ ) increase versus E2 treatment and 55% ( $p=0.012$ ) versus ED, while faslodex further increased staining

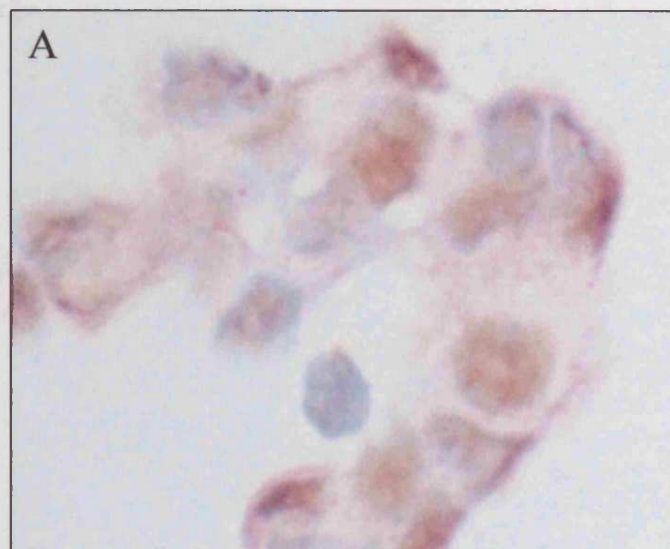
significantly by 339% ( $p=0.004$ ) versus E2 treatment and by 287% ( $p=0.004$ ) versus ED. From these data it appears that the level of Bag-1 in the nucleus with tamoxifen treatment peaked at day 7; however, faslodex treatment had clearly produced the largest increase by day 10 (see Figures 3.61 versus 3.62). Bag-1 is clearly an anti-oestrogen induced gene, as both tamoxifen and faslodex treatment increased nuclear protein staining compared to both E2 treatment and ED. As such the protein levels were thus similar to the mRNA profiles seen with the arrays; however they differed from the RT-PCR results as ED has little or no effect in inducing Bag-1 protein expression. Bag-1 remains a promising anti-oestrogen induced gene.

### 3.4.3.2 Resistance

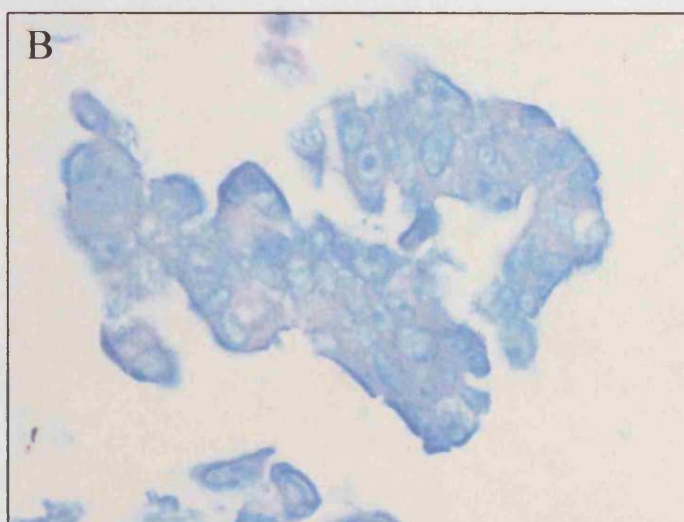
#### 3.4.3.2.1 Immunocytochemistry

The levels of Bag-1 seen in the tamoxifen and faslodex acquired resistance cell lines compared with the parental MCF-7 cells are shown in Figure 3.63. No differences in nuclear staining were observed between MCF-7 cells and TAM-R cells, indicating that the anti-hormone induced effects in MCF-7 cells were transient and not sustained into resistance. In contrast, the nuclear staining of Bag-1 significantly increased by 77% ( $p=0.004$ ) in the FAS-R cells, while the cytoplasmic levels of Bag-1 also increased significantly by 239% ( $p=0.004$ ). Compared with Figure 3.62, these results show that the nuclear staining increase seen after 10 days of faslodex treatment was sustained through to

resistance, with a further marked increase in the cytoplasmic staining occurring between 10 days treatment and resistance.



Localisation of Bag-1 immunostaining



Omission of primary antibody

Figure 3.59 Bag-1 immunostaining and omission of primary antibody control in MCF-7 cells treated with faslodex for 10 days

Photograph A illustrates the predominantly nuclear immunostaining localisation of Bag-1 in MCF-7 cells treated with faslodex for 10 days. Photograph B (original magnification x40) shows that there is no staining with omission of the Bag-1 primary antibody.

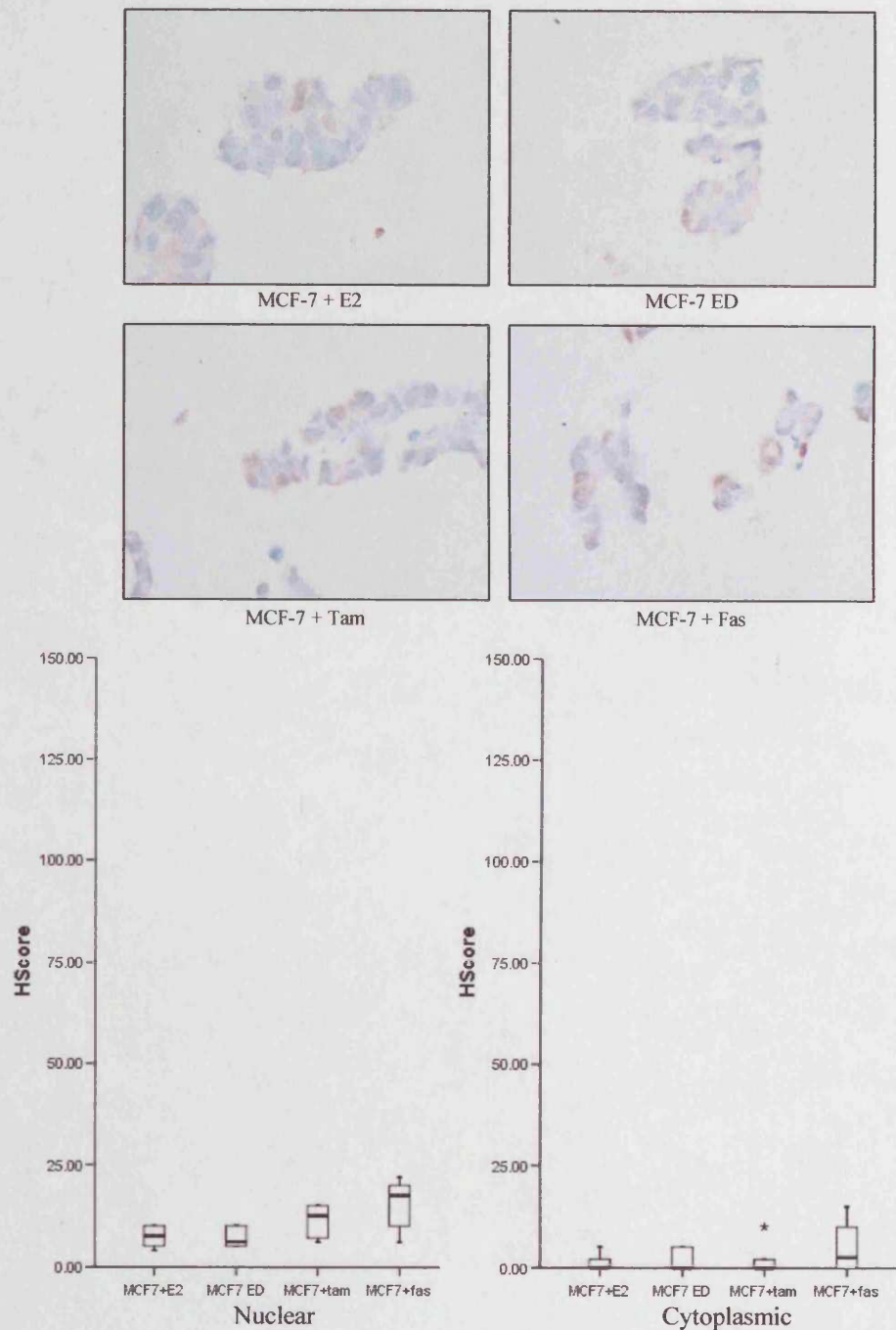


**Figure 3.60** Immunocytochemical staining of Bag-1 in MCF-7 cell pellet preparations after 4 days with/without oestradiol or anti-oestrogen treatment

Day 4 MCF-7 cell pellet treatment arrays were re-hydrated and stained for Bag-1. Annotation is as in Figure 3.55. There are significant differences between E2 and faslodex treatment in the nucleus ( $p=0.027$ ); between ED and tamoxifen treatment in the nucleus ( $p=0.049$ ) and between ED and faslodex treatment in the nucleus ( $p=0.022$ ).

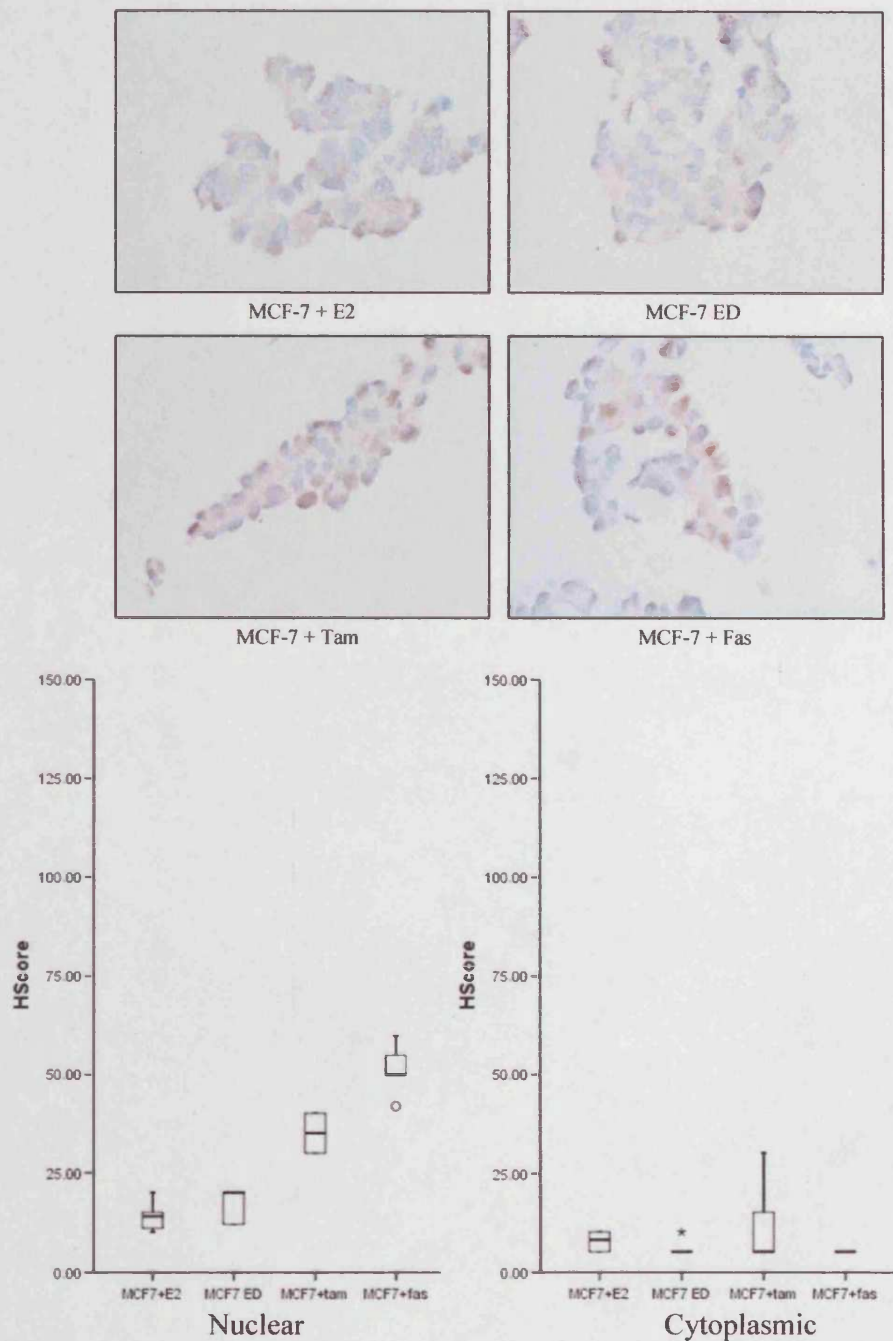


**Figure 3.61** Immunocytochemical staining of Bag-1 in MCF-7 cell pellet preparations after 7 days with/without oestradiol or anti-oestrogen treatment

Day 7 MCF-7 cell pellet treatment arrays were re-hydrated and stained for Bag-1. Annotation is as in Figure 3.55. There are significant differences between E2 and tamoxifen treatment in the nucleus ( $p=0.004$ ) and between E2 and faslodex treatment in the nucleus ( $p=0.004$ ); between ED and tamoxifen treatment in the nucleus ( $p=0.003$ ) and between ED and faslodex treatment in the nucleus ( $p=0.003$ ).

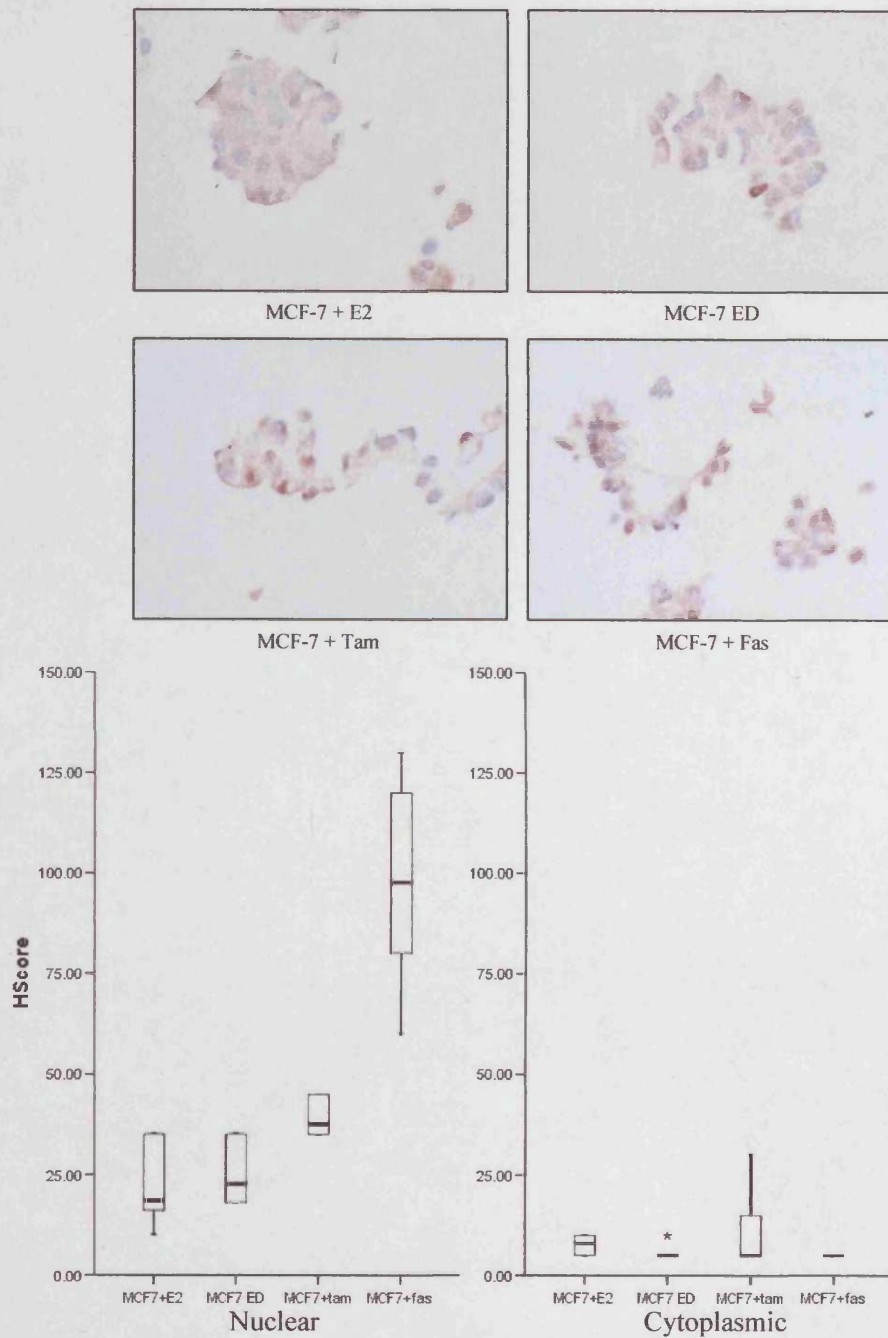


**Figure 3.62** Immunocytochemical staining of Bag-1 in MCF-7 cell pellet preparations after 10 days with/without oestradiol or anti-oestrogen treatment

Day 10 MCF-7 cell pellets treatment arrays were re-hydrated and stained for Bag-1. Annotation is as in Figure 3.55. There are significant differences between E2 and tamoxifen treatment in the nucleus ( $p=0.013$ ) and between E2 and faslodex treatment in the nucleus ( $p=0.004$ ); between ED and tamoxifen treatment in the nucleus ( $p=0.012$ ) and between ED and faslodex treatment in the nucleus ( $p=0.004$ ).

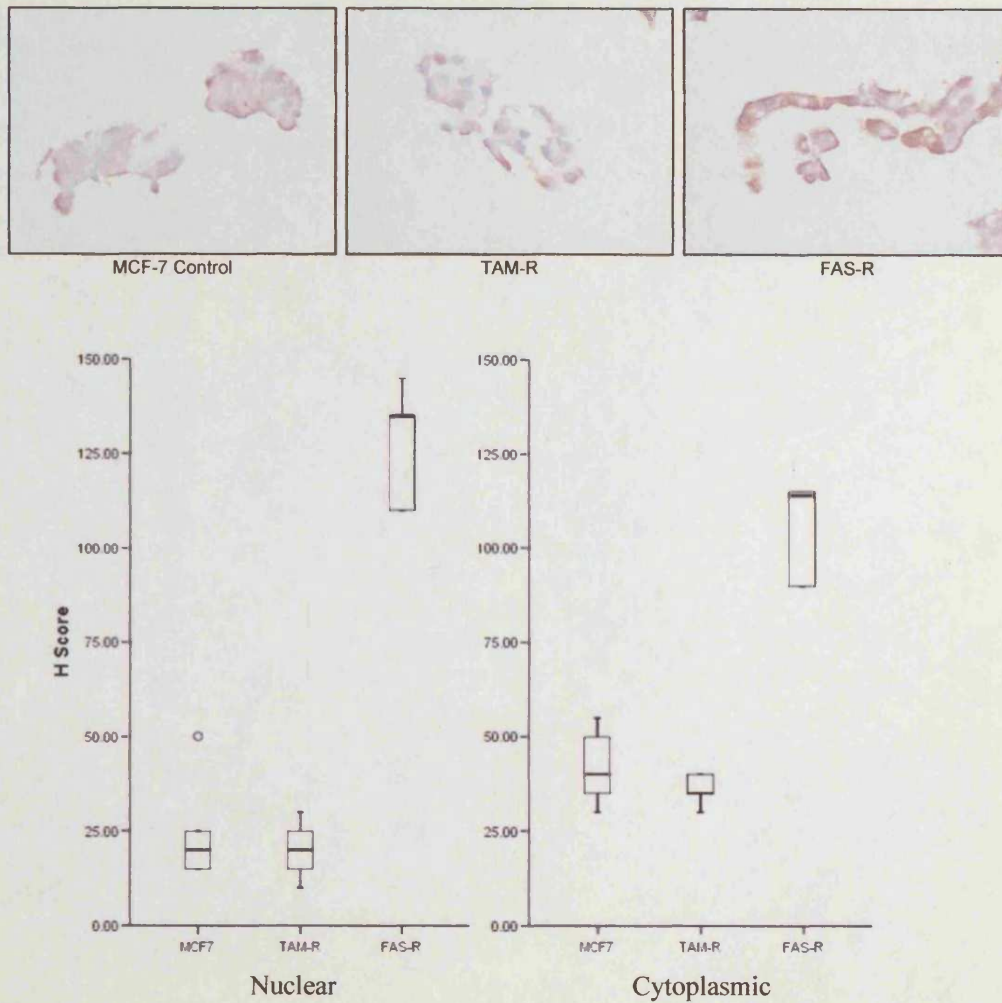


**Figure 3.63 Immunocytochemical staining of Bag-1 levels in MCF-7, TAM-R and FAS-R cell pellet preparations**

Resistant cell line arrays were stained for Bag-1. Annotation is as in Figure 3.55. Shown are the staining levels in MCF-7 cells, acquired tamoxifen resistant (TAM-R) and faslodex resistant (FAS-R) cells. There is a significant increase in the nuclear ( $p=0.004$ ) and cytoplasmic ( $p=0.004$ ) staining, but only in FAS-R cells compared to MCF-7 cells.



### 3.4.4 14-3-3 $\zeta$

#### 3.4.4.1 Oestradiol and anti-hormonal treatments

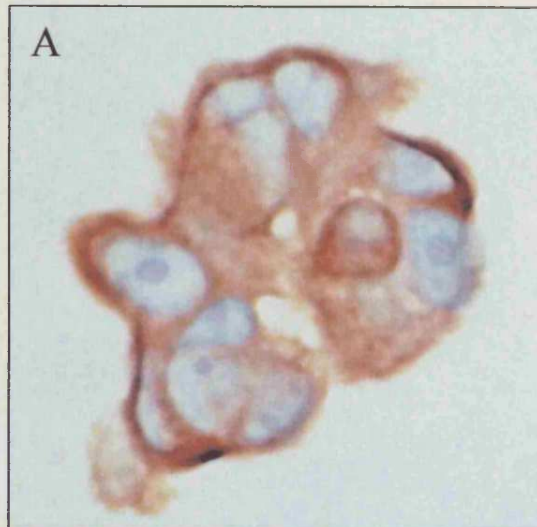
##### 3.4.4.1.1 Immunocytochemistry

Sections of the MCF-7 pellet array of cells treated with anti-hormones or E2 were dehydrated and incubated with a 14-3-3 $\zeta$  specific primary antibody, followed by rabbit secondary antibody and DAB for detection. In general 14-3-3 $\zeta$  staining was relatively homogenous, with a high frequency of stained cells, showing both cytoplasmic and predominant plasma membrane immunocytostaining (Figure 3.64). Such immunostaining was lost when the immunocytochemical assay was carried out in the absence of primary antibody (Figure 3.64), or in the presence of a specific 14-3-3 $\zeta$  blocking peptide showing assay specificity (Figure 3.64). Figure 3.65 shows the protein levels of 14-3-3 $\zeta$  after 4 days of treatment. Tamoxifen or faslodex treatment produced a significant 63% ( $p=0.003$ ) and 54% ( $p=0.003$ ) increase in cytoplasmic staining respectively compared with E2 treatment. Tamoxifen and faslodex treatment also increased cytoplasmic staining significantly versus ED by 35% ( $p=0.003$ ) and 28% ( $p=0.002$ ) respectively. Similarly, there were significant increases in membrane staining in the presence of tamoxifen (140%,  $p=0.003$ ) and faslodex (213%,  $p=0.003$ ) treatment as well as under ED conditions (39%,  $p=0.003$ ) compared with E2 treatment. Again, there was a further significant increase in membrane staining with the anti-oestrogens tamoxifen (73%,  $p=0.003$ ) and faslodex (127%,  $p=0.003$ ) compared to ED conditions. A largely comparable profile was also seen on days 7 (Figure 3.66) and 10 (Figure 3.67). Thus, for

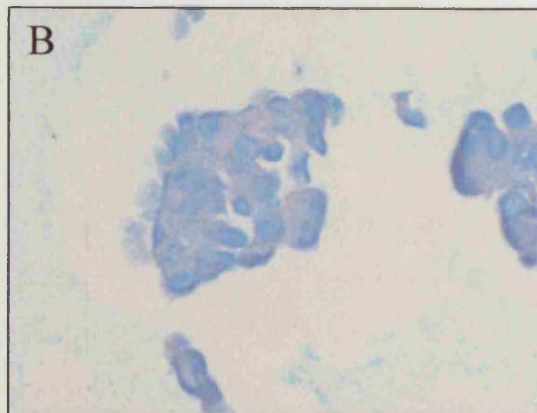
cytoplasmic staining of 14-3-3 $\zeta$  at day 7, there was an 87% ( $p=0.002$ ) increase with tamoxifen and 75% ( $p=0.003$ ) increase with faslodex treatment as well as a 38% ( $p=0.007$ ) increase with ED, compared to levels in MCF-7 cells with E2 treatment. As on day 4, there was a significant increase in cytoplasmic staining with tamoxifen of 36% ( $p=0.001$ ) and a 27% ( $p=0.002$ ) increase with faslodex treatment compared to ED. There were also significant increases with tamoxifen or faslodex treatment of 126% ( $p=0.003$ ) and 136% ( $p=0.003$ ) respectively in membrane staining compared to E2. Versus ED, 14-3-3 $\zeta$  membrane staining was increased 91% ( $p=0.003$ ) with tamoxifen treatment and 186% ( $p=0.003$ ) with faslodex treatment. However, there was no change in membrane staining under ED compared to E2 treatment. At day 10 there were significant increases in cytoplasmic staining of 42% ( $p=0.003$ ) and 31% ( $p=0.002$ ) with tamoxifen and faslodex treatment respectively versus E2 treatment. There was also significant increases with tamoxifen and faslodex treatment compared to ED of 39% ( $p=0.003$ ) and 28% ( $p=0.003$ ) respectively. Although the membrane staining showed no change with tamoxifen treatment compared to E2 treatment, there was a significant increase with faslodex treatment of 148% ( $p=0.004$ ) that also exceeded ED (164%,  $p=0.004$ ). There was again no change in cytoplasmic or membrane levels with ED compared to E2.

#### 3.4.4.1.2 Western blotting

The day 7 western blot results for 14-3-3 $\zeta$  are shown in Figure 3.68 and demonstrate that there was no obvious change in the protein levels in ED versus E2 treatment. There was however an increase with the anti-oestrogen treatments tamoxifen and faslodex, which resulted in a 58% and 50% increase respectively compared to both E2 treatment and ED.



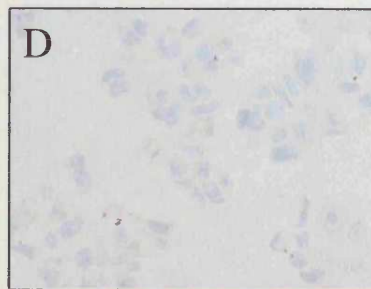
Localisation of 14-3-3 $\zeta$  immunostaining



Omission of primary antibody



MCF-7 + Fas without 14-3-3 $\zeta$  blocking peptide



MCF-7 + Fas with 14-3-3 $\zeta$  blocking peptide

**Figure 3.64** 14-3-3 $\zeta$  immunostaining, omission of primary antibody control and blocking peptide in MCF-7 cells treated with faslodex for 10 days

Photograph A shows localisation of 14-3-3 $\zeta$  in MCF-7 cells treated with faslodex for 10 days. Photograph B shows the lack of immunostaining following omission of primary antibody. Photographs C and D show the immunostaining for 14-3-3 $\zeta$  in the presence (C) and absence (D) of a specific 14-3-3 $\zeta$  blocking peptide (all original magnification x40).

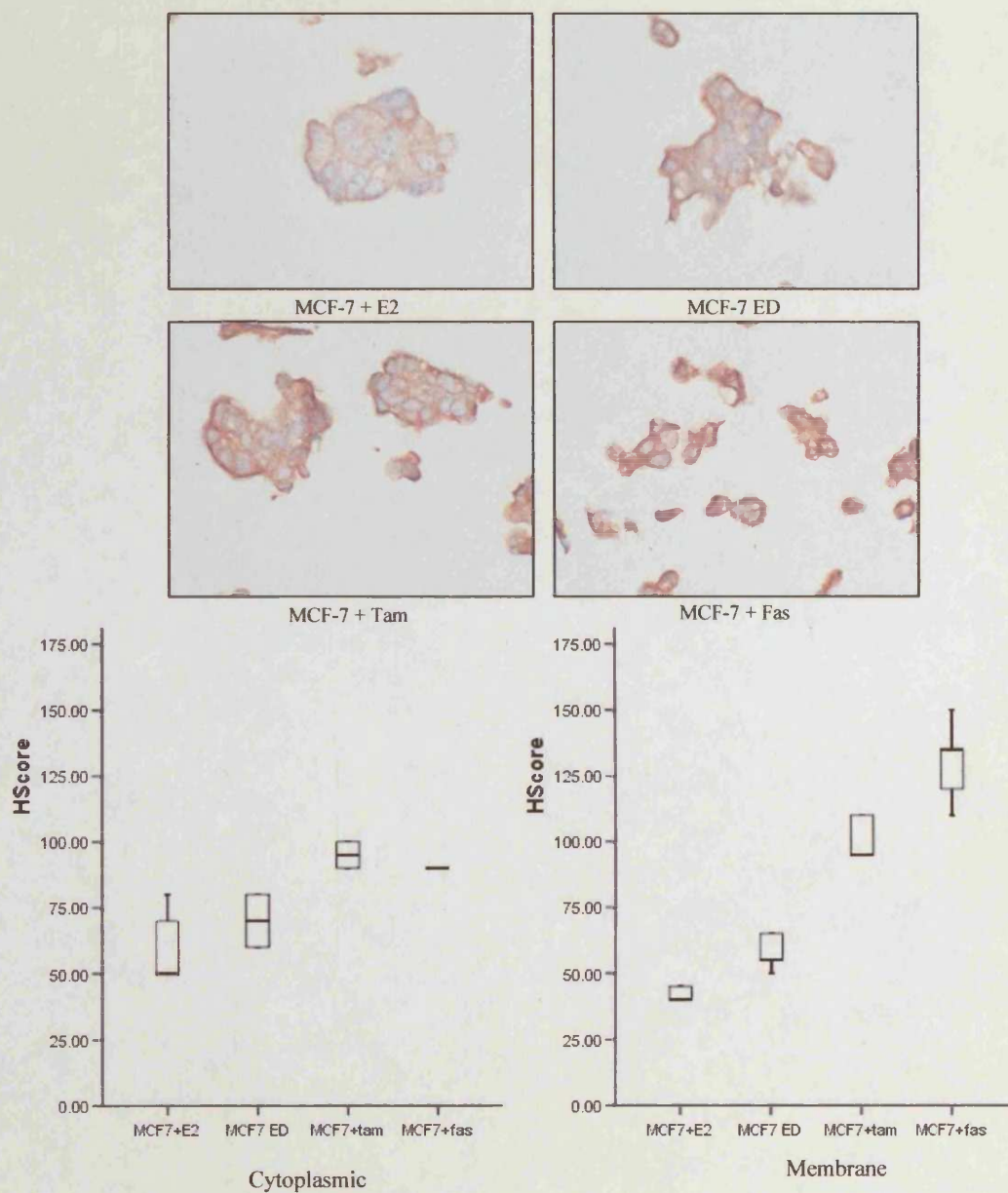


**Figure 3.65** Immunocytochemical staining of 14-3-3ζ in MCF-7 cell pellet preparations after 4 days with/without oestradiol or anti-oestrogen treatment

Day 4 MCF-7 cell pellet treatment arrays were stained for 14-3-3ζ. Annotation is as in Figure 3.55. There are significant differences between ED and E2 treatment in the membrane ( $p=0.003$ ); between E2 and tamoxifen treatment in the cytoplasm ( $p=0.003$ ) and membrane ( $p=0.003$ ); between E2 and faslodex treatment in the cytoplasm ( $p=0.002$ ) and membrane ( $p=0.003$ ); between ED and tamoxifen treatment in the cytoplasm ( $p=0.003$ ) and membrane ( $p=0.003$ ) and between ED and faslodex treatment in the cytoplasm ( $p=0.002$ ) and membrane ( $p=0.003$ ).

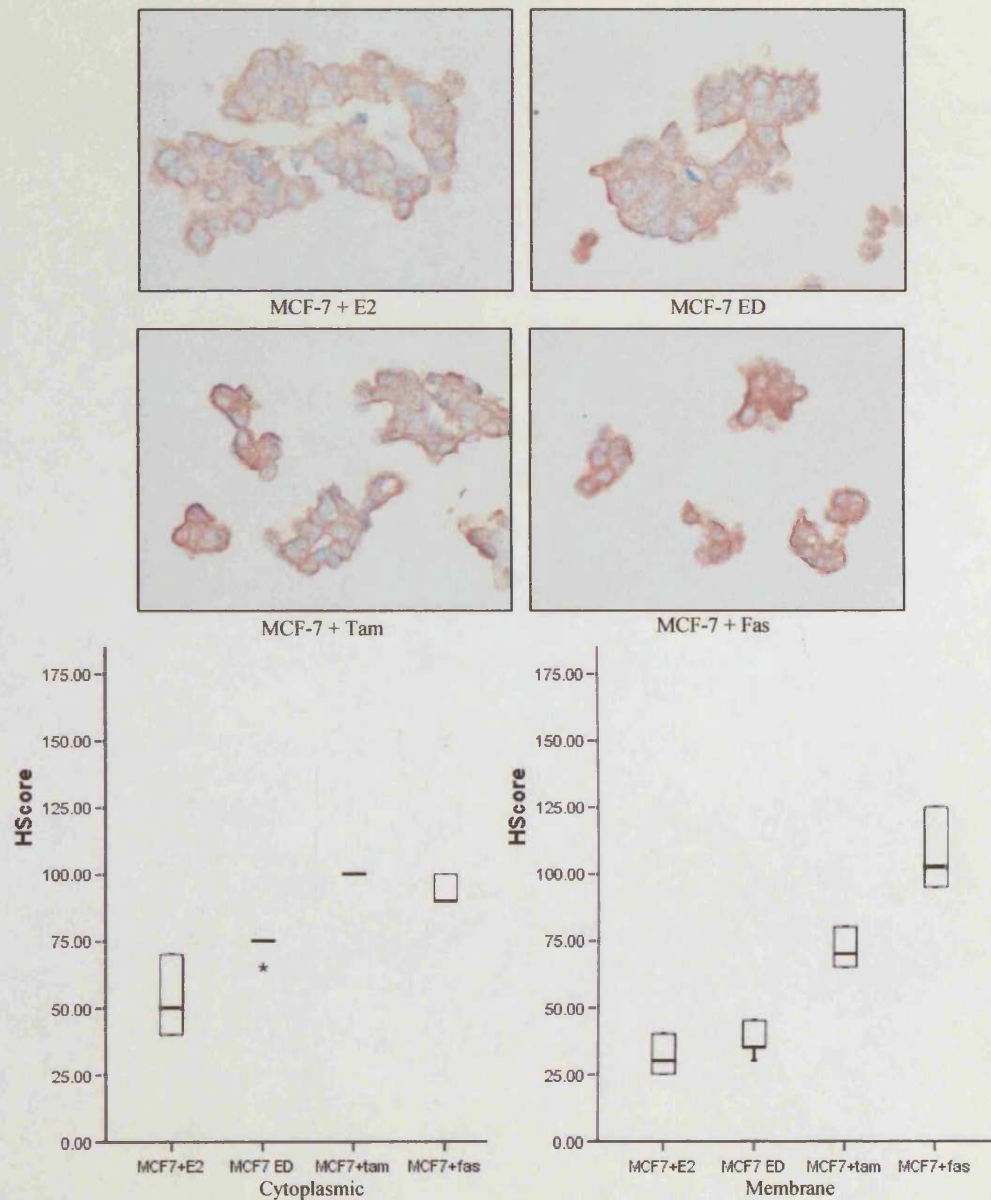


**Figure 3.66** Immunocytochemical staining of 14-3-3ζ in MCF-7 cell pellet preparations after 7 days with/without oestradiol or anti-oestrogen treatment

Day 7 MCF-7 cell pellet treatment arrays were stained for 14-3-3ζ. Annotation is as in Figure 3.55. There are significant differences between ED and E2 treatment in the cytoplasm ( $p=0.007$ ); between E2 and tamoxifen treatment in the cytoplasm ( $p=0.002$ ) and membrane ( $p=0.003$ ); between E2 and faslodex treatment in the cytoplasm ( $p=0.003$ ) and membrane ( $p=0.003$ ); between ED and tamoxifen treatment in the cytoplasm ( $p=0.001$ ) and membrane ( $p=0.003$ ) and between ED and faslodex treatment in the cytoplasm ( $p=0.002$ ) and membrane ( $p=0.003$ ).

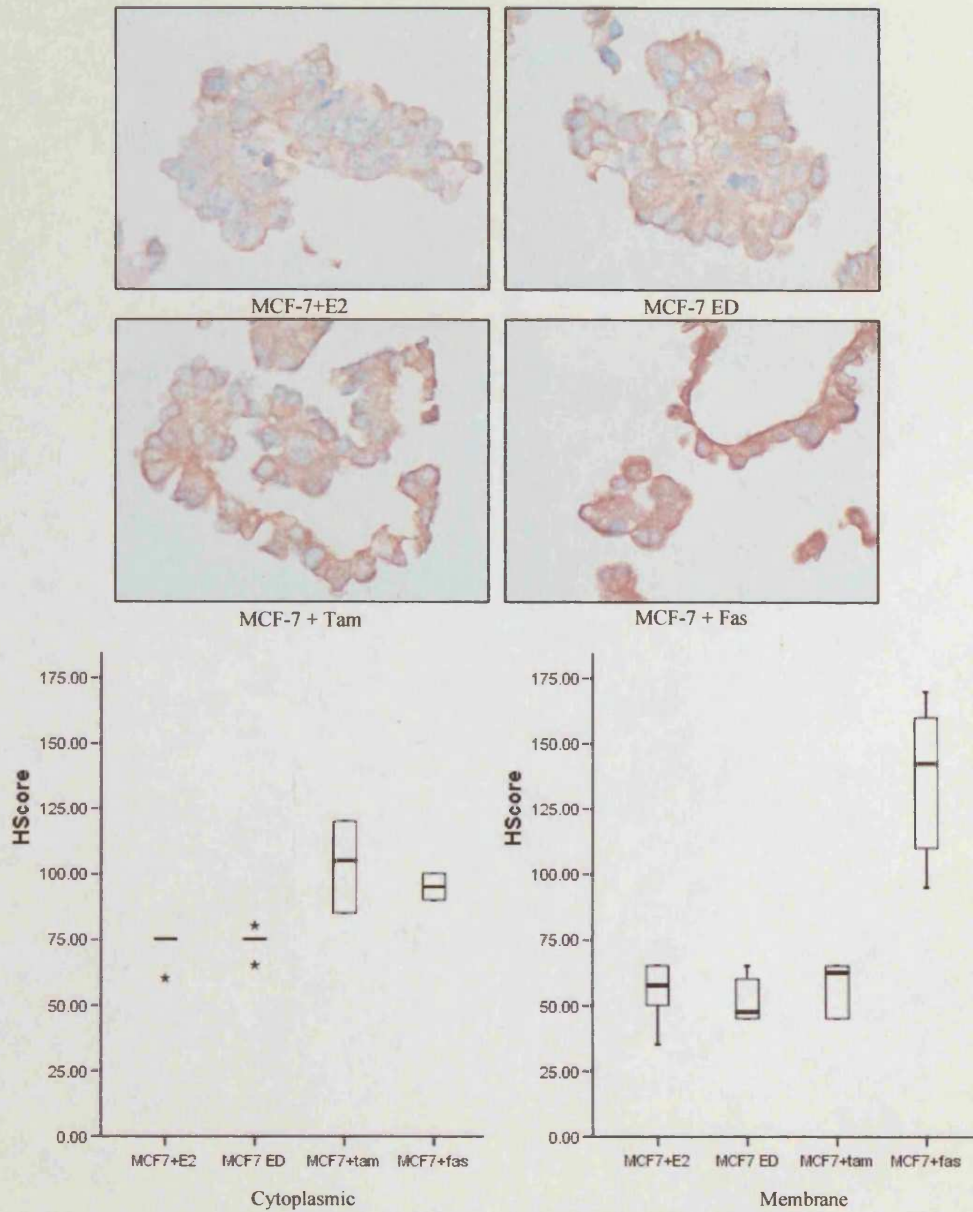


**Figure 3.67** Immunocytochemical staining of 14-3-3ζ in MCF-7 cell pellet preparations after 10 days with/without oestradiol or anti-oestrogen treatment

Day 10 MCF-7 cell pellet treatment arrays were stained for 14-3-3ζ. Annotation is as in Figure 3.55. There are significant differences between E2 and tamoxifen treatment in the cytoplasm ( $p=0.002$ ); between E2 and faslodex treatment in the cytoplasm ( $p=0.002$ ) and membrane ( $p=0.004$ ); between ED and tamoxifen treatment in the cytoplasm ( $p=0.003$ ) and between ED and faslodex treatment for the cytoplasm ( $p=0.003$ ) and membrane ( $p=0.004$ ).

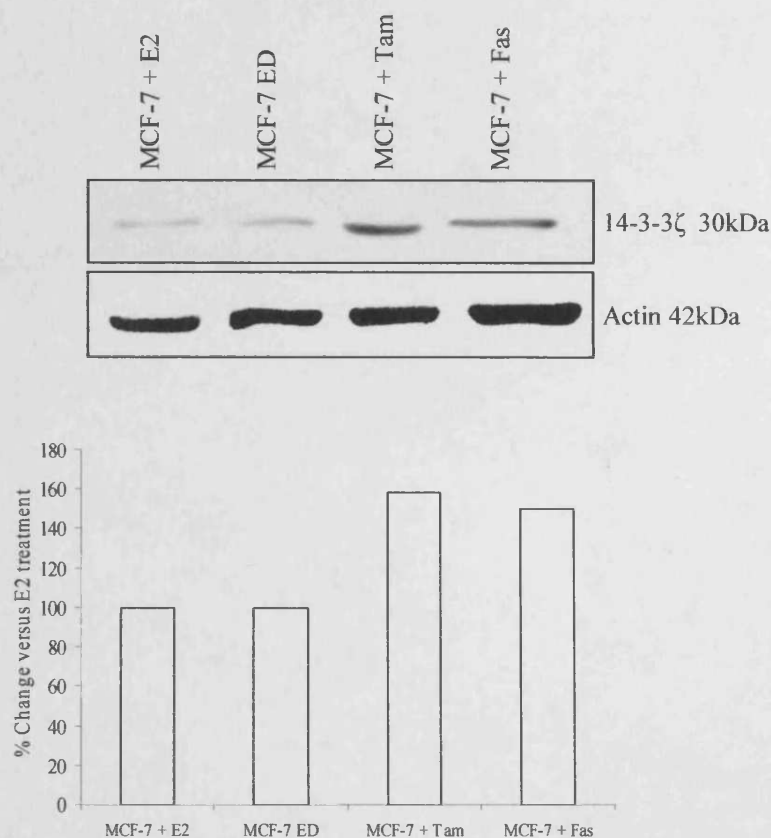


**Figure 3.68** Levels of 14-3-3 $\zeta$  protein by western blotting in MCF-7 cell preparations after 7 days with/without oestradiol or anti-oestrogen treatment

Whole cell extracts from MCF-7 cells either under ED conditions, or treated with E2, tamoxifen or faslodex for 7 days were subject to western blotting. 14-3-3 $\zeta$  and  $\beta$ -actin specific antibodies were used to probe the blotted membranes. The graph shows the percentage change in levels of 14-3-3 $\zeta$  versus E2 levels after scanning densitometry and  $\beta$ -actin normalization (n=1).



### 3.4.5 Hif-1 $\alpha$

#### 3.4.5.1 Oestradiol and anti-hormonal treatments

##### 3.4.5.1.1 Immunocytochemistry

The photographs in Figure 3.69 show the ICC results obtained for Hif-1 $\alpha$ , where staining is only cytoplasmic (but eliminated with omission of primary antibody). After several optimisation attempts using different antigen retrievals and two different primary antibodies, neither a nuclear localisation nor an increase in signal with anti-hormones (e.g. faslodex versus E2, Figure 3.69) could be observed for this transcription factor in keeping with its reported rapid degradation under normoxia.

##### 3.4.5.1.2 Western blotting

Western blotting was also carried out for Hif-1 $\alpha$  and  $\beta$ -actin, where results can be seen in Figure 3.70. No band was observed at the 120kDa size of Hif-1 $\alpha$  as expected under normoxic conditions, although there was an unexpected band at ~50kDa (that was decreased by approximately 40% in the presence of faslodex compared to E2 treated MCF-7 cells). Following achieving no signal at 120kDa and a spurious band at ~50kDa, MCF-7 cells were grown for 7 days and then treated with the iron chelator desferoxamine (DFO, 100 $\mu$ M), a hypoxia mimic, for 4 hours to check if it was possible to induce Hif-1 $\alpha$  protein expression in MCF-7 cells. The resultant blot is shown in Figure 3.71. It clearly shows two bands: a DFO inducible band of approximately 55kDa, and again

the spurious band at ~50kDa band as observed in the control. No band was detected at 120kDa. Due to the obvious experimental problems experienced with both the ICC and western blotting detection of Hif-1 $\alpha$  under normoxic conditions, as well as the results using the DFO hypoxia mimic, no further experiments were carried out in this thesis regarding Hif-1 $\alpha$ .

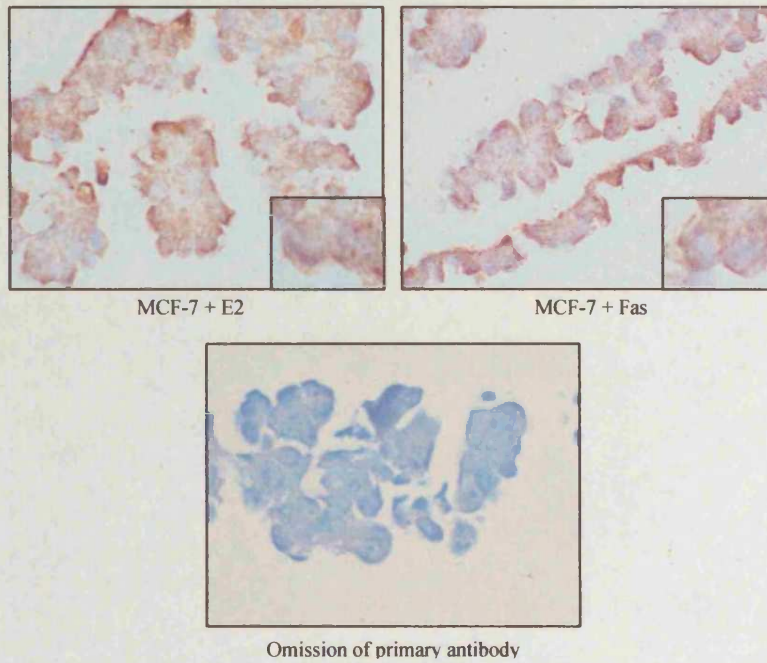


**Figure 3.69 Immunostaining achieved using Hif-1 $\alpha$  antibody and omission of primary antibody control in MCF-7 cells treated with E2 or faslodex for 7 days**

MCF-7 day 7 cell pellets treated with E2 or faslodex were rehydrated and stained for Hif-1 $\alpha$  using a primary antibody followed by secondary antibody and DAB detection. Also shown is the lack of staining following omission of the primary Hif-1 $\alpha$  antibody (all original magnification x40).

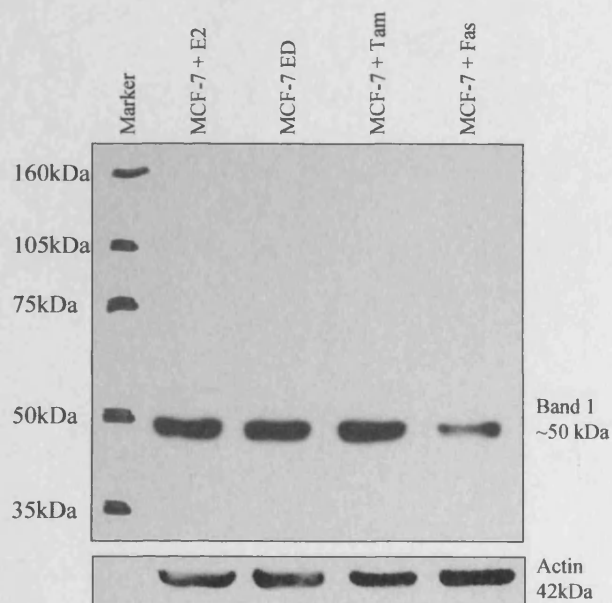


Figure 3.70 Western blot analysis of Hif-1 $\alpha$  in MCF-7 cells after 7 days treatment with/without oestradiol or anti-oestrogens

Whole cell extracts from ED MCF-7 cells, or treated with E2, tamoxifen or faslodex for 7 days were subject to western blotting. Hif-1 $\alpha$  and  $\beta$ -actin specific antibodies were used to probe the blotted membranes.

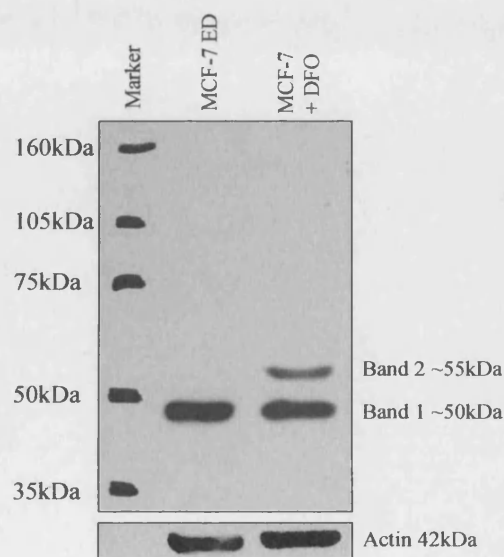


Figure 3.71 Western blot analysis of MCF-7 cells treated with desferoxamine (DFO) for 1 hour versus control

Whole cell extracts from ED MCF-7 cells grown for 7 days followed by DFO (100 $\mu$ M) treatment for 4 hours were subject to western blot analysis. Hif-1 $\alpha$  and  $\beta$ -actin specific antibodies were used to probe the blotted membranes.

### 3.4.6 NME3

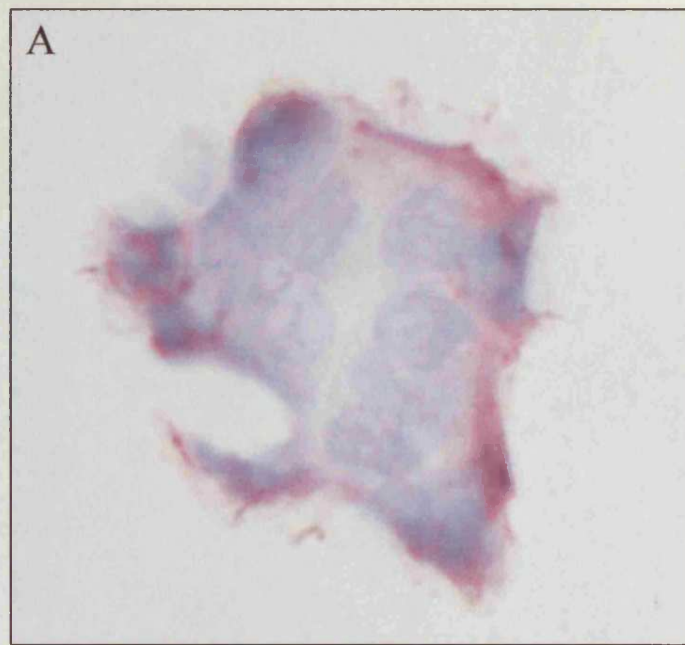
#### 3.4.6.1 Oestradiol and anti-hormonal treatments

##### 3.4.6.1.1 Immunocytochemistry

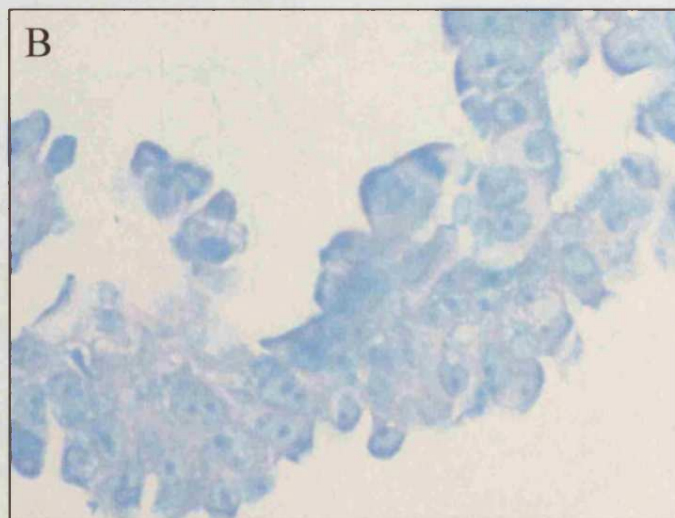
Sections of MCF-7 treatment pellet arrays were immunostained for NME3 using a specific antibody. The resulting staining was heterogeneous and predominantly cytoplasmic, particularly prominent under the plasma membrane (Figure 3.72). Figure 3.72 also shows the lack of staining following primary antibody omission, indicating specificity of the secondary antibody and a working system. At day 4 (Figure 3.73) the level of NME3 in the presence of E2 treatment was very low and remained at this level up to day 10. Relative to the E2 treated group both ED and faslodex treatment produced an increase in the cytoplasmic levels of NME3 on days 4, 7 and 10. While tamoxifen treatment had no effect at day 4 on NME3 levels versus E2 treatment, faslodex treatment resulted in a significant 280% ( $p=0.002$ ) increase compared to E2 treatment, and ED resulted in a significant 170% ( $p=0.002$ ) increase compared with E2 treatment. Faslodex treatment also significantly further increased staining levels by 40% ( $p=0.002$ ) versus ED, although tamoxifen treatment significantly decreased staining by 63% ( $p=0.002$ ) compared to ED at this time point. By day 7 (Figure 3.74), there was a significant increase of 78% ( $p=0.041$ ) with ED, 92% ( $p=0.026$ ) with tamoxifen treatment and 100% ( $p=0.026$ ) with faslodex versus E2 treatment. No difference was seen between ED and tamoxifen or faslodex. By day 10 (Figure 3.75) there was a significant 112% ( $p=0.006$ ) increase in NME3 staining with

ED, an increase of 150% ( $p=0.002$ ) with faslodex treatment but no significant increase with tamoxifen treatment compared to E2. The staining achieved with faslodex treatment was roughly equivalent to that of ED at this time point, although tamoxifen was significantly lower by 32% ( $p=0.041$ ).

The protein staining for NME3 clearly showed evidence of faslodex induction versus E2 treatment at all time points, and at the early time point versus ED. However, induction was not noted consistently with tamoxifen. In general there was some overlap between the array/RT-PCR and protein profiles, but the impact of tamoxifen was discordant. Some E2-suppression was apparent at all time points.



Localisation of NME3 immunostaining



Omission of primary antibody

Figure 3.72 NME3 immunostaining and omission of primary antibody control in MCF-7 cells treated with faslodex for 10 days

Photograph A shows the immunostaining localisation of NME3 in MCF-7 cells treated with faslodex for 10 days. Photograph B (original magnification x40) shows that there is no staining with omission of the NME3 primary antibody.



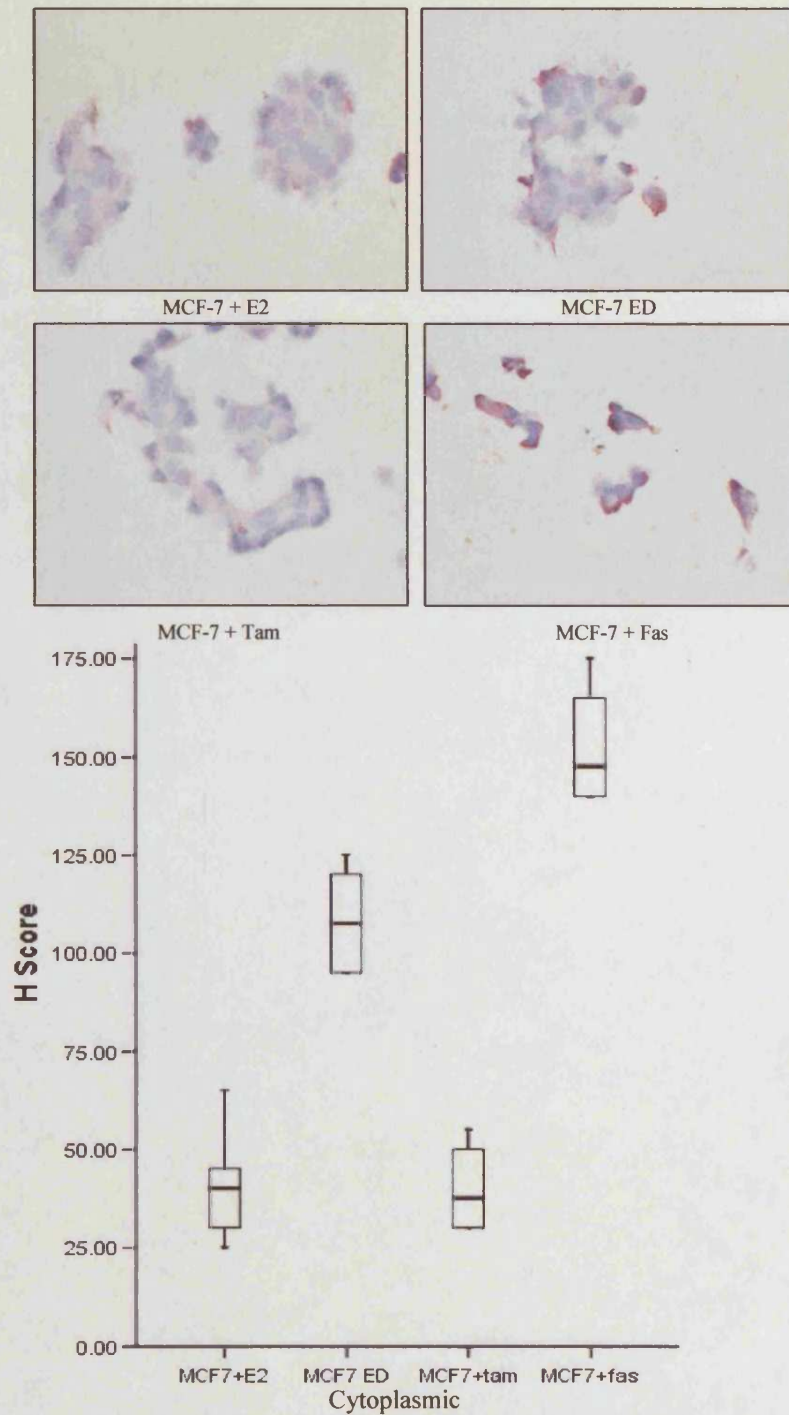
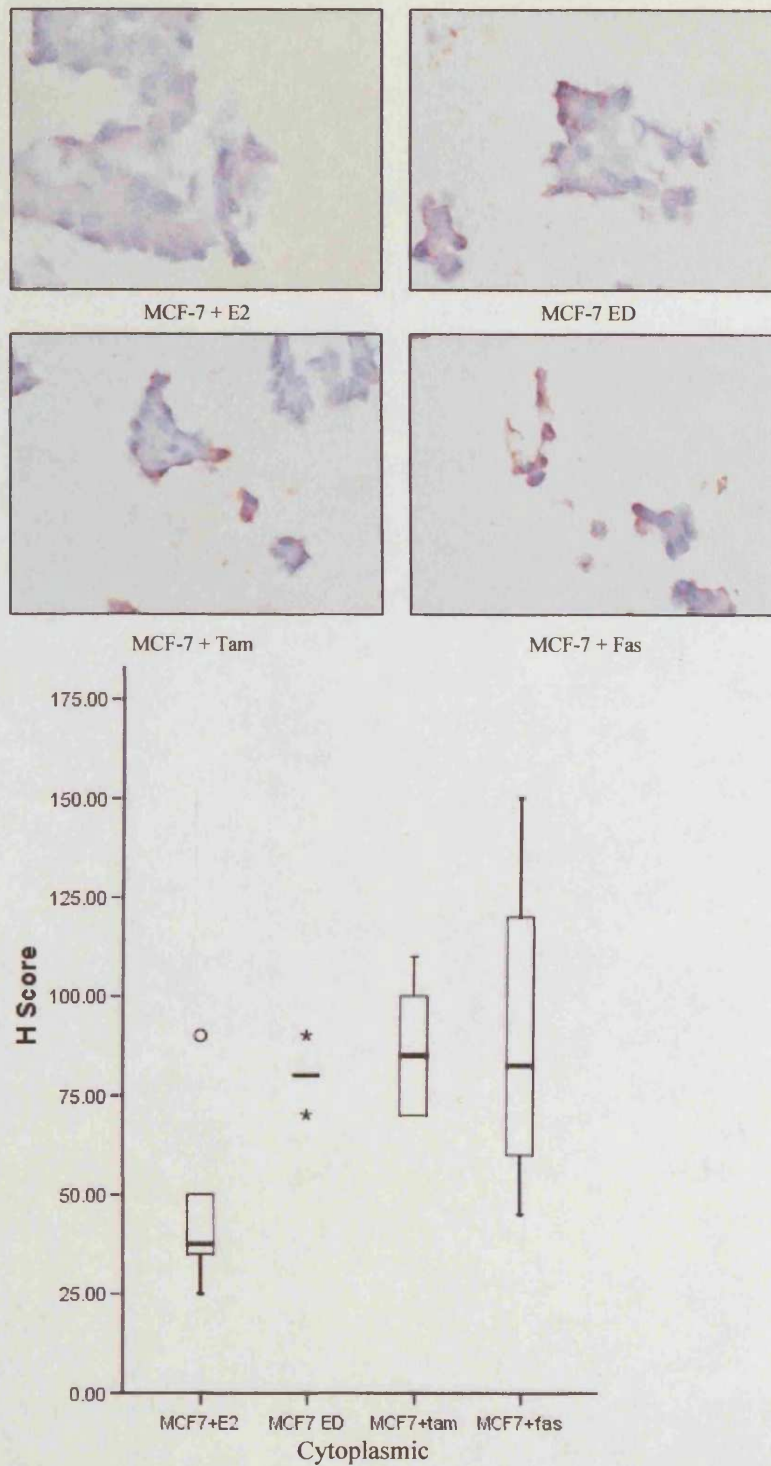


Figure 3.73 Immunocytochemical staining of NME3 in MCF-7 cell pellet preparations after 4 days with/without oestradiol or anti-oestrogen treatment

Day 4 MCF-7 treatment arrays were stained for NME3 with DAB detection. Annotation is as in Figure 3.55. There are significant differences between faslodex and E2 treatment ( $p=0.002$ ); ED and tamoxifen treatment ( $p=0.002$ ) and ED and faslodex treatment ( $p=0.002$ ).



**Figure 3.74 Immunocytochemical staining of NME3 in MCF-7 cell pellet preparations after 7 days with/without oestradiol or anti-oestrogen treatment**

Day 7 MCF-7 treatment arrays were re-hydrated and stained for NME3. Annotation is as in Figure 3.55. There are significant differences in cytoplasmic staining between ED and E2 treatment ( $p=0.041$ ); tamoxifen and E2 treatment ( $p=0.026$ ) and faslodex and E2 treatment ( $p=0.026$ ).

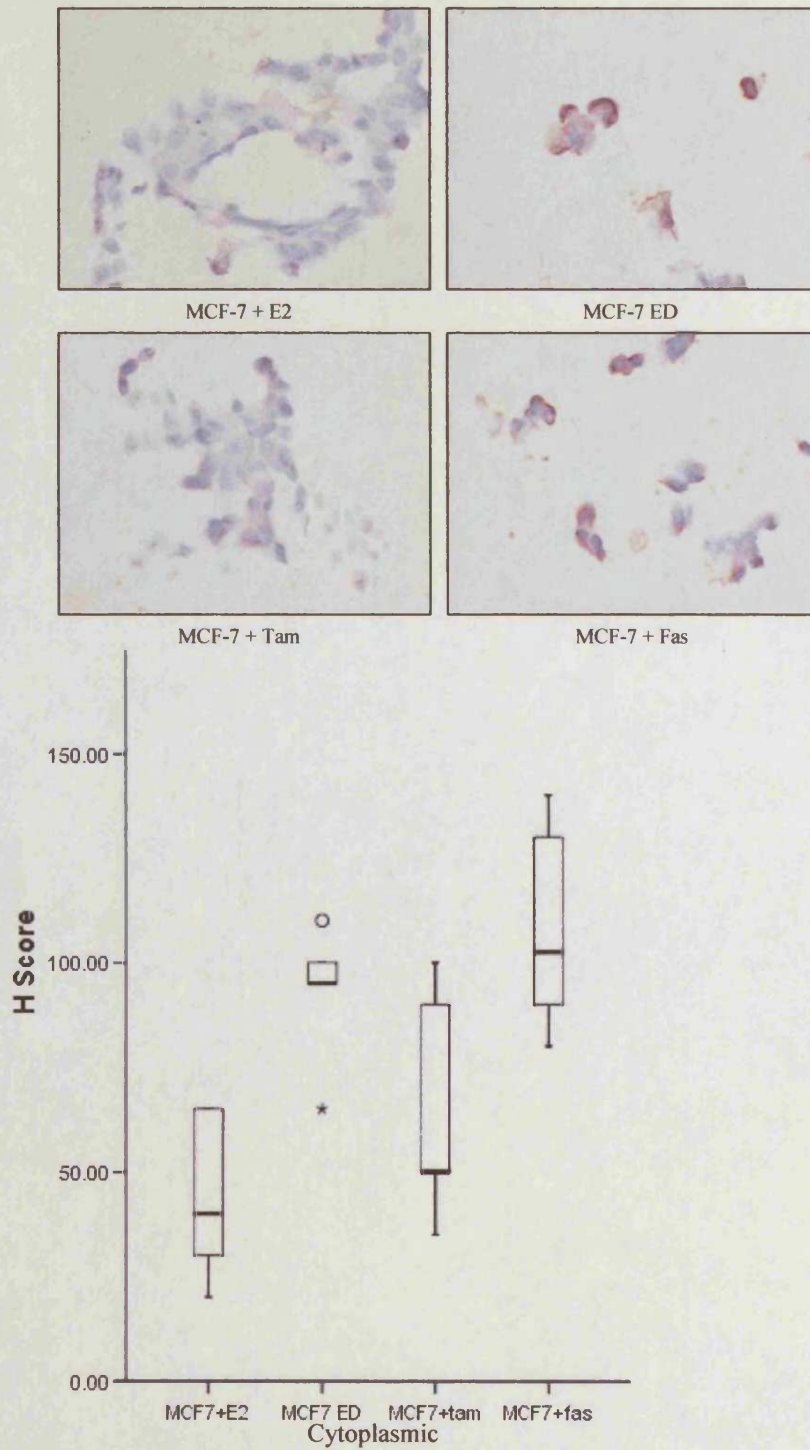


**Figure 3.75** Immunocytochemical staining of NME3 in MCF-7 cells after 10 days with/without oestradiol or anti-oestrogen treatments

Day 10 MCF-7 treatment arrays were re-hydrated and stained for NME3. Annotation is as in Figure 3.55. There are significant differences between ED and E2 treatment ( $p=0.006$ ); faslodex and E2 treatment ( $p=0.002$ ) and tamoxifen treatment and ED ( $p=0.041$ ).

### 3.4.7 NFkB1

#### 3.4.7.1 Oestradiol and anti-hormonal treatments

##### 3.4.7.1.1 Immunocytochemistry

Re-hydrated sections of the MCF-7 cell pellet treatment array were stained for NFkB1 with an antibody that detects both its p50 and p105 isoforms. Staining noted in the nucleus is reported to represent active p50, with cytoplasmic staining reported to represent inactive p105 (Figure 3.76). Also shown in Figure 3.76 is a negative control showing no staining, carried out with the omission of NFkB1 primary antibody which illustrates secondary antibody specificity and a working system. The cytoplasmic staining observed in MCF-7 cell preparations was homogenous and generally constant over treatments at each time point. However, the nuclear staining observed was heterogeneous and differential over treatments and time points. At day 4 (Figure 3.77 and inserts) there were significant increases in nuclear staining with tamoxifen (75%,  $p=0.042$ ) and faslodex (75%,  $p=0.042$ ) treatment compared to E2 treatment. Staining was also increased by ED (71%,  $p=0.039$ ) compared to E2 treatment and so there was no significant difference between staining for ED and for the anti-oestrogens. The various significant differences were represented in the whole cell staining data, as there were no cytoplasmic staining changes. The day 7 (Figure 3.78) and 10 (Figure 3.79) nuclear staining also showed a significant increase with tamoxifen treatment of 83% ( $p=0.003$ ) and 62% ( $p=0.008$ ), with faslodex treatment of 92% ( $p=0.003$ ) and 67% ( $p=0.008$ ), and with ED of 83% ( $p=0.003$ ) and 62% ( $p=0.008$ ) respectively,

compared with E2 treatment. As with day 4, there were no significant increases in nuclear staining between ED and the anti-oestrogens at either time points, although at day 10 only there was an extremely small, but significant, 10% ( $p=0.027$ ) increase in cytoplasmic staining with tamoxifen compared to ED. It was also noted that the total cell staining levels of NFkB1 were significantly increased with anti-hormones by day 10 compared to E2, reflecting a change in expression levels (predominantly nuclear) rather than substantial protein redistribution from an existing NFkB1 cellular pool.

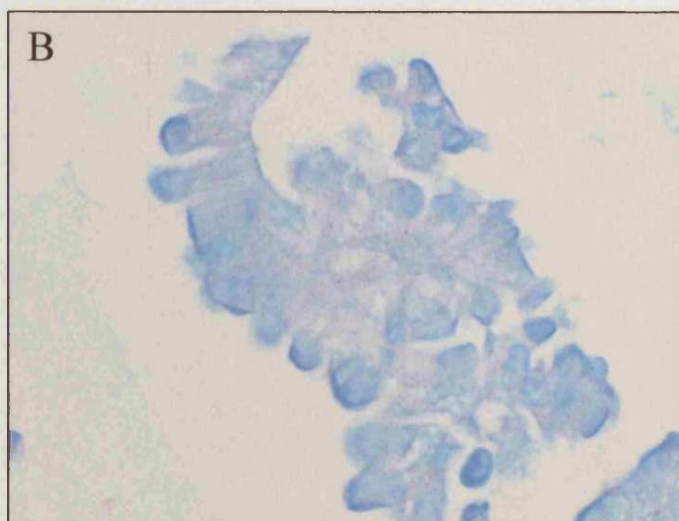
Across the time points it was evident that NFkB1 was an anti-oestrogen-induced, E2-suppressed gene. The protein data was consistent with the RT-PCR results which showed equivalent induction with ED, tamoxifen and faslodex compared to E2 at day 7 and 10, although the array profile differs in that it showed tamoxifen and faslodex also increased levels versus ED (as well as evidence of some E2 induction). NFkB1 remains an interesting gene for further study due to its induction by all anti-hormonal strategies (alongside a strong literature base linking NFkB1 and resistance to other therapy types). Further details of its relationship to anti-hormone treatment have comprised the latter stage of this project.

#### 3.4.7.1.2 NFkB DNA binding activity in MCF-7 cells with oestradiol and anti-hormone treatments

Following on from the above protein studies revealing substantial increases in nuclear NFkB1 with anti-hormones, TransAM assays were carried out to examine the levels of binding activity for different NFkB family members (Renard *et al.*, 2001). The data again indicated active NFkB1 during anti-hormone treatment. Binding activity for all NFkB members except p52 was readily detectable at 7 days (Figures 3.80 and 3.81). In triplicate experiments, the binding activity of NFkB1 p50 (Figure 3.80) increased significantly by 200% ( $p=0.019$ ) in ED cells compared with E2 treatment. There was also a trend for increases of 65% and 57% with the anti-oestrogens tamoxifen ( $p=0.083$ ) and faslodex ( $p=0.131$ ) respectively versus E2 treatment in these studies. The additional NFkB family members (Figure 3.81) were only examined once due to time constraints. p65 was readily detectable with all treatments, but remained constant across the treatment groups. C-rel was also detectable with an apparent increase in binding activity with ED of 67% and with faslodex treatment of 71% versus E2 treatment, although tamoxifen treatment resulted in a 51% decrease in binding activity. The p52 levels were very low and hence no reliable change was detectable.



Localisation of NFkB1 immunostaining



Omission of primary antibody

Figure 3.76 Localisation of NFkB1 staining in MCF-7 cells treated with faslodex for 10 days

Photograph A shows the immunostaining localisation of NFkB in MCF-7 cells treated with faslodex for 10 days. Photograph B (original magnification x40) shows that there is no staining with omission of the NFkB primary antibody.

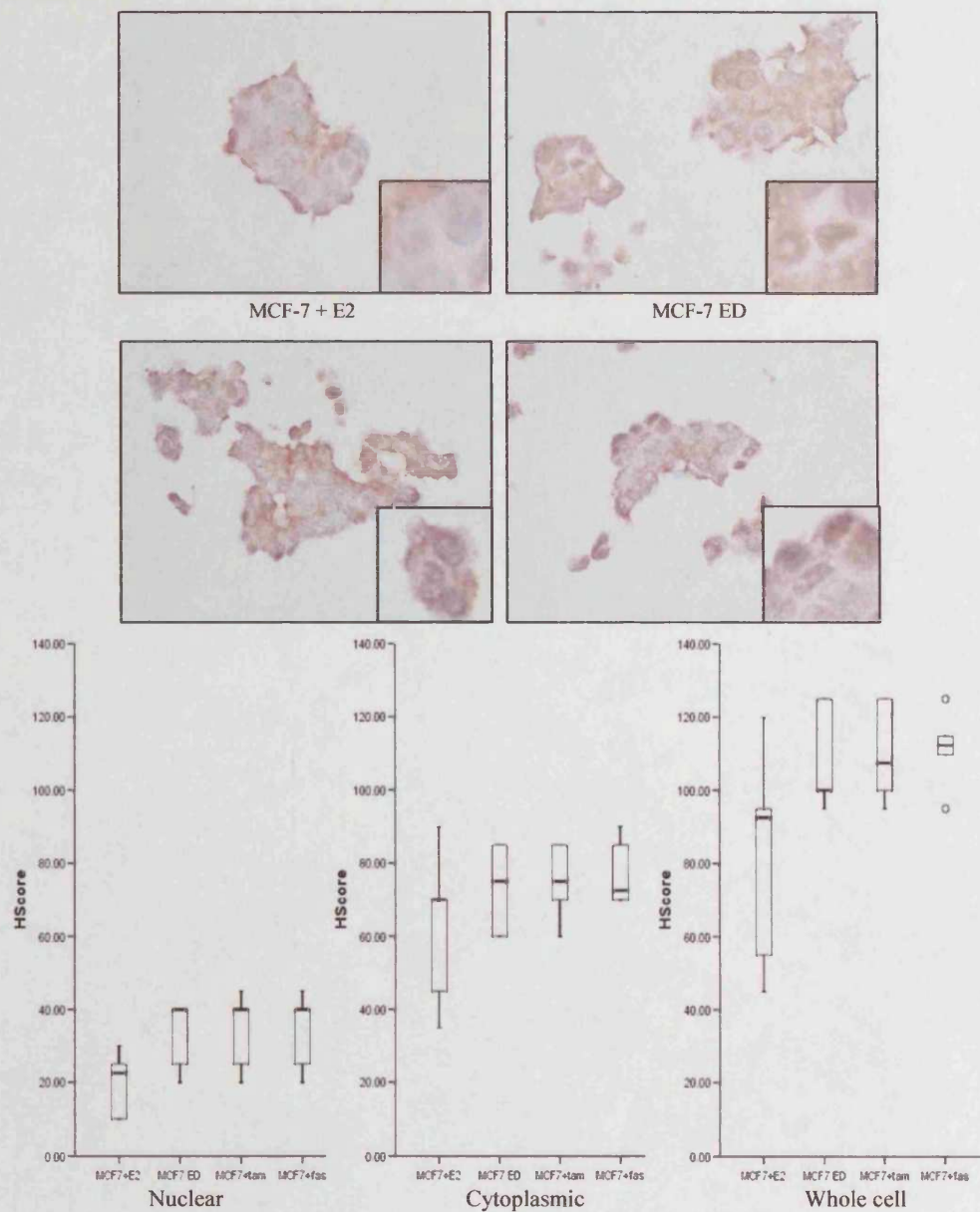


**Figure 3.77** Immunocytochemical staining of NFκB1 in MCF-7 cell pellet preparations after 4 days with/without oestradiol or anti-oestrogen treatment

Day 4 MCF-7 cell pellet treatment arrays were re-hydrated and stained for NFκB1 (p105/p50). Annotation is as seen in Figure 3.55. There are significant differences between E2 treatment and ED in the nucleus ( $p=0.039$ ) and for whole cell staining ( $p=0.034$ ); E2 and tamoxifen treatment in the nucleus ( $p=0.042$ ) and for whole cell staining ( $p=0.036$ ) and between E2 and faslodex treatment in the nucleus ( $p=0.042$ ) and for whole cell staining ( $p=0.05$ ).



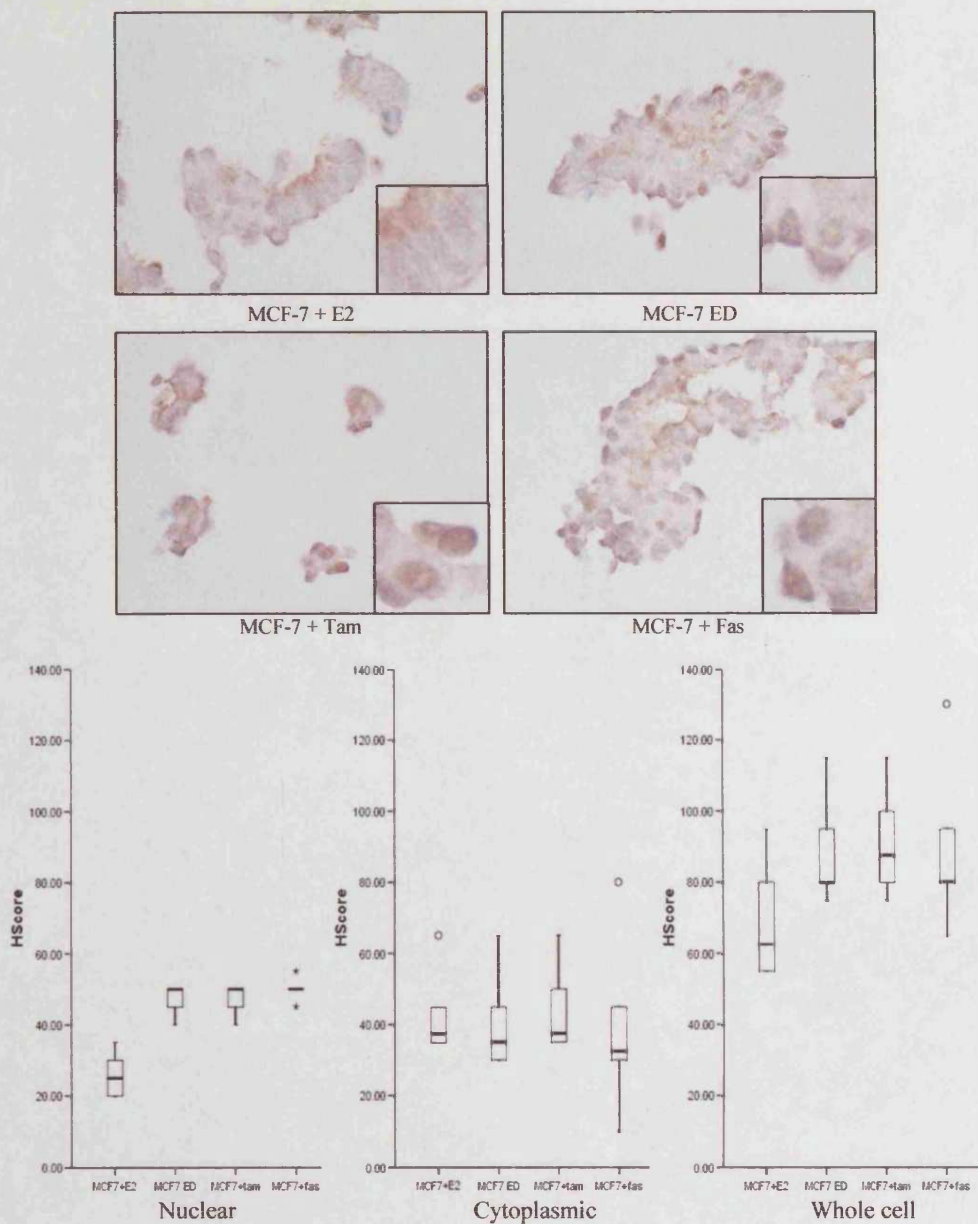


**Figure 3.78** Immunocytochemical staining of NFkB1 in MCF-7 cell pellet preparations after 7 days with/without oestradiol or anti-oestrogen treatment

Day 7 MCF-7 treatment arrays were re-hydrated and stained for NFkB1 (p105/p50). Annotation is as seen in Figure 3.55. There are significant differences between E2 treatment and ED in the nucleus ( $p=0.003$ ); E2 and tamoxifen treatment in the nucleus ( $p=0.003$ ) and for whole cell staining ( $p=0.045$ ) and between E2 and faslodex treatment in the nucleus ( $p=0.003$ ).

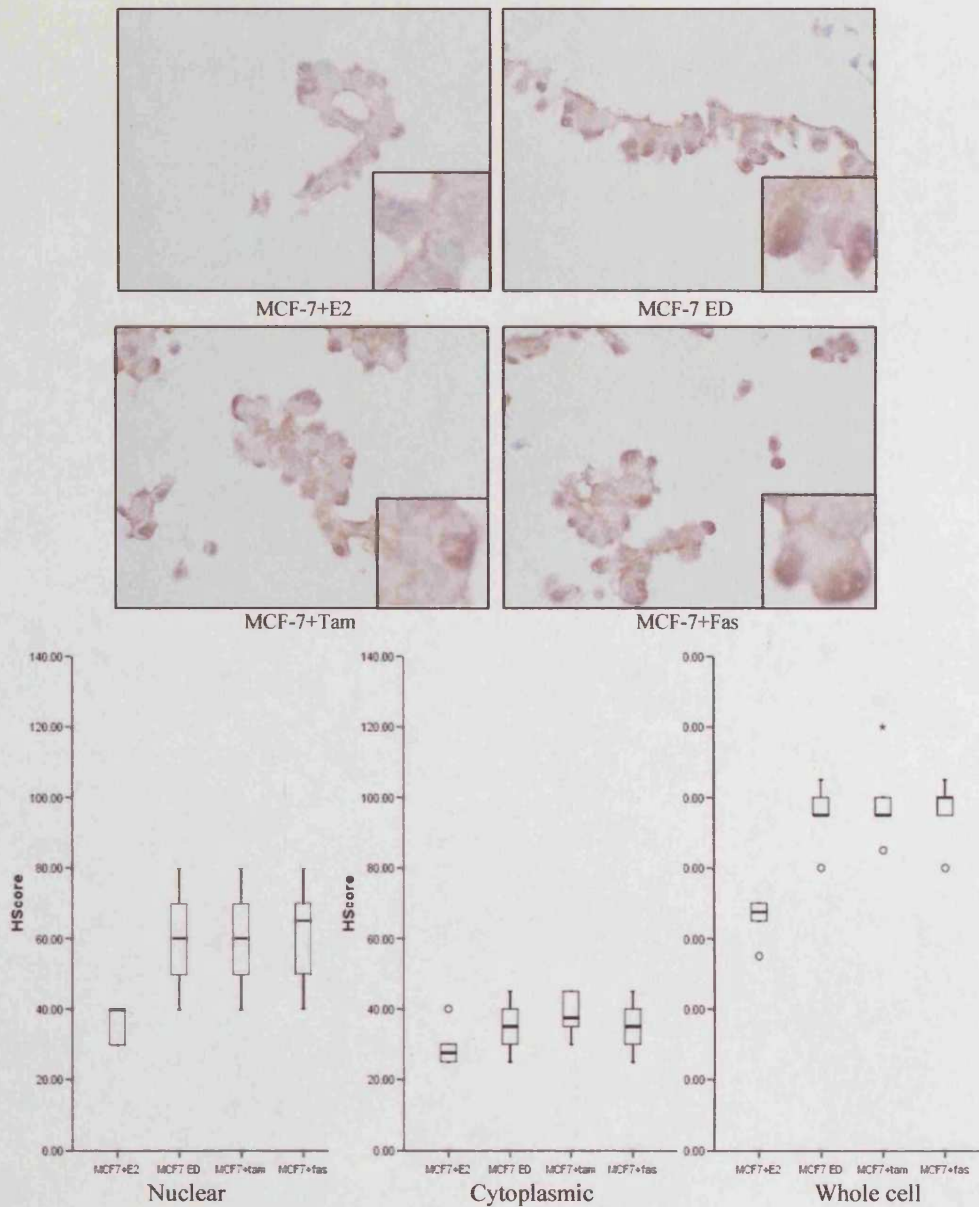


**Figure 3.79** Immunocytochemical staining of NFκB1 in MCF-7 cell pellet preparations after 10 days with/without oestradiol or anti-oestrogen treatment

Day 10 MCF-7 treatment arrays were re-hydrated and stained for NFκB1 (p105/p50). Annotation is as seen in Figure 3.55. There are significant differences between E2 treatment and ED in the nucleus ( $p=0.008$ ) and for whole cell staining ( $p=0.003$ ); E2 and tamoxifen treatment in the nucleus ( $p=0.008$ ), cytoplasmic ( $p=0.027$ ) and for whole cell staining ( $p=0.003$ ) and between E2 and faslodex treatment in the nucleus ( $p=0.008$ ) and for whole cell staining ( $p=0.003$ ).

#### 3.4.7.1.3 NFkB reporter assay in MCF-7 cells with anti-hormone treatments and in the presence and absence of NFkB blockade

To complement the TransAm assay, a reporter assay was performed to assess the total transcriptional activity of the NFkB family in MCF-7 cells treated with E2 or the anti-oestrogen faslodex as well as under ED conditions. Unfortunately due to time constraints this was only performed once and tamoxifen was excluded. Figure 3.82 shows that there was a ~20% increase in luciferase activity with ED and faslodex compared to E2 treatment. With the addition of 3µM of the IKK inhibitor parthenolide, (thus an NFkB inhibitor) there was a ~30% decrease in signal in the presence of E2, ED and faslodex, such that any anti-hormone induction was lost. Equal residual NFkB reporter activity was left in all groups after parthenolide treatment. Although all these changes were small, it needs to be taken into account that they occur after only 8 hours of anti-hormones, E2 or parthenolide treatment in such reporter assays.

#### 3.4.7.1.4 Inhibitor growth studies

In order to explore if blockade of induced NFkB could improve anti-oestrogen response in MCF-7 cells, the effect of increasing doses of the IKK inhibitor parthenolide on faslodex treated MCF-7 cells was examined in growth studies as in Figure 3.83. While there was no effect of 0.5µM parthenolide treatment on growth in the presence of faslodex, 1µM and 3µM produced a 20% and 50% decrease respectively compared with faslodex treatment alone. The maximum decrease in growth was 64% seen with 10µM of parthenolide in

combination with faslodex treatment compared to growth with faslodex alone. Significant changes in the dose response to parthenolide plus faslodex, was confirmed through ANOVA testing ( $p < 0.001$ )

### 3.4.7.2 Resistance

#### 3.4.7.2.1 Immunocytochemistry

NFkB1 protein levels were monitored by ICC in acquired tamoxifen and faslodex resistant cell lines versus the parental cell line, with results shown in Figure 3.84. While nuclear levels of NFkB1 staining were decreased in TAM-R cells by 62% ( $p = 0.003$ ), there was a 312% ( $p = 0.003$ ) increase in nuclear NFkB1 levels in FAS-R cells compared to MCF-7 cells. In contrast, TAM-R cells showed a 214% ( $p = 0.005$ ) increase in cytoplasmic staining, with no significant change in FAS-R cells for cytoplasmic staining compared to MCF-7 cells. This reveals that the nuclear increases in NFkB1 seen during the tamoxifen responsive phase were not sustained through to acquired resistance, although cytoplasmic levels were apparently further increased in TAM-R cells. In contrast, the nuclear increases observed during faslodex treatment (Figure 3.79) appear to be sustained and even further increased in the acquired faslodex resistant cells (with cytoplasmic levels remaining low). The total cell staining levels of NFkB1 staining were also significantly increased in both TAM-R by 64% ( $p = 0.035$ ) and FAS-R by 163% ( $p = 0.004$ ) compared with MCF-7 cells suggesting an increase in overall protein expression rather than a predominant redistribution of protein between the cytoplasm and nucleus. Given the

indication that NFkB activity had increased in the FAS-R cell line, as indicated by an increase in nuclear staining, this relationship was further explored in this project in FAS-R cells.

#### 3.4.7.2.2 NFkB DNA binding activity

A TransAM assay (Figure 3.85) was used to monitor the DNA binding activity for the p50 member of the NFkB family. This revealed an increase in p50 binding activity of 152% in FAS-R cells compared to parental MCF-7 cells.

#### 3.4.7.2.3 Inhibitor growth studies

The role for increased NFkB1 in FAS-R cells was explored further in relation to their growth. The effect of increasing doses of the IKK inhibitor parthenolide on FAS-R cells is shown in Figure 3.86. 0.5µM parthenolide treatment resulted in an 18% decrease in growth; 1µM and 3µM produced a 25% and 80% decrease respectively compared to FAS-R cells with no parthenolide treatment. There was also an 86% decrease in growth with 5µM parthenolide treatment but the maximum decrease in growth was 95% seen with 10µM of parthenolide, both compared to no parthenolide treatment. This agent thus appears to be an effective inhibitor of FAS-R cell growth.

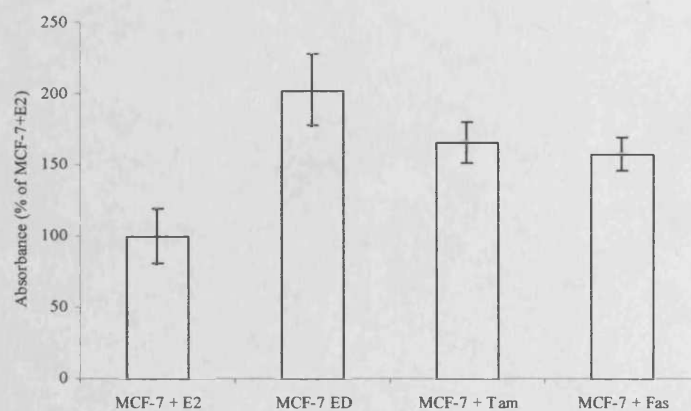


**Figure 3.80 DNA binding activity of the p50 NFkB1 isoform in MCF-7 cells after 7 days with/without oestradiol or anti-oestrogen treatment**

The DNA binding activity of the p50 NFkB1 isoform after 7 days with/without E2, ED, tamoxifen or faslodex treatment was assessed using a TransAM assay. The absorbance represents the amount of active NFkB1 that bound to the NFkB1 consensus DNA sequence which was detected with a p50 specific antibody and colourmetric detection. There is a significant increase in binding activity with ED compared with E2 ( $p=0.019$ ) by Dunnetts t-test ( $n=3$ ).

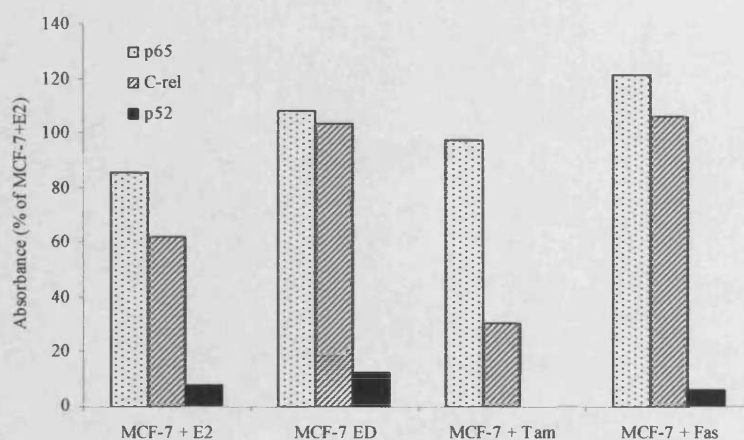


**Figure 3.81 DNA binding activity of the p65, C-rel and p52 NFkB family members in MCF-7 cells after 7 days with/without oestradiol or anti-oestrogen treatment**

The DNA binding activity of NFkB family members (p65, C-rel and p52) after 7 days of treatment with/without E2, ED, tamoxifen or faslodex was assessed using a TransAM assay. The absorbance represents the amount of active NFkB bound to the NFkB consensus DNA sequence which was detected with specific isoform antibodies and colourmetric detection. Only a single experiment was performed for these comparisons ( $n=1$ ).

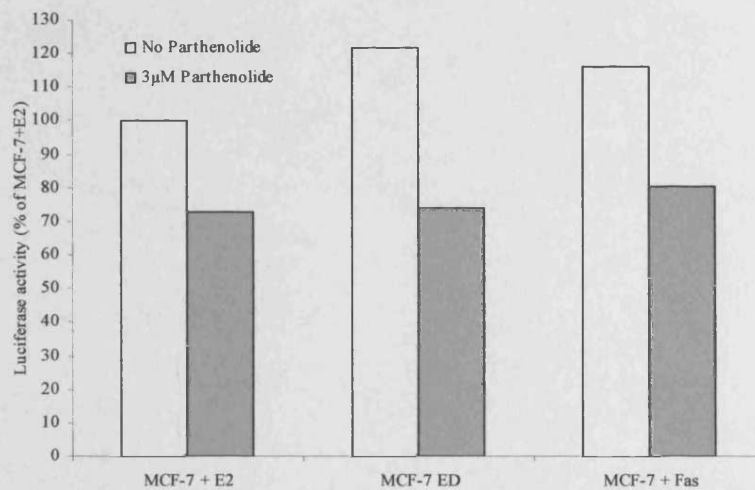
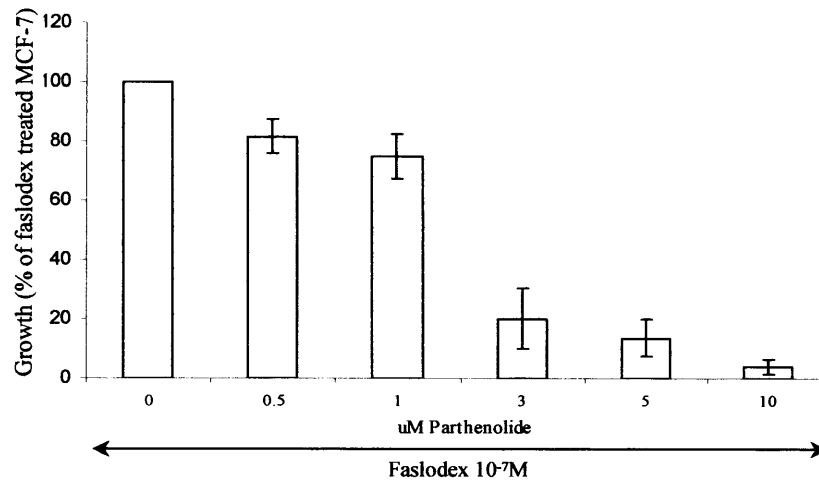


Figure 3.82 NFkB response element reporter activity in MCF-7 cells with treatments in the presence and absence of parthenolide

MCF-7 cells were transfected with a luciferase gene containing the NFkB response element. The cells were then exposed to ED, E2 or faslodex treatment in the presence and absence of 3µM parthenolide. The graph represents the percentage luciferase activity of the MCF-7 + E2 without parthenolide (n=1).



**Figure 3.83 Growth study of MCF-7 cells treated with faslodex plus increasing doses of the IKK inhibitor parthenolide**

MCF-7 cells were grown for 7 days with faslodex treatment ( $10^{-7}\text{M}$ ) plus increasing doses of parthenolide (0-10 $\mu\text{M}$ ) before being Coulter counted, this experiment was repeated three times ( $n=3$ ). An ANOVA test shows that there is a significant difference in the groups ( $p<0.001$ ).



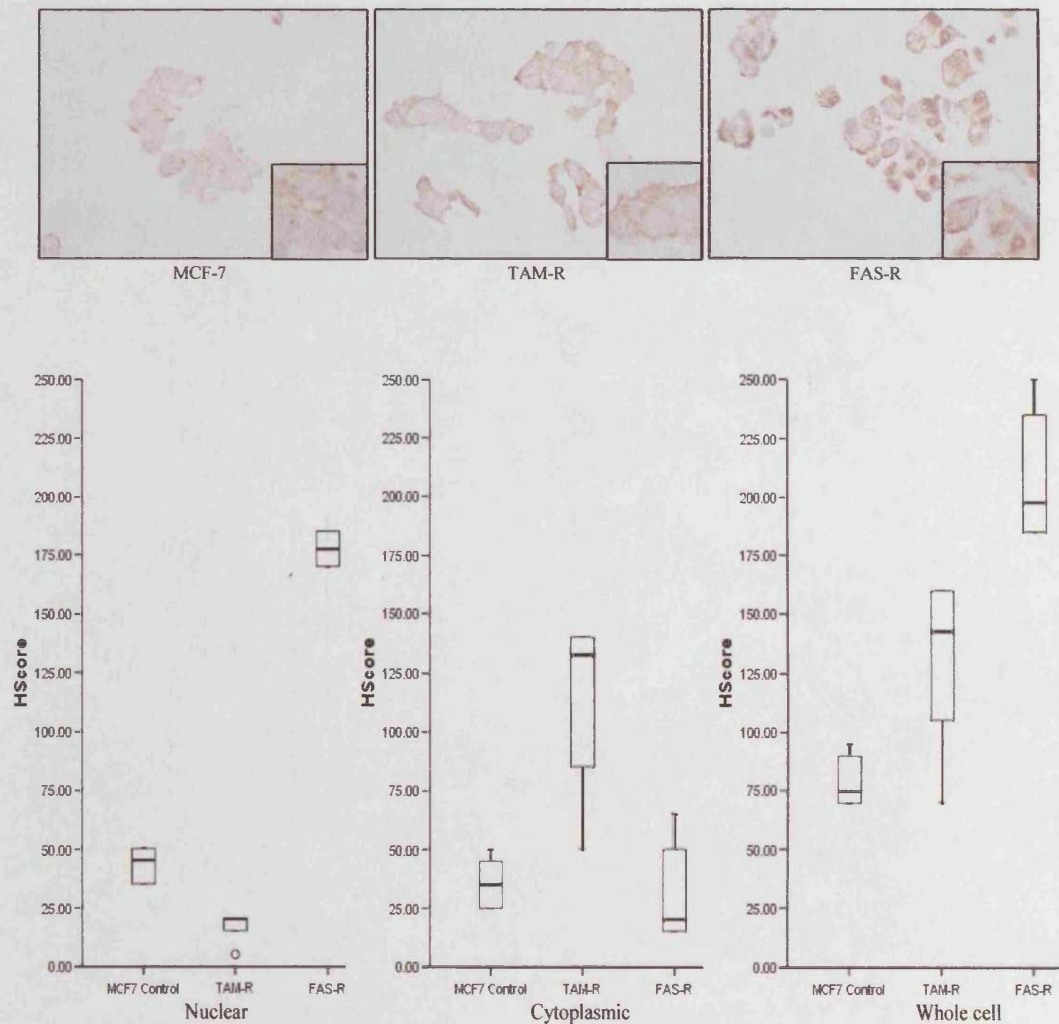


**Figure 3.84** Immunocytochemical staining of NFkB1 in MCF-7, TAM-R and FAS-R cell pellet preparations

Resistant cell line arrays were stained with the NFkB1 (p50/p105) specific antibody. Figure annotation as seen in Figure 3.55. There are significant staining differences between MCF-7 and TAM-R cells in the nucleus ( $p=0.003$ ), cytoplasmic ( $p=0.005$ ) and for whole cell staining ( $p=0.035$ ); there were differences between MCF-7 and FAS-R cells in the nucleus ( $p=0.003$ ) and for whole cell staining ( $p=0.004$ ).

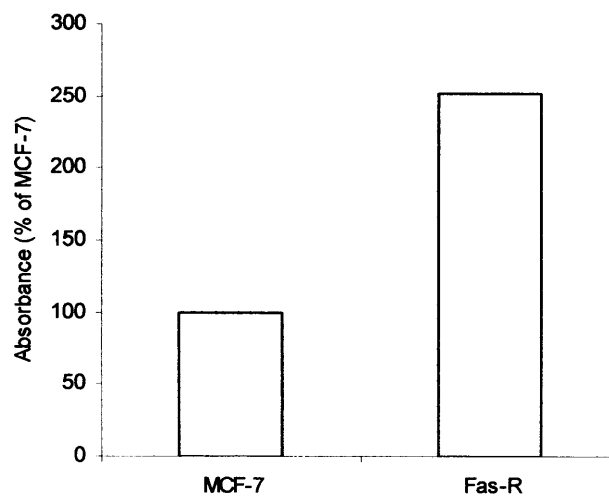
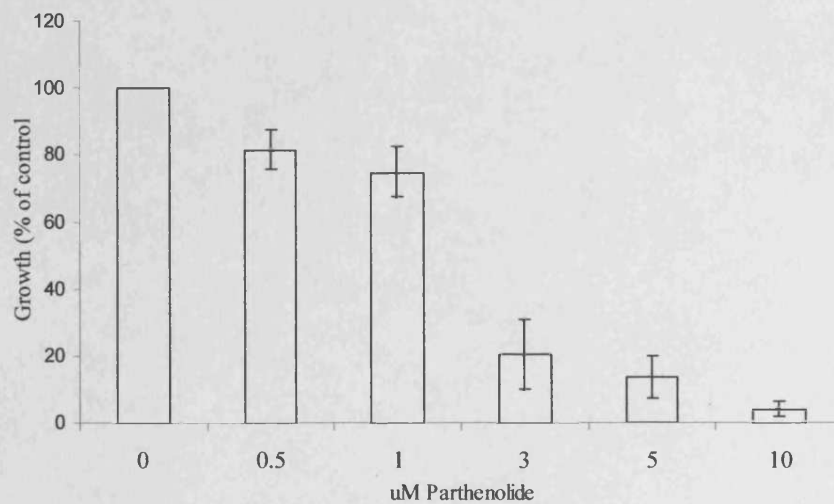


Figure 3.85 DNA binding activity of p50 NFkB1 in parental MCF-7 versus FAS-R cells

Shown is a graph representing the level of p50 NFkB1 binding activity in parental MCF-7 cells and FAS-R cells assessed by TransAm assay. The level of absorbance represents the amount of active NFkB1 that bound to the NFkB1 consensus DNA sequence, which was detected with a p50 specific antibody and colourmetric detection. This is shown graphically as a percentage of MCF-7 level (n=1).



**Figure 3.86 Growth study of FAS-R cells treated plus increasing doses of the IKK inhibitor parthenolide**

FAS-R cells were grown for 7 days in the absence of parthenolide or in the presence of 0.5, 1, 3 5 or 10 $\mu$ M before being Coulter counted. This experiment was repeated three times (n=3). An ANOVA test shows that there is a significant difference between the groups (p<0.001).

## Chapter 4

**~ Discussion ~**

## 4 Discussion

The purpose of this project has been to identify and verify at the RNA and protein level, genes induced by anti-hormones that may contribute to the adverse phenotype associated with endocrine therapy.

### 4.1 Anti-oestrogens induce EGFR/Her2 during response: link to compensatory signalling and improved therapeutic response

The E2-suppression/anti-oestrogen induction of EGFR/Her2 during early response and through to acquired resistance, with its associated adverse phenotype (McClelland *et al.*, 2001; Gee *et al.*, 2003), has provided a model to investigate other E2-suppressed and anti-oestrogen-induced genes that may, along with EGFR/Her2, limit the effectiveness of anti-oestrogens and contribute to acquired resistance (Gee *et al.*, 2006). It is hoped that this may reveal new therapeutic strategies to extend patient response and subvert resistance and progression during anti-hormone treatments, potentially impacting significantly on patient prognosis. To date it has been noted that blockade of EGFR/Her2 in combination with tamoxifen improved cell kill and inhibited proliferation, improving the anti-tumour effect of the anti-oestrogen (Gee *et al.*, 2003; Nicholson *et al.*, 2005). However, this strategy does not completely inhibit growth (Gee *et al.*, 2003) indicating that there are additional important factors involved in the evasion of anti-oestrogen action and

acquisition of resistance. Despite this, anti-hormone/anti-ErbB combination therapies are currently under clinical investigation in breast cancer (Johnston 2005; Johnston 2006b). It is also noteworthy that targeting of EGFR/Her2 in combination with ED may not be as successful as co-treatment with anti-oestrogens, since there is only a small induction of EGFR under these conditions and growth studies have not shown a substantially improved anti-tumour effect for ED when combined with gefitinib (Gee *et al.*, 2003). Indeed, an improved response to ED in combination with gefitinib has only been shown in preclinical studies where tumour cells over-expressed erbB receptors *de novo* (Shou *et al.*, 2004), or in an ER+ve/EGFR+ve clinical setting with the use of aromatase inhibitors in combination with gefitinib (Polychronis *et al.*, 2005). New gene targets for therapy in combination either with ED or anti-oestrogens clearly remain important.

## 4.2 Model system and project comparisons

In this study the *in vitro* model chosen was the ER+ve, hormone responsive MCF-7 breast cancer cell line, where EGFR and Her2 have previously been shown to be inducible by anti-oestrogens (Gee *et al.*, 2003). MCF-7 cells were also used in the study by Frasor *et al.* (2003), where 70% of the genes altered by E2 were suppressed (Frasor *et al.*, 2003). These findings gave much hope that in this project further adverse genes would be uncovered from such a system that would either be linked to the EGFR/Her2 induction or would comprise unique additional elements. Unfortunately, however, EGFR was not

detectable as anti-hormone induced on the nylon arrays as the levels were too low to be detected. This is a known limitation of the array type, and due to this steps were undertaken to ensure all possible candidate genes were identified during the array analysis process in this project.

Comparisons in this project have been made between the anti-oestrogens tamoxifen and faslodex with E2 treatment, and also versus an untreated control. During the course of the study the untreated control arm was designated ED since the media was stripped of its endogenous E2 by charcoal. It has been estimated that this reduces E2 levels to  $10^{-13}$ M (Staka *et al.*, 2005), a concentration of E2 which shows no mitogenic activity in MCF-7 cells (versus  $10^{-9}$ M) and where it is thought that the ER is largely unoccupied (Masamura *et al.*, 1995; Santen *et al.*, 2004).

### **4.3 Arrays were suitable to identify anti-oestrogen induced genes**

The cDNA arrays in this project were generated from RNA extracted from MCF-7 cells either in the absence of ER ligand (hence ED) or treated with E2, tamoxifen or faslodex for 4, 7 and 10 days. The RNA extracted proved to be of high quality and integrity, as validated initially by profiling with the anti-hormone-inhibited gene pS2 and subsequently amphiregulin, as well as a known E2-suppressed, anti-oestrogen induced gene CD59 (Martinez-Lacaci *et al.*, 1996; Rushmere *et al.*, 2004). Unfortunately, after log transformation and

normalisation of the data generated from the nylon arrays, the day 4 arrays did not perform to expected standards and so were excluded from further array analysis. The apparent under performance of the day 4 arrays could feasibly be due to lower levels of gene expression achieved after only 4 days of growth and treatment relative to later time-points, coupled with an unacceptably large spread of the array data obtained across the three replicates at day 4. However, as initial RT-PCR validation studies revealed there were no apparent problems with the RNA quality, it was not deemed necessary to exclude the day 4 experimental material from the subsequent RT-PCR verification steps for the selected genes.

#### **4.4 Overall patterns of gene expression**

The scatter plots generated from the day 7 and 10 array comparisons revealed observations about overall gene expression profiles with the different treatments:

1. When comparing E2 treated and ED samples, there were fewer differences in gene expression than when ED was compared with anti-oestrogen treatment, a feature that was especially evident for higher intensity genes. Subsequent use of Venn diagrams (see below) confirmed that overall there were more genes induced by tamoxifen or faslodex treatment versus ED conditions than when ED and E2 treatment were compared. Thus, globally the E2-occupied ER and ER



in the ED cells resulted in a more similar gene expression profile, data implying some overlap between the transcriptional mechanism and gene targets for ER under both conditions. This is surprising since ED conditions have been associated with co-repressor recruitment to the ER complex and hence transcriptional inactivity of both AF-1 and AF-2 (Martin *et al.*, 2005), in marked contrast to E2 treatment where these functions synergise and are maximised by co-activator recruitment and co-repressor loss (Metivier *et al.*, 2001; Gruber *et al.*, 2002). However, the scatter plot similarities in this project could perhaps be reflective of some residual levels of E2 remaining in the ED media. Significantly, although the residual levels of E2 ( $10^{-13}$ M) fails to translate out into growth comparable with the obvious stimulation by  $10^{-9}$ M E2 in MCF-7 cells *in vitro* (Masamura *et al.*, 1995; Santen *et al.*, 2004), nevertheless, cells grown under these ED conditions are able to grow slowly to confluency and can be inhibited by faslodex. Thus, in such cells a role for E2/ER-regulated genes seems likely to remain (Dowsett *et al.*, 2005).

2. In contrast, it is perhaps not unexpected that the global gene readout achieved by anti-oestrogen occupied ER is obviously different to that for either an E2-occupied or unoccupied receptor, given that the structures of tamoxifen and faslodex perturb the ER complex resulting in co-repressor recruitment and blocking AF-2 function. However, within the altered genes, it is particularly interesting that there appear to be more genes induced with tamoxifen or faslodex treatment than

suppressed among the more abundant gene changes, an observation also made by Levenson *et al.* (2002a).

3. Finally, although it could be anticipated that there might be unique gene inductive effects with tamoxifen versus faslodex, since AF-1 transcriptional activity and hence some gene-specific agonism is partially retained with the former anti-hormone, there was considerable similarity between the scatter plots obtained for tamoxifen and faslodex treatment. These observations are in keeping with previous findings that any anti-oestrogen occupancy of the ER is able to reverse the phenomenon of oestrogen repression of gene expression. Such induced genes could encompass elements potentially involved in the growth inhibitory effects of these agents, as has previously been described for TGF $\beta$  signalling genes (Frasor *et al.*, 2003), but also potentially induction of genes that may act to limit maximal anti-tumour response as has been described for EGFR and Her2 (Gee *et al.*, 2003; Nicholson *et al.*, 2005).

#### **4.5 Identification of genes co-induced by anti-oestrogens**

A 1.5 fold change filter, in combination with Venn diagrams, was used to identify all genes induced by both tamoxifen and faslodex compared to either ED or E2 treatment. A 1.5 fold change was chosen as the only initial filtering approach. This fold change has previously been established as appropriate for use with such arrays under conditions where samples to be compared are all

from the same cell line with relatively short-term treatments (in this instance that all also act via the ER), and thus where extreme fold differences in gene expression profile would have been unlikely (Levenson *et al.*, 2002a).

Venn diagrams of the  $\geq 1.5$  fold induced genes with subsequent hierarchical clustering for profiling across all treatment groups revealed 60 genes that were either anti-hormone induced versus E2 (n=5), anti-hormone induced versus ED (n=35) or anti-hormone induced versus both E2 and ED (n=20). Such induced patterns are likely to be explained by the molecular mechanisms of E2 action previously cited (Introduction section 1.1.5) and parallels the data of Frasor *et al.* (2003) who showed that as many as 70% of E2-regulated genes are suppressed by E2 treatment in an ER+ve breast cancer model using a larger microarray format (Frasor *et al.*, 2003). It is also worth noting that they showed that when combined with E2-treatment, anti-oestrogens could result in reversal of E2-suppression, where gene induction with faslodex was most effective (Frasor *et al.*, 2004). In agreement, superior effectiveness for induction of gene expression with faslodex versus E2 treatment (and indeed versus ED conditions) was also observed in the present study as can be seen in the Venn diagrams (n=67), with fewer inductive events for tamoxifen (n=37) or for ED conditions (n=44) versus the steroid hormone. These data indicate that faslodex has an increased biological potency in reversing ER-repressed events and are no doubt reflective of its potency in depleting both ER activity and level (Frasor *et al.*, 2004; Scafoglio *et al.*, 2006).

Interestingly, further exploration of the profiles of the 55 genes induced by tamoxifen and faslodex versus ED by hierarchical clustering indicated they were invariably also increased somewhat versus E2 treatment, although this did not reach the 1.5 fold induction. Such analysis re-enforces that this is a gene cohort worthy of consideration in this project as potentially anti-oestrogen-induced, E2/ED-repressed, alongside the five genes more obviously induced versus E2 treatment arising from the Venn analysis.

Surprisingly, the Venn diagrams and hierarchical clustering also revealed that among the genes induced by both anti-oestrogens versus ED were a significant number also induced by E2 treatment (although not all to a fold change of 1.5). A similar phenomenon has also been noted by Levenson *et al.*, (2002a) where following array analysis, some E2, raloxifen and faslodex regulated genes clustered together on analysis in ER-ve breast cancer cells transfected with the ER gene. While the underlying mechanism remains unknown and not easily reconciled with classical ER signalling, it was speculated in the Levenson publication that this was perhaps due to non-classical, genomic actions of ER presumably triggered by all these treatments (Levenson *et al.*, 2002a).

#### **4.5.1 Further exploration of induced genes using Venn diagrams**

Alongside the 60 gene cohort of interest in relation to the aims of this project, Venn diagrams also revealed rarer gene patterns. Interestingly, there were some genes induced by both tamoxifen and E2 treatment (n=11), but not by faslodex,

compared to ED conditions. This profile is most likely due to the well documented residual activity of the AF-1 domain of the ER following tamoxifen treatment, resulting in an agonistic response at some classically E2-induced gene promoters (Nicholson and Johnston 2005). More surprisingly, however, the Venn diagrams also identified a small number of genes induced by both faslodex and E2 treatment (n=9), but not by tamoxifen, when compared to ED. This rare, oestrogen-like agonism of faslodex was also noted by Scafoglio *et al.*, whose study revealed that faslodex exhibited an agonistic effect on 20 genes. It was hypothesised that this unexpected phenomenon could be due to the fact that both faslodex and E2 can promote ER degradation, which may allow for occasional common gene profiles (Scafoglio *et al.*, 2006).

#### **4.6 Ontological investigation of the 60 anti-oestrogen induced genes**

Having identified the presence of a large subset of anti-hormone induced genes (versus ED or in some instances E2), an ontological study was undertaken to identify those whose biological properties have previously been linked to proliferation and cell survival rather than to growth inhibition. This subsequent ontological investigation into the cancer-related functions of the 60 anti-oestrogen induced genes revealed, as expected, that several (19%) were involved in the anti-proliferation/pro-apoptotic response to anti-hormone treatment. As hypothesised, however, there also appeared to be genes potentially involved in cell 'protective' effects by promoting cell survival

(12%, e.g. Bag-1 and NFkB1), increasing proliferation (7%, e.g. NDR protein kinase) and immune escape (8%, e.g. CD59) that were induced during tamoxifen and faslodex treatment. Moreover, it was also noted that several genes were induced which could eventually be linked to emergence of the increased invasive and aggressive phenotype that is maximised in tamoxifen and faslodex resistant breast cancer (10%, e.g. Hif-1 $\alpha$ ,  $\delta$ -catenin and RhoE). In addition, several genes (13%, e.g. NME3) had a conflicting ontology in relation to cancer, where their activity was dependent on their phosphorylation state or cell type, or is currently controversial in the literature, and these were retained alongside those elements with more convincing adverse ontology. In total, as many as 37% of the induced genes had the potential to exert an adverse function in the presence of anti-oestrogens. The ontological information compiled about each induced gene following literature review, which included function, localisation for subsequent therapeutic targeting and availability of antibodies/inhibitors, was used together with their array profiles to prioritise and select genes of most interest for further detailed study.

Following initial investigation of overall patterns of expression across the treatments and this subsequent stringent gene selection in part based on adverse ontology, this study has been able to successfully identify, using cDNA nylon arrays, RT-PCR validation and protein studies, 8 previously unrecognised anti-oestrogen induced genes that may limit anti-tumour response. Furthermore, for one gene, NFkB1, studies have been extended to demonstrate the therapeutic promise of additionally targeting such induced genes alongside anti-oestrogen.

#### **4.7 Further investigation of the anti-oestrogen induced genes**

It became apparent in this project that while the array and protein profiles generally correlated (with the exception of NFkB1), the profiles generated by RT-PCR differed in that they suggested the panel of genes were always induced substantially by day 10 by both anti-oestrogens and ED ( $\delta$ -catenin, Bag-1, 14-3-3 $\zeta$ , Hif-1 $\alpha$ , NME3, NFkB1, NDR). This lack of concordance for RT-PCR may possibly be due to the semi-quantitative nature of the RT-PCR technique and hence some inability in discriminating subtle differences in expression. Indeed, other studies have also shown different sensitivities of cDNA nylon arrays versus semi-quantitative RT-PCR (Levenson *et al.*, 2002b).

During this discussion the emphasis, where possible, is on the protein levels of the selected genes, since it is likely that they would be more accurate due to also reflecting mRNA translation, and it is generally the protein products of genes that are amenable to targeting by inhibitors rather than the mRNA.

An overview of the protein expression profiles of the selected induced genes during response as obtained using immunocytochemistry and in some instances western blotting and through to acquired resistance is shown in Table 4.1. Six of the eight anti-oestrogen-induced genes were explored successfully to some degree at protein level. The arrays revealed a number of broad patterns for anti-hormone induced events that may have important implications for future treatment of breast cancer. Thus, the induced genes can be divided into groups depending on whether they were induced versus E2 treatment by anti-oestrogens only, or induced to some degree by both anti-oestrogens and ED. Equally, it is clear that the genes examined in this project are not just transiently induced during anti-hormone response, but like the induced genes EGFR and Her2 (Gee *et al.*, 2003; Knowlden *et al.*, 2003) can be sustained through to acquired resistance (although in this instance only faslodex resistance). Genes can also be further characterised by their potential adverse function during anti-oestrogen treatment, where alongside promotion of cell survival and proliferation, there are genes whose function may be cell context specific and could potentially confer additional adverse features on breast



cancer cells notably invasive behaviour that may have significant bearing when ultimately considering patient outcome.

**Table 4.1 Overview of the protein expression profiles and ontology of the induced genes**

Gene	Early Induction			Resistance		Principle Adverse Ontology
	Tamoxifen	Faslodex	ED	Tamoxifen	Faslodex	
RhoE	Yes	Yes	Yes	No	Yes	Pro-Invasive
NFkB1	Yes	Yes	Yes	No	Yes	Cell Survival
NME3	Yes	Yes	Yes	--	--	Cell Survival
$\delta$ -catenin	Yes	Yes	No	No	Yes	Pro-Invasive
Bag-1	Yes	Yes	No	No	Yes	Cell survival
14-3-3 $\zeta$	Yes	Yes	No	--	--	Cell survival

#### **4.7.1 Genes identified that were induced by anti-oestrogens alone or by both anti-oestrogens and oestrogen deprivation**

Several studies have employed microarrays to decipher the transcriptional impact of E2 during its promotion of breast cancer cell growth, and in turn have evaluated how effective different classes of anti-hormones are in reversing these profiles (Inoue *et al.*, 2002; Levenson *et al.*, 2002a; Cunliffe *et al.*, 2003; Frasar *et al.*, 2003; Hodges *et al.*, 2003). However, these studies have to date primarily focussed on profiling the inductive events of anti-oestrogens that underlie their growth inhibitory effects, rather than exploring

the concept of “compensatory” increases in E2-repressed signalling genes that may serve to attenuate anti-hormone response. During this investigation nylon arrays have been able to successfully identify such potential “compensatory” genes induced by both partial and pure anti-oestrogens. However, it became evident that while some genes were induced by anti-oestrogens alone, others were also induced to some degree by ED. The genes that fell into the induced by anti-oestrogen alone group were:  $\delta$ -catenin, Bag-1 and 14-3-3 $\zeta$ . The remaining genes, RhoE, NME3 and NFkB1 were induced by both anti-oestrogens and ED.

Bag-1, 14-3-3 $\zeta$  and  $\delta$ -catenin (described below) therefore fall in the same category as EGFR which in MCF-7 cells is substantially induced by tamoxifen and faslodex, but increases are minimal or completely absent with ED (McClelland *et al.*, 2001; Gee *et al.*, 2003). As such, their induction may be important in the early evasion of maximal growth inhibition exerted specifically by anti-oestrogen-occupied ER. While induction was common to tamoxifen and faslodex, subsequent verification studies revealed that more substantial, earlier inductive events were particularly apparent when treating with the pure anti-oestrogen, in agreement with reports of more substantial de-repressive effects of this agent (Frasor *et al.*, 2004).

Among these genes, the co-chaperone Bag-1 is known to be a key regulator of apoptosis and thus of particular interest when considering elements that may promote cell survival when induced by anti-oestrogens. It is reported to interact

with heat shock proteins to enhance protein refolding, to interplay with Bcl-2 to influence activity of several nuclear hormone receptors including the ER and growth factor receptors, and to promote proteasomal degradation of denatured proteins to promote cell survival (Cutress *et al.*, 2002; Townsend *et al.*, 2005). The reported interaction of Bag-1 with the proliferation and cell survival-regulating serine/threonine kinase Raf-1 is also potentially interesting, since Raf-1 is known to activate the MAPK pathway which we have shown ultimately promotes ligand independent activation of the ER during anti-oestrogen treatment and thereby resistant growth (Britton *et al.*, 2006; Krajewska *et al.*, 2006). Moreover, it has been reported that p50 Bag-1 can also enhance transcription via the ER and ERE in breast cancer cells through the molecular chaperone proteins Hsc70/Hsp70 (Cutress *et al.*, 2003) that may contribute to residual cell survival in the presence of the anti-oestrogens. Immunocytochemistry with the Bag-1 specific antibody in this study showed that the majority of staining was nuclear and that following anti-oestrogen treatment it was this component of staining that showed the largest increases. This indicates that of the four Bag-1 proteins, the p50 isoform that contains an NLS and is therefore localised to the nucleus (Townsend *et al.*, 2005), is most likely to comprise the main Bag-1 protein found in the MCF-7 breast cancer cells following anti-oestrogen treatment. Bag-1 has previously been reported in several studies of clinical breast cancer samples. While the localisation and definitive prognostic consequences of this expression remains conflicting (as overviewed in Townsend *et al.*, 2002), nevertheless there are studies that show p50 Bag-1 increases cell survival and metastatic capabilities and thus decreases

patient survival. Tang *et al.*, (1999) studied the expression of Bag-1 in clinical breast cancer patients and discovered that, although not significantly increased, nuclear expression of Bag-1 correlated with decreased disease-free period and poorer overall survival (Tang *et al.*, 1999). Xenograft models of the ZR-75-1 breast cancer cell line engineered to over-express p50 Bag-1 resulted in substantially larger tumours than control-transfected cells (Kudoh *et al.*, 2002). Moreover, in prostate cancer, the expression of nuclear p50 Bag-1 has been associated with emergence of hormone refractory disease (Krajewska *et al.*, 2006).

The anti-oestrogen-induced gene 14-3-3 $\zeta$  (or YWHAZ) is also of interest as a member of the 14-3-3 family of phosphoserine binding proteins that regulate many different cellular processes including proliferation and apoptosis. There is significant evidence that 14-3-3 $\zeta$  may act as a pro-survival protein. As an adapter molecule it appears to be able to do this in two different ways, through sequestering Bcl-2 family members or via A20/NF $\kappa$ B (Rosenquist 2003). Furthermore, it is thought that 14-3-3 $\zeta$  is an important regulator of several key signalling pathways that have been implicated in limiting response to anti-oestrogens, for example EGFR signalling (Oksvold *et al.*, 2004) and also Akt and PI3 kinase that are bound and stabilized by 14-3-3 $\zeta$  (Cantley 2002; Powell *et al.*, 2002). In parallel with the observations made in this project, Frasor *et al.* (2006) have also been able to show that the anti-oestrogen tamoxifen upregulated the level of 14-3-3 $\zeta$  in MCF-7 breast cancer cells. They have postulated that this element may contribute to the promotion of tumour

recurrence, although as in the present project their findings have not been extended to further anti-oestrogens (Frasor *et al.*, 2006). Encouragingly, post-analysis of two published clinical studies (van de Vijver *et al.*, 2002; van 't Veer *et al.*, 2002) has also revealed that 14-3-3 $\zeta$  associates with poor prognosis on endocrine therapy (Frasor *et al.*, 2006), data which is highly supportive of an important role for 14-3-3 $\zeta$  in limiting the benefits of such agents.

It is possible that the lack of obvious induction of the above signalling genes under ED conditions is due to the traces of oestrogen ( $\sim 10^{-13}$ M) remaining in the phenol red-free medium containing charcoal stripped serum, repressing gene expression levels to some degree, as with E2 treatment. However, this is not the case for all the induced genes that were identified in this project, since protein investigation of RhoE, NME3 and NFkB1 revealed they are induced by anti-oestrogens and also ED. This indicates that these latter genes may play a role in limiting response to a range of anti-hormonal strategies i.e. as a general protective response to ER blockade, although again the effects appear most substantial with faslodex, in keeping with its profound blockade of ER signalling.

Of particular interest among these anti-hormone-induced genes was NFkB1. This project was able to demonstrate an anti-hormone induced increase in NFkB1 at both the mRNA and protein level. Immunocytochemistry was able to demonstrate parallel increases in total protein expression, but interestingly increases were primarily detectable in the nuclei, a localisation that is

associated with the active (p50) form of NFkB1 following translocation (Karin *et al.*, 2002). In agreement, these changes were accompanied by an increase in active NFkB1 p50 DNA binding activity with tamoxifen and faslodex as well as ED. Some increase in c-Rel was also detected with such assays, while another NFkB family member p65 was readily detectable indicating various p50-containing heterodimers could also potentially be contributory (Karin *et al.*, 2002). In addition, while not examined for tamoxifen, the transcription factor activity of NFkB in reporter gene construct assays could be shown to be modestly increased by ED and faslodex as measured after 8 hours treatment. NFkB has previously been associated with tumourigenesis via its ability to induce expression of genes involved in proliferation and survival of cancer cells (Bours *et al.*, 2000; Karin *et al.*, 2002). Moreover, such signalling is known to be E2-repressed at multiple levels (Kalaitzidis and Gilmore 2005): for example the E2-occupied ER can suppress NFkB activity by blocking its DNA binding, although little has been previously reported regarding impact of ER signalling at the level of expression of NFkB members. Interestingly, NFkB signalling has been previously implicated in ER+ve (and also ER-ve) resistance to anti-oestrogens and also ED in breast cancer (see below). As such, it seems likely that the induction of NFkB1 expression revealed in this project could provide a further means whereby cells could evade maximal anti-tumour effect during the anti-hormone responsive phase.

While RhoE is likely to be anti-proliferative and its anti-hormone induction may play more of a role in promoting invasive behaviour (see below), NME3 is

also of interest among the growth-related genes induced by anti-oestrogens and ED. NME3, originally identified as a member of the nm23 metastasis-suppressor gene family encoding a nucleoside diphosphate kinase (NDPK) (Dusonchet *et al.*, 2003), has been associated with both anti- and pro-apoptotic function. Negroni *et al.* have shown that over-expression of NME3 protected neuroblastoma cells from serum-deprivation induced apoptosis (Negroni *et al.*, 2000). However, over-expression of NME3 in the 32Dcl3 cell line has been shown to increase levels of apoptosis when cells were treated with granulocyte colony stimulating factor (G-CSF) and under interleukin 3 withdrawal (Venturelli *et al.*, 1995). Moreover, contrary to the results found in this study, a genome-wide study of promoter elements for the ER revealed that the promoter region for NME3 contained an ERE, and as such was shown to be an E2-induced gene as measured at the mRNA level in MCF-7 cells (Kamalakaran *et al.*, 2005). However, this has not been confirmed by any other studies nor was the effect of anti-oestrogens examined. In total, it thus seems that the function of NME3 is likely to be cell type and context specific (Negroni *et al.*, 2000), and that it remains possible that NME3 could exert a cell survival role during anti-hormone treatment.

Interestingly, in some instances the induced genes (e.g. Bag-1, 14-3-3 $\zeta$ , NF $\kappa$ B1 and also Hif-1 $\alpha$  that has only been examined successfully in this project at the mRNA level) have also been reported to be inducible by environmental stresses (e.g. hypoxia) and other therapeutic approaches (e.g. in limiting radio/chemoresponse in cancer cells). As such, these genes may comprise

global cell survival mechanisms. For example, 14-3-3 $\zeta$  has been shown to limit the cell kill in human lung cancer cells by ionizing radiation (Qi and Martinez 2003). Bag-1 has been shown to have a positive role in driving proliferation and cell survival to protect ER+ve breast cancer cells from radiation and chemotoxics (Townsend *et al.*, 2003), and interestingly has also been linked to promoting resistance to anti-androgen therapy in prostate cancer (Froesch *et al.*, 1998). Moreover, Bag-1 isoform localisation, including nuclear translocation, is dependent in part on cellular stress (Townsend *et al.*, 2005). NF $\kappa$ B signalling has been implicated substantially in promoting cell survival/proliferation under conditions of environmental stress and again in chemo/radioresistance (Wu and Kral 2005). NF $\kappa$ B activity is inducible by chemotherapy treatment (e.g. daunorubicin, doxorubicin and paclitaxel), an event resulting in initial expression of survival genes that reduced the effectiveness of chemotherapy (Cusack 2003). Hif-1 $\alpha$  was also induced at the mRNA level by anti-hormones in this project, where Hif-1 $\alpha$  is known to also be regulated by hypoxia (Kimbrow and Simons 2006). However, this occurs at the level of nuclear protein expression and activity and so the observations at the mRNA level are perhaps surprising. Moreover, this observation failed to translate into an increase in protein levels by either immunocytochemistry or western blotting in this project. Detection of protein Hif-1 $\alpha$  using western blotting resulted in severe problems, including bands of unexpected size using a Hif-1 $\alpha$  specific antibody. Interestingly while there have been reports of Hif-1 $\alpha$  induction with anti-oestrogen treatment, this was under hypoxic conditions (Kurebayashi *et al.*, 2001) that were not possible to accurately replicate during



the course of this project since even chemical induction of hypoxia with DFO failed to reveal the right sized band for HIF-1 $\alpha$ . Further exploration of this gene is clearly needed.

#### **4.7.2 Some anti-hormone-induced genes identified persist through to acquired resistance**

In addition to investigating the protein levels of the induced gene products during anti-hormonal response, it was also possible in this project to examine the protein levels of RhoE,  $\delta$ -catenin, Bag-1 and NF $\kappa$ B1 in the tamoxifen (TAM-R) and faslodex (FAS-R) acquired resistant MCF-7 cell lines. It was discovered for all these genes that tamoxifen treatment resulted in a transient induction. As there was no sustained induction in the acquired tamoxifen resistant MCF-7 cell line, this indicate that the potential cell survival/proliferative effects of these signalling genes may only serve to limit maximal initial tamoxifen response. Interestingly, however, these signalling genes that were also induced by faslodex treatment were all persistently elevated in acquired faslodex resistance, suggesting a retained critical contribution to growth or to additional adverse features for these genes in this resistant model. Indeed, the retention of their increased expression through to this actively growing phase provides some evidence that anti-hormone induced genes can exert positive, rather than growth inhibitory activity in breast cancer cells. The differential pattern of expression of these signalling genes may reflect the fact that in tamoxifen resistance ER signalling is recovered, thus re-

instating suppressive events on their expression. In contrast, our previous studies have shown that ER signalling is largely lost in the faslodex resistant model. This profound decrease in ER signalling would serve to maintain the depressive effects on expression of these genes and indeed may be further compounded under conditions of very prolonged faslodex exposure which we have shown associates with complete loss of ER expression both at the protein and mRNA level (Nicholson *et al.*, 2005). Interestingly, this profile is different to EGFR/Her2 which has been previously shown to be increased and growth contributory in both the tamoxifen and faslodex resistant MCF-7 cell lines (McClelland *et al.*, 2001; Knowlden *et al.*, 2003). These data suggest EGFR/Her2 expression may not be subject to ER regulation in these anti-oestrogen resistant models, in contrast to the genes identified in this project.

This project revealed that the levels of nuclear, active NFkB1 are very prominently increased in the acquired faslodex resistant MCF-7 cells (FAS-R cells). Constitutive NFkB activity has also been reported in a further cell model of resistance to faslodex, LCC9, compared to the faslodex sensitive MCF-7 cells, although in this instance there were no differences seen in the levels of p50 expression (Riggins *et al.*, 2005). Moreover, while the present study was only able to demonstrate a small cytoplasmic increase of NFkB1 in the tamoxifen resistant MCF-7 cell line, it has previously been shown that the level of NFkB binding activity is substantially increased in further tamoxifen-resistant (ER-positive/ErbB2-positive) breast cancer models. Furthermore that there is constitutive activity of NFkB in ER+ve clinical samples destined for

early tamoxifen relapse (Zhou *et al.*, 2005b) as well as in ER-ve cell lines and tumours (Biswas *et al.*, 2000; Zhou *et al.*, 2005b). NFkB p50 and p65 DNA binding activity were previously evaluated in 81 ER+ve primary breast cancer samples, revealing that p50 containing NFkB dimers were almost twofold more abundant than p65 containing dimers (Zhou *et al.*, 2005a), with this group furthermore reporting that their two anti-oestrogen resistant ER+ve cell lines showed an increase specifically in activity of the p50 NFkB subunit (Zhou *et al.*, 2005b). Finally, increases in NFkB activity have also been shown in ER+ve models of acquired E2 independence (LCC1; Pratt *et al.*, 2003), where this NFkB activity consisted primarily of p50 homodimers (with low levels of p50/p65). It has been postulated by Pratt *et al.* (2003) that the withdrawal of E2 leading to E2 independent growth is facilitated by the increased expression of NFkB p50 in the presence of Bcl-3, since parallel increases in Bcl-3 were observed which can function as a transcriptional co-activator for p50 and p65 hetero/homodimers. These findings together with those made in the present project suggest a key importance for NFkB signalling (notably NfKB1 and its active p50 form) in diverse anti-hormone resistant states.

#### **4.7.3 Several genes induced may confer additional adverse features to the breast cancer cell in the appropriate context**

Interestingly, this project revealed genes that may confer adverse features when tumour cells are in an appropriate cellular context. This has been previously reported for CD59; a complement regulatory protein that defends tumour cells

from immune surveillance (Chen *et al.*, 2000), that is induced in hormone responsive breast cancer cells by anti-oestrogens (confirmed at the mRNA level using arrays and RT-PCR in this project). CD59 induction could be functionally important in the *in vivo* context in enhancing cell survival during treatment, where tumour cells would be vulnerable to the complement cascade. In agreement, through collaboration with Dr. N. Rushmere, UWIC the Tenovus group has previously reported that CD59 induction during exposure to anti-oestrogens does indeed promote increased resistance to complement-mediated lysis (Gee *et al.*, 2004; Gee *et al.*, 2006).

However, of particular interest are the anti-hormone induced genes revealed in this project that may facilitate gain of invasive behaviour. As previously stated, it has been reported that E2 and ER signalling exerts a protective effect on the motility and invasiveness of breast cancer cells. For example, ER+ve disease is known to have a more favourable prognosis (Platet *et al.*, 2004). Furthermore, an inherently low migratory behaviour of ER+ve breast cancer cells such as MCF-7 cells has been shown with matrigel assays in comparison with ER-ve breast cancer cells, where the treatment of ER+ve cells with E2 also resulted in a small increase in the protective effect on invasiveness (Platet *et al.*, 2004; Hiscox *et al.*, 2006a). Although the mechanism by which E2/ER exerts this protective effect is largely unknown, it is thought to require hormone binding, and the DNA binding and AF-2 regions of the ER (Platet *et al.*, 2000; Platet *et al.*, 2004). In part E2 may promote a protective effect via induction of ERE-

containing anti-invasive genes, e.g.  $\alpha$ 1-anti-chymotrypsin, (Platet *et al.*, 2004). However, it is also conceivable that ER protein-protein interactions and transrepression events at heterogenous response elements could contribute if they reduce the expression of key pro-invasive elements in ER+ve breast cancer cells (Platet *et al.*, 2000; Platet *et al.*, 2004). In turn it has been shown that ER blockade with tamoxifen or faslodex *in vitro* results in very modestly increased invasiveness of the MCF-7 cells (Platet *et al.*, 2000; Platet *et al.*, 2004). Interestingly, this project revealed increased expression during treatment of several elements whose ontology implicates them in epithelial-mesenchymal transition (EMT), motility and invasiveness. Of note were RhoE,  $\delta$ -catenin, Hif-1 $\alpha$  and possibly NDR1. There may also be additional roles for p50 Bag-1 since its expression has controversially been reported to increase metastatic potential and worsen patient outlook in various cancer types (Krajewski *et al.*, 1999; Tang *et al.*, 1999; Turner *et al.*, 2001). NF $\kappa$ B has also been linked with increased invasive capacity, especially through the PI3k pathways (Sliva *et al.*, 2002).

Although RhoE has been identified as a supposedly anti-proliferative member of the Rnd family of GTPases, it had been linked to changes in the actin cytoskeleton, cell rounding and increased growth factor-induced cell migratory speed (Guasch *et al.*, 1998; Riento *et al.*, 2005).  $\delta$ -catenin (which is also known as neural plakophilin-related arm repeat protein, NPRAP) is an adhesive junction protein and a member of the p120 catenin protein family (p120<sup>ctn</sup>).

This family is characterized by the presence of ten Armadillo (ARM) repeat domains, which allows for the binding of these plasma membrane proteins to the juxtamembrane segment of the classical cadherins (Lu *et al.*, 1999; Anastasiadis and Reynolds 2000). Via this binding cell-cell adhesion can be modulated. When catenins are deregulated however, transcription can be modulated by their interaction with TCF/LEF and translocation to the nucleus.  $\delta$ -catenin has been shown to be detectable in the nucleus and is associated with the Kaiso transcriptional repressor and member of the Broad complex, Tramtrak, Bric a brac/Pox virus and zinc finger (BTB/POZ) family (Rodova *et al.*, 2004). This is interesting as alongside induction of overall levels of membrane-associated  $\delta$ -catenin by faslodex, by day 10 there was evidence of low levels of nuclear staining for this catenin. The expression of several putative Kaiso regulated gene targets (e.g. cyclin D1, MMP7 and MTA2) have been linked not only with tumorigenesis and cell proliferation but also with metastases (van Roy and McCrean 2005; Daniel 2007). Moreover, ectopic expression of  $\delta$ -catenin has been shown to enhance growth factor-promoted cell scattering, increase formation of lamellipodia and filopodia, as well as promote cell spreading (Lu *et al.*, 1999). Although  $\delta$ -catenin was originally thought to be expressed only in the nervous system, it has also been identified as a marker for prostate cancer where it is linked with increased cell spreading but not proliferation (Burger *et al.*, 2002).

Of further interest is the anti-hormone-induced gene Hif-1 $\alpha$ . The importance of this gene (and indeed detection at the protein level, as described above) may

only be apparent under conditions of hypoxia (Lee *et al.*, 2004), where it could serve to not only maintain proliferation/cell survival by promoting tumour production of angiogenic factors, but also to facilitate invasive behaviour (Lee *et al.*, 2004; Kimbro and Simons 2006). While not explored at the protein level, NDR1 was demonstrated at the RNA level to be a further anti-hormone induced gene. NDR1 is a nuclear serine/threonine kinase and member of the AGC kinase subfamily but little is known about this enzyme with no substrates identified in mammalian cells and no links as yet made to known signalling pathways (Devroe *et al.*, 2004; Hergovich *et al.*, 2006). NDR1 is thought to participate in the regulation of morphology, proliferation and tumour progression (Stegert *et al.*, 2005), and while the role of NDR1 in mammalian cells has not yet been fully established there are some indications that it could act as a proto-oncogene (Hergovich *et al.*, 2006). This is supported by observations that NDR1 levels are increased in ductal carcinoma *in situ* versus normal breast (Adeyinka *et al.*, 2002). Interestingly however, in addition to this feature, regulation of NDR1 has been associated with calcium level through a direct complexing with S100B (a member of the S100 family of EF-hand calcium-binding proteins) an event stimulating NDR1 kinase activity (Millward *et al.*, 1998). Since S100B is over-expressed in over 80% of metastatic melanomas (Devroe *et al.*, 2004) while the closely related S100A4 protein induces a metastatic phenotype in rat mammary cells (Zhang *et al.*, 2005), it could possibly be inferred that NDR1 activity equally has a role in increasing metastatic potential (Devroe *et al.*, 2004).

It is thus feasible that induction of these various genes may contribute to the small promotion of invasiveness by anti-oestrogens. Moreover, they may play a role when acquired anti-oestrogen resistance subsequently emerges with its associated gain of features of EMT and inherently increased aggressiveness (Hiscox *et al.*, 2006a) since, as stated above, RhoE and  $\delta$ -catenin (and both NFkB1 and Bag-1) are retained at increased levels into the FAS-R cell line. Interestingly, these genes were not retained at high levels in tamoxifen resistance, indicating there may be different pro-invasive mechanisms in various anti-oestrogen resistant states. For example, we have previously shown TAM-R invasiveness is highly dependent on deregulation of  $\beta$ -catenin and Src signalling (Hiscox *et al.*, 2006a; Hiscox *et al.*, 2007).

However, it is clear that an apparently substantial induction of pro-migratory genes in MCF-7 cells does not translate out into substantial increases in invasiveness during anti-oestrogen response. Perhaps their full impact may be manifested under conditions of poor cell-cell contact. MCF-7 cells have inherently good cell-cell contacts maintained by functional E-cadherin, in keeping with their low invasiveness (Hiscox *et al.*, 2006a; Hiscox *et al.*, 2007). The largest inductive effects on invasive behaviour are apparent for faslodex (Hiscox *et al.*, 2006b; Hiscox *et al.*, 2007), which is in keeping with the largest gene changes observed with this agent in this project. Clearly, while anti-oestrogens confer only small increases in invasiveness under conditions of good cell-cell contact, this may become substantial in an appropriate context/environment where cell-cell contact is compromised, observations that



may have major implications for patient prognosis when using anti-oestrogens in ER+ve tumours with inherently poor cell-cell contacts.

#### **4.8 Implications for therapy and future directions**

The *in vitro* microarray studies and associated signalling investigations presented in this thesis have revealed a number of E2-repressed, anti-hormone-induced genes whose ontology implies a positive contribution to cell survival/proliferation and as such may act to limit maximal anti-tumour response to anti-hormones and maintain the cellular cohort from which resistance subsequently emerges. Molecular manipulation (e.g. utilizing siRNA technology), in parallel with application of any available selective pharmacological inhibitors to deplete expression/activity of the genes in our models is now essential to definitively prove they promote compensatory growth or enhanced invasiveness in the presence of anti-hormones. The siRNA technique could be used in combination with FACS assay for proliferation, Tunel assays to monitor cell death, and matrigel migration/invasion studies to reveal a more in depth analysis of the gene function, while exploration of procedures to permit longer-term knockdown would be needed to examine impact on quality and duration of anti-tumour response *in vitro* through growth studies. Also of interest would be to explore if the genes are equally inducible in further models representative of ER+ve breast cancer sub-types (Perou *et al.*, 2000; Sorlie *et al.*, 2001) e.g. further luminal breast cancer models, for example ER+ve T47D cell line, as well as Her2-over-expressing ER+ve

models. This is critical, since this may also begin to define the clinical tumour sub-types likely to be responsive to targeting of these elements alongside the anti-hormone therapy. Moreover, since the genes are retained in the faslodex resistant model, it would be relevant to extend study of the genes to models reflective of further resistant states. While apparently not retained in tamoxifen resistance in this project, of particular clinical interest would be to explore the relationship of the genes to acquired resistance to ED. For example alongside available models of this state (e.g. long term oestrogen deprivation, LTED (Santen *et al.*, 2005), the Tenovus laboratories have developed a further model of acquired resistance to severe ED and growth factor deprivation, termed MCF-X cells, that would be relevant to further explore these identified genes (Staka *et al.*, 2005).

While model studies remain important, it is critical that the anti-hormone induced genes are also screened in clinical samples of ER+ve breast cancer. This will confirm if they are expressed and at what level, and in series with follow-up data it would also be possible to correlate the protein levels with time to relapse, breast cancer progression and patient survival. If clinical samples with high levels of the genes are associated with a more aggressive tumour phenotype and shorter overall patient survival it may further support that the genes play a role in the adverse effects of anti-oestrogen treatment. Ideally the gene levels should be investigated in clinical samples pre and post-endocrine therapy and where acquired resistance to the treatment occurs. Obtaining these sequential clinical samples is exceptionally difficult, but

nevertheless has previously been achievable through collaboration of the Tenovus centre for Cancer Research with Nottingham City Hospital (Kenny *et al.*, 2001).

Notwithstanding these future research requirements for the identified genes however, important therapeutic implications already stem from findings made in this thesis.

#### **4.8.1 Oestrogen receptor blockade in combination with targeting of anti-hormone-induced genes could prove worthwhile in improving the anti-tumour properties of anti-hormones**

Proof of principal has previously been provided by studies performed for EGFR. As previously stated EGFR increases during anti-oestrogen challenge and this element has been targeted in the presence of tamoxifen in MCF-7 cells using gefitinib. Co-treatment blocked anti-hormone-induced EGFR signalling (Gee *et al.*, 2003; Nicholson *et al.*, 2005) and was superior in promoting cell death (30% induction) together with inhibiting proliferation (75% fall) versus tamoxifen alone, culminating in a noticeably improved anti-tumour effect *in vitro*, demonstrating the substantial therapeutic potential of such a combination strategy to improve quality and duration of response in ER+ve disease. This effect also extends to other ER+ve breast cancer models and to combination treatment with faslodex plus gefitinib (McClelland *et al.*, 2001; Gee *et al.*, 2003), while supportive *in vivo* model data have also been described for

various anti-EGFR plus anti-hormone strategies (Shou *et al.*, 2004). Excitingly several such combination strategies are currently under clinical evaluation (Johnston 2006a). However, this thesis has been able to reveal several additional signalling targets that could potentially be considered in combined treatments with anti-hormones.

The thesis has also obtained further supportive evidence of the potential for such combined treatments of anti-hormones together with agents targeting their induced elements, in this instance by manipulation of the anti-hormone-induced gene NFkB1 using the Ikb kinase inhibitor parthenolide. This agent was shown to deplete activity of this transcription factor in reporter assays that is induced by faslodex in MCF-7 cells. In parallel, parthenolide plus faslodex combination treatment substantially improved growth inhibitory effects of the anti-hormone in a dose dependent manner. Since NFkB is induced by both anti-oestrogens and ED, such targeting may prove valuable in combination with diverse approaches for ER blockade.

Of course, in deciphering the importance of the identified genes and in considering optimal combination strategies it will be essential in the future to address to what degree the various induced events are interlinked. For example, a key question will be to address whether the new induced genes lie within the EGFR/Her2 signalling pathway that is also induced during anti-oestrogen treatment. Alternatively, the genes may prove independent of this mechanism and thus likely to provide independent therapeutic targets that may be valuable

alongside targeting of EGFR to enhance anti-hormone response and improve outlook in breast cancer patients. Relationship of the identified genes to the EGFR/Her2 signalling pathway could be investigated in the future by looking at the impact of the EGFR-selective TKI gefitinib, or of Her2-inhibitors such as herceptin, on these anti-hormone-induced elements, and in turn addressing whether pharmacological/molecular manipulation of the identified genes impacts on EGFR/Her2 signalling and whether such inhibition further enhances the anti-tumour effects of gefitinib in combination with anti-oestrogen treatment. In this regard, tentative links have been established between 14-3-3 $\zeta$  and EGFR signalling (Oksvold *et al.*, 2004), while NF $\kappa$ B1 has been linked with Her2 and Akt which can contribute to the EGFR signalling pathway. As previously stated, breast cancer cells can be protected from tamoxifen-induced apoptosis by activation of the PI3/Akt pathway which acts via subsequent activation of the NF $\kappa$ B signalling pathway. Significantly higher levels of NF $\kappa$ B DNA binding and transcription-promoting activity as well as increased levels of phosphorylated I $\kappa$ B have been found in tamoxifen-resistant MCF-7 cells with constitutively active Akt compared with the control MCF-7 cells (deGraffenried *et al.*, 2004). Moreover, inhibition of NF $\kappa$ B (either pharmacologically or molecularly) was seen to restore tamoxifen sensitivity in the resistant cell line (deGraffenried *et al.*, 2004). Interestingly it was also noted that trastuzumab (herceptin) treatment of a Her2 over-expressing cell line resulted in inhibition of Akt activation and decreased NF $\kappa$ B binding, suggesting that NF $\kappa$ B can indeed be a significant downstream target of Her2 (Pianetti *et al.*, 2001).

#### **4.8.2 Inhibiting these new gene targets, where their increased expression is retained, could also prove valuable in treating resistance**

Proof of this principal exists as treatment with gefitinib is inhibitory confirming a key role for increased EGFR/Her2 signalling following the acquisition of anti-oestrogen resistance in both the TAM-R and FAS-R cell lines (McClelland *et al.*, 2001; Knowlden *et al.*, 2003). Further resistant models such as MCF-7/Her2 have also shown this (Shou *et al.*, 2004), and anti-erbB therapies are being investigated at present clinically in various anti-hormone resistant states (Johnston 2006a). NFkB is an example of a further potential target in resistance, where the faslodex resistant cells exhibited increased NFkB transcription factor activity which could be noticeably inhibited by parthenolide, observations supported by studies in the LCC9 FAS-R cell line (Riggins *et al.*, 2005). NFkB blockade has also been shown to be growth inhibitory and to restore tamoxifen response in the ER+ve MCF-7/Her2 and also BT474 cell lines (Zhou *et al.*, 2005b) as well as in cells constitutively over-expressing Akt (deGraffenried *et al.*, 2004), and to also inhibit ER-ve models (Biswas *et al.*, 2000). It was also found that pharmacological inhibition of NFkB with the IKK inhibitor parthenolide restored faslodex sensitivity in an acquired faslodex resistant model by enhancing apoptosis (Riggins *et al.*, 2005). Significantly there is already substantial clinical interest in targeting of NFkB signalling in cancer, for example using proteasomal inhibitors such as bortezomib (Zhou *et al.*, 2005a) to subvert NFkB nuclear translocation. It is therefore proposed that such studies should consider both co-treatment with

anti-hormones (either anti-oestrogens or ED) and also NFkB blockade as monotherapy in diverse anti-hormone resistant states.

#### **4.8.3 Targeting of anti-hormone induced genes that may become important according to cell context (notably those driving invasive behaviour) may subvert progression and improve outlook**

The function of some genes induced by anti-hormones may become important according to cell context. Previous studies have shown that complement mediated lysis in MCF-7 cells in the presence of anti-oestrogens can be restored by co-treating with an antibody to neutralise anti-oestrogen-induced CD59 (Gee *et al.*, 2004; Gee *et al.*, 2006). These data provide proof of principle that targeting genes with context-specific function could have considerable therapeutic potential.

Of particular interest is the observation that under certain cell contexts aggressive behaviour in residual cells can be substantially encouraged by anti-oestrogen treatment that induces pro-invasive gene expression. If such progression is to be effectively subverted, ideally combination therapies should aim to achieve early maximal cell kill. However, it is hoped that alongside the future deciphering and targeting of the genes underlying anti-oestrogen-promoted invasive behaviour, embracing of intelligent combination strategies targeting the induced pro-invasive genes may also be therapeutically useful in

extending breast cancer patient survival. Of potential relevance as a target in this regard is RhoE, a Rnd family member identified as anti-oestrogen induced in the present study. RhoE undergoes posttranslational modification by addition of a farnesyl group, which acts as a membrane attachment moiety. There are now farnesyltransferase small molecule inhibitors (FTIs) available that block the enzyme from attaching the farnesyl group to the Rnd/Rac family proteins. In clinical trials these have been shown to be useful as anti-cancer drugs which have led to the inhibition and even regression of tumour growth without major side effects (Tamanoi *et al.*, 2001). Interestingly, the compound FTI-277 has been shown to weakly inhibit the transendothelial migration of MDA-MB-231 breast cancer cells (Kusama *et al.*, 2006) suggesting such compounds may be able to subvert any pro-invasive behaviour of Rnd family members such as RhoE. Equally, the targeting of Hif-1 $\alpha$  may be valuable. This may be achievable by development of small molecule inhibitors of HIF1- $\alpha$ , although no specific Hif-1 $\alpha$  inhibitor have yet been developed the ability of these inhibitor to target multiple pathway involved in cancer progression could be beneficial in anti-tumour therapy (Patiar and Harris 2006). In addition, the Hsp90 inhibitor geldanamycin has been shown to reduce *in vitro* invasion and VEGF expression following chemically induced hypoxia in T24 bladder cancer cells in a mechanism involving blockade of HIF1 $\alpha$  signalling interplay with hepatocyte growth factor receptor signalling (Koga *et al.*, 2007). Excitingly, these various agents are currently being clinically-evaluated in cancer trials, in some instances in combination with anti-hormones in breast cancer (Johnston and Kelland 2001; Head and Johnston 2004).



Chapter 6  
~ **References** ~

- Adeyinka, A., Emberley, E., Niu, Y., Snell, L., Murphy, L. C., Sowter, H., Wykoff, C. C., Harris, A. L. and Watson, P. H. (2002a). "Analysis of gene expression in ductal carcinoma *in situ* of the breast." Clinical Cancer Research **8**: 3788-3795.
- Adeyinka, A., Emberley, E., Niu, Y., Snell, L., Murphy, L. C., Sowter, H., Wykoff, C. C., Harris, A. L. and Watson, P. H. (2002b). "Analysis of gene expression in ductal carcinoma *in situ* of the breast." Clin Cancer Res **8**(12): 3788-95.
- Agrawal, A., Gutteridge, E., Gee, J. M., Nicholson, R. I. and Robertson, J. F. (2005). "Overview of tyrosine kinase inhibitors in clinical breast cancer." Endocr Relat Cancer **12 Suppl 1**: S135-44.
- Anastasiadis, P. Z. and Reynolds, A. B. (2000). "The p120 catenin family: complex roles in adhesion, signaling and cancer." Journal of Cell Science **113**: 1319-1334.
- Baum, M., Buzdar, A., Cuzick, J., Forbes, J., Houghton, J., Howell, A. and Sahmoud, T. (2003). "Anastrozole alone or in combination with tamoxifen versus tamoxifen alone for adjuvant treatment of postmenopausal women with early-stage breast cancer: results of the ATAC (Arimidex, Tamoxifen Alone or in Combination) trial efficacy and safety update analyses." Cancer **98**(9): 1802-10.
- Bentrem, D., Fox, J. E., Pearce, S. T., Liu, H., Pappas, S., Kupfer, D., Zapf, J. W. and Jordan, V. C. (2003). "Distinct molecular conformations of the estrogen receptor alpha complex exploited by environmental estrogens." Cancer Res **63**(21): 7490-6.
- Beral, V. (2003). "Breast cancer and hormone-replacement therapy in the Million Women Study." Lancet **362**(9382): 419-27.
- Biswas, D. K., Cruz, A. P., Gansberger, E. and Pardee, A. B. (2000). "Epidermal growth factor-induced nuclear factor kappa B activation: A major pathway of cell-cycle progression in estrogen-receptor negative breast cancer cells." Proc Natl Acad Sci U S A **97**(15): 8542-7.
- Biswas, D. K., Shi, Q., Baily, S., Strickland, I., Ghosh, S., Pardee, A. B. and Iglehart, J. D. (2004). "NF-kappa B activation in human breast cancer specimens and its role in cell proliferation and apoptosis." Proc Natl Acad Sci U S A **101**(27): 10137-42.
- Biswas, D. K. and Iglehart, J. D. (2006). "Linkage between EGFR family receptors and nuclear factor kappaB (NF-kappaB) signaling in breast cancer." J Cell Physiol **209**(3): 645-52.

- Bogaerts, J., Cardoso, F., Buyse, M., Braga, S., Loi, S., Harrison, J. A., Bines, J., Mook, S., Decker, N., Ravdin, P., Therasse, P., Rutgers, E., van 't Veer, L. J. and Piccart, M. (2006). "Gene signature evaluation as a prognostic tool: challenges in the design of the MINDACT trial." Nat Clin Pract Oncol **3**(10): 540-51.
- Bonizzi, G. and Karin, M. (2004). "The two NF-kappaB activation pathways and their role in innate and adaptive immunity." Trends Immunol **25**(6): 280-8.
- Bours, V., Bentires-Alj, M., Hellin, A. C., Viatour, P., Robe, P., Delhalle, S., Benoit, V. and Merville, M. P. (2000). "Nuclear factor-kappa B, cancer, and apoptosis." Biochem Pharmacol **60**(8): 1085-9.
- Britton, D. J., Hutcheson, I. R., Knowlden, J. M., Barrow, D., Giles, M., McClelland, R. A., Gee, J. M. and Nicholson, R. I. (2006). "Bidirectional cross talk between ERalpha and EGFR signalling pathways regulates tamoxifen-resistant growth." Breast Cancer Res Treat **96**(2): 131-46.
- Burger, M. J., Tebay, M. A., Keith, P. A., Samaratinga, H. M., Clements, J., Lavin, M. F. and Gardiner, R. A. (2002). "Expression analysis of  $\delta$ -catenin and prostate-specific membrane antigen: their potential as diagnostic markers for prostate cancer." International Journal of Cancer **100**(2): 228-237.
- Buzdar, A. U., Jonat, W., Howell, A., Jones, S. E., Blomqvist, C. P., Vogel, C. L., Eiermann, W., Wolter, J. M., Steinberg, M., Webster, A. and Lee, D. (1998). "Anastrozole versus megestrol acetate in the treatment of postmenopausal women with advanced breast carcinoma: results of a survival update based on a combined analysis of data from two mature phase III trials. Arimidex Study Group." Cancer **83**(6): 1142-52.
- Buzdar, A. U. (2004). "Hormonal therapy in early and advanced breast cancer." Breast J **10** Suppl 1: S19-21.
- Cantley, L. C. (2002). "The phosphoinositide 3-kinase pathway." Science **296**(5573): 1655-7.
- Carney, P. A., Miglioretti, D. L., Yankaskas, B. C., Kerlikowske, K., Rosenberg, R., Rutter, C. M., Geller, B. M., Abraham, L. A., Taplin, S. H., Dignan, M., Cutter, G. and Ballard-Barbash, R. (2003). "Individual and combined effects of age, breast density, and hormone replacement therapy use on the accuracy of screening mammography." Ann Intern Med **138**(3): 168-75.

- Carpenter, R. and Miller, W. R. (2005). "Role of aromatase inhibitors in breast cancer." Br J Cancer **93 Suppl 1**: S1-5.
- Chardin, P. (2006). "Function and regulation of Rnd proteins." Nature Reviews molecular cell biology **7**: 54-62.
- Chen, S., Caragine, T., Cheung, N. K. and Tomlinson, S. (2000). "Surface antigen expression and complement susceptibility of differentiated neuroblastoma clones." Am J Pathol **156(3)**: 1085-91.
- Chen, D., Washbrook, E., Sarwar, N., Bates, G. J., Pace, P. E., Thirunuvakkarasu, V., Taylor, J., Epstein, R. J., Fuller-Pace, F. V., Egly, J.-M., Coombes, R. C. and Ali, S. (2002). "Phosphorylation of human estrogen receptor  $\alpha$  at serine 118 by two distinct signal transduction pathways revealed by phosphorylation-specific antisera." Oncogene **21(22)**: 4921-4931.
- Cicatiello, L., Scafoglio, C., Altucci, L., Cancemi, M., Natoli, G., Facchiano, A., Iazzetti, G., Calogero, R., Biglia, N., De Bortoli, M., Sfiligoi, C., Sismondi, P., Bresciani, F. and Weisz, A. (2004). "A genomic view of estrogen actions in human breast cancer cells by expression profiling of the hormone-responsive transcriptome." J Mol Endocrinol **32(3)**: 719-75.
- Clarke, R., Liu, M. C., Bouker, K. B., Gu, Z., Lee, R. Y., Zhu, Y., Skaar, T. C., Gomez, B., O'Brien, K., Wang, Y. and Hilakivi-Clarke, L. A. (2003). "Anti-estrogen resistance in breast cancer and the role of estrogen receptor signaling." Oncogene **22(47)**: 7316-7339.
- Cleator, S. and Ashworth, A. (2004). "Molecular profiling of breast cancer: clinical implications." Br J Cancer **90(6)**: 1120-4.
- Cole, M. P., Jones, C. T. and Todd, I. D. (1971). "A new anti-oestrogenic agent in late breast cancer. An early clinical appraisal of ICI46474." Br J Cancer **25(2)**: 270-5.
- Coombes, R. C., Kilburn, L. S., Snowdon, C. F., Paridaens, R., Coleman, R. E., Jones, S. E., Jassem, J., Van de Velde, C. J., Delozier, T., Alvarez, I., Del Mastro, L., Ortmann, O., Diedrich, K., Coates, A. S., Bajetta, E., Holmberg, S. B., Dodwell, D., Mickiewicz, E., Andersen, J., Lonning, P. E., Cocconi, G., Forbes, J., Castiglione, M., Stuart, N., Stewart, A., Fallowfield, L. J., Bertelli, G., Hall, E., Bogle, R. G., Carpentieri, M., Colajori, E., Subar, M., Ireland, E. and Bliss, J. M. (2007). "Survival and safety of exemestane versus tamoxifen after 2-3 years' tamoxifen treatment (Intergroup Exemestane Study): a randomised controlled trial." Lancet **369(9561)**: 559-70.

- Cooper, C. S. (2001). "Applications of microarray technology in breast cancer research." Breast Cancer Res 3(3): 158-75.
- Cunliffe, H. E., Ringner, M., Bilke, S., Walker, R. L., Cheung, J. M., Chen, Y. and Meltzer, P. S. (2003). "The gene expression response of breast cancer to growth regulators: patterns and correlation with tumor expression profiles." Cancer Res 63(21): 7158-66.
- Curry, E. A., 3rd, Murry, D. J., Yoder, C., Fife, K., Armstrong, V., Nakshatri, H., O'Connell, M. and Sweeney, C. J. (2004). "Phase I dose escalation trial of feverfew with standardized doses of parthenolide in patients with cancer." Invest New Drugs 22(3): 299-305.
- Cusack, J. C. (2003). "Rationale for the treatment of solid tumors with the proteasome inhibitor bortezomib." Cancer Treat Rev 29 Suppl 1: 21-31.
- Cutress, R. I., Townsend, P. A., Brimmell, M., Bateman, A. C., Hague, A. and Packham, G. (2002). "BAG-1 expression and function in human cancer." Br J Cancer 87(8): 834-9.
- Cutress, R. I., Townsend, P. A., Sharp, A., Maison, A., Wood, L., Lee, R., Brimmell, M., Mullee, M. A., Johnson, P. W., Royle, G. T., Bateman, A. C. and Packham, G. (2003). "The nuclear BAG-1 isoform, BAG-1L, enhances oestrogen-dependent transcription." Oncogene 22(32): 4973-82.
- Cuzick, J., Forbes, J., Edwards, R., M. B., Cawthorn, S., A. C., H, H., Howell, A. and T, P. (2002). "First results from the international breast cancer intervention study (IBIS-I): a randomised prevention trial." The Lancet 360(9336): 817-824.
- Daniel, J. M. (2007). "Dancing in and out of the nucleus: p120(ctn) and the transcription factor Kaiso." Biochim Biophys Acta 1773(1): 59-68.
- deGraffenried, L. A., Chandrasekar, B., Friedrichs, W. E., Donzis, E., Silva, J., Hidalgo, M., Freeman, J. W. and Weiss, G. R. (2004). "NF-kappa B inhibition markedly enhances sensitivity of resistant breast cancer tumor cells to tamoxifen." Ann Oncol 15(6): 885-90.
- Devroe, E., Erdjument-Bromage, H., Tempst, P. and Silver, P. A. (2004). "Human Mob proteins regulate the NDR1 and NDR2 serine-threonine kinases." The Journal of Biological Chemistry 279(23): 24444-24451.
- Dobrzycka, K. M., Townson, S. M., Jiang, S. and Oesterreich, S. (2003). "Estrogen receptor corepressors -- a role in human breast cancer?" Endocr Relat Cancer 10(4): 517-36.

- Doisneau-Sixou, S. F., Sergio, C. M., Carroll, J. S., Hui, R., Musgrove, E. A. and Sutherland, R. L. (2003). "Estrogen and antiestrogen regulation of cell cycle progression in breast cancer cells." Endocr Relat Cancer **10**(2): 179-86.
- Dougherty, M. and Morrison, D. (2004). "Unlocking the Code of 14-3-3." The Journal of Cell Science **117**(pt.10): 1875-1884.
- Dowsett, M., Nicholson, R. I. and Pietras, R. J. (2005). "Biological characteristics of the pure antiestrogen fulvestrant: overcoming endocrine resistance." Breast Cancer Res Treat **93 Suppl 1**: S11-8.
- Dunnwald, L. K., Rossing, M. A. and Li, C. I. (2007). "Hormone receptor status, tumor characteristics, and prognosis: a prospective cohort of breast cancer patients." Breast Cancer Res **9**(1): R6.
- Dusonchet, L., Corsale, S., Migliavacca, M., Calo, V., Bazan, V., Amato, A., Cammareri, P., Totaro, M. S., Agnese, V., Casico, S., La Rocca, G., Sisto, P. S., Dardanoni, G., Valerio, M. R., Grassi, N., Latteri, S., Cajozzo, M., Buscemi, M., Castorina, S., Morello, V., Tomasino, R. M., Gebbia, N. and Russo, A. (2003). "Nm23-H1 expression does not predict clinical survival in colorectal cancer patients." Oncology Reports **10**: 1257-1263.
- Ferlay, J., Autier, P., Boniol, M., Heanue, M., Colombet, M. and Boyle, P. (2007). "Estimates of the cancer incidence and mortality in Europe in 2006." Ann Oncol **18**(3): 581-92.
- Filardo, E. J. and Thomas, P. (2005). "GPR30: a seven-transmembrane-spanning estrogen receptor that triggers EGF release." Trends Endocrinol Metab **16**(8): 362-7.
- Finlin, B. S., Gau, C. L., Murphy, G. A., Shao, H., Kimel, T., Seitz, R. S., Chiu, Y. F., Botstein, D., Brown, P. O., Der, C. J., Tamanoi, F., Andres, D. A. and Perou, C. M. (2001). "RERG is a novel ras-related, estrogen-regulated and growth-inhibitory gene in breast cancer." J Biol Chem **276**(45): 42259-67.
- Fisher, B., Costantino, J. P., Redmond, C. K., Fisher, E. R., Wickerham, D. L. and Cronin, W. M. (1994). "Endometrial cancer in tamoxifen-treated breast cancer patients: findings from the National Surgical Adjuvant Breast and Bowel Project (NSABP) B-14." J Natl Cancer Inst **86**(7): 527-37.

- Fisher, B., Jeong, J. H., Bryant, J., Anderson, S., Dignam, J., Fisher, E. R. and Wolmark, N. (2004). "Treatment of lymph-node-negative, oestrogen-receptor-positive breast cancer: long-term findings from National Surgical Adjuvant Breast and Bowel Project randomised clinical trials." Lancet **364**(9437): 858-68.
- Fodor, S. P., Read, J. L., Pirrung, M. C., Stryer, L., Lu, A. T. and Solas, D. (1991). "Light-directed, spatially addressable parallel chemical synthesis." Science **251**(4995): 767-73.
- Frasor, J., Danes, J. M., Komm, B., Chang, K. C., Lyttle, C. R. and Katzenellenbogen, B. S. (2003). "Profiling of estrogen up- and down-regulated gene expression in human breast cancer cells: insights into gene networks and pathways underlying estrogenic control of proliferation and cell phenotype." Endocrinology **144**(10): 4562-74.
- Frasor, J., Stossi, F., Danes, J. M., Komm, B., Lyttle, C. R. and Katzenellenbogen, B. S. (2004). "Selective estrogen receptor modulators: discrimination of agonistic versus antagonistic activities by gene expression profiling in breast cancer cells." Cancer Res **64**(4): 1522-33.
- Frasor, J., Chang, E. C., Komm, B., Lin, C. Y., Vega, V. B., Liu, E. T., Miller, L. D., Smeds, J., Bergh, J. and Katzenellenbogen, B. S. (2006). "Gene expression preferentially regulated by tamoxifen in breast cancer cells and correlations with clinical outcome." Cancer Res **66**(14): 7334-40.
- Froesch, B. A., Takayama, S. and Reed, J. C. (1998). "BAG-1L protein enhances androgen receptor function." J Biol Chem **273**(19): 11660-6.
- Fuqua, S. A., Schiff, R., Parra, I., Moore, J. T., Mohsin, S. K., Osborne, C. K., Clark, G. M. and Allred, D. C. (2003). "Estrogen receptor beta protein in human breast cancer: correlation with clinical tumor parameters." Cancer Res **63**(10): 2434-9.
- Gee, J. M., Robertson, J. F., Ellis, I. O. and Nicholson, R. I. (2001). "Phosphorylation of ERK1/2 mitogen-activated protein kinase is associated with poor response to anti-hormonal therapy and decreased patient survival in clinical breast cancer." Int J Cancer **95**(4): 247-54.
- Gee, J. M., Harper, M. E., Hutcheson, I. R., Madden, T. A., Barrow, D., Knowlden, J. M., McClelland, R. A., Jordan, N., Wakeling, A. E. and Nicholson, R. I. (2003). "The antiepidermal growth factor receptor agent gefitinib (ZD1839/Iressa) improves antihormone response and prevents development of resistance in breast cancer in vitro." Endocrinology **144**(11): 5105-17.

- Gee, J. M. W., Giles, M. G. and Nicholson, R. I. (2004). "Extreme growth factor signalling can promote oestrogen receptor- $\alpha$  loss: therapeutic implications in breast cancer." Breast Cancer Research **6**(4): 162-163.
- Gee, J. M., Robertson, J. F., Gutteridge, E., Ellis, I. O., Pinder, S. E., Rubini, M. and Nicholson, R. I. (2005a). "Epidermal growth factor receptor/HER2/insulin-like growth factor receptor signalling and oestrogen receptor activity in clinical breast cancer." Endocr Relat Cancer **12 Suppl 1**: S99-S111.
- Gee, J. M. W., Robertson, J. F., Gutteridge, E., Ellis, I. O., Pinder, S. E., Rubini, M. and Nicholson, R. I. (2005b). "Epidermal growth factor/HER2/insulin-like growth factor receptor signalling and oestrogen receptor activity in clinical breast cancer." Endocrine-Related Cancer **12**: Suppl S99-S111.
- Gee, J. M., Shaw, V. E., Hiscox, S. E., McClelland, R. A., Rushmere, N. K. and Nicholson, R. I. (2006). "Deciphering antihormone-induced compensatory mechanisms in breast cancer and their therapeutic implications." Endocr Relat Cancer **13 Suppl 1**: S77-88.
- Generali, D., Berruti, A., Brizzi, M. P., Campo, L., Bonardi, S., Wigfield, S., Bersiga, A., Allevi, G., Milani, M., Aguggini, S., Gandolfi, V., Dogliotti, L., Bottini, A., Harris, A. L. and Fox, S. B. (2006). "Hypoxia-inducible factor-1 $\alpha$  expression predicts a poor response to primary chemoendocrine therapy and disease-free survival in primary human breast cancer." Clinical Cancer Research **12**(15): 4562-4568.
- Gibson, L. J., Dawson, C. K., Lawrence, D. H. and Bliss, J. M. (2007). "Aromatase inhibitors for treatment of advanced breast cancer in postmenopausal women." Cochrane Database Syst Rev(1): CD003370.
- Glidewell-Kenney, C., Weiss, J., Lee, E. J., Pillai, S., Ishikawa, T., Ariazi, E. A. and Jameson, J. L. (2005). "ERE-independent ER $\alpha$  target genes differentially expressed in human breast tumors." Mol Cell Endocrinol **245**(1-2): 53-9.
- Glordano, S. H., Buzdar, A. U. and Hortobagyi, G. N. (2002). "Breast cancer in men." Annals Internal Medicine **137**: 678-687.
- Goldhirsch, A., Coates, A. S., Gelber, R. D., Glick, J. H., Thurlimann, B. and Senn, H. J. (2006). "First--select the target: better choice of adjuvant treatments for breast cancer patients." Ann Oncol **17**(12): 1772-6.
- Gruber, C. J., Tschugguel, W., Schneeberger, C. and Huber, J. C. (2002). "Production and actions of estrogens." N Engl J Med **346**(5): 340-52.



- Gruvberger-Saal, S. K., Cunliffe, H. E., Carr, K. M. and Hedenfalk, I. A. (2006). "Microarrays in breast cancer research and clinical practice--the future lies ahead." Endocr Relat Cancer **13**(4): 1017-31.
- Guasch, R. M., Scambler, P., Jones, G. E. and Ridley, A. J. (1998). "RhoE regulates actin cytoskeleton organization and cell migration." Mol Cell Biol **18**(8): 4761-71.
- Gutierrez, M. C., Detre, S., Johnston, S., Mohsin, S. K., Shou, J., Allred, D. C., Schiff, R., Osborne, C. K. and Dowsett, M. (2005). "Molecular changes in tamoxifen-resistant breast cancer: relationship between estrogen receptor, HER-2, and p38 mitogen-activated protein kinase." J Clin Oncol **23**(11): 2469-76.
- Hall, J. M., McDonnell, D. P. and Korach, K. S. (2002). "Allosteric regulation of estrogen receptor structure, function, and coactivator recruitment by different estrogen response elements." Mol Endocrinol **16**(3): 469-86.
- Hayden, M. S. and Ghosh, S. (2004). "Signaling to NF-kappaB." Genes Dev **18**(18): 2195-224.
- Head, J. and Johnston, S. R. (2004). "New targets for therapy in breast cancer: farnesyltransferase inhibitors." Breast Cancer Res **6**(6): 262-8.
- Hellwig-Burgel, T., Rutkowski, K., Metzen, E., Fandrey, J. and Jelkmann, W. (1999). "Interleukin-1beta and tumor necrosis factor-alpha stimulate DNA binding of hypoxia-inducible factor-1." Blood **94**(5): 1561-7.
- Hergovich, A., Stegert, M. R., Schmitz, D. and Hemmings, B. A. (2006). "NDR kinases regulate essential cell processes from yeast to humans." Nat Rev Mol Cell Biol **7**(4): 253-64.
- Hiscox, S., Morgan, L., Barrow, D., Dutkowski, C., Wakeling, A. and Nicholson, R. I. (2004). "Tamoxifen resistance in breast cancer cells is accompanied by an enhanced motile and invasive phenotype: inhibition by gefitinib ('Iressa', ZD1839)." Clin Exp Metastasis **21**(3): 201-12.
- Hiscox, S., Jiang, W. G., Obermeier, K., Taylor, K., Morgan, L., Burmi, R., Barrow, D. and Nicholson, R. I. (2006a). "Tamoxifen resistance in MCF7 cells promotes EMT-like behaviour and involves modulation of beta-catenin phosphorylation." Int J Cancer **118**(2): 290-301.
- Hiscox, S., Jordan, N. J., Jiang, W., Harper, M., McClelland, R., Smith, C. and Nicholson, R. I. (2006b). "Chronic exposure to fulvestrant promotes overexpression of the c-Met receptor in breast cancer cells: implications for tumour-stroma interactions." Endocr Relat Cancer **13**(4): 1085-99.

- Hiscox, S., Jordan, N. J., Morgan, L., Green, T. P. and Nicholson, R. I. (2007). "Src kinase promotes adhesion-independent activation of FAK and enhances cellular migration in tamoxifen-resistant breast cancer cells." Clin Exp Metastasis **24**(3): 157-67.
- Hodges, L. C., Cook, J. D., Lobenhofer, E. K., Li, L., Bennett, L., Bushel, P. R., Aldaz, C. M., Afshari, C. A. and Walker, C. L. (2003). "Tamoxifen functions as a molecular agonist inducing cell cycle-associated genes in breast cancer cells." Mol Cancer Res **1**(4): 300-11.
- Howell, A., Osborne, C. K., Morris, C. and Wakeling, A. E. (2000). "ICI 182,780 (Faslodex): development of a novel, "pure" antiestrogen." Cancer **89**(4): 817-25.
- Howell, A., Robertson, J. F., Abram, P., Lichinitser, M. R., Elledge, R., Bajetta, E., Watanabe, T., Morris, C., Webster, A., Dimery, I. and Osborne, C. K. (2004). "Comparison of fulvestrant versus tamoxifen for the treatment of advanced breast cancer in postmenopausal women previously untreated with endocrine therapy: a multinational, double-blind, randomized trial." J Clin Oncol **22**(9): 1605-13.
- Huang, E., Cheng, S. H., Dressman, H., Pittman, J., Tsou, M. H., Horng, C. F., Bild, A., Iversen, E. S., Liao, M., Chen, C. M., West, M., Nevins, J. R. and Huang, A. T. (2003). "Gene expression predictors of breast cancer outcomes." Lancet **361**(9369): 1590-6.
- Hynes, N. E. and Lane, H. A. (2005). "ERBB receptors and cancer: the complexity of targeted inhibitors." Nat Rev Cancer **5**(5): 341-54.
- Inoue, A., Yoshida, N., Omoto, Y., Oguchi, S., Yamori, T., Kiyama, R. and Hayashi, S. (2002). "Development of cDNA microarray for expression profiling of estrogen-responsive genes." J Mol Endocrinol **29**(2): 175-92.
- Jansen, M. P., Foekens, J. A., van Staveren, I. L., Dirkzwager-Kiel, M. M., Ritstier, K., Look, M. P., Meijer-van Gelder, M. E., Sieuwerts, A. M., Portengen, H., Dorssers, L. C., Klijn, J. G. and Berns, E. M. (2005). "Molecular classification of tamoxifen-resistant breast carcinomas by gene expression profiling." J Clin Oncol **23**(4): 732-40.
- Jatoi, I. and Miller, A. B. (2003). "Why is breast-cancer mortality declining?" Lancet Oncol **4**(4): 251-4.
- Jensen, E. V. and Jordan, V. C. (2003). "The estrogen receptor: a model for molecular medicine." Clin Cancer Res **9**(6): 1980-9.

- Joel, P. B., Smith, J., Sturgill, T. W., Fisher, T. L., Blenis, J. and Lannigan, D. A. (1998a). "pp90rsk1 regulates estrogen receptor-mediated transcription through phosphorylation of Ser-167." Mol Cell Biol **18**(4): 1978-84.
- Joel, P. B., Traish, A. M. and Lannigan, D. A. (1998b). "Estradiol-induced phosphorylation of serine 118 in the estrogen receptor is independent of p42/p44 mitogen-activated protein kinase." J Biol Chem **273**(21): 13317-23.
- Johnson, K. H. and Millard, P. S. (1996). "Oral contraceptives and breast cancer." J Fam Pract **43**(4): 340-1.
- Johnston, S. R. and Kelland, L. R. (2001). "Farnesyl transferase inhibitors--a novel therapy for breast cancer." Endocr Relat Cancer **8**(3): 227-35.
- Johnston, S. R. and Dowsett, M. (2003). "Aromatase inhibitors for breast cancer: lessons from the laboratory." Nat Rev Cancer **3**(11): 821-31.
- Johnston, S. R. (2005a). "Clinical trials of intracellular signal transductions inhibitors for breast cancer--a strategy to overcome endocrine resistance." Endocr Relat Cancer **12 Suppl 1**: S145-57.
- Johnston, S. R. (2005b). "Combinations of endocrine and biological agents: present status of therapeutic and presurgical investigations." Clin Cancer Res **11**(2 Pt 2): 889s-99s.
- Johnston, S. R. (2006a). "Clinical efforts to combine endocrine agents with targeted therapies against epidermal growth factor receptor/human epidermal growth factor receptor 2 and mammalian target of rapamycin in breast cancer." Clin Cancer Res **12**(3 Pt 2): 1061s-1068s.
- Johnston, S. R. (2006b). "Targeting downstream effectors of epidermal growth factor receptor/HER2 in breast cancer with either farnesyltransferase inhibitors or mTOR antagonists." Int J Gynecol Cancer **16 Suppl 2**: 543-8.
- Johnston, S. R. and Leary, A. (2006c). "Lapatinib: a novel EGFR/HER2 tyrosine kinase inhibitor for cancer." Drugs Today (Barc) **42**(7): 441-53.
- Jones, H. E., Gee, J. M., Taylor, K. M., Barrow, D., Williams, H. D., Rubini, M. and Nicholson, R. I. (2005). "Development of strategies for the use of anti-growth factor treatments." Endocr Relat Cancer **12 Suppl 1**: S173-82.

- Jordan, N. J., Gee, J. M., Barrow, D., Wakeling, A. E. and Nicholson, R. I. (2004). "Increased constitutive activity of PKB/Akt in tamoxifen resistant breast cancer MCF-7 cells." Breast Cancer Res Treat **87**(2): 167-80.
- Jordan, V. C. (2003). "Is tamoxifen the Rosetta stone for breast cancer?" J Natl Cancer Inst **95**(5): 338-40.
- Kalaitzidis, D. and Gilmore, T. D. (2005). "Transcription factor cross-talk: the estrogen receptor and NF-kappaB." Trends Endocrinol Metab **16**(2): 46-52.
- Kamalakaran, S., Radhakrishnan, S. K. and Beck, W. T. (2005). "Identification of estrogen-responsive genes using a genome-wide analysis of promoter elements for transcription factor binding sites." J Biol Chem **280**(22): 21491-7.
- Kamei, Y., Xu, L., Heinzl, T., Torchia, J., Kurokawa, R., Gloss, B., Lin, S. C., Heyman, R. A., Rose, D. W., Glass, C. K. and Rosenfeld, M. G. (1996). "A CBP integrator complex mediates transcriptional activation and AP-1 inhibition by nuclear receptors." Cell **85**(3): 403-14.
- Karin, M., Cao, Y., Greten, F. R. and Li, Z. W. (2002). "NF-kappaB in cancer: from innocent bystander to major culprit." Nat Rev Cancer **2**(4): 301-10.
- Katzenellenbogen, B. S. and Katzenellenbogen, J. A. (2000). "Estrogen receptor transcription and transactivation: Estrogen receptor alpha and estrogen receptor beta: regulation by selective estrogen receptor modulators and importance in breast cancer." Breast Cancer Res **2**(5): 335-44.
- Kelley, K. M., Rowan, B. G. and Ratnam, M. (2003). "Modulation of the folate receptor alpha gene by the estrogen receptor: mechanism and implications in tumor targeting." Cancer Res **63**(11): 2820-8.
- Kenny, F. S., Willsher, P. C., Gee, J. M., Nicholson, R., Pinder, S. E., Ellis, I. O. and Robertson, J. F. (2001). "Change in expression of ER, bcl-2 and MIB1 on primary tamoxifen and relation to response in ER positive breast cancer." Breast Cancer Res Treat **65**(2): 135-44.
- Kim, K. N., Pie, J. E., Park, J. H., Park, Y. H., Kim, H. W. and Kim, M. K. (2006). "Retinoic acid and ascorbic acid act synergistically in inhibiting human breast cancer cell proliferation." J Nutr Biochem **17**(7): 454-62.
- Kimbrow, K. S. and Simons, J. W. (2006). "Hypoxia-inducible factor-1 in human breast and prostate cancer." Endocr Relat Cancer **13**(3): 739-49.

- Klijn, J. G., Blamey, R. W., Boccardo, F., Tominaga, T., Duchateau, L. and Sylvester, R. (2001). "Combined tamoxifen and luteinizing hormone-releasing hormone (LHRH) agonist versus LHRH agonist alone in premenopausal advanced breast cancer: a meta-analysis of four randomized trials." J Clin Oncol **19**(2): 343-53.
- Klinge, C. M. (2000). "Estrogen receptor interaction with co-activators and co-repressors." Steroids **65**(5): 227-251.
- Klinge, C. M. (2001). "Estrogen receptor interaction with estrogen response elements." Nucleic Acids Research **29**(14): 2905-2919.
- Knowlden, J. M., Hutcheson, I. R., Jones, H. E., Madden, T., Gee, J. M., Harper, M. E., Barrow, D., Wakeling, A. E. and Nicholson, R. I. (2003). "Elevated levels of epidermal growth factor receptor/c-erbB2 heterodimers mediate an autocrine growth regulatory pathway in tamoxifen-resistant MCF-7 cells." Endocrinology **144**(3): 1032-44.
- Knowlden, J. M., Hutcheson, I. R., Barrow, D., Gee, J. M. and Nicholson, R. I. (2005). "Insulin-like growth factor-I receptor signaling in tamoxifen-resistant breast cancer: a supporting role to the epidermal growth factor receptor." Endocrinology **146**(11): 4609-18.
- Koga, F., Tsutsumi, S. and Neckers, L. M. (2007). "Low Dose Geldanamycin Inhibits Hepatocyte Growth Factor and Hypoxia-Stimulated Invasion of Cancer Cells." Cell Cycle **6**(11):1393-1402.
- Krajewska, M., Turner, B. C., Shabaik, A., Krajewski, S. and Reed, J. C. (2006). "Expression of BAG-1 protein correlates with aggressive behavior of prostate cancers." Prostate **66**(8): 801-10.
- Krajewski, S., Krajewska, M., Turner, B. C., Pratt, C., Howard, B., Zapata, J. M., Frenkel, V., Robertson, S., Ionov, Y., Yamamoto, H., Perucho, M., Takayama, S. and Reed, J. C. (1999). "Prognostic significance of apoptosis regulators in breast cancer." Endocr Relat Cancer **6**(1): 29-40.
- Kudoh, M., Knee, D. A., Takayama, S. and Reed, J. C. (2002). "Bag-1 proteins regulate growth and survival of ZR-75-1 human breast cancer cells." Cancer Research **62**(6): 1904-1909.
- Kurebayashi, J., Otsuki, T., Moriya, T. and Sonoo, H. (2001). "Hypoxia reduces hormone responsiveness of human breast cancer cells." Jpn J Cancer Res **92**(10): 1093-101.

- Kusama, T., Mukai, M., Tatsuta, M., Nakamura, H. and Inoue, M. (2006). "Inhibition of transendothelial migration and invasion of human breast cancer cells by preventing geranylgeranylation of Rho." Int J Oncol **29**(1): 217-23.
- Kushner, P. J., Agard, D. A., Greene, G. L., Scanlan, T. S., Shiau, A. K., Uht, R. M. and Webb, P. (2000). "Estrogen receptor pathways to AP-1." J Steroid Biochem Mol Biol **74**(5): 311-7.
- Kuss, J. T., Muss, H. B., Hoen, H. and Case, L. D. (1997). "Tamoxifen as initial endocrine therapy for metastatic breast cancer: long term follow-up of two Piedmont Oncology Association (POA) trials." Breast Cancer Res Treat **42**(3): 265-74.
- Lannigan, D. A. (2003). "Estrogen receptor phosphorylation." Steroids **68**(1): 1-9.
- Laronga, C., Yang, H.-Y., Neal, C. and Lee, M.-H. (2000). "Association of the cyclin-dependent kinases and 14-3-3 sigma negatively regulates cell cycle progression." The Journal of Biological Chemistry **275**(30): 23106-23112.
- Lash, T. L. and Aschengrau, A. (2000). "Alcohol Drinking and Risk of Breast Cancer." Breast J **6**(6): 396-399.
- Lee, J. W., Bae, S. H., Jeong, J. W., Kim, S. H. and Kim, K. W. (2004). "Hypoxia-inducible factor (HIF-1)alpha: its protein stability and biological functions." Exp Mol Med **36**(1): 1-12.
- Levenson, A. S., Kliakhandler, I. L., Svoboda, K. M., Pease, K. M., Kaiser, S. A., Ward, J. E., 3rd and Jordan, V. C. (2002a). "Molecular classification of selective oestrogen receptor modulators on the basis of gene expression profiles of breast cancer cells expressing oestrogen receptor alpha." Br J Cancer **87**(4): 449-56.
- Levenson, A. S., Svoboda, K. M., Pease, K. M., Kaiser, S. A., Chen, B., Simons, L. A., Jovanovic, B. D., Dyck, P. A. and Jordan, V. C. (2002b). "Gene expression profiles with activation of the estrogen receptor alpha-selective estrogen receptor modulator complex in breast cancer cells expressing wild-type estrogen receptor." Cancer Res **62**(15): 4419-26.
- Levin, E. R. (2005). "Integration of the extranuclear and nuclear actions of estrogen." Mol Endocrinol **19**(8): 1951-9.

- Lin, C. Y., Strom, A., Vega, V. B., Kong, S. L., Yeo, A. L., Thomsen, J. S., Chan, W. C., Doray, B., Bangarusamy, D. K., Ramasamy, A., Vergara, L. A., Tang, S., Chong, A., Bajic, V. B., Miller, L. D., Gustafsson, J. A. and Liu, E. T. (2004). "Discovery of estrogen receptor alpha target genes and response elements in breast tumor cells." Genome Biol **5**(9): R66.
- Lipshutz, R. J., Fodor, S. P., Gingeras, T. R. and Lockhart, D. J. (1999). "High density synthetic oligonucleotide arrays." Nat Genet **21**(1 Suppl): 20-4.
- Liu, Y., Liu, H., Han, B. and Zhang, J.-T. (2006). "Identification of 14-3-3 $\sigma$  as a contributor to drug resistance in human breast cancer cells using functional proteomic analysis." Cancer Research **66**(6): 3248-3255.
- Lockhart, D. J., Dong, H., Byrne, M. C., Follettie, M. T., Gallo, M. V., Chee, M. S., Mittmann, M., Wang, C., Kobayashi, M., Horton, H. and Brown, E. L. (1996). "Expression monitoring by hybridization to high-density oligonucleotide arrays." Nat Biotechnol **14**(13): 1675-80.
- Lonning, P. E. (2004). "Aromatase inhibitors in breast cancer." Endocr Relat Cancer **11**(2): 179-89.
- Lu, Q., Paredes, M., Medina, M., Zhou, J., Cavallo, R., Peifer, M., Orecchio, L. and Kosik, K. S. (1999). "delta-catenin, an adhesive junction-associated protein which promotes cell scattering." J Cell Biol **144**(3): 519-32.
- Lyons, P. (2003). "Advances in spotted microarray resources for expression profiling." Brief Funct Genomic Proteomic **2**(1): 21-30.
- MacGregor, J. I. and Jordan, C. (1998). "Basic guide to the mechanisms of antiestrogen action." Pharmacological Reviews **50**(2): 151-196.
- Mackie, S. and Aitken, A. (2005). "Novel brain 14-3-3 interacting proteins involved in neurodegenerative disease." FEBS Journal **272**(16): 4202-4210.
- Magnani, M., Crinelli, R., Bianchi, M. and Antonelli, A. (2000). "The ubiquitin-dependent proteolytic system and other potential targets for the modulation of nuclear factor-kB (NF-kB)." Curr Drug Targets **1**(4): 387-99.
- Martin, L. A., Farmer, I., Johnston, S. R., Ali, S. and Dowsett, M. (2005a). "Elevated ERK1/ERK2/estrogen receptor cross-talk enhances estrogen-mediated signaling during long-term estrogen deprivation." Endocr Relat Cancer **12 Suppl 1**: S75-84.

- Martin, L. A., Pancholi, S., Chan, C. M., Farmer, I., Kimberley, C., Dowsett, M. and Johnston, S. R. (2005b). "The anti-oestrogen ICI 182,780, but not tamoxifen, inhibits the growth of MCF-7 breast cancer cells refractory to long-term oestrogen deprivation through down-regulation of oestrogen receptor and IGF signalling." Endocr Relat Cancer **12**(4): 1017-36.
- Martinez-Lacaci, I., Johnson, G. R., Salomon, D. S. and Dickson, R. B. (1996). "Characterization of a novel amphiregulin-related molecule in 12-*O*-tetradecanoylphorbol-13-acetate treated breast cancer cells." Journal of Cellular Physiology **169**: 497-508.
- Masamura, S., Santner, S. J., Heitjan, D. F. and Santen, R. J. (1995). "Estrogen deprivation causes estradiol hypersensitivity in human breast cancer cells." J Clin Endocrinol Metab **80**(10): 2918-25.
- Masters, S. (2002). "Survival-promoting functions of 14-3-3 proteins." Biochemical Society **30**(4): 360-365.
- Matsuda, T., Yamamoto, T., Muraguchi, A. and Saatcioglu, F. (2001). "Cross-talk between transforming growth factor-beta and estrogen receptor signaling through Smad3." J Biol Chem **276**(46): 42908-14.
- Mauriac, L., Debled, M. and MacGrogan, G. (2005). "When will more useful predictive factors be ready for use?" Breast **14**(6): 617-23.
- McClelland, R. A., Manning, D. L., Gee, J. M., Anderson, E., Clarke, R., Howell, A., Dowsett, M., Robertson, J. F., Blamey, R. W., Wakeling, A. E. and Nicholson, R. I. (1996). "Effects of short-term antiestrogen treatment of primary breast cancer on estrogen receptor mRNA and protein expression and on estrogen-regulated genes." Breast Cancer Res Treat **41**(1): 31-41.
- McClelland, R. A., Barrow, D., Madden, T. A., Dutkowski, C. M., Pamment, J., Knowlden, J. M., Gee, J. M. and Nicholson, R. I. (2001). "Enhanced epidermal growth factor receptor signaling in MCF7 breast cancer cells after long-term culture in the presence of the pure antiestrogen ICI 182,780 (Faslodex)." Endocrinology **142**(7): 2776-88.
- McDonnell, D. P., Connor, C. E., Wijayaratne, A., Chang, C. Y. and Norris, J. D. (2002). "Definition of the molecular and cellular mechanisms underlying the tissue-selective agonist/antagonist activities of selective estrogen receptor modulators." Recent Prog Horm Res **57**: 295-316.
- McPherson, K., Steel, C. M. and Dixon, J. M. (2000). "ABC of breast diseases. Breast cancer-epidemiology, risk factors, and genetics." Bmj **321**(7261): 624-8.



- Metivier, R., Penot, G., Flouriot, G. and Pakdel, F. (2001). "Synergism between ERalpha transactivation function 1 (AF-1) and AF-2 mediated by steroid receptor coactivator protein-1: requirement for the AF-1 alpha-helical core and for a direct interaction between the N- and C-terminal domains." Mol Endocrinol **15**(11): 1953-70.
- Mhawech, P. (2005). "14-3-3 proteins - an update." Cell Research **15**(4): 228-236.
- Milde-Langosch, K., Janke, S., Wagner, I., Schroder, C., Streichert, T., Bamberger, A. M., Janicke, F. and Loning, T. (2007). "Role of Fra-2 in breast cancer: influence on tumor cell invasion and motility." Breast Cancer Res Treat Mar 28 (Epub ahead of print).
- Millward, T. A., Heizmann, C. W., Schafer, B. W. and Hemmings, B. A. (1998). "Calcium regulation of Ndr protein kinase mediated by S100 calcium-binding proteins." Embo J **17**(20): 5913-22.
- Montano, M. M., Jaiswal, A. K. and Katzenellenbogen, B. S. (1998). "Transcriptional regulation of the human quinone reductase gene by antiestrogen-liganded estrogen receptor-alpha and estrogen receptor-beta." J Biol Chem **273**(39): 25443-9.
- Murphy, D. (2002). "Gene expression studies using microarrays: principles, problems, and prospects." Adv Physiol Educ **26**(1-4): 256-70.
- Nahta, R., Hortobagyi, G. N. and Esteva, F. J. (2003). "Growth factor receptors in breast cancer: potential for therapeutic intervention." Oncologist **8**(1): 5-17.
- Negrone, A., Venturelli, D., Tanno, B., Amendola, R., Ransac, S., Cesi, V., Calabretta, B. and Raschella, G. (2000a). "Neuroblastoma specific effects of DR-nm23 and its mutant forms on differentiation and apoptosis." Cell Death Differ **7**(9): 843-50.
- Negrone, A., Venturelli, D., Tanno, B., Amendola, R., Ransac, S., Cesi, V., Calabretta, B. and Raschella, G. (2000b). "Neuroblastoma specific effects of DR-nm23 and its mutant forms on differentiation and apoptosis." Cell Death and Differentiation **7**(9): 843-850.
- Newman, S. P., Bates, N. P., Vernimmen, D., Parker, M. G. and Hurst, H. C. (2000). "Cofactor competition between the ligand-bound oestrogen receptor and an intron 1 enhancer leads to oestrogen repression of ERBB2 expression in breast cancer." Oncogene **19**(4): 490-7.

- Nicholson, R. I., McClelland, R. A., Gee, J. M., Manning, D. L., Cannon, P., Robertson, J. F., Ellis, I. O. and Blamey, R. W. (1994). "Transforming growth factor-alpha and endocrine sensitivity in breast cancer." Cancer Res **54**(7): 1684-9.
- Nicholson, R. I., Hutcheson, I. R., Harper, M. E., Knowlden, J. M., Barrow, D., McClelland, R. A., Jones, H. E., Wakeling, A. E. and Gee, J. M. (2001). "Modulation of epidermal growth factor receptor in endocrine-resistant, oestrogen receptor-positive breast cancer." Endocr Relat Cancer **8**(3): 175-82.
- Nicholson, R. I., Hutcheson, I. R., Hiscox, S. E., Knowlden, J. M., Giles, M., Barrow, D. and Gee, J. M. (2005a). "Growth factor signalling and resistance to selective oestrogen receptor modulators and pure anti-oestrogens: the use of anti-growth factor therapies to treat or delay endocrine resistance in breast cancer." Endocr Relat Cancer **12 Suppl 1**: S29-36.
- Nicholson, R. I. and Johnston, S. R. (2005b). "Endocrine therapy - current benefits and limitations." Breast Cancer Research and Treatment **93: Suppl 1**: S3-S10.
- Nobes, C. D., Lauritzen, I., Mattei, M. G., Paris, S., Hall, A. and Chardin, P. (1998). "A new member of the Rho family, Rnd1, promotes disassembly of actin filament structures and loss of cell adhesion." J Cell Biol **141**(1): 187-97.
- Oesterreich, S., Deng, W., Jiang, S., Cui, X., Ivanova, M., Schiff, R., Kang, K., Hadsell, D. L., Behrens, J. and Lee, A. V. (2003). "Estrogen-mediated down-regulation of E-cadherin in breast cancer cells." Cancer Res **63**(17): 5203-8.
- Office for National Statistics, Cancer Statistics registrations: registrations of cancer diagnosed in 2003, England. Series MB1 no.34. London, National Statistics.
- Oh, D. S., Troester, M. A., Usary, J., Hu, Z., He, X., Fan, C., Wu, J., Carey, L. A. and Perou, C. M. (2006). "Estrogen-regulated genes predict survival in hormone receptor-positive breast cancers." J Clin Oncol **24**(11): 1656-64.
- Oksvold, M. P., Huitfeldt, H. S. and Langdon, W. Y. (2004a). "Identification of 14-3-3 $\zeta$  as an EGF receptor interacting protein." FEBS Letters **569**(1-3): 207-210.

- Okubo, S., Kurebayashi, J., Otsuki, T., Yamamoto, Y., Tanaka, K. and Sonoo, H. (2004). "Additive antitumour effect of the epidermal growth factor receptor tyrosine kinase inhibitor gefitinib (Iressa, ZD1839) and the antioestrogen fulvestrant (Faslodex, ICI 182,780) in breast cancer cells." Br J Cancer **90**(1): 236-44.
- Olivier, S., Robe, P. and Bours, V. (2006). "Can NF-kappaB be a target for novel and efficient anti-cancer agents?" Biochem Pharmacol **72**(9): 1054-68.
- O'Regan, R. M. and Jordan, C. V. (2002). "The evolution of tamoxifen therapy in breast cancer: selective oestrogen-receptor modulators and downregulators." The Lancet Oncology **3**(4): 207-214.
- Osborne, C. K., Coronado-Heinsohn, E. B., Hilsenbeck, S. G., McCue, B. L., Wakeling, A. E., McClelland, R. A., Manning, D. L. and Nicholson, R. I. (1995). "Comparison of the effects of a pure steroidal antiestrogen with those of tamoxifen in a model of human breast cancer." J Natl Cancer Inst **87**(10): 746-50.
- Patiar, S. and Harris, A. L. (2006). "Role of hypoxia-inducible factor-1alpha as a cancer therapy target." Endocr Relat Cancer **13 Suppl 1**: S61-75.
- Pearce, S. T., Liu, H. and Jordan, V. C. (2003). "Modulation of estrogen receptor alpha function and stability by tamoxifen and a critical amino acid (Asp-538) in helix 12." J Biol Chem **278**(9): 7630-8.
- Perou, C. M., Jeffrey, S. S., van de Rijn, M., Rees, C. A., Eisen, M. B., Ross, D. T., Pergamenschikov, A., Williams, C. F., Zhu, S. X., Lee, J. C., Lashkari, D., Shalon, D., Brown, P. O. and Botstein, D. (1999). "Distinctive gene expression patterns in human mammary epithelial cells and breast cancers." Proc Natl Acad Sci U S A **96**(16): 9212-7.
- Perou, C. M., Sorlie, T., Eisen, M. B., van de Rijn, M., Jeffrey, S. S., Rees, C. A., Pollack, J. R., Ross, D. T., Johnsen, H., Akslén, L. A., Fluge, O., Pergamenschikov, A., Williams, C., Zhu, S. X., Lonning, P. E., Borresen-Dale, A. L., Brown, P. O. and Botstein, D. (2000). "Molecular portraits of human breast tumours." Nature **406**(6797): 747-52.
- Peruzzi, F., Prisco, M., Dews, M., Salomoni, P., Grassilli, E., Romano, G., Calabretta, B. and Baserga, R. (1999). "Multiple signaling pathways of the insulin-like growth factor 1 receptor in protection from apoptosis." Molecular and Cellular biology **19**(10): 7203-7215

- Pianetti, S., Arsura, M., Romieu-Mourez, R., Coffey, R. J. and Sonenshein, G. E. (2001). "Her-2/neu overexpression induces NF-kappaB via a PI3-kinase/Akt pathway involving calpain-mediated degradation of IkappaB-alpha that can be inhibited by the tumor suppressor PTEN." Oncogene **20**(11): 1287-99.
- Piccart, M. J., de Valeriola, D., Dal Lago, L., de Azambuja, E., Demonty, G., Lebrun, F., Bernard-Marty, C., Colozza, M. and Cufer, T. (2005). "Adjuvant chemotherapy in 2005: standards and beyond." Breast **14**(6): 439-45.
- Platet, N., Cathiard, A. M., Gleizes, M. and Garcia, M. (2004). "Estrogens and their receptors in breast cancer progression: a dual role in cancer proliferation and invasion." Crit Rev Oncol Hematol **51**(1): 55-67.
- Platet, N., Cunat, S., Chalbos, D., Rochefort, H. and Garcia, M. (2000). "Unliganded and liganded estrogen receptors protect against cancer invasion via different mechanisms." Mol Endocrinol **14**(7): 999-1009.
- Polychronis, A., Sinnett, H. D., Hadjiminias, D., Singhal, H., Mansi, J. L., Shivapatham, D., Shousha, S., Jiang, J., Peston, D., Barrett, N., Vigushin, D., Morrison, K., Beresford, E., Ali, S., Slade, M. J. and Coombes, R. C. (2005). "Preoperative gefitinib versus gefitinib and anastrozole in postmenopausal patients with oestrogen-receptor positive and epidermal-growth-factor-receptor-positive primary breast cancer: a double-blind placebo-controlled phase II randomised trial." Lancet Oncol **6**(6): 383-91.
- Pore, N., Jiang, Z., Gupta, A., Cerniglia, G., Kao, G. D. and Maity, A. (2006). "EGFR tyrosine kinase inhibitors decrease VEGF expression by both hypoxia-inducible factor (HIF)-1-independent and HIF-1-dependent mechanisms." Cancer Res **66**(6): 3197-204.
- Powell, D. W., Rane, M. J., Chen, Q., Singh, S. and McLeish, K. R. (2002). "Identification of 14-3-3zeta as a protein kinase B/Akt substrate." J Biol Chem **277**(24): 21639-42.
- Pratt, M. A., Bishop, T. E., White, D., Yasvinski, G., Menard, M., Niu, M. Y. and Clarke, R. (2003). "Estrogen withdrawal-induced NF-kappaB activity and bcl-3 expression in breast cancer cells: roles in growth and hormone independence." Mol Cell Biol **23**(19): 6887-900.
- Qi, W. and Martinez, J. D. (2003). "Reduction of 14-3-3 proteins correlates with increased sensitivity to killing of human lung cancer cells by ionizing radiation." Radiat Res **160**(2): 217-23.

- Rae, J. M., Johnson, M. D., Scheys, J. O., Cordero, K. E., Larios, J. M. and Lippman, M. E. (2005). "GREB 1 is a critical regulator of hormone dependent breast cancer growth." Breast Cancer Res Treat **92**(2): 141-9.
- Rajendran, R. R., Nye, A. C., Frasor, J., Balsara, R. D., Martini, P. G. and Katzenellenbogen, B. S. (2003). "Regulation of nuclear receptor transcriptional activity by a novel DEAD box RNA helicase (DP97)." J Biol Chem **278**(7): 4628-38.
- Ravi, R. and Bedi, A. (2004). "NF-kappaB in cancer--a friend turned foe." Drug Resist Updat **7**(1): 53-67.
- Razandi, M., Pedram, A., Merchenthaler, I., Greene, G. L. and Levin, E. R. (2004). "Plasma membrane estrogen receptors exist and functions as dimers." Mol Endocrinol **18**(12): 2854-65.
- Renard, P., Ernest, I., Houbion, A., Art, M., Le Calvez, H., Raes, M. and Remacle, J. (2001). "Development of a sensitive multi-well colorimetric assay for active NFkappaB." Nucleic Acids Res **29**(4): E21.
- Richard, D. E., Berra, E. and Pouyssegur, J. (2000). "Nonhypoxic pathway mediates the induction of hypoxia-inducible factor 1alpha in vascular smooth muscle cells." J Biol Chem **275**(35): 26765-71.
- Riento, K., Guasch, R. M., Garg, R., Jin, B. and Ridley, A. J. (2003). "RhoE binds to ROCK I and inhibits downstream signaling." Mol Cell Biol **23**(12): 4219-29.
- Riento, K., Villalonga, P., Garg, R. and Ridley, A. (2005). "Function and regulation of RhoE." Biochemical Society **33**(4): 649-651.
- Riggins, R. B., Zwart, A., Nehra, R. and Clarke, R. (2005). "The nuclear factor kappa B inhibitor parthenolide restores ICI 182,780 (Faslodex; fulvestrant)-induced apoptosis in antiestrogen-resistant breast cancer cells." Mol Cancer Ther **4**(1): 33-41.
- Ring, A. and Dowsett, M. (2004). "Mechanisms of tamoxifen resistance." Endocr Relat Cancer **11**(4): 643-58.
- Robertson, J. F. R. (2001). "Faslodex (ICI 182,780), a novel estrogen receptor downregulator - future possibilities in breast cancer." Journal of Steroid Biochemistry & Molecular Biology **79**(1-5): 209-212.

- Robertson, J. F., Semiglazov, V., Nemsadze, G., Dzagnidze, G., Janjalia, M., Nicholson, R. I., Gee, J. M. and Armstrong, J. (2007). "Effects of fulvestrant 250mg in premenopausal women with oestrogen receptor-positive primary breast cancer." Eur J Cancer **43**(1): 64-70.
- Rocheftort, H., Glondu, M., Sahla, M. E., Platet, N. and Garcia, M. (2003). "How to target estrogen receptor-negative breast cancer?" Endocrine-Related Cancer **10**: 261-266.
- Rodova, M., Kelly, K. F., VanSaun, M., Daniel, J. M. and Werle, M. J. (2004). "Regulation of the rapsyn promoter by kaiso and delta-catenin." Mol Cell Biol **24**(16): 7188-96.
- Rosenquist, M. (2003a). "14-3-3 proteins in apoptosis." Braz J Med Biol Res **36**(4): 403-8.
- Rosenquist, M., 14-3-3 proteins in apoptosis. Brazilian Journal of Medical and Biological Research. 36:403-408 (2003) (2003b). "14-3-3 proteins in apoptosis." Brazilian Journal of Medical and Biological Research **36**: 403-408.
- Ross, D. T., Scherf, U., Eisen, M. B., Perou, C. M., Rees, C., Spellman, P., Iyer, V., Jeffrey, S. S., Van de Rijn, M., Waltham, M., Pergamenschikov, A., Lee, J. C., Lashkari, D., Shalon, D., Myers, T. G., Weinstein, J. N., Botstein, D. and Brown, P. O. (2000). "Systematic variation in gene expression patterns in human cancer cell lines." Nat Genet **24**(3): 227-35.
- Rushmere, N. K., Knowlden, J. M., Gee, J. M. W., Harper, M. E., Robertson, J. F., Morgan, B. P. and Nicholson, R. I. (2004). "Analysis of the level of mRNA expression of the membrane regulators of complement, CD59, CD55 and CD46 in breast cancer." International Journal of Cancer **108**(6): 930-936.
- Santen, R. J., Song, R. X., Zhang, Z., Yue, W. and Kumar, R. (2004). "Adaptive hypersensitivity to estrogen: mechanism for sequential responses to hormonal therapy in breast cancer." Clin Cancer Res **10**(1 Pt 2): 337S-45S.
- Santen, R. J., Song, R. X., Zhang, Z., Kumar, R., Jeng, M. H., Masamura, A., Lawrence, J., Jr., Berstein, L. and Yue, W. (2005a). "Long-term estradiol deprivation in breast cancer cells up-regulates growth factor signaling and enhances estrogen sensitivity." Endocr Relat Cancer **12** **Suppl 1**: S61-73.

- Santen, R. J., Song, R. X., Zhang, Z., Kumar, R., Jeng, M. H., Masamura, S., Lawrence, J., Jr., MacMahon, L. P., Yue, W. and Berstein, L. (2005b). "Adaptive hypersensitivity to estrogen: mechanisms and clinical relevance to aromatase inhibitor therapy in breast cancer treatment." J Steroid Biochem Mol Biol **95**(1-5): 155-65.
- Scafoglio, C., Ambrosino, C., Cicatiello, L., Altucci, L., Ardovino, M., Bontempo, P., Medici, N., Molinari, A. M., Nebbioso, A., Facchiano, A., Calogero, R. A., Elkon, R., Menini, N., Ponzzone, R., Biglia, N., Sismondi, P., De Bortoli, M. and Weisz, A. (2006). "Comparative gene expression profiling reveals partially overlapping but distinct genomic actions of different antiestrogens in human breast cancer cells." J Cell Biochem **98**(5): 1163-84.
- Schena, M., Shalon, D., Davis, R. W. and Brown, P. O. (1995). "Quantitative monitoring of gene expression patterns with a complementary DNA microarray." Science **270**(5235): 467-70.
- Schiff, R., Massarweh, S. A., Shou, J., Bharwani, L., Arpino, G., Rimawi, M. and Osborne, C. K. (2005). "Advanced concepts in estrogen receptor biology and breast cancer endocrine resistance: implicated role of growth factor signaling and estrogen receptor coregulators." Cancer Chemother Pharmacol **56 Suppl 1**: 10-20.
- Schiff, R., Massarweh, S. A., Shou, J., Bharwani, L., Mohsin, S. K. and Osborne, C. K. (2004). "Cross-talk between estrogen receptor and growth factor pathways as a molecular target for overcoming endocrine resistance." Clin Cancer Res **10**(1 Pt 2): 331S-6S.
- Schulze, A. and Downward, J. (2001). "Navigating gene expression using microarrays--a technology review." Nat Cell Biol **3**(8): E190-5.
- Shou, J., Massarweh, S., Osborne, C. K., Wakeling, A. E., Ali, S., Weiss, H. and Schiff, R. (2004). "Mechanisms of tamoxifen resistance: increased estrogen receptor-HER2/neu cross-talk in ER/HER2-positive breast cancer." J Natl Cancer Inst **96**(12): 926-35.
- Simoncini, T. and Genazzani, A. R. (2003). "Non-genomic actions of sex steroid hormones." Eur J Endocrinol **148**(3): 281-92.
- Singletary, S. E. (2003). "Rating the risk factors for breast cancer." Ann Surg **237**(4): 474-82.
- Sliva, D., Rizzo, M. T. and English, D. (2002). "Phosphatidylinositol 3-kinase and NF-kappaB regulate motility of invasive MDA-MB-231 human breast cancer cells by the secretion of urokinase-type plasminogen activator." J Biol Chem **277**(5): 3150-7.

- Sommer, A., Hoffmann, J., Lichtner, R. B., Schneider, M. R. and Parczyk, K. (2003). "Studies on the development of resistance to the pure antiestrogen Faslodex in three human breast cancer cell lines." J Steroid Biochem Mol Biol **85**(1): 33-47.
- Song, R. X., Barnes, C. J., Zhang, Z., Bao, Y., Kumar, R. and Santen, R. J. (2004). "The role of Shc and insulin-like growth factor 1 receptor in mediating the translocation of estrogen receptor alpha to the plasma membrane." Proc Natl Acad Sci U S A **101**(7): 2076-81.
- Sorlie, T., Perou, C. M., Tibshirani, R., Aas, T., Geisler, S., Johnsen, H., Hastie, T., Eisen, M. B., van de Rijn, M., Jeffrey, S. S., Thorsen, T., Quist, H., Matese, J. C., Brown, P. O., Botstein, D., Eystein Lonning, P. and Borresen-Dale, A. L. (2001). "Gene expression patterns of breast carcinomas distinguish tumor subclasses with clinical implications." Proc Natl Acad Sci U S A **98**(19): 10869-74.
- Sorlie, T., Wang, Y., Xiao, C., Johnsen, H., Naume, B., Samaha, R. R. and Borresen-Dale, A. L. (2006). "Distinct molecular mechanisms underlying clinically relevant subtypes of breast cancer: gene expression analyses across three different platforms." BMC Genomics **26**(7): 127.
- Soulez, M. and Parker, M. G. (2001). "Identification of novel oestrogen receptor target genes in human ZR75-1 breast cancer cells by expression profiling." J Mol Endocrinol **27**(3): 259-74.
- Spicer, D. V. and Pike, M. C. (2000). "Future possibilities in the prevention of breast cancer: luteinizing hormone-releasing hormone agonists." Breast Cancer Res **2**(4): 264-7.
- Staka, C. M., Nicholson, R. I. and Gee, J. M. (2005). "Acquired resistance to oestrogen deprivation: role for growth factor signalling kinases/oestrogen receptor cross-talk revealed in new MCF-7X model." Endocr Relat Cancer **12 Suppl 1**: S85-97.
- Stegert, M. R., Hergovich, A., Tamaskovic, R., Bichsel, S. J. and Hemmings, B. A. (2005). "Regulation of NDR protein kinase by hydrophobic motif phosphorylation mediated by the mammalian Ste20-like kinase MST3." Molecular and Cellular biology **25**(24): 11019-11029.
- Stein, B. and Yang, M. X. (1995). "Repression of the interleukin-6 promoter by estrogen receptor is mediated by NF-kappa B and C/EBP beta." Mol Cell Biol **15**(9): 4971-9.



- Tamanoi, F., Gau, C. L., Jiang, C., Edamatsu, H. and Kato-Stankiewicz, J. (2001). "Protein farnesylation in mammalian cells: effects of farnesyltransferase inhibitors on cancer cells." Cell Mol Life Sci **58**(11): 1636-49.
- Tamaskovic, R., Bichsel, S. and Hemmings, B. (2003). "NDR family of AGC kinases - essential regulators of the cell cycle and morphogenesis." FEBS Letters **546**: 73-80.
- Tang, S. C., Shehata, N., Chernenko, G., Khalifa, M. and Wang, X. (1999). "Expression of BAG-1 in invasive breast carcinomas." J Clin Oncol **17**(6): 1710-9.
- Townsend, P. A., Cutress, R. I., Sharp, A., Brimmell, M. and Packham, G. (2002a). "BAG-1: a multifunctional regulator of cell growth and survival." Biochimica et Biophysica Acta **1603**: 83-98.
- Townsend, P. A., Dublin, E., Hart, I. R., Kao, R. H., Hanby, A. M., Cutress, R. I., Poulsom, R., Ryder, K., Barnes, D. M. and Packham, G. (2002b). "BAG-1 expression in human breast cancer: interrelationship between BAG-1 RNA, protein, HSC70 expression and clinico-pathological data." J Pathol **197**(1): 51-9.
- Townsend, P. A., Cutress, R. I., Sharp, A., Brimmell, M. and Packham, G. (2003). "BAG-1 prevents stress-induced long-term growth inhibition in breast cancer cells via a chaperone-dependent pathway." Cancer Res **63**(14): 4150-7.
- Townsend, P. A., Stephanou, A., Packham, G. and Latchman, D. S. (2005). "BAG-1: a multi-functional pro-survival molecule." Int J Biochem Cell Biol **37**(2): 251-9.
- Turner, B. C., Krajewski, S., Krajewska, M., Takayama, S., Gumbs, A. A., Carter, D., Rebeck, T. R., Haffty, B. G. and Reed, J. C. (2001). "BAG-1: a novel biomarker predicting long-term survival in early-stage breast cancer." J Clin Oncol **19**(4): 992-1000.
- Tzivion, G., Gupta, V. S., Kaplun, L. and Balan, V. (2006). "14-3-3 proteins as potential oncogenes." Seminars in Cancer Biology **16**(3): 203-213.
- van de Vijver, M. J., He, Y. D., van't Veer, L. J., Dai, H., Hart, A. A., Voskuil, D. W., Schreiber, G. J., Peterse, J. L., Roberts, C., Marton, M. J., Parrish, M., Atsma, D., Witteveen, A., Glas, A., Delahaye, L., van der Velde, T., Bartelink, H., Rodenhuis, S., Rutgers, E. T., Friend, S. H. and Bernards, R. (2002). "A gene-expression signature as a predictor of survival in breast cancer." N Engl J Med **347**(25): 1999-2009.

- van Roy, F. M. and McCrea, P. D. (2005). "A role for Kaiso-p120ctn complexes in cancer?" Nat Rev Cancer **5**(12): 956-64.
- van 't Veer, L. J., Dai, H., van de Vijver, M. J., He, Y. D., Hart, A. A., Mao, M., Peterse, H. L., van der Kooy, K., Marton, M. J., Witteveen, A. T., Schreiber, G. J., Kerkhoven, R. M., Roberts, C., Linsley, P. S., Bernards, R. and Friend, S. H. (2002). "Gene expression profiling predicts clinical outcome of breast cancer." Nature **415**(6871): 530-6.
- Venturelli, D., Martinez, R., Melotti, P., Casella, I., Peschle, C., Cucco, C., Spampinato, G., Darzynkiewicz, Z. and Calabretta, B. (1995). "Overexpression of DR-nm23, a protein encoded by a member of the nm23 gene family, inhibits granulocyte differentiation and induces apoptosis in 32Dc13 myeloid cells." Proc Natl Acad Sci U S A **92**(16): 7435-9.
- Villalonga, P., Guasch, R. M., Riento, K. and Ridley, A. J. (2004). "RhoE inhibits cell cycle progression and ras-induced transformation." Molecular and Cellular biology **24**(18): 7829-7840.
- Villeneuve, D. J., Hembruff, S. L., Veitch, Z., Cecchetto, M., Dew, W. A. and Parissenti, A. M. (2006). "cDNA microarray analysis of isogenic paclitaxel- and doxorubicin-resistant breast tumor cell lines reveals distinct drug-specific genetic signatures of resistance." Breast Cancer Res Treat **96**(1): 17-39.
- Vincenz, C. and Dixit, V. M. (1996). "14-3-3 proteins associate with A20 in an isoform-specific manner and function both as chaperone and adapter molecules." The Journal of Biological Chemistry **271**(22): 20029-20034.
- Wakeling, A. E. and Bowler, J. (1992). "ICI 182,780, a new antioestrogen with clinical potential." J Steroid Biochem Mol Biol **43**(1-3): 173-7.
- Wang, D. Y., Fulthorpe, R., Liss, S. N. and Edwards, E. A. (2004). "Identification of estrogen-responsive genes by complementary deoxyribonucleic acid microarray and characterization of a novel early estrogen-induced gene: EEIG1." Mol Endocrinol **18**(2): 402-11.
- Wang, J., He, F. T., Tzang, C. H., Fong, W. F., Xiao, P. G., Han, R. and Yang, M. S. (2005). "Differential gene expression profiles in paclitaxel-induced cell cycle arrest and apoptosis in human breast cancer MCF-7 cells." Yao Xue Xue Bao **40**(12): 1099-104.

- Webb, P., Valentine, C., Nguyen, P., Price, R. H., Jr., Marimuthu, A., West, B. L., Baxter, J. D. and Kushner, P. J. (2003). "ERbeta Binds N-CoR in the Presence of Estrogens via an LXXLL-like Motif in the N-CoR C-terminus." Nucl Recept **1**(1):4 1-15.
- West, M., Blanchette, C., Dressman, H., Huang, E., Ishida, S., Spang, R., Zuzan, H., Olson, J. A., Jr., Marks, J. R. and Nevins, J. R. (2001). "Predicting the clinical status of human breast cancer by using gene expression profiles." Proc Natl Acad Sci U S A **98**(20): 11462-7.
- Wilson, M. A. and Chrysogelos, S. A. (2002). "Identification and characterization of a negative regulatory element within the epidermal growth factor receptor gene first intron in hormone-dependent breast cancer cells." J Cell Biochem **85**(3): 601-14.
- Wu, J. T. and Kral, J. G. (2005). "The NF-kappaB/IkappaB signaling system: a molecular target in breast cancer therapy." J Surg Res **123**(1): 158-69.
- Yamamoto, T., Saatcioglu, F. and Matsuda, T. (2002). "Cross-talk between bone morphogenic proteins and estrogen receptor signaling." Endocrinology **143**(7): 2635-42.
- Yarden, R. I., Wilson, M. A. and Chrysogelos, S. A. (2001). "Estrogen suppression of EGFR expression in breast cancer cells: A possible mechanism to modulate growth." J Cell Biochem **81**(S36): 232-246.
- Zelzer, E., Levy, Y., Kahana, C., Shilo, B. Z., Rubinstein, M. and Cohen, B. (1998). "Insulin induces transcription of target genes through the hypoxia-inducible factor HIF-1alpha/ARNT." Embo J **17**(17): 5085-94.
- Zhang, S., Wang, G., Liu, D., Bao, Z., Fernig, D. G., Rudland, P. S. and Barraclough, R. (2005). "The C-terminal region of S100A4 is important for its metastasis-inducing properties." Oncogene **24**(27): 4401-11.
- Zhang, Y., Karas, M., Zhao, H., Yakar, S. and LeRoith, D. (2004). "14-3-3 $\sigma$  mediation of cell cycle progression is p53-independent in response to insulin-like growth factor-1 receptor activation." The Journal of Biological Chemistry **279**(13): 34353-34360.
- Zhong, H., De Marzo, A. M., Laughner, E., Lim, M., Hilton, D. A., Zagzag, D., Buechler, P., Isaacs, W. B., Semenza, G. L. and Simons, J. W. (1999). "Overexpression of hypoxia-inducible factor 1alpha in common human cancers and their metastases." Cancer Res **59**(22): 5830-5.
- Zhou, Y., Eppenberger-Castori, S., Eppenberger, U. and Benz, C. C. (2005a). "The NFkappaB pathway and endocrine-resistant breast cancer." Endocr Relat Cancer **12 Suppl 1**: S37-46.

- Zhou, Y., Eppenberger-Castori, S., Marx, C., Yau, C., Scott, G. K., Eppenberger, U. and Benz, C. C. (2005b). "Activation of nuclear factor-kappaB (NFkappaB) identifies a high-risk subset of hormone-dependent breast cancers." Int J Biochem Cell Biol **37**(5): 1130-44.
- Zubairy, S. and Oesterreich, S. (2005). "Estrogen-repressed genes -- key mediators of estrogen action?" Breast Cancer Res **7**(4): 163-4.

